AIT Austrian Institute of Technology GmbH

Center for Health and Bioresources

Competence Unit Molecular Diagnostics

(Supervisor: Priv.-Doz. Dipl.-Ing. Dr. Winfried Neuhaus)

From DNA methylation to protein: Selection and evaluation of regulated targets in a human cerebral ischemia *in vitro* model of the blood-brain barrier

Thesis submitted in partial fulfilment of the requirements for the degree of

Master of Science (MSc)

University of Veterinary Medicine Vienna

Submitted by

Barbora Valentová, BSc

Vienna, July 2021

I. Supervision

Internal Supervisor: Dr. rer. nat. Sabine Lagger

External Supervisor: Priv.-Doz. Dipl.-Ing. Dr. Winfried Neuhaus

Reviewer: Ao. Univ.-Prof. Dr. rer. nat. Ralf Steinborn

II. Declaration of honour

“I declare on my word of honour that I have written this paper on my own and that I have not used any sources or resources other than stated and that I have marked those passages and/or ideas that were either verbally or textually extracted from sources. This also applies to drawings, sketches, graphic representations as well as to sources from the internet.
The paper has not been submitted in this or similar form for assessment at any other domestic or foreign post-secondary educational institution and has not been published elsewhere. The present paper complies with the version submitted electronically.”

Date: 30.07.2021

Signature: 

III. Acknowledgements

Firstly, I would like to express my gratitude to my external supervisor Priv.-Doz. Dipl.-Ing. Dr. Winfried Neuhaus who gave me the opportunity to realize my master thesis internship in his research group at Austrian Institute of Technology in Vienna. Thank you for your always present patience, guidance, and support during my internship.

I would like to thank the lab members Anna Gerhartl, Sarah Grabner, Andreas Brachner, Peter Friedl, Christina Gruber, Léna Czeloth, Grace Lin, and Ana Spilak for their unceasing help and encouragement with my research project as well as for their company and nice time spent together.

My gratitude belongs to Lisa Frühbauer, Anna Gerhartl, Sonja Peric, and Iris Soliman for providing me with initial data, primer design, and samples that were used for structuring and later successful completion of my work.

In the end, I would like to acknowledge my internal supervisor Dr. rer. nat. Sabine Lagger for her motivation, great care, and kind assistance during this time.

IV. Abstract

Background: Stroke and traumatic brain injury (TBI) are two threatening disorders of the central nervous system (CNS) that in case of survival usually result in serious permanent disabilities. Course of both diseases is accompanied by cerebral ischemia. The blood-brain barrier (BBB) represents a neuroprotective border formed by brain capillary endothelial cells. Loss of the BBB integrity is a consequence of cerebral ischemia. Recent studies demonstrated that the restorative processes initiated at the BBB after cerebral ischemia are regulated by epigenetic mechanisms, namely DNA methylation. The aim of this study was to evaluate the effect of oxygen-glucose deprivation (OGD) on the expression and function of targets selected from DNA methylation arrays of OGD treated human cerebral microvascular endothelial cell line (hCMEC/D3).

Methods: Targets were chosen based on Kegg Pathway Database, Gene Set Enrichment Analysis, and STRING database analysis. Their expression was examined at mRNA and protein level. For analysis at mRNA level, RNA samples from different conditions were used: hCMEC/D3 in co-culture with astrocytes and pericytes, hiPS-EC in co-culture with astrocytes and pericytes, and human TBI biopsy samples. For analysis at protein level, hCMEC/D3 mono-culture was exposed to OGD at 0.1% oxygen for 5 hours followed by recovery phase for additional 19 hours. For inhibitor studies, transwell models with hCMEC/D3 cells in co-culture with glioma C6 cells were subjected to 5-hour OGD treatment at 0.1% oxygen.

Results: Selected 13 regulated targets showed significant changes at mRNA level as well as at protein level in different experimental set-ups after two distinct OGD timepoints. Data analysis of qPCRs with human TBI biopsy samples from four patients revealed changes in the expression of DNA methylation targets over the time. Inhibitor studies performed with *SGK1* inhibitor demonstrated greater damage and injury to the BBB when applied at higher concentrations, while displayed powerful protective response upon the cells in lower concentrations.

Conclusion: Epigenetics, namely DNA methylation, emerges as a valuable tool for understanding complex processes arising at the BBB during and after cerebral ischemia. Identification and characterization of novel DNA methylation targets may help to tackle currently restricted treatment strategies as well as to develop means of restoring permanent damage resulting from stroke and TBI in case of survival.

Key words: blood-brain barrier, cerebral ischemia, DNA methylation targets

V. Abstrakt

Hintergrund: Schlaganfall und Schädel-Hirn Trauma (SHT) sind zwei bedrohliche Erkrankungen des Zentralnervensystems, die im Falle des Überlebens normalerweise zu schweren und dauerhaften Behinderungen führen. Beide Krankheiten werden von zerebraler Ischämie begleitet. Die Blut-Hirn-Schranke (BHS) stellt eine neuroprotektive Grenze dar, die durch Hirnkapillarendothelzellen gebildet wird. Der Verlust der BHS-Integrität ist eine Folge der zerebralen Ischämie. Jüngste Studien zeigten, dass die an der BHS nach zerebraler Ischämie initiierten restaurativen Prozesse von epigenetischen Mechanismen, nämlich DNA-Methylierung, reguliert sind. Ziel dieser Studie war es, den Effekt die Wirkung von Sauerstoff- und Glukoseentzug (SGE) auf die Expression und die Funktion der Ziele aus DNA-Methylierungsanordnungen der SGE-behandelten menschlichen, geistigen, mikrovaskulären Endothelzelllinie hCMEC/D3 auszuwerten.

Methoden: Die Ziele wurden basierend auf der KEGG-Pathway-Datenbank, der Gene-Set-Anreicherungsanalyse und der String-Datenbankanalyse ausgewählt. Ihre Expression wurde auf mRNA- und Eiweißebene untersucht. Für die Analyse auf mRNA-Ebene wurden RNA-Proben verschiedener Zustände verwendet: hCMEC/D3 in der Co-Kultur mit Astrozyten und Perizyten, hiPS-EC in Co-Kultur mit Astrozyten und Perizyten sowie Human-TBI-Biopsie-Proben. Bei der Analyse des Proteinspiegels wurde die hCMEC/D3-Monokultur für 5 Stunden SGE mit Sauerstoff von 0,1% ausgesetzt, gefolgt von einer Erholungsphase für weitere 19 Stunden. Bei Inhibitorstudien wurden Transwell-Modelle mit hCMEC/D3-Zellen in der Co-Kultur mit Gliom-C6-Zellen einer 5-stündigen SGE Behandlung mit 0,1% Sauerstoff unterzogen.

Ergebnisse: 13 ausgewählte regulierte Ziele zeigten erhebliche Veränderungen auf mRNA-Ebene sowie Veränderungen des Proteinspiegels in verschiedenen experimentellen Setups nach zwei unterschiedlichen SGE-Zeitpunkten. Die Datenanalyse von qPCRs mit humanen TBI-Biopsie-Proben von vier Patienten ergab Änderungen der Expression der DNA-Methylierungsziele über die Zeit. Inhibitorstudien, die mit *SGK1*-Inhibitor durchgeführt wurden, zeigten größere Beschädigungen und Verletzungen der BHS bei höheren Konzentrationen, während die Zellen in niedrigeren Konzentrationen eine leistungsstarke Schutzreaktion anzeigten.

Schlussfolgerung: Epigenetik, nämlich DNA-Methylierung, ist ein wertvolles Werkzeug, um komplexe Prozesse zu verstehen, die während und nach der zerebralen Ischämie auf der

BHS ablaufen. Die Identifizierung und Charakterisierung neuartiger DNA-Methylierungsziele kann dazu beitragen, die derzeit eingeschränkten Behandlungsstrategien zu verbessern und dauerhafte Schäden zu bewältigen, welche sich aus Schlaganfall und SHT ergeben.

Key-Wörter: Blut-Hirn-Schranke, zerebrale Ischämie, DNA-Methylierungsziele

VI. Table of contents

1. Introduction

1.1 Blood-brain barrier and its discovery

The blood-brain barrier (BBB) is defined as a highly selective and tightly regulated continuous semi-permeable layer composed of capillary endothelial cells (ECs) [1]. The BBB was originally discovered by Paul Ehrlich in 1885, despite the fact that he denied its unique property related to the permeability of cerebral vessels. In reality, the concept of BBB is rather attributed to the collective work of Max Lewandowsky, Edwin Goldmann, Lina Stern, and Raymond Gautier. Their studies demonstrated that toxins were unable to penetrate the blood-brain interface of the vertebrae brain. For instance, trypan blue dye injected into the brain remained localized only in the brain area. The same dye injected outside of the brain became evenly distributed in the entire organism with exclusion of the brain [2]. Intactness between blood, brain, and cerebrospinal fluid was also confirmed in embryos. This revelation is associated with George B. Wislocki, who injected a guinea pig embryo with trypan blue in 1920 [3]. The anatomical site of the BBB was resolved in 1967 due to extensive electron microscopy studies of Thomas Karnovsky and Morris Reese. Injection with electron-dense horseradish peroxidase (HRP) showed that HRP confined specifically to the cerebral capillary endothelium [4].

1.2 Role of the blood-brain barrier

The central nervous system (CNS) is kept distinct from the rest of the body by the BBB, the arachnoid barrier, and the blood-cerebrospinal fluid barrier at the choroid plexus. From these three types of barriers, the BBB is the most crucial for proper function of the brain [5]. More precisely, the BBB provides the greatest control over the microenvironment of brain cells required for a reliable neuronal signaling. It can be viewed as a physical barrier as the complex tight junctions between the adjacent ECs block the molecular transport via the paracellular pathway. The BBB also acts as a selective transport barrier due to the presence of multiple transport systems that regulate the molecular transport via the transcellular pathway. Furthermore, it is known under the term of a metabolic barrier due to the presence of a variety of intracellular and extracellular enzymes [6]. From the physiological point of view, the BBB maintains ionic homeostasis, controls levels of neurotransmitters, restricts leakage of plasma proteins into the brain, and provides the brain with constant nutrient and oxygen supply [7]. Additionally, this neuroprotective border limits the entry of potentially harmful blood-borne agents such as neurotoxins, pathogens, or immune cells into the brain [8].

1.3 Structure of the blood-brain barrier

Capillary blood vessels represent the major site of the BBB. The smallest cerebral blood vessels actually take up 85% of the total length of all blood vessels in the brain [9]. The BBB is a dynamic structure composed of brain capillary ECs, astrocyte feet, pericytes, and extracellular matrix (ECM) components. Apart from these elements, the BBB belongs to the neurovascular unit (NVU) which additionally refers to neurons, microglia, peripheral immune cells, and the basement membrane (BM). Specifically, BM is defined as a specialized type of ECM that is secreted by astrocytes, pericytes, and ECs [10,11]. Members of the NVU share complex associations forming the multicellular relationship between the brain and the blood vessels. All of the elements mentioned above interact with brain capillary ECs and are thus responsible for the development, maintenance, and function of the BBB [12,13].

ECs developed from squamous epithelial cells and derived from the mesoderm are in control of building the walls of the blood vessels [14]. Brain ECs lining the cerebral vasculature differ from peripheral ECs by stronger barrier properties due to the expression of the tight junction proteins as well as the restrictive transcellular transport controlled by transporters [12]. In comparison to muscle ECs, they are 39% thinner which makes them in general extremely thin [15]. Covering the highest surface area at the blood-CNS interface equal to approximately 12 m^2 with mean intercapillary distance of 40 μm^2, brain capillary ECs regulate the most effective influx and efflux of proteins and other molecules [9].

Astrocytes lie between neurons and brain ECs. Their endfeet surround and cover brain capillaries which makes the communication between astrocytes and brain ECs simple and efficient. In fact, astrocytes represent the most numerous brain cells. They help to maintain and repair the BBB through a release of several effector molecules. Astrocytes and brain ECs are characterized by a symbiotic relationship. While astrocytes are capable of inducing BBB phenotype of ECs, brain ECs encourage their differentiation [12,16].

Pericytes sit along the microvasculature of the brain capillaries, in contact with the underlying endothelium and localized within the vascular BM. Being in charge of regulation of angiogenesis and ECM deposition, pericytes maintain and stabilize the continuous layer of brain ECs. Pericytes have also an indispensable role in the development of tight junctions [12,16].

Neurons can be found in the proximity of 8-20 μm from the brain capillaries, associated with the astrocyte feet. Close proximity of neurons to the brain ECs enables them to regulate blood

flow, microvascular permeability, or to interact with ECM. Brain ECs, astrocytes, pericytes, and neurons communicate all together to initiate formation of the BBB as well as to regulate its function and structure [12,16]. ECM components establish formation and integrity of the BBB, while BM assures and drives crosstalk between the individual elements of the NVU [10,17].

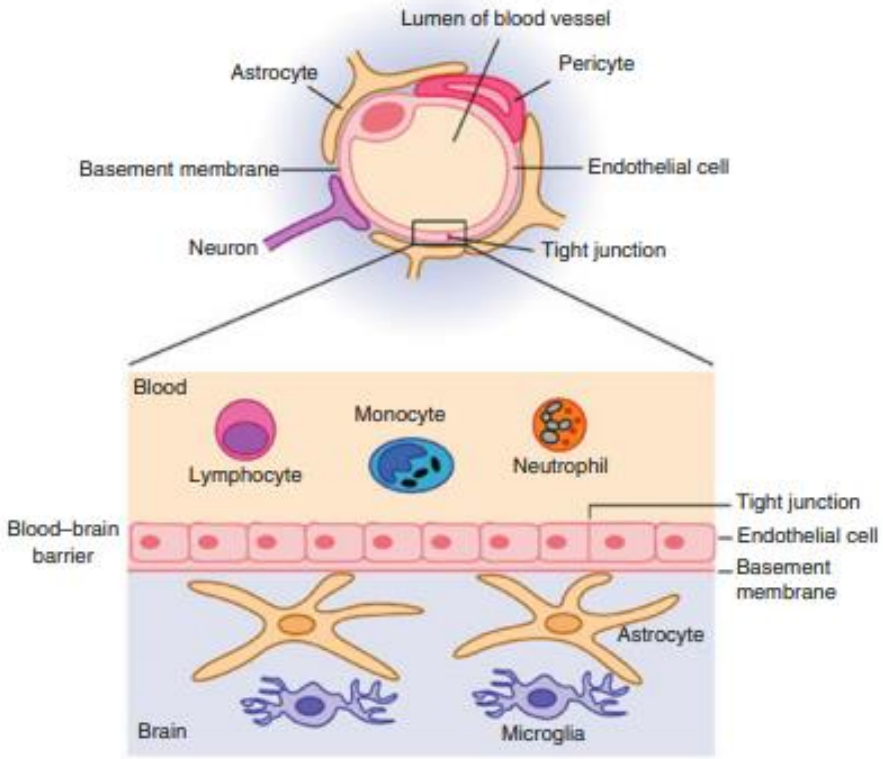

Figure 1: Structure of the blood-brain barrier; BBB is composed out of brain capillary ECs, astrocyte feet, pericytes, and ECM components; BBB is also part of the NVU that additionally comprises microglia, neurons, peripheral immune cells, and BM; Together all of these elements contribute to the development, maintenance, and function of the BBB [18].

1.4 Blood-brain barrier in disease

Disruption of the BBB may result in brain edema, altered signaling, infiltration with immune cells, or disruption of brain homeostasis. These consequences can lead to neuronal dysfunction followed by a neuronal degeneration. Breakdown of the BBB is common in several disorders of the CNS including stroke, traumatic brain injury (TBI), Alzheimer´s disease (AD), epilepsy, or multiple sclerosis [15].

During disease, internalization or down-regulation of the tight junctions between adjacent brain capillary ECs precedes BBB dysfunction. This further induces leakage for proteins and other agents from the cerebral blood vessels into the CNS. Modulation of the transcellular transport and transporters causes insufficient oxygen and nutrient supply for the brain. Equally, metabolites to be excluded from the brain with potentially harmful chemicals are not restricted from the brain invasion. Changing of the BBB structure and altered signaling accompanied with increased expression of leukocytes and microglia gives rise to inflammation, oxidative stress, and neuronal damage [14].

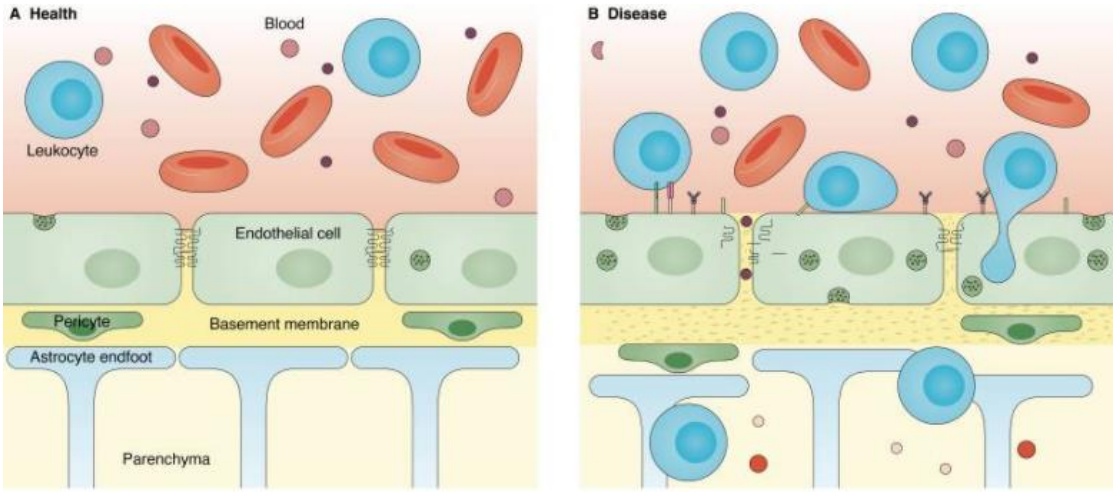

Figure 2: Blood-brain barrier in health and disease; A: In health, tight junctions are present together with low rates of transcytosis and no leukocyte adhesion; astrocytes and pericytes maintain the structure of BBB; B: During disease, tight junctions become leaky, transcytosis and leukocyte adhesion increase; BM disintegrates; astrocytes and pericytes surround and maintain BBB less tightly [19]; Creative Commons Attribution-Noncommercial-ShareAlike 4.0 International License.

1.4.1 Cerebral ischemia

Cerebral ischemia causes high rates of morbidity and mortality worldwide. It occurs from cessation of the blood flow leading to brain damage [20]. Stroke represents one form of cerebral ischemia that often results in a permanent disability [21]. Stroke is also the 2nd most common cause of dementia and the 4th most common cause of death in developed countries. During lifetime, one out of seven individuals suffers from stroke [22]. There are two main types of the stroke: ischemic and hemorrhagic. Ischemic stroke is more common as it affects 87% of the population while the hemorrhagic stroke affects only 13% of the population [23]. Ischemic stroke occurs when an area deprived of blood is formed due to the interruption of the blood flow by generation of a vascular thrombus. Hemorrhagic stroke causes a bleeding area in the

brain after rupture of the blood vessel due to aneurysms, weakening of the blood vessel walls, or arteriovenous malformations. As brain requires substantial amount of nutrients and oxygen for its proper function, stroke occurrence is a manifestation of potentially severe brain damage resulting in further neurological disorders. Current treatment possibilities for cerebral ischemia and stroke include use of anti-thrombolytics and hypothermia in hyperacute stages [24]. Even though these interventions seem to be successful in decreasing the burden of mortality rates and severe neuronal injury, long-term disabilities of post-stroke survivors are not avoided. This is the reason why it is essential to identify novel targets, biomarkers, and therapeutics in order to improve post-stroke neurological recovery [25].

TBI represents the most common cause of a long-term disability, chronic neurobehavioral sequelae [26]. TBI often provokes significant injury to the brain vasculature accompanied by ischemia, hypoxia, hemorrhage, BBB breakdown, hypoperfusion, and edema. As the research on TBI is mostly focused on neuroprotective strategies, it lacks development of efficient therapeutic agents for clinical treatment [27,28]. Equally, there are currently only very few biomarkers available such as S100B to track brain recovery or to determine an accurate TBI diagnosis [29,30].

1.5 Impact of epigenetics

Epigenetics focuses on modifications able of altering gene expression or cellular phenotype without changing the DNA sequence. In the last years, epigenetic mechanisms emerged as key regulators of the enhanced plasticity observed during repair processes after cerebral ischemia. Repair processes originate at the affected area and include angiogenesis, neurogenesis, oligodendrogenesis, synaptogenesis, and axonal outgrowth. Together they promote post-stroke neurological recovery. For instance, common epigenetic mechanisms include DNA methylation, histone modifications, and non-coding RNAs [25].

1.5.1 DNA methylation and cerebral ischemia

DNA methylation known also under the term “silencing epigenetic mark” occurs after covalent addition of a methyl group to form 5-methylcytosine. Its main role is to repress genes or to inhibit binding of a transcription factor. CpG sites cover 1% of human genome and are heavily methylated with exception of CpG islands. CpG island represents a DNA region of at least 500 base pairs with CG content greater than 55%. Unmethylated CpG islands are usually located in the close proximity of promoter regions which allows them to regulate gene expression. Methylation of CpG islands is catalyzed by family of writing enzymes, DNA methyltransferases

(Dnmts). In particular, Dnmt1 is the most abundant and active during DNA replication to copy the methylation pattern of paternal strain to the newly synthesized daughter strain. While *de novo* Dnmts, Dnmt3a and Dnmt3b, establish a novel methylation pattern [31]–[33]. *In vivo* studies with mice showed that in case of Dnmt1 knockout, the role of this essential DNA methylation enzyme is compensated by an increased expression of Dnmt3b [34]. Erasers are enzymes that remove or modify the methyl group. One of the known DNA demethylation mechanisms is mediated by the ten-eleven translocation (Tet) enzymes, namely Tet1, Tet2, and Tet3. Readers are enzymes that bind the methyl group and thus possess eventual control over the gene expression. Reading DNA methylation enzymes include family of MBD proteins, UHRF proteins, and zinc-finger proteins. Mechanism of DNA methylation is fundamental for mammalian development, and vital for silencing of retroviral elements, genomic imprinting, or chromosome X inactivation [31].

More recent evidence demonstrates that DNA methylation may occur also in non-CpG context (mCHG and mCHH, where H = A, C or T). For instance in human embryonic stem cells, non-CG methylation was identified in approximately 25% of all cytosines [35].

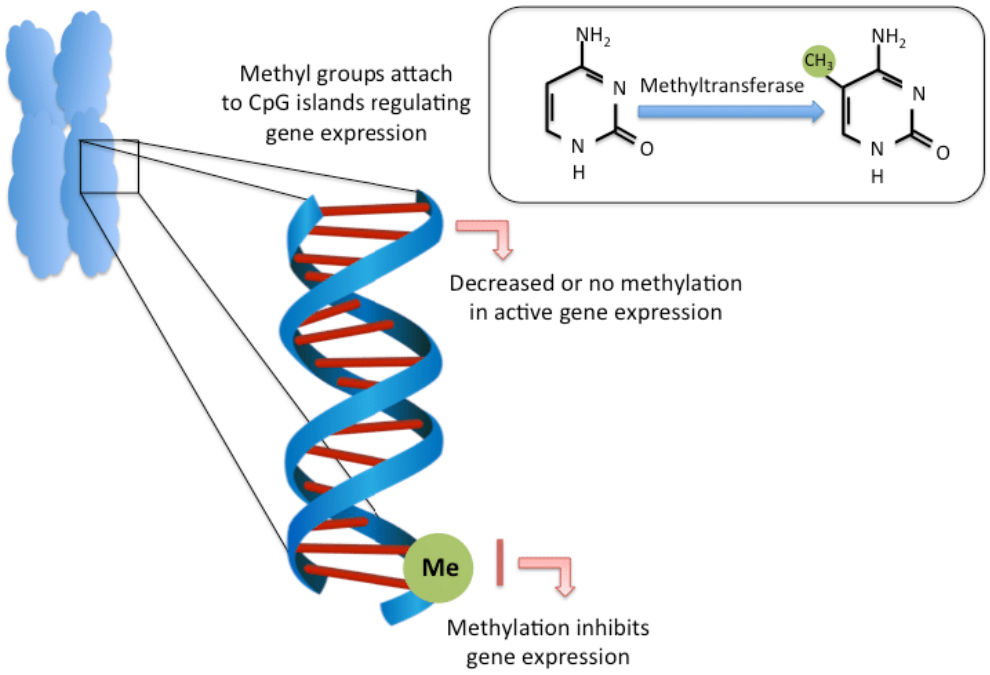

Figure 3: Epigenetic modulation by DNA methylation; DNA methylation is catalyzed by family of Dnmt enzymes and occurs by covalent addition of methyl group to cytosine to form 5-methylcytosine; DNA methylation of CpG island

results in inhibition of gene transcription and thus in silencing of gene expression [36]; Creative Commons Attribution-ShareAlike 4.0 International License.

After cerebral ischemic insult the consequence may be either increased or decreased DNA methylation of different genes [37]. Aberration of DNA methylation is associated with increased risk of stroke incidence. Pharmacological inhibition of Dnmts induces lower levels of DNA methylation. It is well established that in a rat model of middle cerebral artery occlusion (MCAO), Dnmt inhibition evokes reduction of infarct size and cerebral ischemic damage [38]. On the other hand, it was shown that DNA methylation is implicated in the regenerative processes such as adult neurogenesis and synaptic plasticity. For instance, reading DNA methylation protein methyl-CpG-binding protein 2 (MECP2) induces restorative mechanisms 24 hours after stroke in rat brain [25]. It was equally demonstrated that the expression of genes regulating apoptosis and angiogenesis including *Casp1*, *Casp9*, *VEGFa*, *Epo*, *Hif 1α* increases shortly after hypoxic-ischemic brain damage [37]. Another study showed that blood DNA hypomethylation is attributed to a high risk of stroke insult followed by death. This suggests that Dnmts act in a dual and sometimes contrary manner. To fully understand the role of DNA methylation during and after stroke, it is crucial to examine specific genes with changed methylation patterns and to observe the alteration of this pattern over specific timepoints [39].

1.6 *In vitro* models of the blood-brain barrier

In vitro models of the BBB are used to translate knowledge acquired through basic research into applied science. They help to tackle complex interactions and processes of the BBB as well as to better understand what happens at the BBB during disease. Moreover, *in vitro* BBB models are an indispensable tool for evaluation of drugs destined for the disorders of the CNS. Applied drugs need to be able to cross the BBB and reach their site of action [40]. Cell lines for *in vitro* studies come from different species origins including human, rodent, and porcine [41]. These are based on immortalized, tumor, or primary brain ECs. For instance, BBB *in vitro* models can be also derived from stem cells acquired from umbilical cord blood. Models based on human induced pluripotent stem cells (hiPSCs) have broader applicability and as first demonstrate *in vivo* like paracellular barrier properties [42].

1.6.1 Human cerebral ischemia *in vitro* blood-brain barrier model

Human cerebral ischemia *in vitro* BBB model can be set up with immortalized human brain endothelial cell line hCMEC/D3. hCMEC/D3 cell line represents the most commonly used human BBB model cell line. To better mimic physiological *in vivo* conditions of the BBB, cultivation of hCMEC/D3 cells is often performed in transwell models [43]. Transwell system

consists of a porous semi-permeable membrane that separates the vascular compartment (apical chamber) from the compartment of the brain parenchyma (basolateral chamber). Cell culture of hCMEC/D3 cells takes place on a filter membrane mimicking natural BBB environment [41]. hCMEC/D3 cells can be cultured on transwell inserts alone as mono-culture, or more cell lines can be added to them. When cultivating cells in co-culture or triple-culture conditions, astrocytes and pericytes are usually added [42]. Equally, co-culture with rat glioma cell line C6 is favourable as its contribution to the BBB breakdown was proven in a mouse as well as human ischemia models [42,43].

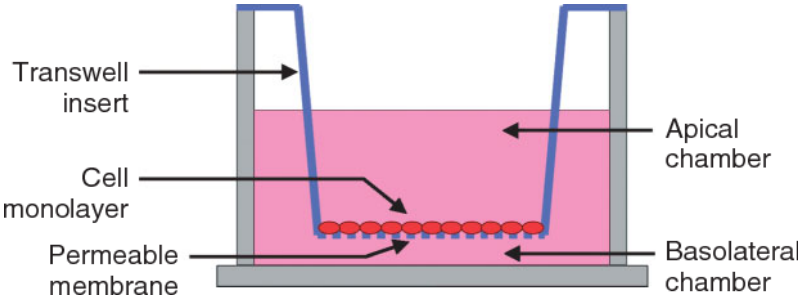

Figure 4: Cultivation of brain endothelial mono-culture (cell monolayer) in transwell model mimicking physiological BBB environment [45].

To help elucidate novel molecular mechanisms in stroke or TBI, cerebral ischemia can be stimulated using OGD treatment. OGD conditions together with nutrient deprivation induce BBB disruption accompanied with higher paracellular diffusion across the membrane [46]. BBB integrity can be then assessed by measurement of reduction in transepithelial/transendothelial electrical resistance (TEER) values [47]. For greater accuracy, transport studies involving paracellular markers such as fluorescein isothiocyanate-dextran (FITC-dextran) can be performed. This allows calculation of permeability coefficients which then serve for the evaluation of the BBB tightness [43].

1.7 Objectives

Cerebral ischemia is implicated in the development of numerous diseases of the CNS including stroke and TBI. In order to decrease its amplifying clinical and economic burden on the society, it is important to elucidate molecular mechanisms hidden behind this condition. During the course of cerebral ischemia, an array of targets is regulated at mRNA level as well as at protein level. Many of these targets play a role either in the induction of damage or regenerative processes at the BBB that follow after the insult. Recently, it was shown that one key regulation site is found at the level of DNA methylation. Principal aim of this project was to investigate

whether observed epigenetic changes at the DNA level are also translated via the mRNA level to the protein level. The hypothesis was stated as following: Epigenetic changes detected after cerebral ischemia at the DNA methylation level are translated further to the mRNA level, protein level, as well as to the functional level. Understanding regulation already at the DNA methylation level might lead to characterization of novel targets with potential use as biomarkers. For instance, these could be employed as biomarkers for cerebral ischemia induced BBB damage. In general, this study could reveal underlying processes causing brain injury, but also those that contribute to the neurological recovery of the BBB.

The research question posed was generated as follows:

How are the epigenetic changes detected at the DNA methylation level translated via the mRNA level to the protein level using a human cerebral ischemia in vitro model of the blood-brain barrier?

3. Materials and methods

List of materials used in this Master´s thesis:

Table 1: List of reagents with corresponding product number and company name

Material/Reagent	**Product number, company**
Ammonium persulfate (APS)	102029-95-8, Sigma-Aldrich
Bovine serum albumin (BSA)	9048-46-8, Sigma-Aldrich
Dimethyl sulfoxide (DMSO)	#SHBG7041V, Sigma-Aldrich
Glycine	A1067, Applichem
Immun-Blot® PVDF Membranes for Protein Blotting	#1620177, Biorad
Isopropanol	67-63-0, Merck
4x Laemmli sample buffer	#161-0747, Biorad
2-Mercaptoethanol	M3148-250ML, Sigma-Aldrich
Methanol	20864.320, VWR
Milk powder	A0830.0500, Applichem
Nuclease-free water	AM9937, Thermo Fisher Scientific
Page Ruler	26616, Thermo Fisher Scientific
PBS tablets	18912-014, Gibco
PhosStop tablets	4906837001, Sigma-Aldrich

PowerUp SybrGreen MasterMix	A2 5742, Applied Biosystems/Thermo Fisher Scientific
Quantitative polymerase chain reaction (qPCR) plate seals	4ti-0560, 4titude
RNase AWAY™ Decontamination Reagent	10328011, Thermo Fisher Scientific
ROTIPHORESE® Gel 40, 37.5:1	T802.2, Roth
Sodium dodecyl sulfate (SDS)	A1112.0500, Applichem
Tetramethylethylenediamine (TEMED)	#BCBR4495V, Sigma-Aldrich
Tris(Hydroxymethyl)aminomethane TRIS	#5429.3, Roth
Tween 20	#SLCC6910, Sigma-Aldrich
96-well qPCR plates	710877, Biozym Scientific

Table 2: List of primary antibodies with corresponding product number, company name, and dilution factor

Gene name	**Product number, company**	**Dilution factor for western blotting**
ß-Actin	A3854-200UL, Sigma-Aldrich	1:20.000, 1:5000
EVI-1 (MECOM)	ab124934, Abcam	1:400
MTA2	sc-55566, Santa Cruz Biotechnology	1:100
RBP-Jk	sc-271128, Santa Cruz Biotechnology	1:100

RUNX1	sc-365644, Santa Cruz Biotechnology	1:100
Tankyrase-1/2	sc-365897, Santa Cruz Biotechnology	1:100

Table 3: List of secondary antibodies with corresponding product number, company name, and dilution factor

Antibody name	**Product number, company**	**Dilution factor for western blotting**
Anti-Mouse IgG-POD	12015218001, Roche Diagnostics GmbH	1:400
Anti-Rabbit IgG-POD	12015218001, Roche Diagnostics GmbH	1:400

Some of the listed primer sequences in the table below possess different transcript variants. For instance for gene *EPC1*, abbreviation tr1-2/4 suggests that the used transcript has transcript variants 1 and 2 out of the total number of 4 transcript variants that are available. Furthermore, all of the listed primers were tested for the amplification efficiency.

Table 4: List of primary sequences with corresponding transcript variant used where applicable

Gene name	**Transcript**	**Direction**	**Sequence**
18SrRNA		FW	ATGGTTCCTTTGGTCGCTCG
		RV	GAGCTCACCGGGTTGGTTTT
B2M		FW	TGAGTGCTGTCTCCATGTTTGA
		RV	TCTGCTCCCCACCTCTAAGTTG
CLEC14A		FW	GACAGCTCCCGATCTCAGTTA
		RV	CCAAGTCGTCTAGGCAGTTAGG
EPC1	tr1-2/4	FW	TTCCCCAGAGCGGAGAGGTA

		RV	ATGATGTTCCGACTCCTCTTCCTT
EVI-1	tr1-8.10-17/17	FW	TATCCACGAAGAACGGCAATATC
		RV	CATGGAAACTTTTGGTGATCTGC
FGFR1	tr1-4,10-18/18	FW	CCCGTAGCTCCATATTGGACA
		RV	TTTGCCATTTTTCAACCAGCG
H4C3		FW	CGGCATAACATCCAGGGCAT
		RV	GGTCACGGCGTCTCGAATAA
MTA2	tr1-2/2	FW	ACTGGTGTTTGACCCCGTG
		RV	TCTACTAGGCGATCTGGGATCT
NLK	tr1/1	FW	CCAACCTCCACACATTGACTATT
		RV	ACTTTGACATGATCTGAGCTGAG
NOTCH3		FW	CCTGTGGCCCTCATGGTATC
		RV	CATGGGTTGGGGTCACAGTC
PPIA		FW	GTTCTTCGACATTGCCGTCG
		RV	TGAAGTCACCACCCTGACAC
RBPJ	tr1-5/5	FW	CTGACTCAGACAAGCGAAAGC
		RV	AGGAACACACCAATGTCATCAC
RUNX1	tr1-3/3	FW	CTGCCCATCGCTTTCAAGGT
		RV	GCCGAGTAGTTTTCATCATTGCC
SCARB1	tr1-6.8.9.13	FW	ACTTCTGGCATTCCGATCAGT
		RV	ACGAAGCGATAGGTGGGGAT
SGK1	tr1-4/5	FW	CATATTATGTCGGAGCGGAATGT
		RV	TGTCAGCAGTCTGGAAAGAGA
SGK1	tr1-5/5	FW	GATGACGGTGAAACCTGAGGC
		RV	CGATGAGAATTGCCACCATGC
TNKS2	tr1/1	FW	GCTGAGCCAACCATCCGAAAT
		RV	ACTTGCGTGGCAGTTGACA

Table 5: List of cell lines with corresponding product number and company name

Cell line name	**Product number, company**
Human endothelial cell line (hCMEC/D3)	SCC066, Merck Millipore
Rat glioma cell line (C6)	ATCC

Table 6: List of cell culture material with corresponding product number and company name

Material/Reagent	**Product number, company**
Ascorbic acid	A4544-25G, Sigma-Aldrich
Cell scraper	541070, Greiner
D-(+)-Glucose	G7528-1KG, Sigma-Aldrich
DMEM with glucose 4,5 g/L (DMEM +G)	D5796-1L, Sigma-Aldrich
DMEM with glucose 4,5 g/L (DMEM +G)	31966-021, Gibco®, Thermo Fisher Scientific
DMEM without glucose (DMEM -G)	11966 025, Gibco®, Thermo Fisher Scientific
DPBS	14190194, Gibco®
Dulbecco´s Phosphate Buffered Saline	D8662-500ML, Sigma-Aldrich
EBM-2 basal medium	CC 3156, Lonza

Fetal bovine serum (FBS)	F9665, lot:19A124, Sigma-Aldrich
Fibronectin bovine plasma	F1141-5MG, Sigma-Aldrich
Fluorescein isothiocyanate-dextran	FD4-250MG, Sigma-Aldrich
Gelatin	151067, Serva Electrophoresis GmbH
GSK-650394	SML0773-5MG, Sigma-Aldrich
hbFGF	F0291-25UG, Sigma-Aldrich
HEPES (1 M)	H0887, Sigma-Aldrich
Penicillin/Streptomycin (10 000 units of Penicillin/mL; 10 mg Streptomycin/mL)	P4333, Sigma-Aldrich
T-25 cell culture flasks	690160, Cellstar®, Greiner
T-75 cell culture flasks	658170, Cellstar®, Greiner
Trypsin + EDTA solution (0.05% trypsin/ 0.02% EDTA)	L2143, Biochrom GmbH
6-well plates	08-771-24, Fisher Scientific, Falcon™
24-well plates	BDL353504, Falcon®, Szabo-Scandic
24-well plates	662160, Cellstar®, Greiner
24-well plate inserts	662641, Greiner

Table 7: List of kits with corresponding product number and company name

Kit name	**Product number, company**
Biorad Clarity™ Western ECL Substrate	200 mL #1705060
High Capacity cDNA Reverse Transcription kit	4368814, Applied Biosystems/Thermo Fisher Scientific
Lumi-Light^{Plus} Western Blotting Kit (Mouse/Rabbit)	12015218001, Roche Diagnostics GmbH
Pierce™ BCA Protein Assay Kit	23225, Thermo Fisher Scientific

Table 8: List of equipment used with corresponding product number and company name where applicable

Material	**Product number, company**
Blotting chamber	Mini-PROTEAN Tetra Cell, Biorad
Centrifuge	Eppendorf
Heating block	Labnet
Hypoxia chamber	Biospherix
Imager	ChemiDOC, Biorad
Incubator	Thermo Fisher Scientific HERACell Vios 160i CO2 Incubator
Lamina Air Flow	Thermo Fisher Scientific
LightCycler 480	Roche Diagnostics GmbH

Multimode Plate Reader	Enspire®, PerkinElmer
Nanodrop	2000c, 10021778 0
Shaker Titramax 1000	Heidolph
Table plate spinner	89184-610, VWR PCR plate spinner
Thermocycler	Biometra

3.1 DNA methylation EPIC arrays for OGD treated hCMEC/D3 cells

DNA methylation EPIC arrays were done for OGD treated hCMEC/D3 brain ECs. Ilumina HumanMethylationEPIC BeadChip (EPIC) covers over 850.000 CpGs distributed genome-wide. It is used to investigate DNA methylation in human tissues [48].

3.1.1 Selection of targets

After DNA methylation EPIC array analysis, 39 most promising targets were selected based on the p-values and the highest plus delta b-values as well as the highest minus delta b-values. Link between each of these 39 targets and function in brain and disease, merely stroke and cerebral ischemia was investigated. Moreover, impact of these targets on ischemia reperfusion (I/R) in other organs such as kidney and heart was assessed.

To explain the meaning and use of b-values in DNA methylation array analysis, Beta-value method represents a method recommended by the manufacturer of Illumina Infinium HumanMethylation27 BeadChip microarrays for determination of DNA methylation levels. In fact, Beta-value is defined as the ratio of the methylated probe intensity and the overall intensity while the overall intensity depicts sum of methylated and unmethylated probe intensities. Range of the Beta-value varies from zero to one and can be interpreted as an approximation of the percentage of methylation. In general, a value of zero shows that no methylated molecules were measured, and thus all copies identified at the CpG site were unmethylated. On the other hand, value of one suggests that every copy of the CpG site in the sample was methylated [49].

3.1.2 Pathway analysis

The 39 chosen targets of OGD treated hCMEC/D3 brain ECs were examined more closely with Kegg Pathway Database: https://www.genome.jp/kegg/pathway.html. Here, it was studied in which pathways are the individual proteins active as well as connected to each other.

Search for common nodes and interactions was also performed through Gene Set Enrichment Analysis: https://www.gsea-msigdb.org/gsea/msigdb/index.jsp. Gene Set Enrichment Analysis uses a database of predefined gene sets that have been grouped together for instance by common biological pathway, regulation, or chromosomal location [50].

3.1.3 Protein interactions analysis

Protein interactions analysis was conducted with help of STRING database that constructs known and predicted protein-protein interaction networks: https://string-db.org/. Generation of multiple networks allowed thorough investigation of targets and their interactions.

3.2 Samples to be examined on mRNA level

Initial target data originated from OGD treated mono-cultures of hCMEC/D3 cells at the mRNA level. OGD treatment was performed with samples taken directly after five hours (5 h samples) and after an additional 19 hour phase of reoxygenation where glucose was added (24 h samples). This analysis involved many targets, encompassing also our 13 best targets.

These initial experiments were performed via collaboration of MSc student Sonja Peric and intern Iris Soliman.

3.2.1 hCMEC/D3 triple-culture samples

First RNA samples to be analyzed were samples from OGD experiments with two different timepoints, namely 5 h and 24 h time points. This OGD experiment was performed in two experimental weeks, providing two sets of samples. Every condition was done in triplicate per experiment. Samples chosen to be examined on mRNA level came from six different conditions and are summarized in the **Table 1**.

Table 9: Conditions of hCMEC/D3 triple-culture samples to be examined with 13 selected targets (per one experimental week)

No.	Condition
1	5 h OGD treated triple-culture in DMEM medium without glucose

2	5 h treated triple-culture in EBM-2 medium (control for medium exchange from EBM-2 to DMEM)
3	5 h treated triple-culture in DMEM medium with glucose (normoxic control)
4	24 h OGD treated triple-culture in DMEM medium without glucose
5	24 h treated triple-culture in EBM-2 medium (control for medium exchange from EBM-2 to DMEM)
6	24 h treated triple-culture in DMEM medium with glucose (normoxic control)

Different media were used during this experiment to exclude medium as the factor that may influence the results.

These samples were provided by MSc student Lisa Frühbauer from AIT.

3.2.2 hiPS-EC triple-culture samples

Brain ECs were obtained using differentiation protocol for hiPSCs as previously published [51]. Here, hiPS-EC cells were also co-cultured with astrocytes and pericytes. OGD experiment performed with these cells was similar to the one with hCMEC/D3 with slightly different timepoints, directly after 6 h OGD and after 18 hours reoxygenation with glucose addition after OGD. Individual samples were derived from two different differentiations and samples chosen to be examined at mRNA level came from four different conditions and are summarized in the **Table 2**.

Table 10: Conditions of hiPS-EC samples to be examined with 13 selected targets (per one differentiation)

No.	**Condition**
1	6 h OGD treated triple-culture
2	6 h treated triple-culture (normoxic control)
3	24 h OGD treated triple-culture
4	24 h treated triple-culture (normoxic control)

These samples were provided by PhD student Anna Gerhartl from AIT.

3.2.3 Human brain biopsy samples

In overall, samples from four patients from University Hospital Wurzburg in Germany were analyzed. There were always four samples per one patient. The reason for this is that the samples were taken separately from the whole brain and from brain capillaries. Also, samples

were taken separately from contusional and contralateral brain/capillaries. However, every individual suffered from TBI and succumbed to it after different amount of time. More detailed information about patient samples to be analyzed on the mRNA level can be found in the **Table 3**.

Table 11: Conditions of patient samples from the University Hospital Wurzburg to be examined with 13 selected targets [52]

Patient number and characteristics	**RNA sample type**
Patient 1 (TBI + 0 h survival)	Capillary – contusional
	Capillary – contralateral
	Brain – contusional
	Brain – contralateral
Patient 2 (TBI + 4 h survival)	Capillary – contusional
	Capillary - contralateral
	Brain – contusional
	Brain – contralateral
Patient 3 (TBI + 7 h survival)	Capillary – contusional
	Capillary – contralateral
	Brain – contusional
	Brain – contralateral
Patient 4 (TBI + 21 h survival)	Capillary – contusional
	Capillary – contralateral
	Brain – contusional
	Brain - contralateral

In addition, to estimate whether targets examined at mRNA level were upregulated or downregulated in the capillaries after the respective TBIs, ratios between corresponding x-fold values of the contralateral and contusional capillaries were determined. Calculation of ratios was performed by dividing x-fold value of contusional capillary by the x-fold value of contralateral capillary which was followed by division of the obtained value by the x-fold value of divided contusional brain by the x-fold value of the contralateral brain as summarized in the formula below:

$$Ratio = \frac{\left(\frac{x-fold\ value\ of\ the\ contusional\ capillary}{x-fold\ value\ of\ the\ contralateral\ capillary}\right)}{\left(\frac{x-fold\ value\ of\ the\ contusional\ brain}{x-fold\ value\ of\ the\ contralateral\ brain}\right)}$$

3.3 cDNA synthesis

Synthesis of DNA of a RNA template, via reverse transcription, results in complementary DNA (cDNA). Mastermix for cDNA synthesis was prepared based on the composition listed in the **Table 4**. Volume of 10 µL of mastermix was added per one PCR tube.

Table 12: Composition of mastermix for one cDNA reaction (for total volume of 20 µL of cDNA)

Reagent	**Volume [µL]**
Nuclease-free H_2O	3.2
10* RT Buffer	2
10* RT Random Primers	2
25* dNTP Mix (100 mM)	0.8
Multiscripe Reverse Transcriptase	1
RNAse Inhibitor	1
Total volume of mastermix	**10**

For RNA samples, calculated amount of RNA had to be diluted in nuclease-free water. For hCMEC/D3 and hiPS-EC triple-culture samples, the goal was to obtain 1000 ng of RNA in the total volume of 10 µL. While for Wurzburg patient samples comprising of capillary and total brain samples, 250 ng of RNA was prepared for one cDNA reaction in the total volume of 10 µL.

Respective volumes of nuclease-free water were added to each PCR tube containing mastermix. Diluted RNA was added to the PCR tubes with mastermix and nuclease-free water to achieve total cDNA reaction volume of 20 µL.

Samples were placed in the thermocycler and the cDNA synthesis run was initiated.

Table 13: Description of steps in the cDNA synthesis program

Step	**Temperature [°C]**	**Time [min]**	**Phase**
1	25	10	Primer annealing

2	37	120	Reverse transcription
3	85	5	Deactivation of enzymes, Termination of reactions
4	4	∞	Cooling

After the cDNA synthesis run was finished, concentrated cDNA was stored at -80°C.

3.4 Quantitative PCR

qPCR is used to detect, characterize, and quantify nucleic acids for numerous applications. Preparation of qPCR was initiated by primer dilutions. Forward and reverse primer for each target (100 pmol/µL) were diluted with nuclease-free water in ratio of 1:33. The same applied for housekeeping gene *18SrRNA*. This control gene was used for analysis of gene expression with every RNA sample. For Wurzburg patient samples, housekeeping genes *PPIA* and *B2M* were used additionally. In order to obtain 200 µL of diluted primer pair, 6.06 µL of forward primer and 6.06 µL pf reverse primer were added to 187.88 µL of nuclease-free water in a 1.5 mL microcentrifuge tube. Complete mastermix for qPCR reaction was prepared based on the composition in the **Table 6**.

Table 14: Mastermix composition for one qPCR reaction, respectively for one well of a 96-well plate

Reagent	**Volume [µL]**
Nuclease-free water	3.2
Primer pair 1:33	2.8
PowerUp SYBR Green Master Mix	10

16 µL of qPCR mastermix were pipetted per one well of a 96-well plate by reverse pipetting. Concentrated cDNA was diluted in ratio of 1:10 with nuclease-free water. 4 µL of diluted cDNA were added to wells, making total volume of 20 µL per one qPCR reaction. Due to reproducibility and statistical reasons, technical triplicates were measured for every sample. Finalized 96-well qPCR plate was sealed tightly with qPCR seal and spun down for 12 seconds in a table plate spinner. This was followed by the placement of the qPCR plate in the LightCycler 480. PowerUp SYBR Green program was initiated after that.

Table 15: qPCR run settings

Step	**Temperature [°C]**	**Time [sec]**	**Phase**

1	95	20	Holding stage
2	95	3	
3	60	30	
4			Repeat step 2 and 3 for 40 cycles
5	96	15	Melting curve stage
6	60	60	
7	95	15	

3.4.1 Analysis of qPCR data

Melting curves were examined directly in the LightCycler 480 after every single qPCR run. Obtained results were exported as an excel file. This excel file was then imported to the external LightCycler 480 Software, where it was analyzed, and the Ct values were exported into a new excel file. Noise ratios were set up manually for every target. More precisely, for every target measured on different plates, also when applying different experimental conditions, same noise ratio was used. In order to analyze samples, the relative quantification method was chosen. Relative quantification method measures the relative change in the mRNA expression levels. Here, the mRNA expression of a gene of interest is compared to an endogenous control such as *18SrRNA*, *PPIA*, or *B2M*. Endogenous controls are considered as constantly expressed reference genes. For analysis, firstly averages of the triplicates of the endogenous control were calculated. This was followed by the subtraction of the calculated averages from the copied Ct values which delivered ΔCt values. In the next step, it was necessary to obtain 2^-ΔCt value of each triplicate by exponentiation. Obtained values were used for calibration to the untreated control group. Final x-fold change values of the genes of interest were determined after dividing every respective 2^-ΔCt value by the respective normalized value. Control values were set to one in order to compare x-fold values of the investigated targets to the different experimental conditions.

The description of the qPCR data analysis complies with the Minimum Information for Publication of Quantitative Digital PCR experiments [53].

3.5 Cell culture

3.5.1 Cell lines

3.5.1.1 hCMEC/D3 cell line

Cell line hCMEC/D3 was derived from human temporal lobe microvessels isolated from tissue excised during surgery for control of epilepsy. In the first passage, cells were immortalized by the lentiviral vector transduction. hCMEC/D3 cells are widely used for the establishment of a human *in vitro* BBB model [54].

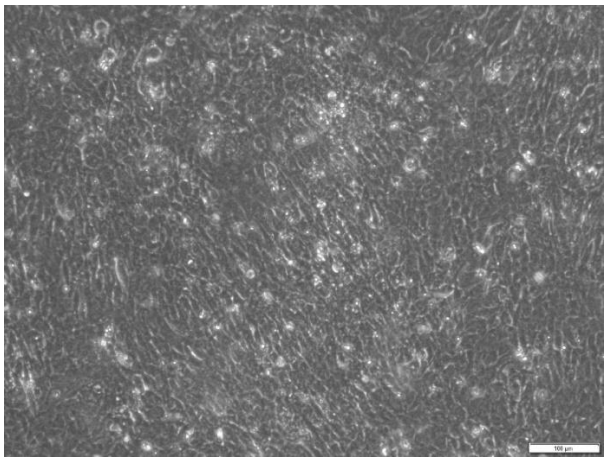

Figure 5: hCMEC/D3 cell line at passage 15 shows a spindle-shaped elongated morphology, similar to primary cultures of brain endothelial cells; bar size: 100 µm

3.5.1.2 Rat glioma cell line

The glial cell strain, C6, was cloned from a rat glial tumor after adult Wistar-Furth rats were repetitively exposed to the N-nitroso-N-methylurea. Rat glioma cell line is mostly used to study biological features of the brain tumors such as tumor growth, tumor invasion, angiogenesis, or BBB disruption [55].

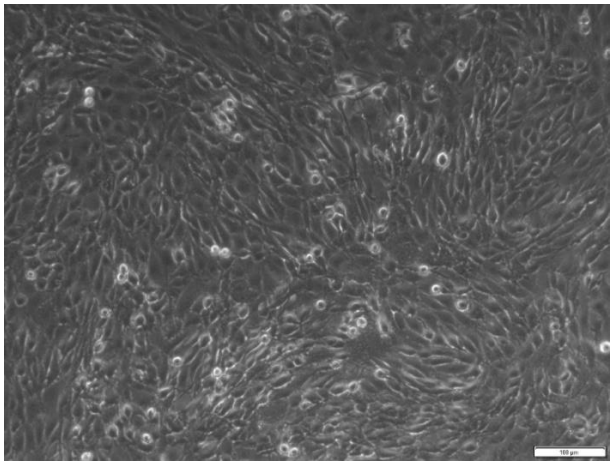

Figure 6: Rat glioma cell line C6 at passage 35; bar size: 100 µm

3.5.2 Cell culture maintenance

Media were firstly pre-warmed for 30 minutes at 37°C for every cell line. All cells were grown in T-25 and T-75 cell culture flasks at 37°C in an incubator with air O_2, 5% CO_2, and 95% humidity. hCMEC/D3 cell line was maintained in cell culture flasks coated with 0.5% gelatin solution. Cells were passaged once a week, using Trypsin/EDTA solution. They were subcultivated in a ratio of 1:3. Medium exchange was done three times per week. For cell cultivation, Endothelial Cell Growth Basal Medium-2 (EBM-2) was used. Medium was supplemented with 5% FBS, 1% Penicillin/Streptomycin, 5 µg/mL ascorbic acid, 10 mM HEPES, and 1 ng/mL of hbFGF. hbFGF was added to the medium only shortly before use. Detailed preparation of the EBM-2 medium for 52 mL of total volume can be seen in the **Table 8**.

Table 16: Composition of EBM-2 medium with 5% FBS and other supplements for total volume of 52 mL

Material	**Volume**
EBM-2	48 mL
FBS	2.65 mL
Penicillin/Streptomycin	531 µL
HEPES (stock solution concentration = 1M)	531 µL

Ascorbic acid (dissolved in EBM-2 medium; stock solution concentration = 1mg/mL)	265 µL
hbFGF (dissolved in 0.1% BSA solution; stock solution concentration = 200 ng/mL)	265 µL

Rat glioma cell line C6 was maintained in the cell culture flasks coated with 0.5% gelatin solution. For passaging, cells were split using Trypsin/EDTA solution once a week. They were passaged in a ratio of 1:20. Medium exchange was done three times per week. For cell cultivation, DMEM medium with high glucose content was used. It was supplemented with 10% FBS and 1% Penicillin/Streptomycin. Respectively, for one 50 mL centrifuge tube of DMEM medium with supplements were needed 40 mL of DMEM medium high in glucose, 4 mL of FBS, and 400 µL of Penicillin/Streptomycin.

3.5.3 Experimental set-up for OGD experiment with hCMEC/D3 cells

OGD experiment was repeated three times in total. It involved use of hCMEC/D3 cells from passages 21-23. Experimental setup for one experiment consisted of four 6-well plates. Apart from having one plate for 5 h OGD timepoint and another plate for 24 h OGD timepoint, additional medium controls for both timepoints with DMEM high in glucose were set.

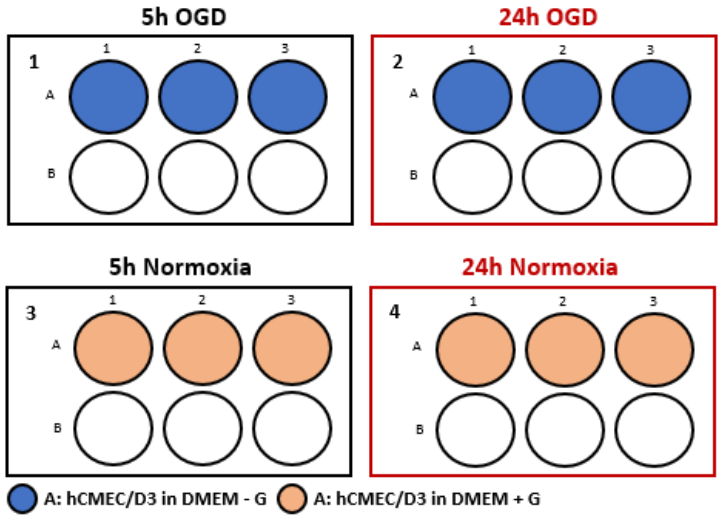

Figure 7: Experimental set-up of OGD experiment with hCMEC/D3 cells in 6-well plates. Medium was adapted to the desired condition. OGD plates 1-2 contained DMEM without glucose. 5 h OGD plate was incubated for 5 h under OGD conditions. Cells on plates 2 were fed with glucose and incubated for additional 19 hours. OGD treatment was performed at 0.1% O_2 and 5% CO_2 in hypoxia chamber from Biospherix. Control normoxia plates 3-

4 contained DMEM medium with high glucose content. Plates 1 and 3 were lysed for protein after 5 hours. Plates 2 and 4 were lysed for protein after 24 hours.

3.5.3.1 Seeding hCMEC/D3 cells into 6-well plates

Prior to cell seeding, 6-well plates were coated with 1 mL of 0.5% gelatin solution per well. Gelatin solution was distributed evenly across the whole surface area by gentle shaking of the plates. Plates coated with gelatin were left at room temperature for 30 minutes. Meanwhile, cells were checked under the microscope for confluency. For a T-75 flask, 10 minutes before the gelatin was ready, cells were washed twice with 5 mL of PBS. Trypsinization of cells was done with 2 mL of Trypsin/EDTA solution. Solution was distributed evenly across the T-75 flask and cells were put in the incubator at 37°C for 5 minutes. In case T-25 flask was used for the splitting of the hCMEC/D3 cells, cells were washed twice with 2 mL of PBS and detached with 700 µL of Trypsin/EDTA solution. After 5 minutes, flask was inspected under the microscope and tapped to see if the cells were detaching. To the T-75 flask with cells, 7 mL of EBM-2 medium were added. Again, in case a smaller T-25 flask was used, only 5.3 mL of EBM-2 were added to the flask with detached cells. To homogenize cells, the 9-point rule was used. Thus, medium was flushed over 9 separate points on the cell culture flask to dissociate adherent cells. Cells were pipetted up and down for 6 times in order to further resuspend them and to obtain a single cell suspension. Single cell suspension was then transferred into a 15 mL centrifuge tube. Cells were counted with a Thoma cell counting chamber. Total volume of 20 µL of the cell suspension was applied per one counting chamber. As hCMEC/D3 cells had to be seeded in a cell density of 80.000 cells/cm^2, appropriate calculation was done. Cell seeding suspension was prepared by taking the calculated amount of the cell suspension into a 50 mL centrifuge tube. Furthermore, 50 mL centrifuge tube was filled with EBM-2 medium and hbFGF according to the calculation. Gelatin solution was aspirated from the 6-well plates. Cell seeding suspension was resuspended to get a homogenized solution. 2 mL of cell seeding solution were added per one well of the 6-well plate. Plates were gently mixed in order to obtain an even distribution of the cell layer across the plates. Freshly seeded cells were incubated at 37°C. When seeding hCMEC/D3 cells into 6-well plates, always only three wells were used for the seeding. The residual three wells stayed empty to ease the working process during the experiment day. Media exchange was performed every 2 or 3 days with regular EBM-2 medium with 5% FCS.

3.5.3.2 OGD experiment with hCMEC/D3 cells in 6-well plates

OGD experiments were performed 6 days after seeding as by that time 100% confluency should have been reached. Glucose solution needed for 24 h OGD plates was prepared by weighting 1.116 g of glucose in a 50 mL centrifuge tube. DMEM medium without glucose was added to the tube until the total volume of 8 mL. Centrifuge tube was left on shakers until the glucose was completely dissolved. Glucose solution was then sterile filtered using a 0.22 µm filter and a 30 mL syringe. Final concentration of sterile glucose solution per one well was 4.5 g/L, thus of the same concentration as DMEM high glucose medium has. On the day of the experiment, cells were initially checked under the microscope for confluency and potential contamination. Wells containing cells were washed two times with 1 mL warm PBS. To the wells of two OGD plates, 3 mL of DMEM without glucose were added. Two petri dishes were filled with water and put inside OGD chamber without lids in order to establish appropriate conditions during OGD experiment. OGD chamber was turned on and set on O_2 concentration of 0.1% and CO_2 concentration of 5%. Two OGD plates were put in the OGD chamber, their lids taken off. Switches for gases were switched on, and the OGD experiment started. A timer was set. To the wells of the two normoxia plates, 3 mL of DMEM with high glucose content were added. Normoxia plates were placed in the incubator at 37°C. Another timer was set.

RIPA lysis buffer needed for protein lysis of samples and subsequent experiments was prepared based on the composition in the **Table 9** and **Table 10**.

Table 17: RIPA buffer composition

Reagent	**Volume**
1 M TRIS pH 8	25 mL
NaCl	4.38 g
693.5 mM SDS	2.5 mL
Na-Deoxycholate	2.5 g
NP-40 Substitute	5 mL
Double-distilled water	Fill up to 500 mL

Table 18: RIPA lysis buffer composition

Reagent	**Amount**
RIPA buffer	10 mL
Phosphatase Inhibitor (PhosSTOP)	1 tablet

Protease Inhibitor (PIC)	1 tablet

20 minutes before the 5 hours from the start of OGD experiment were over, 139.5 g/L glucose solution was warmed up in the water bath at 37°C. 15 mL aliquot of Dulbecco´s Phosphate Buffered Saline stored at 4°C was taken. Furthermore, it was kept on ice together with RIPA lysis buffer. After 5 hours of OGD treatment, hypoxia chamber was turned off. Lids were placed back on the 6-well plates and petri dishes containing water were removed. To the plate labelled as 24 h OGD plate, 100 µL of glucose solution were added. Glucose was evenly distributed over the wells. 24 h OGD plate was put into the normoxic 37°C incubator for 19 additional hours for recovery period. 24 h normoxia plate remained in the normoxic incubator at 37°C. However, 5 h normoxia plate was taken out from the incubator. Both 5 h OGD and 5 h normoxia plates were washed one time with 1 mL of the Dulbecco´s Phosphate Buffered Saline (D-PBS). After washing, the plates were placed on the ice. D-PBS was aspirated outside the laminar and cells were washed one more time. The residual buffered saline was aspirated using a 1000 µL pipette. 50 µL of RIPA lysis buffer were added quickly by drops across every well containing cells. Timer was set for 5 minutes. Meanwhile, 1.5 mL microcentrifuge tubes were labelled properly for storage of protein lysates. After 5 minutes, wells were scraped with help of cell scrapers. After one well was scraped, cell lysate was transferred to the microcentrifuge tube with help of a 200 µL pipette. When finished, protein lysates of cells from 5 h OGD experiment were stored at -80°C.

24 hours after starting the OGD experiment, 24 h OGD plate and 24 h normoxia plate were taken out of the incubator at 37°C. They were washed with D-PBS and lysed for protein the same way as the previous plates. Equally, protein lysates of cells from 24 h OGD experiment were stored at -80°C until further use.

3.6 Western blots

hCMEC/D3 protein lysates from OGD experiments were used for western blotting procedure. This widely used analytical technique serves for detection of specific proteins in the sample. Purpose of this experiment was to examine selected targets not only at mRNA level, but also at protein level.

Table 19: List of hCMEC/D3 samples from OGD experiments used for western blotting

Sample number	**Treatment**	**Date of finished OGD experiment**

1, 2, 3	5 h OGD DMEM – G	13.10.2020
4, 5, 6	5 h Normoxia DMEM + G	13.10.2020
7, 8, 9	5 h OGD DMEM – G + 19h Reoxygenation	14.10.2020
10, 11, 12	24 h Normoxia DMEM + G	14.10.2020
13, 14, 15	5 h OGD DMEM – G	20.10.2020
16, 17, 18	5 h Normoxia DMEM + G	20.10.2020
19, 20, 21	5 h OGD DMEM – G + 19h Reoxygenation	21.10.2020
22, 23, 24	24 h Normoxia DMEM + G	21.10.2020
25, 26, 27	5 h OGD DMEM – G	27.10.2020
28, 29, 30	5 h Normoxia DMEM + G	27.10.2020
31, 32, 33	5 h OGD DMEM – G + 19h Reoxygenation	28.10.2020
34, 35, 36	24 h Normoxia DMEM + G	28.10.2020

3.6.1 Protein quantification

Protein concentration of hCMEC/D3 samples lysed for protein was determined using a BCA protein assay kit. Pre-prepared BSA standard solution and RIPA buffer were used for preparation of samples for BSA standard curve in 1.5 mL centrifuge tubes following the manufacturer´s instructions. BSA was pipetted on the principle of serial dilutions. 25 µL of every standard curve sample were reversely pipetted on two plates in triplicates after proper vortexing and spinning down of the tubes. To the residual wells where protein lysate samples in triplicates were supposed to be added, 23 µL of RIPA buffer was reversely pipetted first. Every thawed protein sample was spun down and all the samples were centrifuged together for 3 minutes at 4°C and 2.000 g. This step was followed by pipetting 2 µL of protein samples from supernatants to the plates based on the working scheme. Next, the reagent was prepared. In general, for 10 mL of reagent solution, 10 mL of reagent A and 200 µL of reagent B are needed. Reagent solution had to be prepared only right before use. For this BCA protein assay, 40 mL of reagent solution were prepared by mixing 40 mL of reagent A and 800 µL of reagent B. Prepared solution was shortly vortexed and then 200 µL of solution per well were reversely pipetted into every well, including BSA standard samples wells. For this purpose, a multi-channel pipette was used. It was important to pipette up and down 3 to 4 times for every sample. Bubble formation was avoided. Plates were covered with aluminum foil and incubated for 30 minutes at 37°C. Afterwards, plates remained at room temperature for 5 more minutes to avoid results dependency in relation to higher the temperature. Using multi-mode reader,

absorbance of samples was measured at 562 nm. Data was collected and analyzed. Sample volume needed for 20 µg protein was determined for following western blotting.

3.6.2 Buffer preparation

List of buffers needed for western blotting procedure:

Table 20: Composition of Gel buffer for Resolving gel (1.5 M TRIS-HCl, pH 8.8)

Reagent	**Volume/Amount**
TRIS	92.5 g
Double-distilled water	350 mL
HCl 6N	Add until pH is adjusted to 8.8
Double-distilled water	Fill up to 500 mL

Table 21: Composition of Gel buffer for Stacking gel (0.5 M TRIS-HCl, pH 6.8)

Reagent	**Volume/Amount**
TRIS	30 g
Double-distilled water	300 mL
HCl 6 N	Add until pH is adjusted to 6.8
Double-distilled water	Fill up to 500 mL

Table 22: Composition of 10* Electrophoresis buffer

Reagent	**Volume/Amount**
TRIS	60.4 g
Glycine	376 g
SDS	20 g
Double-distilled water	Fill up to 2 L

10* Electrophoresis buffer needed to be diluted 1:10 before use to 1* Electrophoresis buffer with double-distilled water.

Table 23: Composition of Towbin transfer buffer

Reagent	**Volume/Amount**
TRIS	6.06 g
Glycine	28.83 g

Methanol	400 mL
10 % SDS solution	7.5 mL
Double-distilled water	Fill up to 2 L

Transfer buffer for blotting could be reused two to three times consecutively until it turned greenish.

Table 24: Composition of Harsh stripping buffer for one membrane

Reagent	**Volume/Amount**
10 % SDS solution	20 mL
Stacking gel buffer	12.5 mL
2-Mercaptoethanol	800 µL
Double-distilled water	67.5 mL

Table 25: Composition of PBST buffer

Reagent	**Volume/Amount**
PBS tablets	2 tablets
Tween	1 mL
Double-distilled water	1 L

Table 26: Composition of Blocking buffer (5% skimmed milk in PBST)

Reagent	**Amount**
Milk powder	10 g
PBST buffer	200 mL

Blocking buffer needed to be stirred with a magnet stirrer at least for 10 minutes. It was stored up to three days from the day of production at 4°C.

3.6.3 SDS-PAGE gel

SDS-PAGE represents a discontinuous electrophoretic system used to separate proteins on the basis of differences in their molecular weight. To produce SDS-PAGE gel, resolving gel and stacking gel had to be prepared. Gels were prepared separately in two 50 mL centrifuge

tubes based on the composition in the table below. TEMED and 10% APS were not added until the very end to both gels.

Table 27: Composition of Resolving gel (10%) and Stacking gel (5%) for SDS-PAGE

Substance	**Resolving gel (10%)**	**Stacking gel (5%)**
Double-distilled water	3.8 mL	2.975 mL
ROTIPHORESE gel (Acrylamide/Bis-acrylamide 30%)	3.4 mL	670 µL
Gel buffer	2.6 mL	1.25 mL
10% SDS	100 µL	50 µL
TEMED	10 µL	5 µL
10% APS	100 µL	50 µL

All parts belonging to the Biorad chamber for running of the SDS-PAGE gel were cleaned with distilled water and left to dry. Then, chamber for running of the gels was assembled. Glass plates were clamped and inserted into the casting stand. Leakproofness of the apparatus was checked beforehand with water. Under the hood, 10% APS and TEMED were added to the resolving gel. Tube with resolving gel was shaken gently by hand. Around 10 mL of the resolving gel were added in between the glass slides of the chamber. However, space of 2 cm from the upper side of the glasses was left empty for stacking gel. 1 mL of isopropanol was distributed evenly across the top of the resolving gel immediately. Resolving gel was left to run for the duration of 30 minutes.

After the resolving gel polymerized, isopropanol was poured out and space in between glasses rinsed with distilled water thoroughly. Glasses were also dried from the inside using a paper towel without touching the gel. 10% APS and TEMED were added to the stacking gel under the hood. Tube with stacking gel was shaken gently by hand. Around 2.5 mL of the stacking gel was added on top of the hardened resolving gel until it overflowed the glass. Paper towels were placed around the chamber and the comb with 15 slots was inserted in between the glasses. This step was done carefully, making sure that no bubbles were formed in the proximity of the comb slots. Stacking gel was left to run for 25 minutes.

3.6.3.1 Sample preparation and gel electrophoresis

Protein samples were put on ice to thaw them already during the polymerisation of the resolving gel. Centrifuge was cooled down shortly to 4°C. Thawed samples were centrifuged

for 3 minutes at 4°C and 2.000 g. Based on the analysis from the BCA protein assay, appropriate amounts of nuclease-free water were added to the empty 1.5 mL microcentrifuge tubes. Next, calculated amounts of protein samples were added. Pipette tip was changed every time in order to deliver equal protein concentration of samples in the end. Lastly, 10 µL of laemmli buffer were added per one microcentrifuge tube. Laemmli buffer was prepared by mixing 2-mercaptoethanol and 4* laemmli sample buffer in ratio of 1:10. Here it was again important to change the tip every time in order to deliver equal protein concentration. Total volume of every tube after addition of all components was 40 µL. All tubes containing nuclease-free water, protein sample, and laemmli buffer were shortly vortexed and spun down. Then, they were put on the heating block pre-heated to 95°C for the duration of 5 minutes. Tubes were shortly vortexed and spun down one more time. This step was followed by cooling of the samples on ice.

Polymerized SDS-PAGE gel was clamped inside the gel electrophoresis chamber, while the smaller glass was facing the inner side. In case that only one gel was supposed to be run, a dummy plate was included. Chamber was filled with 1* electrophoresis buffer until the corresponding line was reached. Comb was gently removed. Based on the prepared scheme for pipetting of the samples, 4 µL of marker or 30 µL of sample were added per slot made by the comb. If necessary, more electrophoresis buffer was added after pipetting of the samples was finished. The lid with the electrodes was connected to the gel electrophoresis chamber. The chamber was connected to the power supply. Gels were run firstly for 20 minutes at 80 V and then at 120 V until sufficient amount of the gels was run. Whole gel electrophoresis run required usually around 2 hours of time in total.

3.6.4 Blotting

Blotting was used to transfer proteins from the SDS-PAGE gel onto the hydrophilic polyvinylidene fluoride (PVDF) membrane. For one gel, two blotting filters and one PVDF membrane for protein blotting were prepared. Prepared filters and membranes were stored in the dark until further use. Fiber pads were pre-wetted in a fresh transfer buffer. Blotting filters were pre-wetted in the fresh transfer buffer only shortly before the assembly of the blotting sandwich. Membrane was activated for 60 seconds in methanol. Afterwards, it was put in the fresh transfer buffer. Gels from gel electrophoresis chamber were also placed in the fresh transfer buffer. Shorter glass was loosened from the longer glass and the stacking gel was removed from the resolving gel. Resolving gel was carefully detached from the glass plate and left in the buffer. Chamber from the gel electrophoresis run was cleaned with distilled water and dried with paper towels. Assembly of the blotting sandwich was performed based on the **Figure 8**.

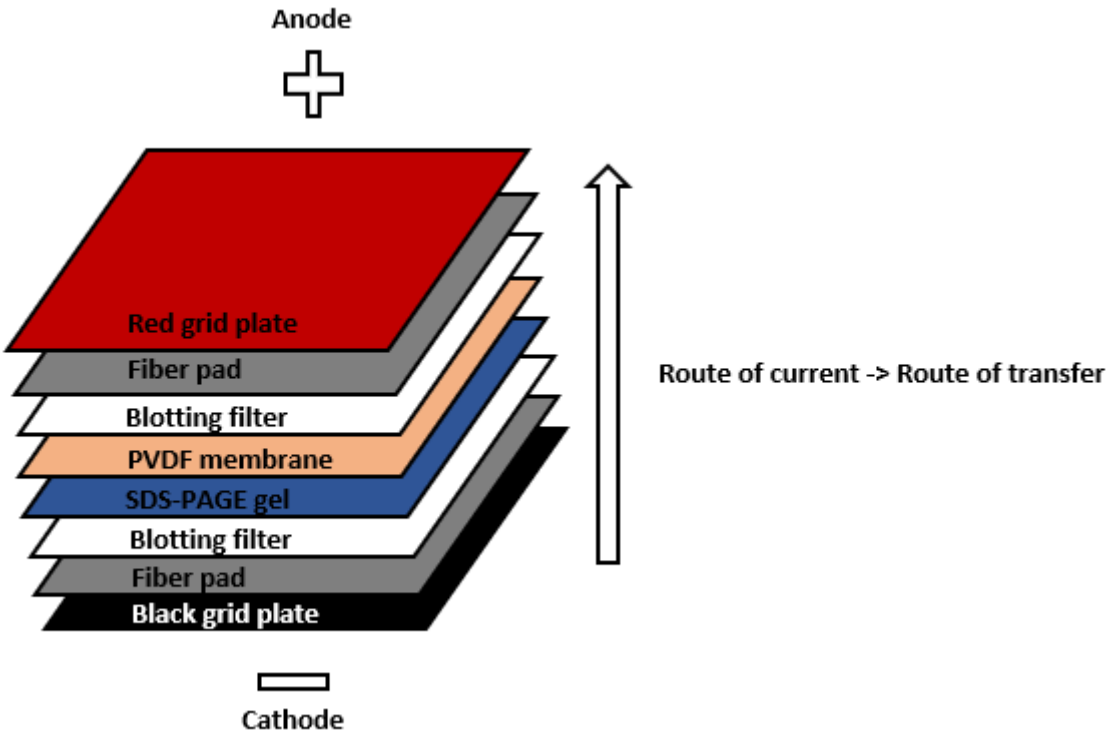

Figure 8: Blotting sandwich assembly

Blotting sandwich was placed to the chamber with the black side and the black grid plate in the direction of the electrodes and closer to the closure of the chamber lid. A magnet stirrer and 50 mL centrifuge tubes containing a cooling solution were added inside as well. Chamber was filled with transfer buffer used for pre-wetting of the materials for the assembly of the blot. The

rest of the chamber was filled with transfer buffer that could have been also already used before. Since the blotting process generates heat, the whole blotting apparatus was transferred to the cold room at 4°C. Overnight, blotting was run at 40 mA per one gel. During this time, contents of the chamber were mixed with the magnet stirrer.

3.6.5 Blocking step

Membrane was removed from the blotting sandwich with black side facing the bottom side. Next, membrane was placed in the blocking buffer and placed on the shaker for 2 hours at room temperature. This step prevented any non-specific proteins from binding to the membrane.

3.6.6 Incubation with primary antibody

Incubation with primary antibodies was done in 50 mL centrifuge tubes. Goal of the primary antibody was to bind the protein of interest. One tube was used for one antibody and one membrane. Every tube contained in minimum 3.5 mL of the blocking buffer. Exact amount of the blocking buffer needed was dependent on the size of the membrane. The bigger the membrane, the higher volume of the blocking buffer was used as the surface of the membrane had to be completely covered by the buffer. Primary antibody was then dissolved in the blocking buffer at the appropriate concentration. Antibody solution was turned around and the membrane was carefully inserted into the centrifuge tube using tweezers. It was essential to put the membrane inside in the correct position and without scratching it. Correct position involved insertion of the membrane with the bands facing the inside of the tube. Membranes with primary antibody dilutions were incubated overnight at 4°C on the rolling shaker.

3.6.7 Incubation with secondary antibody

Incubation with labelled secondary antibody enabled protein of interest to become detected as it was coupled with HRP enzyme. After incubation with the primary antibody, membrane was washed in PBST buffer for 25 minutes. During this time, PBST was changed two to three times. For handling of the membranes, tweezers were used. It was important to use only one pair of tweezers for one specific antibody. Incubation with the secondary antibody was done in the blocking buffer added to the 50 mL centrifuge tubes or to the ´boxes´. Based on the species of the primary antibody, either anti-mouse or anti-rabbit secondary antibody was dissolved in the blocking buffer in ratio of 1:400. Again, it was important to ensure that membrane was completely covered by the secondary antibody dilution. Antibody solution was turned around and the membrane was carefully inserted into the centrifuge tube or to the respective box. It

was essential to put the membrane inside in the correct position and without scratching it. Membranes with secondary antibody dilutions were incubated for 1 h at room temperature on the shaker.

3.6.8 Detection

After the incubation with the secondary antibody, membranes were washed in the PBST buffer for the duration of 25 minutes. During the washing step, PBST was changed two to three times. This was followed by HRP-ECL reaction. For this purpose, reagents from Lumi-light western blotting kit were used. When these solutions were used up, they were replaced by ECL reagents from Biorad. ECL reagent 1 and 2 had to be mixed only right before use in the ratio of 1:1. Then, solution was shaken by hand. Membrane was put on the glass slide and overlayed with ECL solution using 1000 µL pipette. Membrane was incubated in the dark for 5 minutes. Afterwards, membrane was transferred to the transparent foils used for imaging and furthermore to the black tray of the imager for western blots. Protein of interest was detected on the basis of the principle of chemiluminescence. Imager settings were set to ''Chemiluminescence'' and 'rapid auto exposure''. Image was recorded. Based on the resolution of this image, exposure time could be manually modified for next images. First image served also as a quality control to see if every band was present in the blot. To make the bands of the protein marker visible, an additional colorimetric image was taken. If more membranes were to be imaged in a row, residual membranes were left in the PBST buffer until imaging. For every membrane, a new HRP-ECL reaction was made. Transparent foils and the black tray as well as glass slide were cleaned after every membrane with 70% ethanol. After imaging, recorded pictures were exported as JPG files and saved until further analysis.

Membranes were stored in 50 mL centrifuge tubes filled with 50 mL of PBST buffer at 4°C. Due to conservation reasons, 1 mL of 0.02% sodium azide was added to every tube.

3.6.9 *ß-actin* antibody

As *ß-actin* primary antibody was already directly coupled to HRP enzyme, it required no further incubation with secondary antibody. Immediately after the blocking step, membrane was incubated in the blocking buffer with appropriate concentration of *ß-actin*. This incubation step took place at room temperature for the duration of 60 minutes on the shaker. Subsequently, membrane was washed with PBST buffer for 25 minutes. PBST buffer was changed during this time two to three times. HRP-ECL substrate reaction and membrane imaging followed.

3.6.10 Stripping

Stripping was done to remove primary and secondary antibodies from the western blot. Due to limited number of protein amounts of samples, membranes had to be often stripped so that different antibodies of similar molecular weights could have been detected on the same membranes. One membrane was stripped for maximum of three times. Stripping procedure started with the preparation of the stripping buffer in the 50 mL centrifuge tube. Last component to be added was 2-mercaptoethanol. Harsh stripping buffer was shaken gently by hand. Membrane was added inside and the whole tube was sealed tightly with a thick layer of parafilm. Centrifuge tube was then placed on the shaker pre-heated to 52°C for 45 minutes. Next, the sealed tube was opened under the hood and the membrane was transferred to double-distilled water. When the harsh stripping buffer cooled down, the tube was disposed safely. Membrane was washed in double-distilled water on the shaker for 15 minutes. In between, water was changed two times. Then, membrane was washed in PBST for 15 minutes with fresh PBST every five minutes. After this step, blocking procedure was done again followed by incubation with new antibodies.

3.6.11 Analysis of the blots

Blot images were examined by a densitometric analysis using Image lab software 5.2.1. This was preceded by optimum adjustment of the images using auto contrast function. In the analysis toolbox, the volume tools were chosen to manually quantify the bands of the proteins of interest. Every single band was framed with boxes of the same rectangular size. Obtained data was then exported as an excel file. Newly determined values of the proteins of interest were divided by the corresponding ß-actin values. Lastly, normalization of averages to the control group DMEM+G or to the control group DMEM-G took place. Additionally, normalization of averages to the 5h DMEM+G and DMEM-G conditions was performed in order to evaluate the effect of control and OGD treatment over time.

3.7 Experimental set-up for transwell OGD experiments with hCMEC/D3 cells and C6 cells

Next, OGD experiments involving hCMEC/D3 cells co-cultured with rat glioma C6 cells with different concentrations of *SGK1* inhibitor were performed. Both cell lines were cultured separately until the day of the experiment. This experiment was repeated six times in total. However, during the first two experiments different conditions were used. These experiments involved use of hCMEC/D3 cells from passages 15-20 and use of C6 cells from passages 32-

35. Experimental setup for one experiment consisted out of two 24-well plates. One plate was used for control normoxia conditions and one for stimulation of OGD conditions.

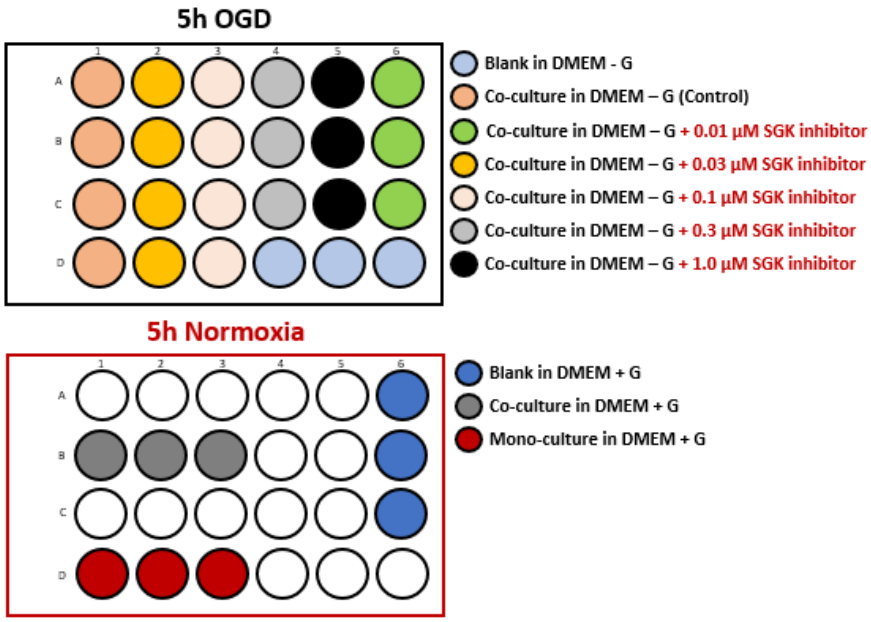

Figure 9: Experimental set-up of transwell OGD experiments with hCMEC/D3 cells and C6 cells. All inserts apart from blanks were seeded with hCMEC/D3 cells, mimicking the apical site (blood side). Cell culture inserts were placed in 24-well plates without cells (blue/blanks and red/mono-culture), or with C6 cells (other colors), which simulated the basolateral side (CNS side). Medium was adapted to the desired condition. OGD plate contained DMEM without glucose and was incubated for 5 h under OGD conditions. Control normoxia plate contained DMEM medium with high glucose content. OGD treatment was performed at 0.1% O_2 and 5% CO_2 in hypoxia chamber from Biospherix.

3.7.1 Seeding hCMEC/D3 cells on inserts into 24-well plates

Transwell inserts were placed into the 24-well plates using sterile tweezers based on the working scheme. Inserts had to keep same order and exact position on the plates. Prior to cell seeding, transwell inserts were coated with 100 µL of fibronectin/collagen IV solution. In order to prepare 10 mL of fibronectin/collagen IV solution, 15 mL centrifuge tube was taken. Inside, 5 mL of sterile double-distilled water, 4 mL of collagen IV (0.1 mg/mL dissolved in 0.25% acetic acid and PBS/fibronectin (1 mg/mL in PBS)), and 1 mL of fibronectin bovine plasma were mixed. Double-distilled water could be also replaced by PBS. Prepared solution was shaken by hand and ready to use. It was stored at 4°C and could be reused 3 times in total. After adding fibronectin/collagen IV solution, 24-well plates were incubated at least for 2 hours at 37°C.

hCMEC/D3 cells were split regularly in ratio of 1:3. Single cell suspension was kept in a 15 mL centrifuge tube. For inserts with filter area of 0.336 cm^2, 300 µL of medium were used for the apical compartment and 900 µL of medium were used for the basolateral compartment. Thus, a 50 mL centrifuge tube of calculated volume of EBM-2 medium needed was prepared. hbFGF was freshly added to the medium before use. Fibronectin/collagen IV solution was removed from the transwell inserts and stored until further use. Inserts were washed with PBS. More precisely, four to six drops of PBS using 5 mL serological pipette were added per one insert. PBS was poured out of the inserts into a petri dish. This step was done with help of tweezers. Washing step with PBS was repeated 3 times in overall. Residual PBS was removed from the inserts using a 1000 µL pipette. It was checked whether any PBS leaked into the basolateral compartment. In case that there was some PBS, it had to be removed in addition. The inserts remained to dry at room temperature for 10 minutes. Meanwhile, hCMEC/D3 cells were counted and seeding solution with them was prepared. Firstly, 900 µL of EBM-2 medium enriched with hbFGF were added to the basolateral compartment as well as 300 µL of medium were added to the apical compartment for blanks. Prepared cell seeding solution with 40.000 cells/cm^2 was mixed thoroughly with serological pipette. Next, 300 µL of cell suspension were added to the apical compartment per insert based on the working scheme. Correct position of inserts was adjusted, if needed. Both compartments were examined under the microscope. Cells were incubated at 37°C in the cell culture incubator.

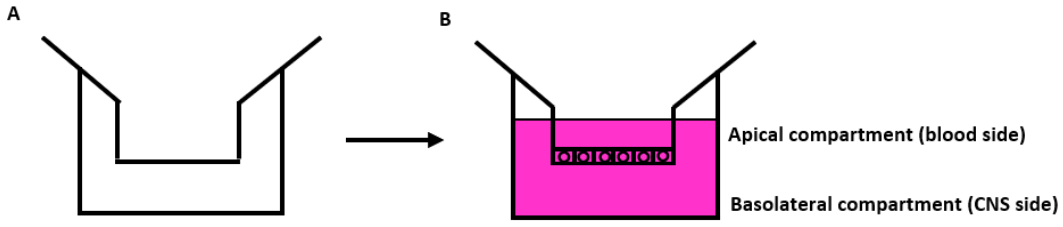

Figure 10: Seeding of hCMEC/D3 cells into transwell inserts; A: empty insert with filter area of 0.336 cm^2 placed in the well of a 24-well plate; B: 40.000 cells/cm^2 seeded in the apical compartment in volume of 300 µL with EBM-2 medium 5% FBS and fresh hbFGF; 900 µL of EBM-2 medium 5% FBS with fresh hbFGF in the basolateral compartment

3.7.2 Medium exchange of hCMEC/D3 cells on inserts

Medium exchange was done every two to three days. It was performed with EBM-2 medium with 5% FBS. However, last medium exchange before the experiment day was performed with only 0.25% FBS to minimize serum dependent results during OGD experiment as well as to increase tightness of the cell layers. Prior to the medium exchange, the inserts were transferred

to the exchange plates. Initial order and position of the inserts were kept. Basolateral compartment was investigated for any sign of contamination. Plate was tilted and medium was aspirated from the wells with an aspirator. 900 µL of freshly prepared EMB-2 medium with hbFGF were added per well into the basolateral compartment. Liquid in inserts was discarded to the petri dish using sterile tweezers. Meanwhile, inserts were placed back to their initial plates. Subsequently, 300 µL of newly prepared medium were added into the apical compartment. As the inserts contained cells, medium was added inside only carefully along the wall, without disturbing the intact cell layer. Cells were examined under the microscope and further incubated at 37°C.

Table 28: Composition of EBM-2 medium with 0.25% FBS and other supplements for total volume of 52 mL

Material	**Volume**
EBM-2	50.5 mL
FBS	130 µL
Penicillin/Streptomycin	531 µL
HEPES (stock solution concentration = 1 M)	531 µL
Ascorbic acid (dissolved in EBM-2 medium; stock solution concentration = 1 mg/mL)	265 µL
hbFGF (dissolved in 0.1% BSA solution; stock solution concentration = 200 ng/mL)	265 µL

3.7.3 Seeding rat glioma C6 cells into 24-well plates

Coating of 24-well plates was performed with 1 mL of 0.5% gelatin per well. Coated plates were left at room temperature for the duration of 30 minutes. Rat glioma C6 cells were split regularly in the ratio of 1:20. Obtained single cell suspension was used for the cell counting. Based on the calculation of the volume of cells needed, cell seeding solution was prepared. Gelatin solution was aspirated from the 24-well plates. Cell seeding solution consisted out of 20.000 cells/cm^2 and appropriate volume of DMEM high glucose medium enriched in 10% FBS and 1% Penicillin/Streptomycin. Using this solution, 1 mL of medium with cells was seeded per one well of a 24-well plate.

3.7.4 Transwell OGD experiment with hCMEC/D3 in co-culture with C6 cells

Prior to start of the experiment, it was crucial to examine the confluency of hCMEC/D3 cells and C6 cells. Especially, confluency of the C6 cells was a prerequisite for a successful experiment. Original 50 mM solution of the GSK-650394 inhibitor was dissolved in DMSO. Three additional GSK-650394 inhibitor dilutions in DMSO were prepared in 1.5 mL centrifuge tubes. All GSK-650394 inhibitor solutions were stored at 4°C, and when possible kept in dark. As DMSO freezes at 4°C, 15 minutes before the start of the experiment, GSK-650394 inhibitor solutions were left at room temperature to thaw.

Table 29: Preparation of GSK-650394 inhibitor dilutions in DMSO

GSK-650394 inhibitor solution in DMSO	**Dilution approach**
5 mM	90 µl of DMSO + 10 µl of 50 mM GSK-650394 inhibitor
0.5 mM	90 µl of DMSO + 10 µl of 5 mM GSK-650394 inhibitor
0.05 mM	90 µl of DMSO + 10 µl of 0.5 mM GSK-650394 inhibitor

Next, preparation of media stock solutions was performed. Beforehand, it was necessary to calculate how much of different stock solutions was needed based on the number of the wells. It was also important to count with additional volumes of media solutions needed for the later transport study as well as with some spare volume. One 50 mL centrifuge tube was filled with 16 mL of DMEM medium with high glucose content. Another 50 mL centrifuge tube was filled with 52 mL of DMEM medium without glucose. These two tubes were used only as the means of how to distribute media furthermore and to minimize the risk of contamination. Seven more 50 mL centrifuge tubes were taken and properly labelled. Here, one tube out of seven represented one medium stock condition out of seven conditions in total. DMEM media were pipetted into 7 tubes based on the volumes in the **Table 22**. It was essential to use 1000 µL pipette and do not touch the walls of the tube so that pipetting was precise and accurate. Sterile DMSO aliquot was shaken gently by hand. GSK-650394K inhibitor solutions were vortexed and spun down. Afterwards, appropriate volumes of DMSO and GSK-650394 inhibitor solutions were added to the media.

Table 30: Composition of stock media solutions with different concentrations of GSK-650394 inhibitor for OGD experiment

No.	Condition	DMEM - G	DMEM + G	DMSO	GSK-650394 inhibitor solution
1	DMEM + G	-	14.991 mL	9 µL	-
2	DMEM – G	14.991 mL	-	9 µL	-
3	DMEM – G + 0.01 µM GSK-650394 inhibitor	4.997 mL	-	2 µL	1 µL (0.05 mM)
4	DMEM – G + 0.03 µM GSK-650394 inhibitor	9.994 mL	-	-	6 µL (0.05 mM)
5	DMEM – G + 0.1 µM GSK-650394 inhibitor	9.994 mL	-	4 µL	2 µL (0.5 mM)
6	DMEM – G + 0.3 µM GSK-650394 inhibitor	4.997 mL	-	-	3 µL (0.5 mM)
7	DMEM – G + 1.0 µM GSK-650394 inhibitor	4.997 mL	-	2 µL	1 µL (5 mM)

In addition, 7 mL aliquot of DMEM medium with high glucose content was transferred into a 15 mL centrifuge tube. Into another tube, 7 mL aliquot of DMEM medium without glucose was added. Into another tube, 7 mL aliquot of sterile 70% ethanol was taken. These aliquots were used for later TEER measurements.

Medium was aspirated from the wells of C6 cells. Cells were washed with 1 mL of PBS per well. Liquid in inserts was discarded into a petri dish using sterile tweezers. Empty inserts were transferred into an exchange plate. Inserts were washed with 450 µL using a 5 mL serological pipette. PBS was aspirated from the wells of C6 cells. Cells were washed one more time with 1 mL of PBS. PBS in inserts was discarded into a petri dish, and hCMEC/D3 cells on inserts were washed one more time with 450 µL of PBS. All tubes with stock solutions were vortexed. PBS was aspirated from the wells of C6 cells. Based on the **Figure 9**, 900 µL of different media solutions were added into the corresponding wells of the 24-well plates in the basolateral compartment. PBS from inserts was discarded into the petri dish. Transwell inserts were transferred to the plates of C6 cells. Any residual PBS in inserts was removed using a 1000 µL pipette. Again, based on the working scheme in the **Figure 9**, 300 µL of different

media solutions were added into the apical compartment of the 24-well plates. Thus, until then separately cultivated hCMEC/D3 cells and C6 cells were merged together.

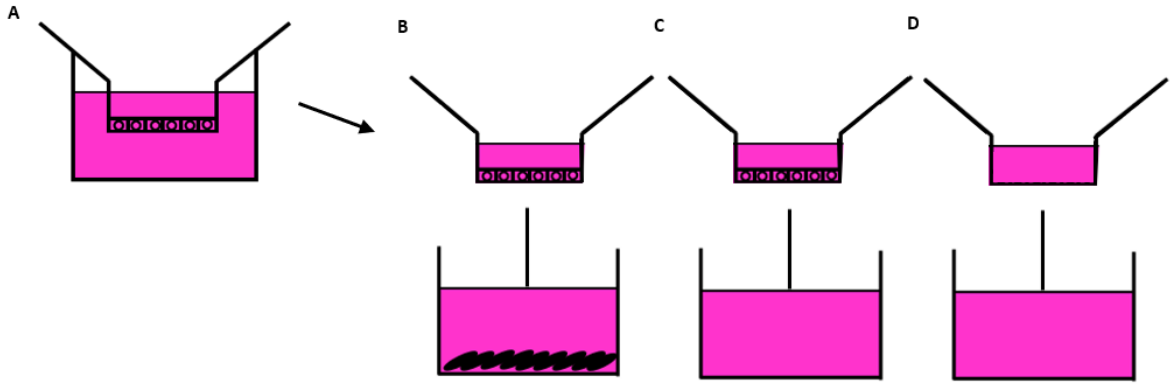

Figure 11: Three different cell cultivation set-ups during transwell OGD experiment; A: Prior to experiment, 40.000 cells/cm^2 seeded in the apical compartment in volume of 300 µL with EBM-2 medium 0.25% FBS; 900 µL of EBM-2 medium 0.25% FBS in the basolateral compartment; B: Co-culture of hCEMC/D3 cells and C6 cells; C: Mono-culture of hCMEC/D3 cells; D: Blank control

Normoxia plate and OGD plate remained at room temperature in the laminar until a TEER measurement was initiated, leaving the cells to adapt to the medium exchange. TEER values offer information about the integrity of the cellular barriers such as of the hCMEC/D3 cells in the blood-brain barrier model [56]. TEER device was wiped with 70% ethanol, turned on, and set to measure resistance. Electrode connected to the TEER device was put in the 7 mL aliquot of sterile 70% ethanol for 2 minutes. Then, the TEER device was transferred to the 7 mL aliquot of DMEM medium with high glucose due to proper calibration for the duration of 40 minutes. TEER values in the normoxia plate were measured, starting from the blanks. While measuring the TEER values, electrode was hold vertically and measurement of every insert was done at the same site in the same position of the well. Measured TEER values were written down. After all the wells in the normoxia plate were measured, the electrode was transferred to the 7 mL aliquot of DMEM medium without glucose for 2 minutes. Next, TEER values in the OGD plate were recorded, starting from the blanks, control wells, and then media conditions with the lowest concentration of the *SGK*1 inhibitor. Measured TEER values were written down. After all the wells in the OGD plate were measured, the electrode was transferred to the 7 mL aliquot of 70% sterile ethanol for 2 minutes. The TEER device was turned off. Stock media solutions remained in the laminar until further use.

Both 24-well plates were examined under the microscope mostly to check the cell layer of rat glioma C6 cells in the basolateral compartment. Normoxia plate was incubated for 5 hours at 37°C. OGD plate was placed in the OGD chamber. Settings of the hypoxia chamber were set to O_2 of 0.1% and CO_2 of 5%. OGD experiment was initiated and a timer for 5 hours was set.

After 5 hour OGD timepoint, normoxia plate and OGD plate were placed back to the cell culture laminar. Plates stayed at room temperature until TEER measurement was initiated, leaving the cells to adapt to the temperature shift. Measurement of TEER values was performed exactly the same way as before the OGD treatment. TEER values were measured before and after the OGD treatment in order to observe the effect of OGD on the cells. This effect also needed to be compared with control normoxia values.

3.7.5 Transport study with fluorescein isothiocyanate-dextran

Fluorescein isothiocyanate-dextran also known as FITC-dextran or FD4 has fluorescent properties and is often used in microcirculation and cell permeability research. Purpose of the transport study with dextran was to investigate how much dextran permeates into the basolateral compartment after the 5 hour OGD experiment. Simply, the more fluorescence permeated the barrier, the more was the barrier disrupted after the OGD treatment. FITC-dextran was added into the initial stock media solutions in such volumes that in the end, its concentration was equal in every tube. Furthermore, dextran was added in the ratio of 1:100 to reach 10 µM as it was a 1 mM solution. All seven tubes were vortexed thoroughly. Medium from the inserts of both 24-well plates was aspirated from the blanks to the highest concentration of *SGK1* inhibitor, using the 1000 µL pipette. Pipette tip was changed only after one plate. Again, 300 µL of respective media stock solutions was added into the apical compartment of the wells. It was crucial that no drop got to the basolateral compartment. Both plates were incubated at 37°C for 1 hour. After 60 minutes of the transport study, inserts were quickly transferred with help of tweezers into the exchange plates. This step was initiated with the transfer of blanks as those leaked the fastest. Using the 1000 µL pipette, the maximum volume of the apical samples (300 µL) was taken to the 1.5 mL centrifuge tubes. Again, aspiration started from blanks until the inserts with the highest concentrations of the SGK inhibitor were reached. One 1.5 mL centrifuge tube was labelled for every apical and basolateral sample. Then, 1 mL of every basolateral sample was transferred to the 1.5 mL centrifuge tubes. Furthermore, 1 mL of every media stock solution was collected as well as that of the blank media (7 mL aliquots of DMEM media used for the calibration of the TEER electrode). Collected samples were covered with aluminum foil as fluorescent samples are

light sensitive. Samples were stored at 4°C in the maximum for the duration of 2 days. Until then, fluorescence measurement of the collected samples was performed.

Samples were tapped by finger for proper mixing of their contents and spun down. 100 µL of every sample was pipetted in appropriate black 96-wellplates in triplicates. Blank media and stock media solutions needed to be added to every plate used. Apical samples were pipetted only in duplicates due to the restricted volume availability. Plates were covered with the aluminum foil as soon as the pipetting of samples was finished. Fluorescence of the samples was measured at excitation wavelength of 488 nm and emission wavelength of 520 nm. Obtained results were exported as an excel file and saved until further analysis.

3.7.6 Establishment of *SGK1* inhibitor concentrations

To establish experimental set-up for the transwell OGD experiments with hCMEC/D3 cells in co-culture with C6 cells, different concentrations of the *SGK1* inhibitor were tested initially. In the first experiment, serum content in the EBM-2 medium was not decreased to 0.25% FBS. Thus, regular EBM-2 medium with 5% FBS was used during medium exchange until the day of the experiment. In addition, OGD treatment was stimulated at O_2 levels of 1% and CO_2 levels of 5%.

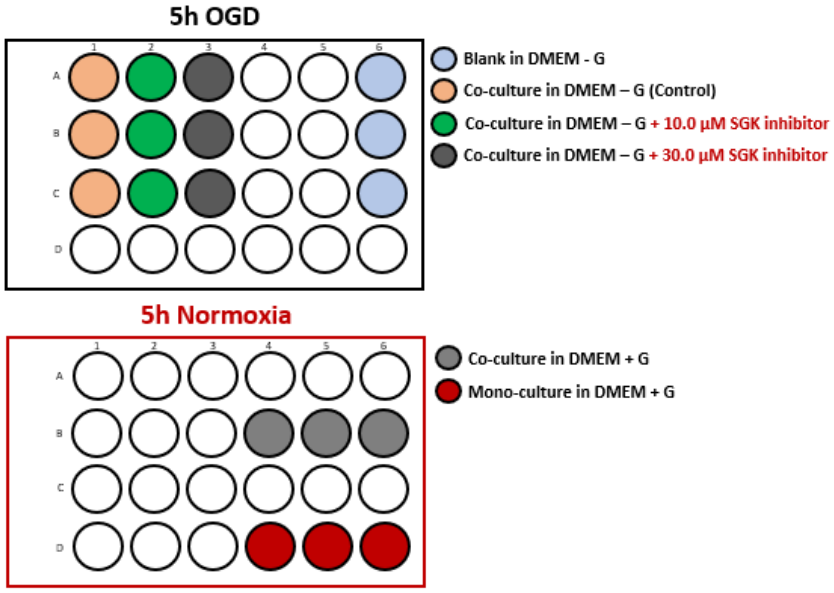

Figure 12: Establishment of *SGK1* inhibitor concentrations – First experiment

In the second experiment, serum content during medium exchange was already changed to 0.25% FBS in the EBM-2 medium one day prior to the experiment. OGD treatment was performed at O_2 concentration of 0.1% and CO_2 concentration of 5%. Concentrations of the *SGK1* inhibitor applied were lower in comparison to the first experiment.

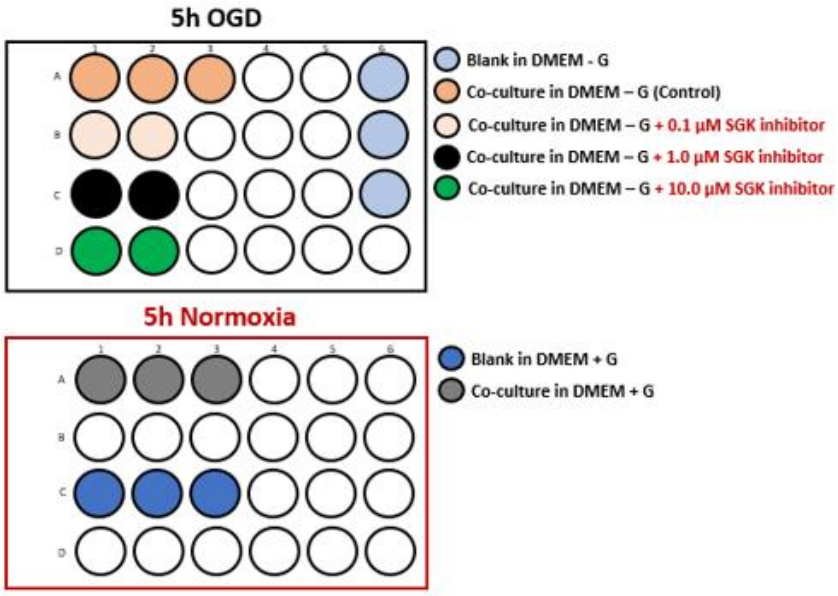

Figure 13: Establishment of *SGK1* inhibitor concentrations – Second experiment

3.7.7 Analysis of the fluorescence data and TEER measurement values

With fluorescence data, calculations in excel were performed, leading to the calculation of the permeability coefficients [µm/min] of all samples taken from the basolateral side of the transwell model. To determine permeability coefficients, firstly mean fluorescence values of the fluorescence data per condition were calculated. From these, respective blank values were subtracted. In the next step passage [%] numbers were obtained by multiplying fluorescence value of every sample by 100, and then by dividing it with the fluorescence value of corresponding stock solution. This step was followed by the calculation of cleared volume [µL]. Cleared volume was determined by multiplying fluorescence value of every sample by 200, and then by dividing it with the fluorescence value of corresponding stock solution. Cleared volume together with time [min] of the respective transport study represented two factors used for plotting of the standard curves. From standard curves, linear regressions from all basolateral samples were obtained by determination of respective trendline equations. Slopes after linear regressions analysis and surface area [cm^2] of inserts used for transwell experiments were further used for calculation of PEall (permeability coefficient through the

membrane insert and cell layer) and PEblank (permeability coefficient without cell layer). From this, PEcell (permeability coefficient only through the cell layer) was calculated. Permeability coefficients [µm/min] were in the end determined by multiplying respective PEcell values by factor of 10 000.

Values obtained from the TEER measurement were analyzed by firstly subtracting the blank averages from individual samples. This step was performed separately for values from TEER measurement before and after the OGD treatment. Then, the separate values were merged by calculating percentage values of TEER change during the course of every individual experiment.

3.8 Statistics

Results of mRNA expression, protein expression, and cell culture experiments were analyzed with GraphPad Prism Software 9.1.2. For calculation of mean differences between the two groups, student t-test was used. For calculation of mean differences between more than two groups, One-Way ANOVA was used followed by a Dunnett´s post-hoc test. The level of significance was set to $p < 0.05$. In addition, data was checked for normal distribution with Shapiro-Wilk test where applicable due to sample size limitations and scanned for outliers with use of Grubbs´s test.

4. Results

4.1 Selection of 13 regulated targets of cerebral ischemia

OGD treatment of hCMEC/D3 mono-culture was followed by the DNA methylation EPIC arrays which were performed by MSc student Sonja Peric at AIT. More precisely, this DNA methylation technique allowed to detect the total DNA methylation level of over 850.000 DNA methylation sites at single nucleotide resolution based on bisulfide conversion, where unmethylated cytosines were converted to uracils while methylated cytosines remained unchanged. The level of total methylation was then determined from the loci, which were beforehand interrogated by the array technology, by calculating the ratio of the fluorescent signals from the methylated vs. unmethylated sites. From the outcome of the DNA methylation array analysis technique, the 39 most promising targets were selected based on the p-values, the highest delta b-values, and the bumphunt analysis. These targets were tested at mRNA level firstly in hCMEC/D3 mono-culture after the OGD treatment by intern Iris Soliman at AIT.

Table 31: Most promising regulated targets based on the DNA methylation EPIC array analysis of the OGD treated hCMEC/D3 mono-culture

No.	Name of the target	No.	Name of the target	No.	Name of the target
1	*MECOM*	14	*ZNF365*	27	*SMG6*
2	*RUNX1*	15	*MAN1A1*	28	*CCT6A*
3	*FRMD4A*	16	*GFRA2*	29	*RBMS3*
4	*SGK1*	17	*MLIP*	30	*FRMPD2*
5	*FGFR1*	18	*FAM13C*	31	*EPC1*
6	*FOXK1*	19	*RBM47*	32	*ATP6V1G3*
7	*RO60*	20	*MTA2*	33	*NOTCH3*
8	*SCARB1*	21	*ACAA2*	34	*SESN3*
9	*TP73*	22	*TNKS2*	35	*AK2*
10	*CCDC30*	23	*TM9SF3*	36	*CLEC14A*
11	*CHST11*	24	*NFIC*	37	*RNF168*
12	*RBPJ*	25	*ADORA2B*	38	*H4C3*
13	*UBE2E1*	26	*NLK*	39	*CENPF*

The next step required another selection of the targets for further analysis. Function and expression of each single target of the 39 targets were investigated in relation to the brain and to cerebral ischemia, stroke, as well as I/R in other organs such as kidney and heart. The aim of the analysis with Kegg Pathway Database was to look for the active target proteins in different signaling cascades and thus to identify potential target clustering.

Subsequently, search for clustering and evidence of regulation continued using Gene Set Enrichment Analysis. This database is focused on grouping of specific proteins based on the common characteristics between them. Gene Set Enrichment Analysis of 39 targets set to top 20 gene sets generated a matrix as output. Its outcome then served as a guide in protein-protein interactions analysis performed by STRING tool. STRING database is used to generate known as well as predicted protein-protein interaction networks. Using STRING database, interactions between the 39 targets were examined (**Figure 14**). Analysis using STRING database was done by simple search of interactions between multiple proteins. Thus, proteins to be investigated were just listed by their protein names and searched in the database. In addition, interactions of 39 targets with ABC transporter protein family, CDH5, FOXO3, MECP2, and tight junction proteins were examined (**Figure 15-19**). Also, predicted interactions between FOXO3, SGK1, and NLK were confirmed (**Figure 20**). Observation of the interactions with additional proteins was performed due to their close relationship with the BBB. For instance, ABC transporter proteins at the BBB contribute to the efflux of small compounds and xenobiotics from the CNS into the bloodstream [57]. CDH5 belongs to the adherens junctions that represent a prerequisite for the tight junctions which are very relevant at the BBB [58]. For the proper function of the CNS, protein levels of MECP2 need to be tightly regulated as any aberration in their levels may lead to severe neuronal dysfunction. However, MECP2 protein is mostly known for primary cause of Rett syndrome which occurs due to loss of function mutations in the *MECP2* gene [59]. Tight junction proteins included in the analysis together with 39 hCMEC/D3 targets were in particular ZO-1, CDH1 and CDH5, as well as CLDN1-23. All these proteins play a crucial role in the molecular structure of the tight junctions and are thus fundamental for the proper function of the BBB.

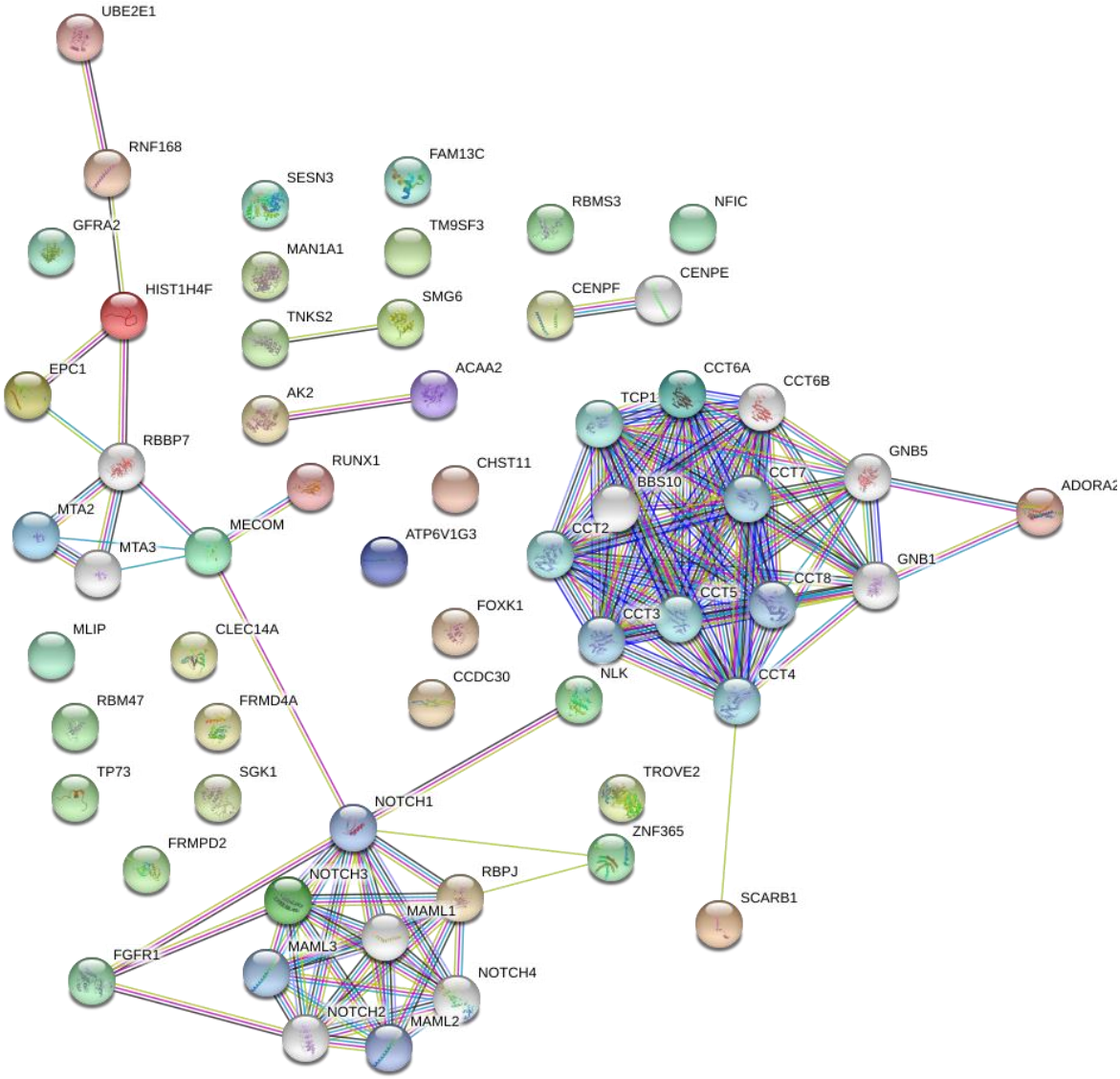

Figure 14: Interactions between 39 hCMEC/D3 targets by STRING analysis

As can be observed in the **Figure 15** below, ABC transporters ABCB1, ABCC1-4, and ABCG2 are linked to NLK, FGFR1, RBPJ, NOTCH3, and MECOM (EVI-1) via NOTCH1. The present linkage of ABC transporters with EVI-1 further continues to RUNX1, MTA2, and EPC1.

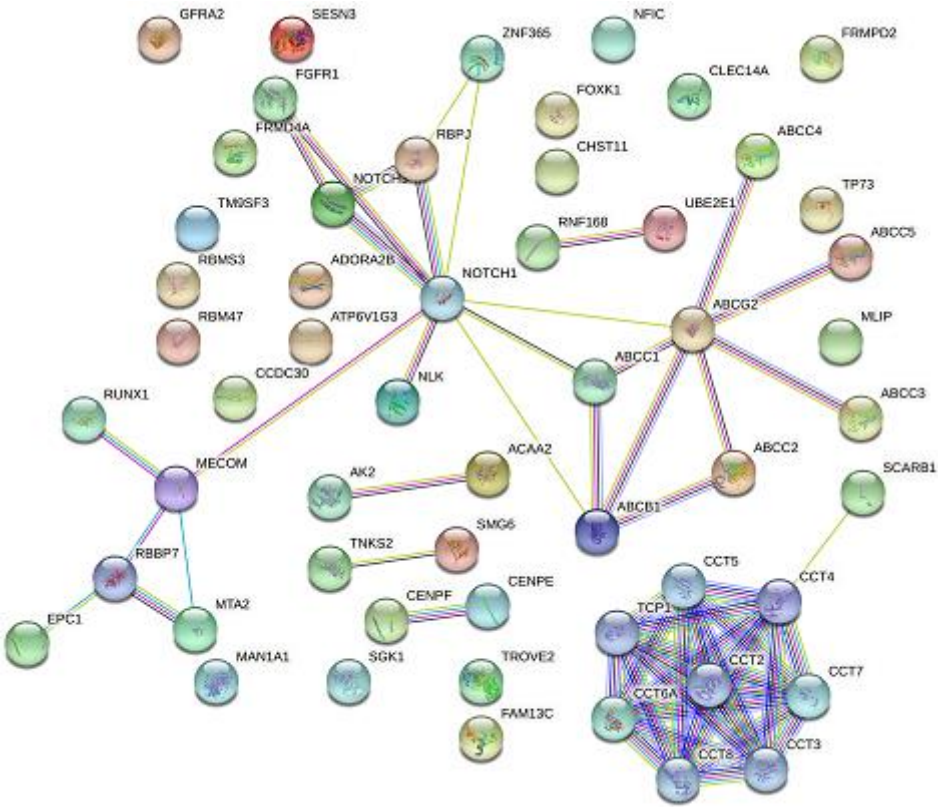

Figure 15: Interactions between 39 hCMEC/D3 targets and ABC transporters ABCB1, ABCG2, ABCC1, ABCC2, ABCC3, ABCC4, and ABCC5 by STRING analysis

Investigation of interactions between the 39 targets and CDH5 by STRING analysis revealed linkage of CDH5 to CLEC14A, NOTCH3 via NOTCH1, as well as to the targets RBPJ and NLK (**Figure 16**).

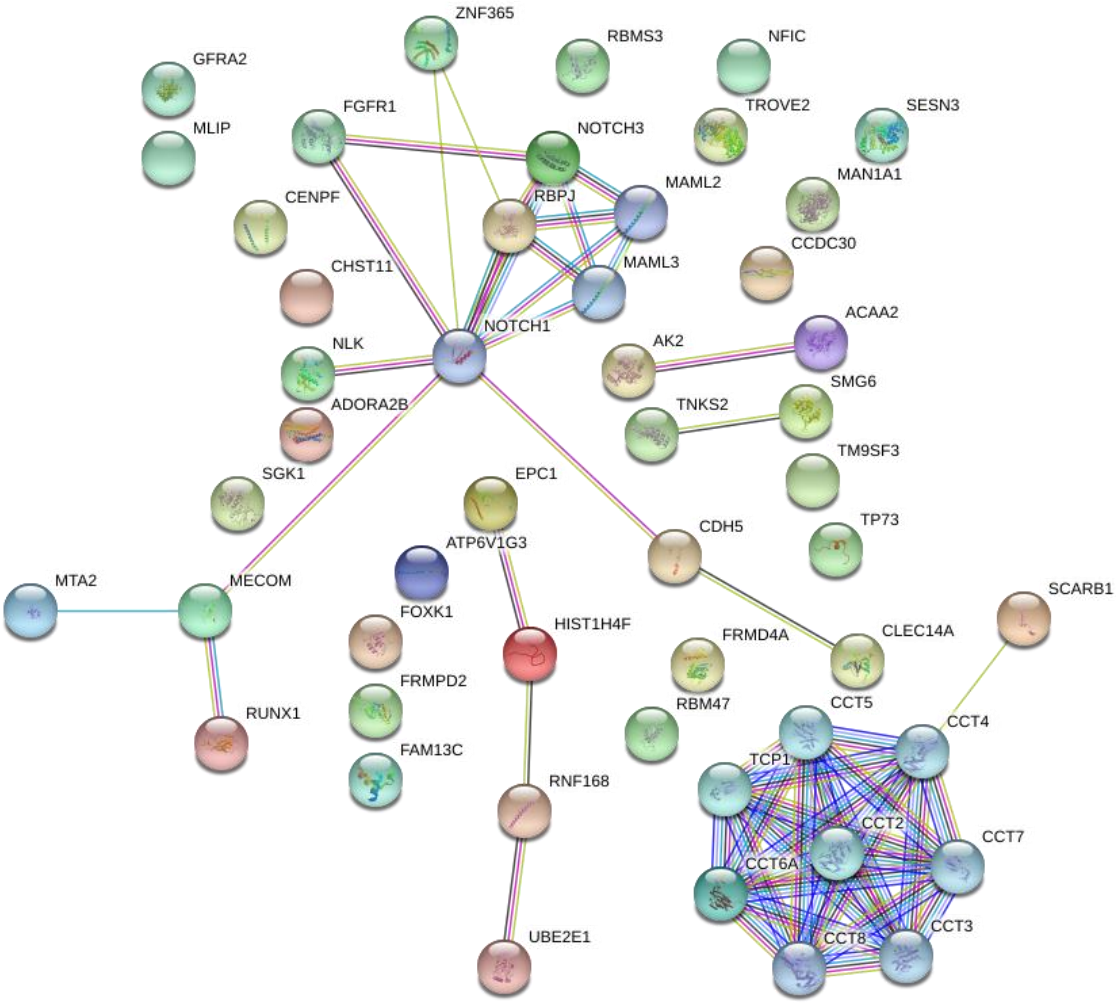

Figure 16: Interactions between 39 hCMEC/D3 targets and CDH5 by STRING analysis

Next, identified interactions between the 39 targets and FOXO3 depicted linkage between FOXO3 and RUNX1, MECOM (EVI-1), MTA2 via NOTCH1, RBPJ, NLK, FGFR1, as well as SGK1 (**Figure 17**).

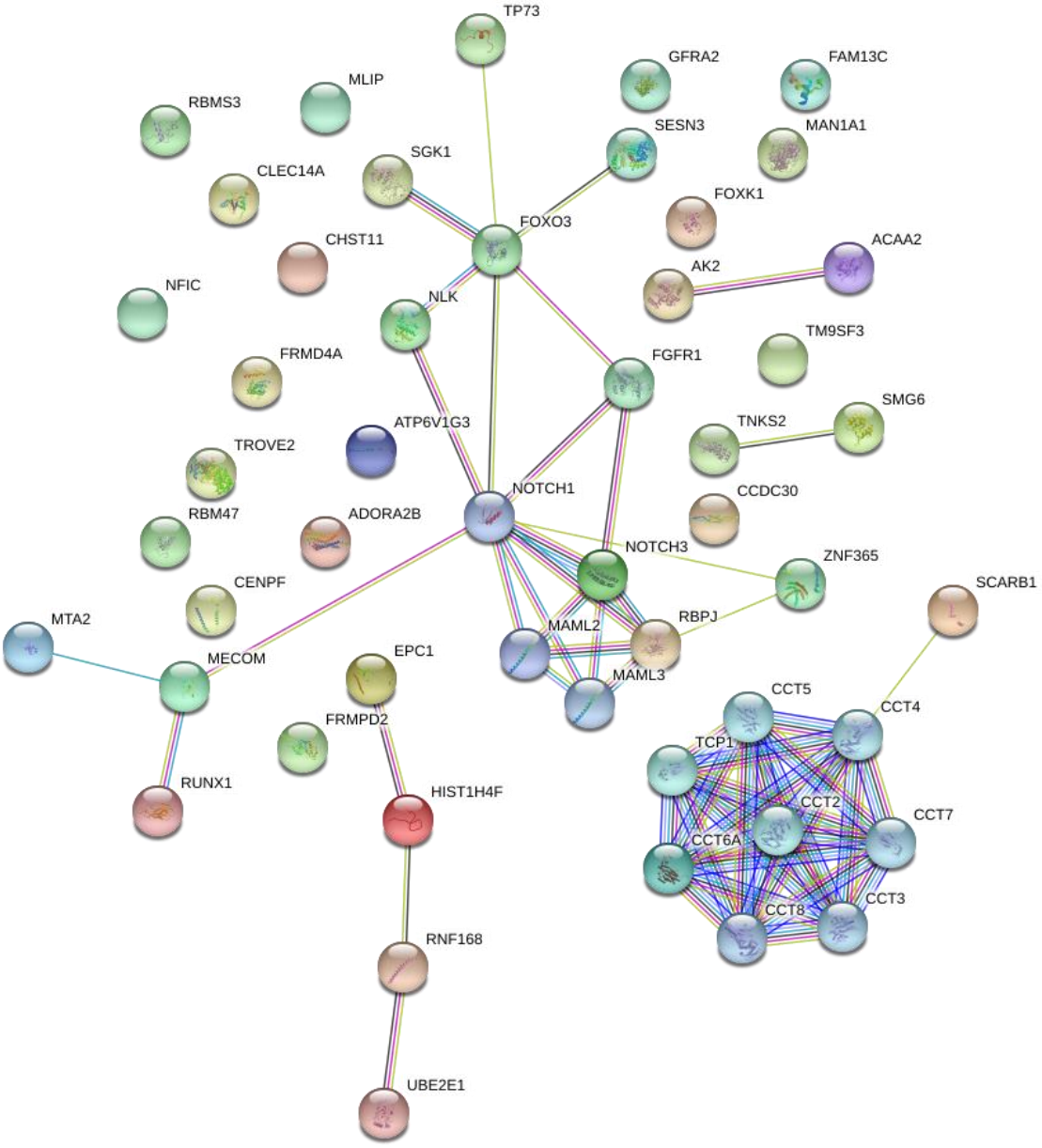

Figure 17: Interactions between 39 hCMEC/D3 targets and FOXO3 by STRING analysis

Furthermore, MECP2 as epigenetic regulating protein was linked to some of the found targets such as RBPJ, NOTCH3, FGFR1, NLK, but also to another strand consisting of MTA2, MECOM (EVI-1), and RUNX1 (**Figure 18**).

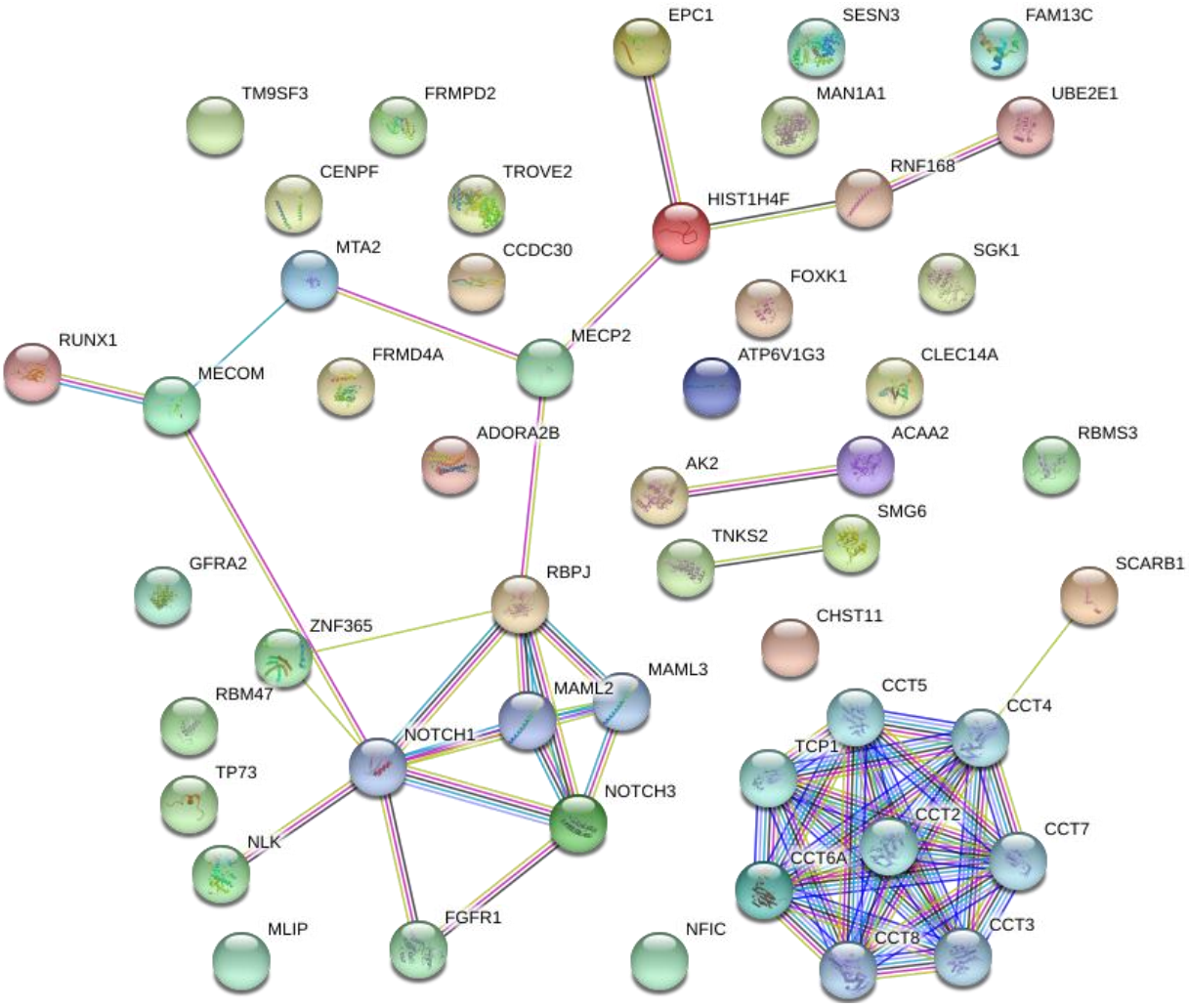

Figure 18: Interactions between 39 hCMEC/D3 targets and MECP2 by STRING analysis

Observed interactions between the 39 targets and tight junction proteins in STRING database suggest linkage of NOTCH3, RBPJ, FGFR1, NLK, TNKS2, SMG6 via CTNNB1 (β-catenin) and cadherins to TJP1 (ZO-1) as well as via MTA2, MECOM (EVI-1), and RUNX1 also to TJP1 (ZO-1). Specifically, TJP1 (ZO-1) is associated very closely with several claudins. Independently from these findings, it seems that SCABR1 is directly linked to some claudins (**Figure 19**).

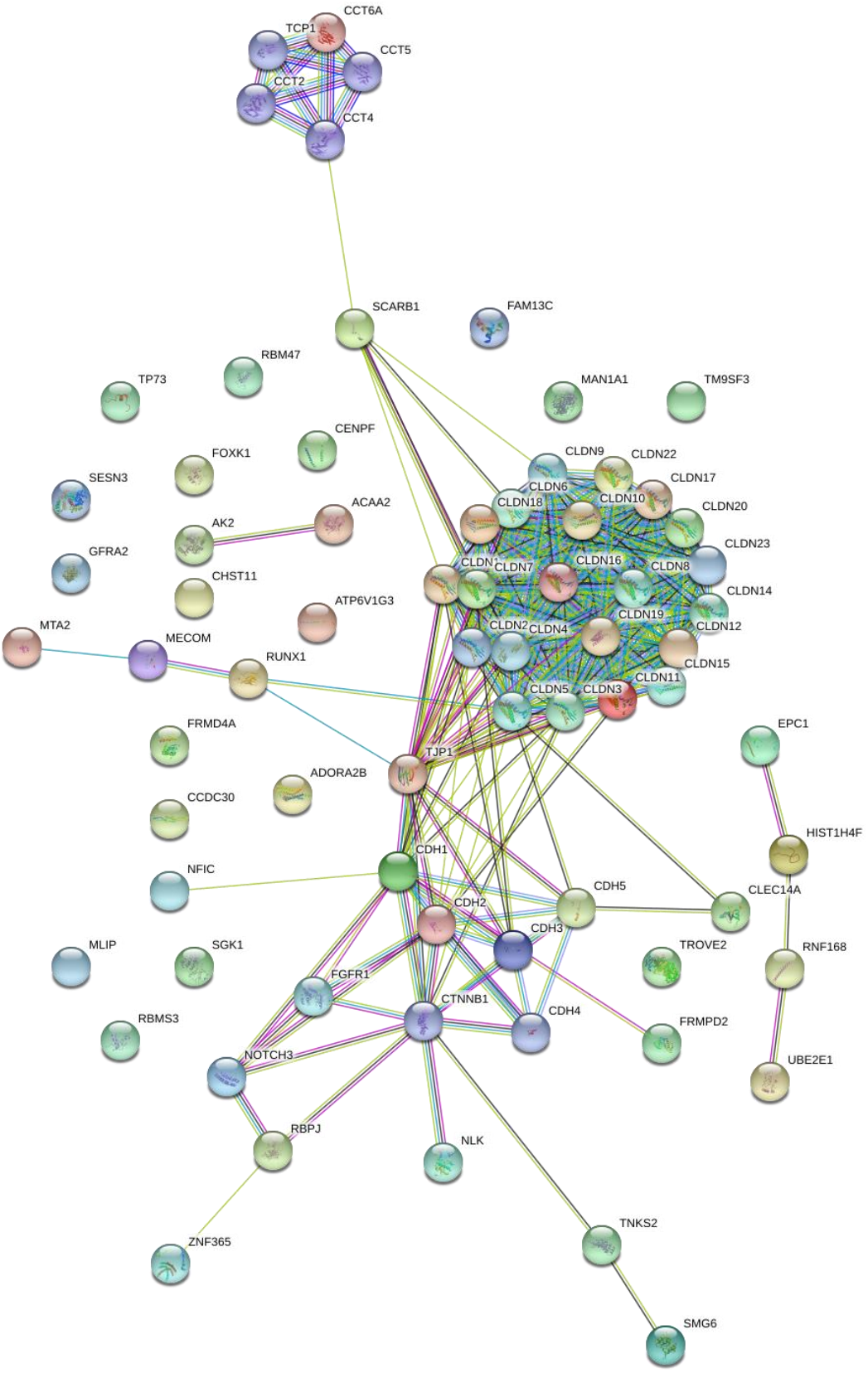

Figure 19: Interactions between 39 hCMEC/D3 targets and tight junction proteins by STRING analysis

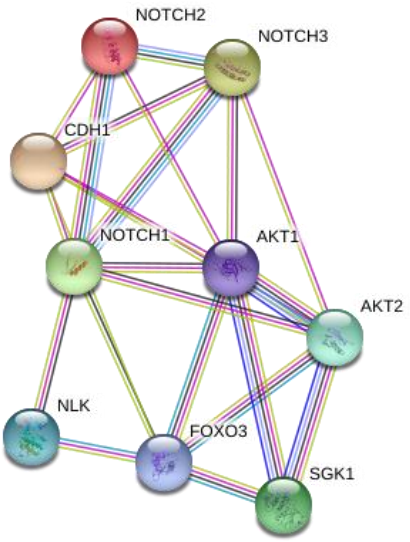

Figure 20: Confirmation of interactions between FOXO3, SGK1, and NLK including AKT1 and CDH1 by STRING analysis

Generation of multiple networks of protein-protein interactions allowed thorough investigation of the targets and resulted in the selection of 13 regulated targets of cerebral ischemia to be used for further analysis (**Table 24**). Thorough investigation consisted of dividing the targets into several clusters. Targets of every cluster cooperated and were related to each other. Such behaviour was shown for example by close proximity of the targets to each other in the STRING analysis or because they shared common pathways. Including of additional proteins which are fundamental for the proper function of the BBB to the analysis made selection of the targets more relevant. Furthermore, targets to be chosen were ideally significantly upregulated at mRNA level after the OGD treatment at both distinct OGD timepoints (5 h OGD treatment and 24 h OGD treatment including 19 h reoxygenation).

Table 32: Selected regulated targets for further analysis

No.	Name of the target
1	*CLEC14A*
2	*EPC1*
3	*MECOM*
4	*FGFR1*
5	*H4C3*
6	*MTA2*

7	*NLK*
8	*NOTCH3*
9	*RBPJ*
10	*RUNX1*
11	*SCARB1*
12	*SGK1 (tr1-4/5)*
	SGK1 (tr1-5/5)
13	*TNKS2*

CLEC14A is a type I transmembrane protein involved in mediation of inflammatory responses and cell-to-cell adhesion. At the BBB, CLEC14A contributes to the stability of endothelial junctions and vascular integrity. Equally, it was demonstrated that MCAO model of *CLEC14A*-KO mice induces an increased BBB leakage accompanied by an increased inflammatory response [60]. EPC1 protein is an epigenetic factor located in the nucleus. *EPC1* is implicated in the DNA damage protection by directly activating *E2F1* that further promotes the expression of anti-apoptotic genes such as *BCL-2* [61]. MECOM known also under the term EVI-1 and positive regulatory domain zinc finger protein 3 (PRDM3) represents a protein encoded by *MECOM* gene. In multiple cancer types, *MECOM* is considered to be a proto-oncogene due to exhibition of anti-apoptotic effects [62]. FGFR1 is a transmembrane protein of the fibroblast growth factor receptor family. *FGFR1* gene has a role in cancer pathogenesis and represents often a site of molecular aberrations [63]. For instance, hypoxia-induced resistance to conventional therapy in cancer is associated with overexpression of FGFR1 [64]. H4 clustered histone 3 is a protein encoded in humans by *HIST1H4C* gene. In general, histones are responsible for building of nucleosomes structure [65]. MTA2 is often overexpressed in human cancer. Higher level of MTA2 dysregulation correlates also with tumour invasiveness and metastasis [66]. NLK is an enzyme and member of the mitogen-activated protein kinase family (MAPK). MAPK regulates wide range of cellular processes including inflammation and stress responses. In addition, it plays a pivotal role in stroke pathology [67]. *NLK* specifically controls cell proliferation, migration, or apoptosis. Based on cancer type, *NLK* can be considered either a tumour suppressor or an oncogene [68]. NOTCH3 is a protein involved in cell fate and tissue maintenance [69]. Mutations in *NOTCH3* are associated mostly with cerebral autosomal dominant arteriopathy with subcortical infarcts and leukoencephalopathy and AD. Despite this fact, it seems that *NOTCH3* mutations do not significantly correspond with stroke occurrence

[70]. RBPJ represents a protein known also under the name CBF1. *RBPJ* is a transcription factor and mediator of Notch1 signaling cascade [71]. Thus, role of *RBPJ* is closely intertwined with stroke progression too. In one study, postnatal inactivation of *RBPJ* gene in mice increased local TGFβ signaling and triggered profound changes in endothelial cell phenotype. Noticeably, loss of *RBPJ* gene in adult mice promoted aggravated brain damage upon stroke incidence [72]. Another study demonstrated that *RBPJ* knockdown which subsequently blocked Notch signaling, and combined with stroke insult, resulted in a higher recruitment of astrocytes to neurogenesis. Equally, it was deduced that blockage of Notch signaling in stroke raised the neurogenic response to stroke by a factor of 3.5 fold [73]. RUNX1 is a protein known also under the name AML1 or CBFA2. In general, transcription factor RUNX1 is responsible for regulation of normal hematopoietic development. Any arising mutations in *RUNX1* gene are usually associated with malignancies of the hematopoietic system including acute myeloid leukemia (AML) [74]. SCARB1 is a high-density lipoprotein receptor [75]. Thus, polymorphisms in *SCARB1* gene may influence the susceptibility to coronary heart disease or cerebral infarction [76]. SGK1 is a member of serine/threonine kinase family located downstream of phosphatidylinositide-3 kinase (PI3K) signaling pathway [77]. Activity of SGK1 enzyme is induced for instance by stress or growth factors. *SGK1* expression is also stimulated by TGFβ while at the same time *SGK1* promotes inhibitory action towards TGFβ degradation in a feedback loop [78]. Action of *SGK1* contributes to the proper function and regulation of ion channel opening, metabolite transport, hormone release, inflammation, cell proliferation, and apoptosis. Moreover, overexpression of *SGK1* was over the past years associated with multiple pathological conditions and their progression such as hypertension, diabetes, stroke, ischemia, thrombosis, obesity, tumour growth, fibrosis, or neurodegenerative diseases [77], [79], [80]. TNKS2 is a member of poly(ADP-ribose)polymerase protein superfamily. Tankyrases are enzymes involved in Wnt/β-catenin signaling pathway that represent an attractive drug target for various cancer types and heritable diseases [81]. Equally, Wnt/β-catenin signaling pathway plays an essential role in BBB development [17].

4.2 Determination of mRNA expression of selected targets in hCMEC/D3 mono-culture and triple-culture with astrocytes and pericytes after OGD treatment

To confirm the reproducibility of the first data, hCMEC/D3 cells were cultivated on well plates as a mono-culture and treated under the OGD conditions. Mono-culture experiments were done via collaboration of MSc student Sonja Peric and intern Iris Soliman from AIT. Separately, hCMEC/D3 cells were also cultivated and treated under OGD conditions on transwell model system as triple-culture with astrocytes and pericytes. In both experimental set-ups, mRNA expression of selected targets for further analysis was investigated.

4.2.1 *CLEC14A* mRNA expression in hCMEC/D3 after OGD treatment

To observe how the OGD treatment affects individual groups, all values (shown as bar plots – difference between means ± SEM, p-value) were related to the normoxia group of the respective culture condition. Assessment of *CLEC14A* gene expression in hCMEC/D3 mono-culture after 5 h OGD treatment as well as after 5 h OGD treatment with 19 h of reoxygenation (24 h treatment) showed no statistically significant change.

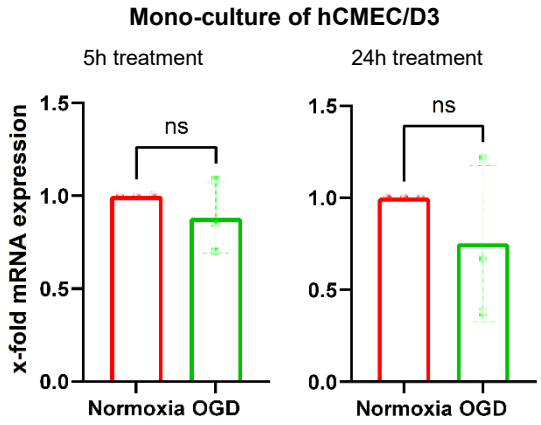

Figure 21: *CLEC14A* x-fold mRNA expression (shown as bar plots) related to respective normoxia (DMEM + G) of culture condition in hCMEC/D3 mono-culture after five hours OGD and 19 hours reoxygenation and five hours OGD only; Normoxia: Dulbecco´s Modified Eagle´s Medium with glucose (DMEM + G), normoxic conditions 21% O_2, n=3; OGD: Dulbecco´s Modified Eagle´s Medium without glucose (DMEM - G), 0.1% O_2 , n=3; hCMEC/D3 cells cultivated in mono-culture on well plates; housekeeping gene: *18SrRNA*; ns: p>0.05

After 24 h OGD treatment, consisting out of 5 h OGD treatment and 19 h recovery phase, expression of *CLEC14A* was significantly increased in the EBM-2 control group (1.76 ± 0.25, p=0.0379) as well as in the OGD group (2.68 ± 0.26, p<0.0001) of hCMEC/D3 triple-culture.

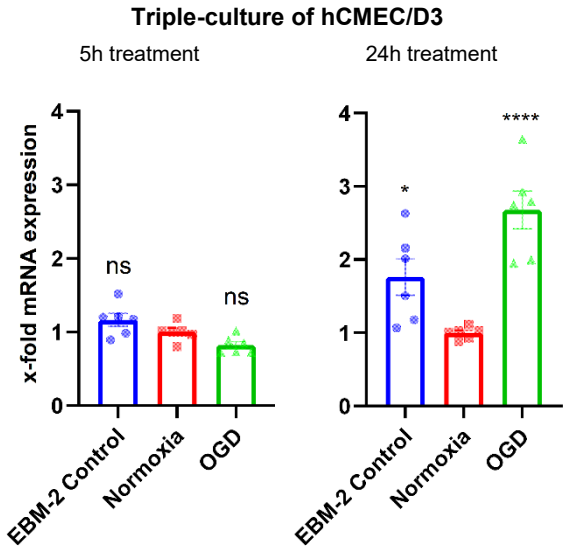

Figure 22: *CLEC14A* x-fold mRNA expression (shown as bar plots) related to nornoxia culture condition in hCMEC/D3 triple-culture after five hours OGD and 19 hours reoxygenation and five hours OGD only; EBM-2 Control: Endothelial Cell Growth Basal Medium-2 (EBM-2), normoxic conditions 21% O_2, n=6; Normoxia: Dulbecco´s Modified Eagle´s Medium with glucose (DMEM + G), normoxic conditions 21% O_2, n=6; OGD: Dulbecco´s Modified Eagle´s Medium without glucose (DMEM - G), 0.1% O_2 , n=6; hCMEC/D3 triple-culture with human astrocytes and human pericytes; housekeeping gene: *18SrRNA*; ns: p>0.05, *: p≤0.05, **:p≤0.01, ***: p≤0.001, ****:p≤0.0001

4.2.2 *EPC1* mRNA expression in hCMEC/D3 after OGD treatment

Determination of *EPC1* mRNA expression in hCMEC/D3 mono-culture after 5 h OGD treatment and consecutive 5 h OGD treatment followed by 19 h reoxygenation showed no significant upregulation or downregulation of the target.

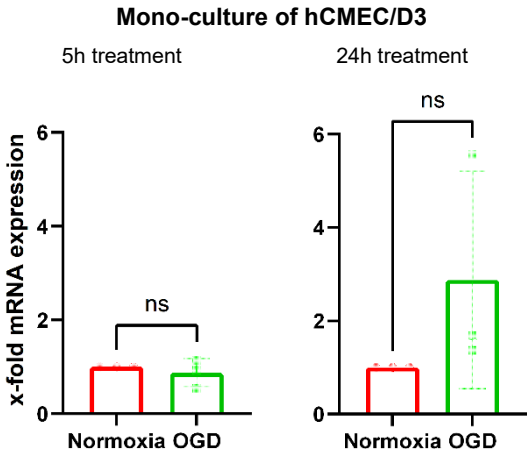

Figure 23: *EPC1* x-fold mRNA expression (shown as bar plots) related to respective normoxia (DMEM + G) of culture condition in hCMEC/D3 mono-culture after five hours OGD and 19 hours reoxygenation and five hours OGD only; Normoxia: Dulbecco´s Modified Eagle´s Medium with glucose (DMEM + G), normoxic conditions 21% O_2, n=3; OGD: Dulbecco´s Modified Eagle´s Medium without glucose (DMEM - G), 0.1% O_2 , n=3; hCMEC/D3 cells cultivated in mono-culture on well plates; housekeeping gene: *18SrRNA*; ns: p>0.05

In hCMEC/D3 triple-culture experimental set-up, *EPC1* mRNA expression increased significantly in the OGD group after 5 h treatment (1.38 ± 0.11, p=0.0096) as well as after 24 h treatment (1.33 ± 0.15, p=0.0471).

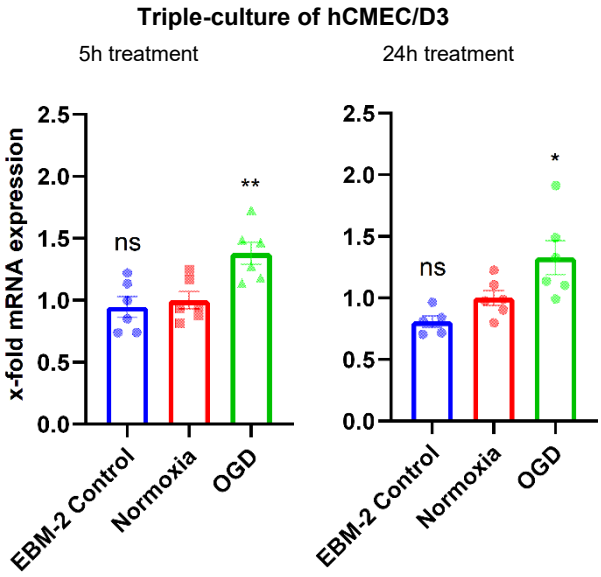

Figure 24*: EPC1* x-fold mRNA expression (shown as bar plots) related to normoxia culture condition in hCMEC/D3 triple-culture after five hours OGD and 19 hours reoxygenation and five hours OGD only; EBM-2 Control: Endothelial Cell Growth Basal Medium-2 (EBM-2), normoxic conditions 21% O_2, n=6; Normoxia: Dulbecco´s Modified Eagle´s Medium with glucose (DMEM + G), normoxic conditions 21% O_2, n=6; OGD: Dulbecco´s Modified Eagle´s Medium without glucose (DMEM - G), 0.1% O_2 , n=6; hCMEC/D3 triple-culture with human astrocytes and human pericytes; housekeeping gene: *18SrRNA*; ns: p>0.05, *: p≤0.05, **:p≤0.01

4.2.3 *MECOM* mRNA expression in hCMEC/D3 after OGD treatment

MECOM mRNA expression in hCMEC/D3 mono-culture after 5 h OGD treatment decreased significantly (0.43 ± 0.04, p=0.0002). However, after 5 h of OGD treatment with 19 additional hours of reoxygenation change in the *MECOM* gene expression was not significant.

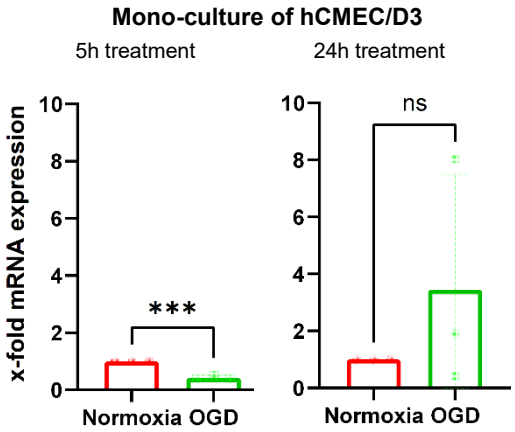

Figure 25: *MECOM* x-fold mRNA expression (shown as bar plots) related to respective normoxia (DMEM + G) of culture condition in hCMEC/D3 mono-culture after five hours OGD and 19 hours reoxygenation and five hours OGD only; Normoxia: Dulbecco´s Modified Eagle´s Medium with glucose (DMEM + G), normoxic conditions 21% O_2, n=3; OGD: Dulbecco´s Modified Eagle´s Medium without glucose (DMEM - G), 0.1% O_2 , n=3; hCMEC/D3 cells cultivated in mono-culture on well plates; housekeeping gene: *18SrRNA*; ns: p>0.05, *: p≤0.05, **:p≤0.01, ***: p≤0.001

The effect of triple-culture conditions on independent groups in relation to *MECOM* gene expression is represented in the **Figure 26**. Significant changes on the mRNA level were determined in the OGD group after 5 h OGD treatment (0.60 ± 0.06, p=0.0454) as well as in the EBM-2 control group after 24 h OGD treatment (1.59 ± 0.16, p=0.0222).

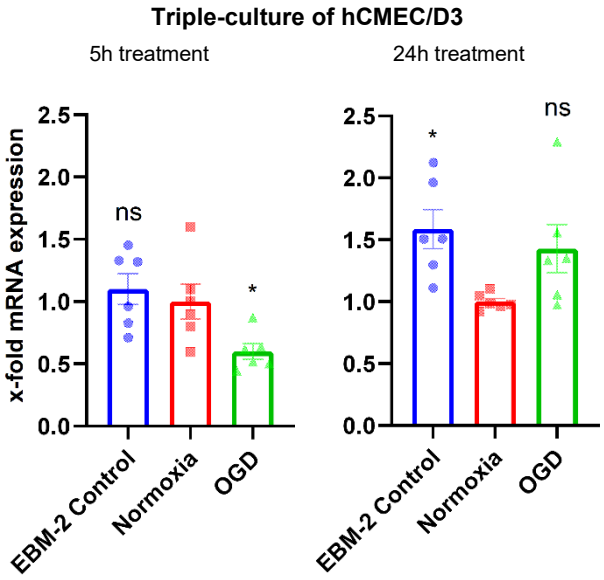

Figure 26: *MECOM* x-fold mRNA expression (shown as bar plots) related to normoxia culture condition in hCMEC/D3 triple-culture after five hours OGD and 19 hours reoxygenation and five hours OGD only; EBM-2 Control: Endothelial Cell Growth Basal Medium-2 (EBM-2), normoxic conditions 21% O_2, n=6; Normoxia: Dulbecco´s Modified Eagle´s Medium with glucose (DMEM + G), normoxic conditions 21% O_2, n=6; OGD: Dulbecco´s Modified Eagle´s Medium without glucose (DMEM - G), 0.1% O_2 , n=6; hCMEC/D3 triple-culture with human astrocytes and human pericytes; housekeeping gene: *18SrRNA*; ns: p>0.05, *: p≤0.05

4.2.4 *FGFR1* mRNA expression in hCMEC/D3 after OGD treatment

As can be seen in the **Figure 27** below, there was a significant decrease in mRNA expression of *FGFR1* in the hCMEC/D3 mono-culture after 5 h OGD treatment (0.43 ± 0.06, p=0.0007). The *FGFR1* expression change after 24 h treatment consisting out of 5 h OGD treatment with 19 additional hours of recovery phase was not significant.

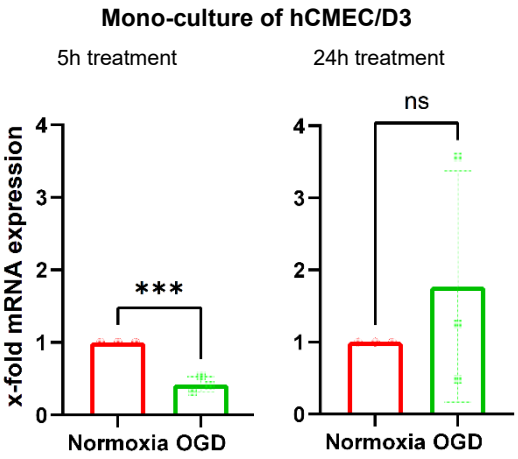

Figure 27: *FGFR1* x-fold mRNA expression (shown as bar plots) related to respective normoxia (DMEM + G) of culture condition in hCMEC/D3 mono-culture after 5 hours OGD and 19 hours reoxygenation and 5 hours OGD only; Normoxia: Dulbecco´s Modified Eagle´s Medium with glucose (DMEM + G), normoxic conditions 21% O_2, n=3; OGD: Dulbecco´s Modified Eagle´s Medium without glucose (DMEM - G), 0.1% O_2 , n=3; hCMEC/D3 cells cultivated in mono-culture on well plates; housekeeping gene: *18SrRNA*; ns: p>0.05, *: p≤0.05, **:p≤0.01, ***: p≤0.001

The OGD effect on normoxia DMEM+G group of hCMEC/D3 triple-culture showed a downregulation of *FGFR1* gene expression in the OGD group after 5 h treatment (0.64 ± 0.03, p=0.0006) and an upregulation in the OGD group after 24 h treatment (1.41 ± 0.11, p=0.0057). Moreover, a significant decrease of *FGFR1* expression was recorded in the EBM-2 control group after 5 h OGD treatment (0.74 ± 0.03, p=0.0056) (**Figure 28**).

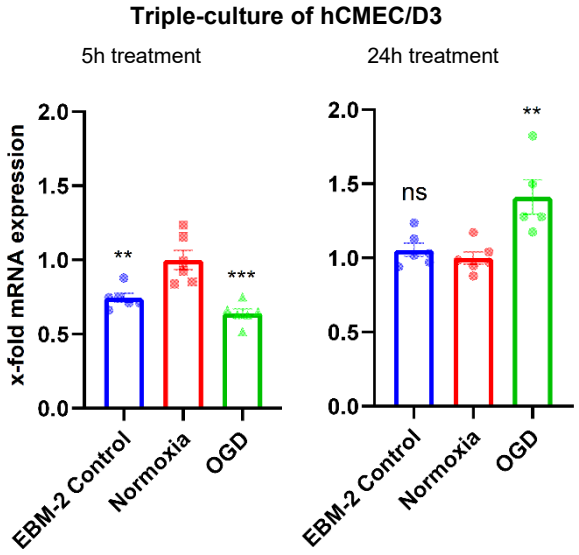

Figure 28: *FGFR1* x-fold mRNA expression (shown as bar plots) related to normoxia culture condition in hCMEC/D3 triple-culture after 5 hours OGD and 19 hours reoxygenation and 5 hours OGD only; EBM-2 Control: Endothelial Cell Growth Basal Medium-2 (EBM-2), normoxic conditions 21% O_2, n=6; Normoxia: Dulbecco´s Modified Eagle´s Medium with glucose (DMEM + G), normoxic conditions 21% O_2, n=6; OGD: Dulbecco´s Modified Eagle´s Medium without glucose (DMEM - G), 0.1% O_2 , n=5-6; hCMEC/D3 triple-culture with human astrocytes and human pericytes; in OGD group of 5h treatment an outlier was removed (Grubbs´s test); housekeeping gene: *18SrRNA*; ns: p>0.05, *: p≤0.05, **:p≤0.01, ***: p≤0.001

4.2.5 *H4C3* mRNA expression in hCMEC/D3 after OGD treatment

Simulation of OGD in hCMEC/D3 mono-culture by the OGD treatment resulted in a significantly decreased *H4C3* gene expression after 5 h timepoint (0.26 ± 0.05, p<0.0001).

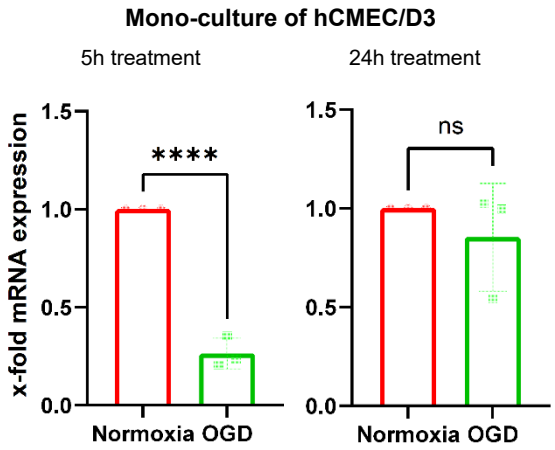

Figure 29: *H4C3* x-fold mRNA expression (shown as bar plots) related to respective normoxia (DMEM + G) of culture condition in hCMEC/D3 mono-culture after 5 hours OGD and 19 hours reoxygenation and 5 hours OGD only; Normoxia: Dulbecco´s Modified Eagle´s Medium with glucose (DMEM + G), normoxic conditions 21% O_2, n=3; OGD: Dulbecco´s Modified Eagle´s Medium without glucose (DMEM - G), 0.1% O_2 , n=3; hCMEC/D3 cells cultivated in mono-culture on well plates; housekeeping gene: *18SrRNA*; ns: p>0.05, *: p≤0.05, **:p≤0.01, ***: p≤0.001, ****:p≤0.0001

OGD treatment of hCMEC/D3 triple-culture resulted in a significant decrease in *H4C3* gene expression in the OGD group (0.58 ± 0.05 p<0.0001) and in the EBM-2 control group (0.78 ± 0.04, p=0.0071) after 5 h OGD timepoint.

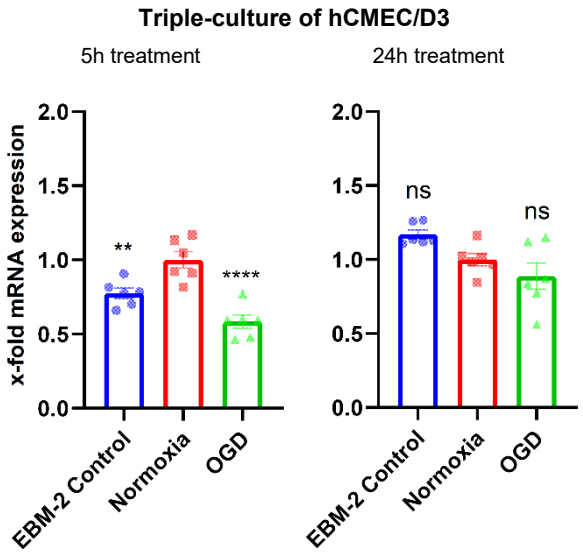

Figure 30: *H4C3* x-fold mRNA expression (shown as bar plots) related to normoxia culture condition in hCMEC/D3 triple-culture after 5 hours OGD and 19 hours reoxygenation and 5 hours OGD only; EBM-2 Control: Endothelial Cell Growth Basal Medium-2 (EBM-2), normoxic conditions 21% O_2, n=6; Normoxia: Dulbecco´s Modified Eagle´s Medium with glucose (DMEM + G) normoxic conditions 21% O_2, n=6; OGD: Dulbecco´s Modified Eagle´s Medium without glucose (DMEM - G), 0.1% O_2 , n=6; hCMEC/D3 triple-culture with human astrocytes and human pericytes; housekeeping gene: *18SrRNA*; ns: p>0.05, *: p≤0.05, **:p≤0.01, ***: p≤0.001, ****:p≤0.0001

4.2.6 *MTA2* mRNA expression in hCMEC/D3 after OGD treatment

When assessing the effect of OGD simulation on the hCMEC/D3 mono-culture, target *MTA2* was significantly downregulated after 5 h OGD treatment (0.36 ± 0.09, p=0.0024) (**Figure 31**).

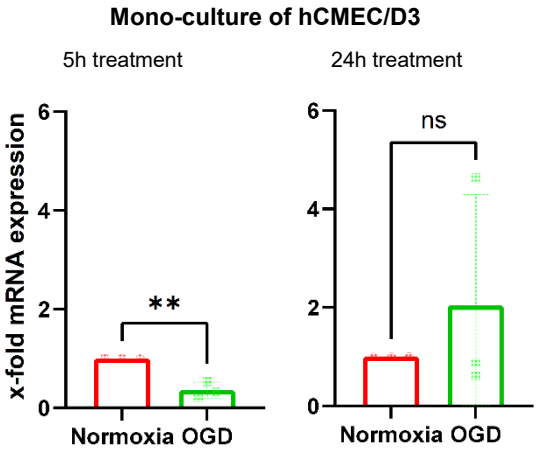

Figure 31: *MTA2* x-fold mRNA expression (shown as bar plots) related to respective normoxia (DMEM + G) of culture condition in hCMEC/D3 mono-culture after 5 hours OGD and 19 hours reoxygenation and 5 hours OGD only; Normoxia: Dulbecco´s Modified Eagle´s Medium with glucose (DMEM + G), normoxic conditions 21% O_2, n=3; OGD: Dulbecco´s Modified Eagle´s Medium without glucose (DMEM - G), 0.1% O_2 , n=3; hCMEC/D3 cells cultivated in mono-culture on well plates; housekeeping gene: *18SrRNA*; ns: p>0.05, *: p≤0.05, **:p≤0.01

The impact of OGD conditions resulted in a significant change of *MTA2* gene expression in 5 h OGD timepoint of the OGD group of hCMEC/D3 triple-culture (0.63 ± 0.07, p=0.0160) (**Figure 32**).

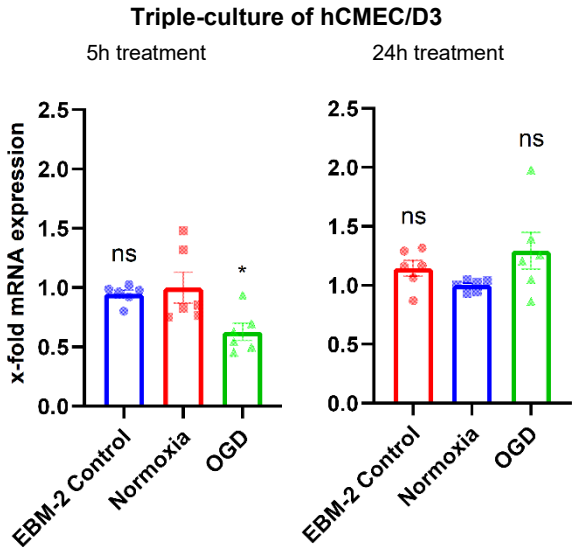

Figure 32: *MTA2* x-fold mRNA expression (shown as bar plots) related to normoxia culture condition in hCMEC/D3 triple-culture after 5 hours OGD and 19 hours reoxygenation and 5 hours OGD only; EBM-2 Control: Endothelial Cell Growth Basal Medium-2 (EBM-2), normoxic conditions 21% O_2, n=6; Normoxia: Dulbecco´s Modified Eagle´s Medium with glucose (DMEM + G), normoxic conditions 21% O_2, n=6; OGD: Dulbecco´s Modified Eagle´s Medium without glucose (DMEM - G), 0.1% O_2 , n=6; hCMEC/D3 triple-culture with human astrocytes and human pericytes; housekeeping gene: *18SrRNA*; ns: p>0.05, *: p≤0.05

4.2.7 *NLK* mRNA expression in hCMEC/D3 after OGD treatment

In hCMEC/D3 mono-culture, the OGD treatment did not lead to any significant changes in the *NLK* mRNA expression.

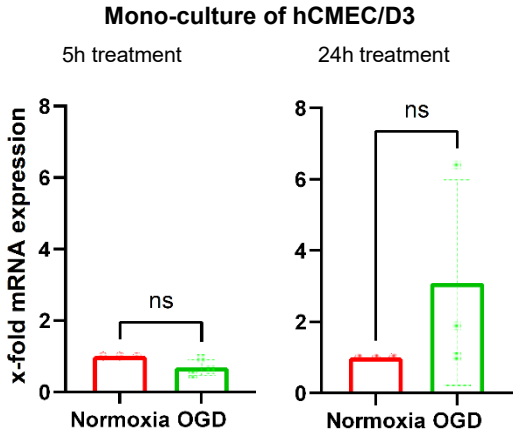

Figure 33: *NLK* x-fold mRNA expression (shown as bar plots) related to respective normoxia (DMEM + G) of culture condition in hCMEC/D3 mono-culture after 5 hours OGD and 19 hours reoxygenation and 5 hours OGD only; Normoxia: Dulbecco´s Modified Eagle´s Medium with glucose (DMEM + G), normoxic conditions 21% O_2, n=3; OGD: Dulbecco´s Modified Eagle´s Medium without glucose (DMEM - G), 0.1% O_2 , n=3; hCMEC/D3 cells cultivated in mono-culture on well plates; housekeeping gene: *18SrRNA*; ns: p>0.05

The effect of the OGD treatment did not lead to a significant change in *NLK* mRNA expression in hCMEC/D3 triple-culture after neither of the two distinct OGD timepoints.

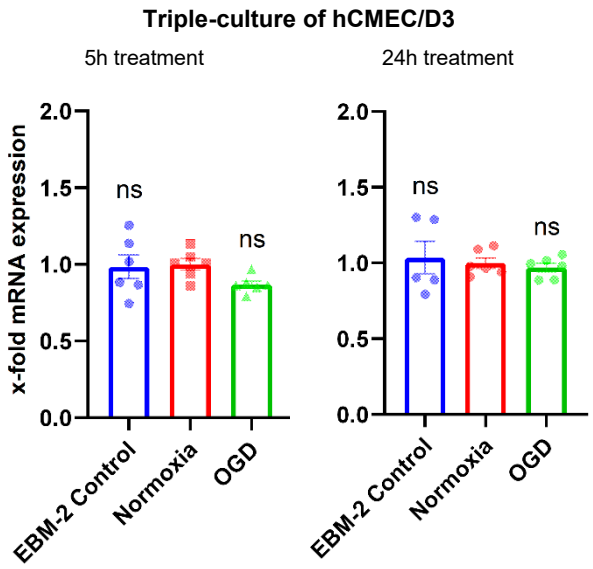

Figure 34: *NLK* x-fold mRNA expression (shown as bar plots) related to normoxia culture condition in hCMEC/D3 triple-culture after 5 hours OGD and 19 hours reoxygenation and 5 hours OGD only; EBM-2 Control: Endothelial Cell Growth Basal Medium-2 (EBM-2), normoxic conditions 21% O_2, n=6; Normoxia: Dulbecco´s Modified Eagle´s Medium with glucose (DMEM + G), normoxic conditions 21% O_2, n=6; OGD: Dulbecco´s Modified Eagle´s Medium without glucose (DMEM - G), 0.1% O_2 , n=6; hCMEC/D3 triple-culture with human astrocytes and human pericytes; in EBM-2 control group of 5h treatment an outlier was removed (Grubbs´s test); housekeeping gene: *18SrRNA*; ns: $p>0.05$

4.2.8 *NOTCH3* mRNA expression in hCMEC/D3 after OGD treatment

The effect of OGD treatment on hCMEC/D3 mono-culture lead to no significant change in *NOTCH3* gene expression after 5 h or 24 h OGD timepoint.

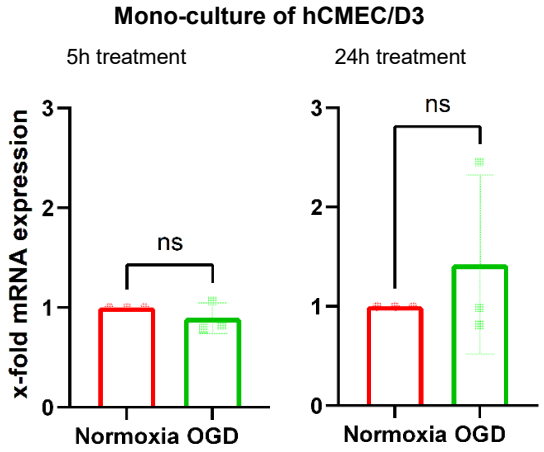

Figure 35: *NOTCH3* x-fold mRNA expression (shown as bar plots) related to respective normoxia (DMEM + G) of culture condition in hCMEC/D3 mono-culture after 5 hours OGD and 19 hours reoxygenation and 5 hours OGD only; Normoxia: Dulbecco´s Modified Eagle´s Medium with glucose (DMEM + G), normoxic conditions 21% O_2, n=3; OGD: Dulbecco´s Modified Eagle´s Medium without glucose (DMEM - G), 0.1% O_2 , n=3; hCMEC/D3 cells cultivated in mono-culture on well plates; housekeeping gene: *18SrRNA*; ns: p>0.05

In hCMEC/D3 triple-culture experimental set-up, a significant *NOTCH3* upregulation in the EBM-2 control group was demonstrated after 5 h OGD treatment (1.55 ± 0.21, p=0.0297) as well as after 24 h OGD treatment (1.75 ± 0.17, p=0.0135).

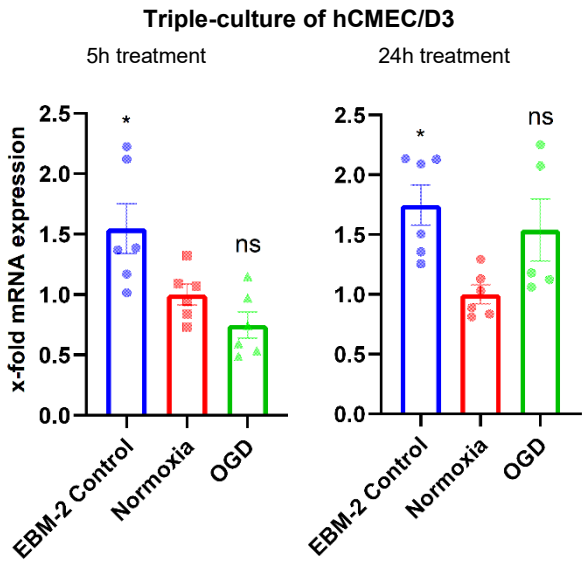

Figure 36: *NOTCH3* x-fold mRNA expression (shown as bar plots) related to normoxia culture condition in hCMEC/D3 triple-culture after 5 hours OGD and 19 hours reoxygenation and 5 hours OGD only; EBM-2 Control: Endothelial Cell Growth Basal Medium-2 (EBM-2), normoxic conditions 21% O_2, n=6; Normoxia: Dulbecco´s Modified Eagle´s Medium with glucose (DMEM + G), normoxic conditions 21% O_2, n=6; OGD: Dulbecco´s Modified Eagle´s Medium without glucose (DMEM - G), 0.1% O_2 , n=5-6; hCMEC/D3 triple-culture with human astrocytes and human pericytes; housekeeping gene: *18SrRNA*; in OGD group of 24h treatment an outlier was removed (Grubbs´s test); ns: p>0.05, *: p≤0.05

4.2.9 *RBPJ* mRNA expression in hCMEC/D3 after OGD treatment

After simulation of cerebral ischemia in hCMEC/D3 mono-culture by OGD treatment, no significant changes in *RBPJ* gene expression levels were determined.

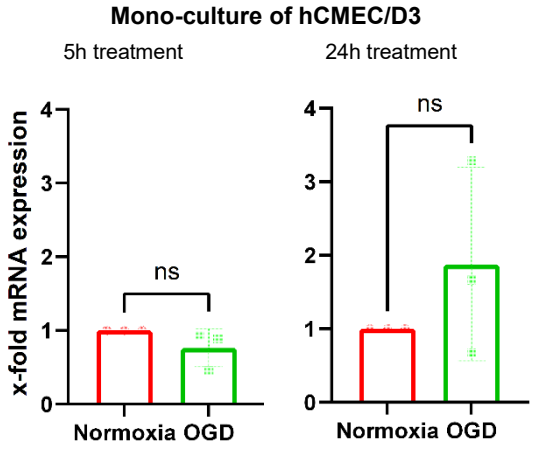

Figure 37: *RBPJ* x-fold mRNA expression (shown as bar plots) related to respective normoxia (DMEM + G) of culture condition in hCMEC/D3 mono-culture after 5 hours OGD and 19 hours reoxygenation and 5 hours OGD only; Normoxia: Dulbecco´s Modified Eagle´s Medium with glucose (DMEM + G), normoxic conditions 21% O_2, n=3; OGD: Dulbecco´s Modified Eagle´s Medium without glucose (DMEM - G), 0.1% O_2 , n=3; hCMEC/D3 cells cultivated in mono-culture on well plates; housekeeping gene: *18SrRNA*; ns: p>0.05

In triple-culture conditions, the effect of the OGD treatment showed upregulation of *RBPJ* gene expression in the OGD group after 24 h OGD timepoint in respect to the normoxia DMEM+G group (1.46 ± 0.12, p=0.0034).

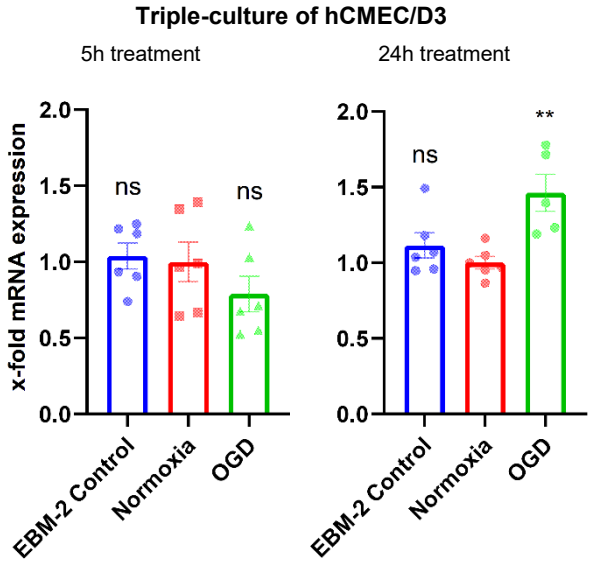

Figure 38: *RBPJ* x-fold mRNA expression (shown as bar plots) related to normoxia culture condition in hCMEC/D3 triple-culture after 5 hours OGD and 19 hours reoxygenation and 5 hours OGD only; EBM-2 Control: Endothelial Cell Growth Basal Medium-2 (EBM-2), normoxic conditions 21% O_2, n=6; Normoxia: Dulbecco´s Modified Eagle´s Medium with glucose (DMEM + G), normoxic conditions 21% O_2, n=6; OGD: Dulbecco´s Modified Eagle´s Medium without glucose (DMEM - G), 0.1% O_2 , n=5-6; hCMEC/D3 triple-culture with human astrocytes and human pericytes; in OGD group of 24h treatment an outlier was removed (Grubbs´s test); housekeeping gene: *18SrRNA*; ns: p>0.05, *: p≤0.05, **:p≤0.01

4.2.10 *RUNX1* mRNA expression in hCMEC/D3 after OGD treatment

OGD treatment of hCMEC/D3 mono-culture revealed a significant downregulation of *RUNX1* mRNA expression levels after 5 h OGD timepoint (0.53 ± 0.14, p=0.0265).

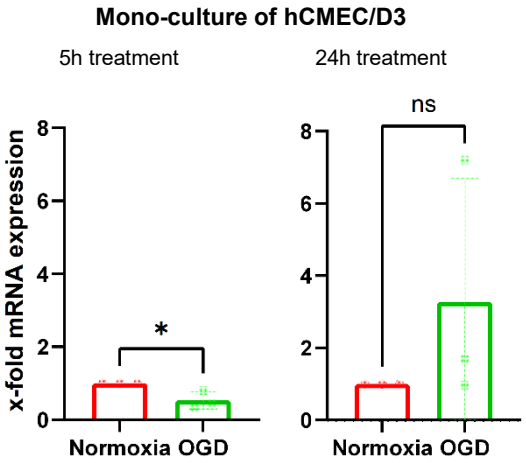

Figure 39: *RUNX1* x-fold mRNA expression (shown as bar plots) related to respective normoxia (DMEM + G) of culture condition in hCMEC/D3 mono-culture after 5 hours OGD and 19 hours reoxygenation and 5 hours OGD only; Normoxia: Dulbecco´s Modified Eagle´s Medium with glucose (DMEM + G), normoxic conditions 21% O_2, n=3; OGD: Dulbecco´s Modified Eagle´s Medium without glucose (DMEM - G), 0.1% O_2 , n=3; hCMEC/D3 cells cultivated in mono-culture on well plates; housekeeping gene: *18SrRNA*; ns: p>0.05, *: p≤0.05

In **Figure 40**, the effect of OGD treatment on mRNA expression of *RUNX1* is summarised. In comparison to normoxia DMEM+G group, significant upregulation of *RUNX1* was recorded in EBM-2 control group (1.27 ± 0.07, p=0.0485) and OGD group (1.52 ± 0.11, p=0.0005) after 5 h OGD timepoint. Significant downregulation of *RUNX1* was observed in the EBM-2 control group after 24 h OGD timepoint that included 19 h of recovery phase after initial 5 h of OGD treatment (0.77 ± 0.05, p=0.0177).

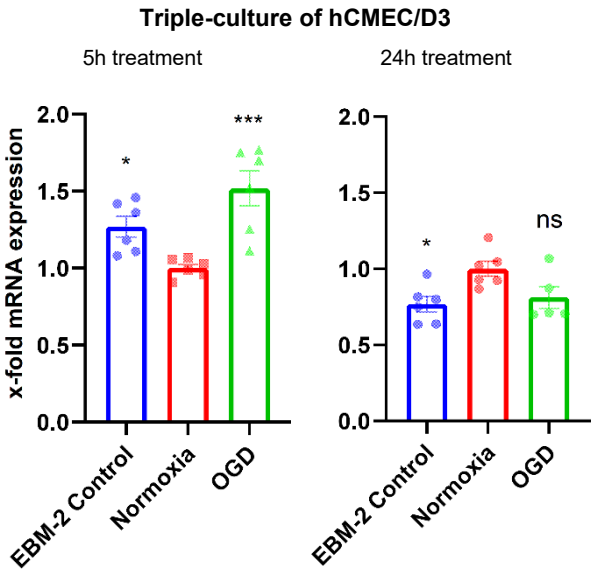

Figure 40: *RUNX1* x-fold mRNA expression (shown as bar plots) related to normoxia culture condition in hCMEC/D3 triple-culture after 5 hours OGD and 19 hours reoxygenation and 5 hours OGD only; EBM-2 Control: Endothelial Cell Growth Basal Medium-2 (EBM-2), normoxic conditions 21% O_2, n=6; Normoxia: Dulbecco´s Modified Eagle´s Medium with glucose (DMEM + G), normoxic conditions 21% O_2, n=6; OGD: Dulbecco´s Modified Eagle´s Medium without glucose (DMEM - G), 0.1% O_2 , n=5-6; hCMEC/D3 triple-culture with human astrocytes and human pericytes; in OGD group of 24h treatment an outlier was removed (Grubbs´s test); housekeeping gene: *18SrRNA*; ns: p>0.05, *: p≤0.05, **:p≤0.01, ***: p≤0.001

4.2.11 *SCARB1* mRNA expression in hCMEC/D3 after OGD treatment

In hCMEC/D3 mono-culture, OGD treatment with two different timepoints resulted in a significant decrease in *SCARB1* gene expression levels after 24 hours (0.29 ± 0.04, p=0.0002).

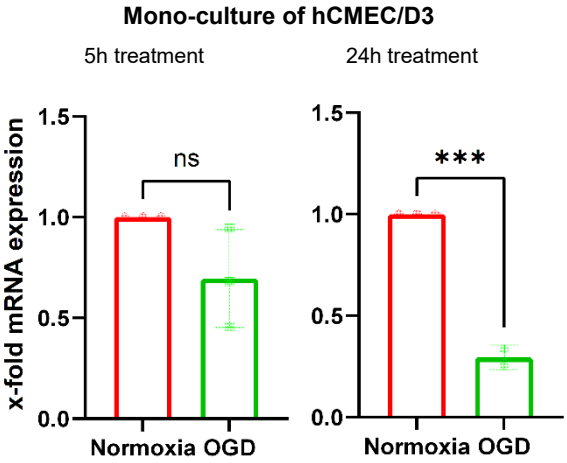

Figure 41: *SCARB1* x-fold mRNA expression (shown as bar plots) related to respective normoxia (DMEM + G) of culture condition in hCMEC/D3 mono-culture after 5 hours OGD and 19 hours reoxygenation and 5 hours OGD only; Normoxia: Dulbecco´s Modified Eagle´s Medium with glucose (DMEM + G), normoxic conditions 21% O_2, n=3; OGD: Dulbecco´s Modified Eagle´s Medium without glucose (DMEM - G), 0.1% O_2 , n=2-3; hCMEC/D3 cells cultivated in mono-culture on well plates; in OGD group of 24h treatment an outlier was removed (Grubbs´s test); housekeeping gene: *18SrRNA*; ns: p>0.05, *: p≤0.05, **:p≤0.01, ***: p≤0.001

In triple-culture conditions, OGD treatment resulted in a significant change of *SCARB1* gene expression. Specifically, *SCARB1* downregulation was recorded in the OGD group after 5 h OGD timepoint (0.59 ± 0.05, p=0.0016) as well as in the OGD group after 24 h OGD timepoint (0.42 ± 0.03, p<0.0001).

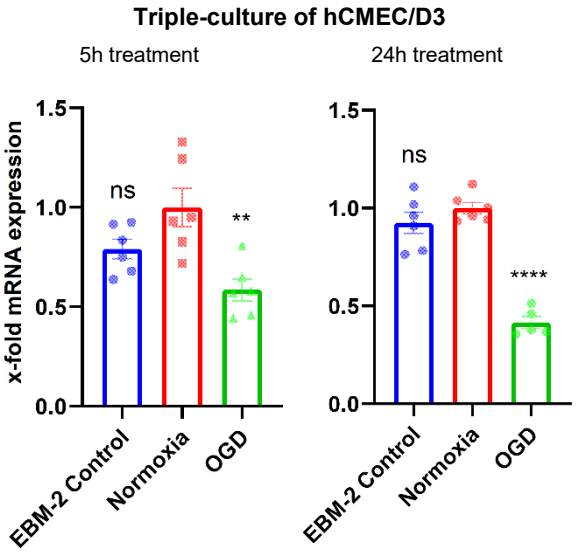

Figure 42: *SCARB1* x-fold mRNA expression (shown as bar plots) related to normoxia culture condition in hCMEC/D3 triple-culture after 5 hours OGD and 19 hours reoxygenation and 5 hours OGD only; EBM-2 Control: : Endothelial Cell Growth Basal Medium-2 (EBM-2), normoxic conditions 21% O_2, n=6; Normoxia: Dulbecco´s Modified Eagle´s Medium with glucose (DMEM + G), normoxic conditions 21% O_2, n=6; OGD: Dulbecco´s Modified Eagle´s Medium without glucose (DMEM - G), 0.1% O_2 , n=5-6; hCMEC/D3 triple-culture with human astrocytes and human pericytes; in OGD group of 24h treatment an outlier was removed (Grubbs´s test); housekeeping gene: *18SrRNA*; ns: p>0.05, *: p≤0.05, **:p≤0.01, ***: p≤0.001, ****:p≤0.0001

4.2.12 *SGK1* mRNA expression in hCMEC/D3 after OGD treatment

Simulation of ischemia by OGD treatment in hCMEC/D3 mono-culture showed a significant *SGK1* (transcript variant 1-4/5) overexpression after 5h OGD conditions followed by 19 h of reoxygenation (3.52 ± 0.34, p=0.0017). *SGK1* upregulation was confirmed also with second *SGK1* transcript variant (transcript variant 1-5/5). Here, a significant *SGK1* overexpression was observed after 5 h OGD timepoint (1.53 ± 0.01, p<0.0001) as well as after 24 h OGD timepoint that included recovery phase (3.64 ± 0.40, p=0.0027).

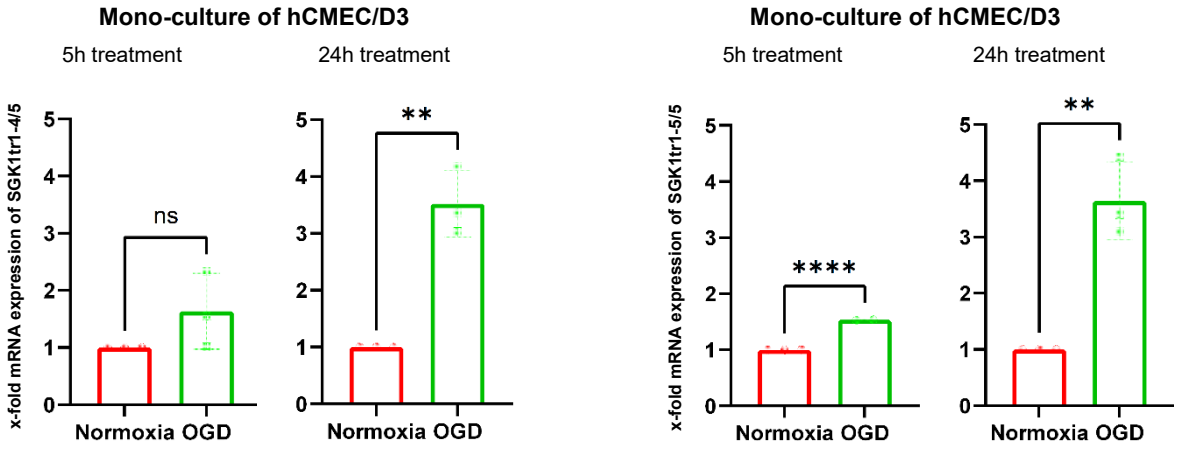

Figure 43: *SGK1* x-fold mRNA expression (shown as bar plots) related to respective normoxia (DMEM + G) of culture condition in hCMEC/D3 mono-culture after 5 hours OGD and 19 hours reoxygenation and 5 hours OGD only; Normoxia: Dulbecco´s Modified Eagle´s Medium with glucose (DMEM + G), normoxic conditions 21% O_2, n=3; OGD: Dulbecco´s Modified Eagle´s Medium without glucose (DMEM - G), 0.1% O_2 , n=2-3; hCMEC/D3 cells cultivated in mono-culture on well plates; in OGD group of 5h treatment (SGK1tr1-5/5) an outlier was removed (Grubbs´s test); housekeeping gene: *18SrRNA*; ns: p>0.05, *: p≤0.05, **:p≤0.01, ***: p≤0.001, ****:p≤0.0001

In relation to normoxia DMEM+G samples, *SGK1* expression (transcript variant 1-5/5) displayed an upregulation in the respective OGD groups after 5 h OGD treatment (2.02 ± 0.14, p<0.0001) as well as after 24 h OGD treatment (1.93 ± 0.07, p<0.0001). *SGK1* downregulation was observed in EBM-2 control group after 24 h OGD timepoint (0.68 ± 0.02, p=0.0003) (**Figure 44**).

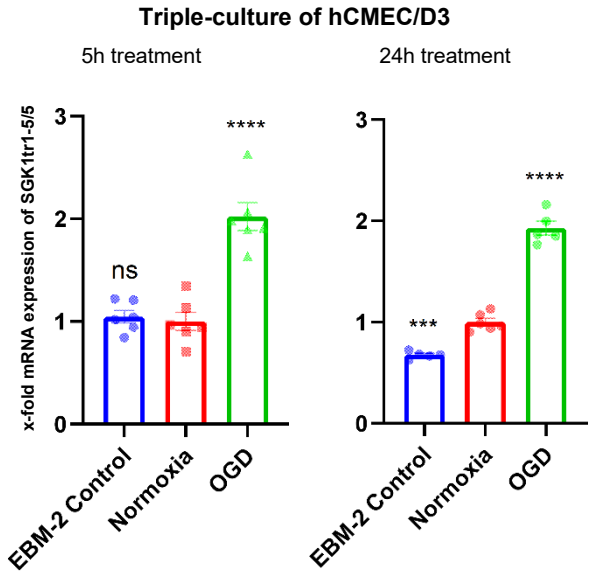

Figure 44: *SGK1* x-fold mRNA expression (shown as bar plots) related to normoxia culture condition in hCMEC/D3 triple-culture after 5 hours OGD and 19 hours reoxygenation and 5 hours OGD only; EBM-2 Control: Endothelial Cell Growth Basal Medium-2 (EBM-2), normoxic conditions 21% O_2, n=5-6; Normoxia: Dulbecco´s Modified Eagle´s Medium with glucose (DMEM + G), normoxic conditions 21% O_2, n=6; OGD: Dulbecco´s Modified Eagle´s Medium without glucose (DMEM - G), 0.1% O_2 , n=5-6; hCMEC/D3 triple-culture with human astrocytes and human pericytes; in OGD group and EBM-2 control group of 24h treatment (SGK1tr1-5/5) an outlier was removed (Grubbs´s test); housekeeping gene: *18SrRNA*; ns: p>0.05, *: p≤0.05, **:p≤0.01, ***: p≤0.001, ****:p≤0.0001

4.2.13 *TNKS2* mRNA expression in hCMEC/D3 after OGD treatment

OGD treatment in hCMEC/D3 mono-culture promoted a significant change in *TNKS2* mRNA expression in form of downregulation after 5 h OGD timepoint (0.36 ± 0.06, p=0.0004) (**Figure 45**).

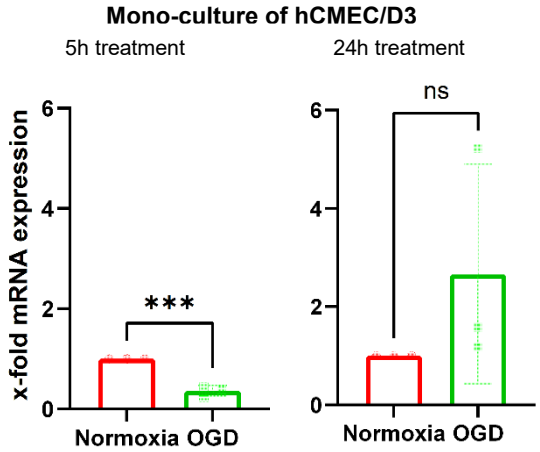

Figure 45: *TNKS2* x-fold mRNA expression (shown as bar plots) related to respective normoxia (DMEM + G) of culture condition in hCMEC/D3 mono-culture after 5 hours OGD and 19 hours reoxygenation and 5 hours OGD only; Normoxia: Dulbecco´s Modified Eagle´s Medium with glucose (DMEM + G), normoxic conditions 21% O_2, n=3; OGD: Dulbecco´s Modified Eagle´s Medium without glucose (DMEM - G), 0.1% O_2 , n=3; hCMEC/D3 cells cultivated in mono-culture on well plates; housekeeping gene: *18SrRNA*; ns: p>0.05, *: p≤0.05, **:p≤0.01, ***: p≤0.001

In hCMEC/D3 triple-culture samples, the two distinct OGD timepoints influenced *TNKS2* gene expression levels significantly. More precisely, *TNKS2* gene expression levels significantly decreased in the OGD group after 5 h OGD treatment (0.54 ± 0.04, p=0.0025), while significantly increased in the OGD group after 24 h OGD treatment (1.25 ± 0.04, p=0.0014).

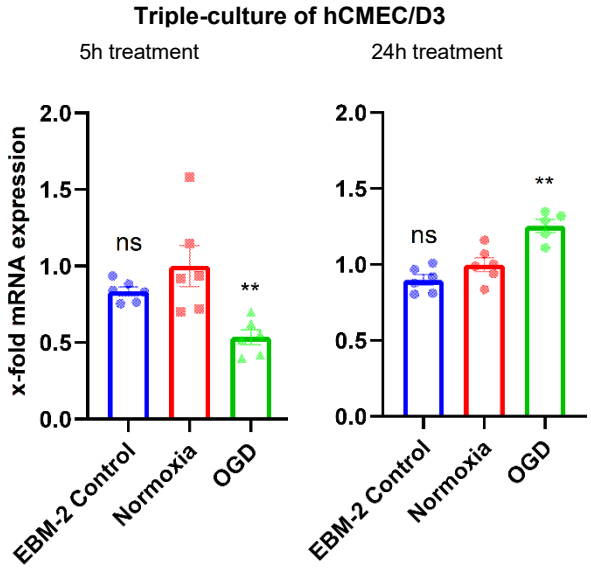

Figure 46: *TNKS2* x-fold mRNA expression (shown as bar plots) related to normoxia culture condition in hCMEC/D3 triple-culture after 5 hours OGD and 19 hours reoxygenation and 5 hours OGD only; EBM-2 Control: Endothelial Cell Growth Basal Medium-2 (EBM-2), normoxic conditions 21% O_2, n=6; Normoxia: Dulbecco´s Modified Eagle´s Medium with glucose (DMEM + G), normoxic conditions 21% O_2, n=6; OGD: Dulbecco´s Modified Eagle´s Medium without glucose (DMEM - G), 0.1% O_2 , n=5-6; hCMEC/D3 triple-culture with human astrocytes and human pericytes; in OGD group of 24h treatment an outlier was removed (Grubbs´s test); housekeeping gene: *18SrRNA*; ns: p>0.05, *: p≤0.05, **:p≤0.01

4.2.14 Summary of mRNA expression studies with selected targets in hCMEC/D3 triple-culture with astrocytes and pericytes after OGD treatment

To make a summary of the effect that OGD treatment exerted on the mRNA expression of selected regulated targets of cerebral ischemia in the hCMEC/D3 triple-culture with astrocytes and pericytes, expression of all targets was summarised. Specifically, **Figure 47** shows all OGD values of mRNA expression levels of the respective targets from the two distinct OGD timepoints. OGD groups used in this figure were calibrated to the corresponding normoxic control DMEM+G groups equal to one.

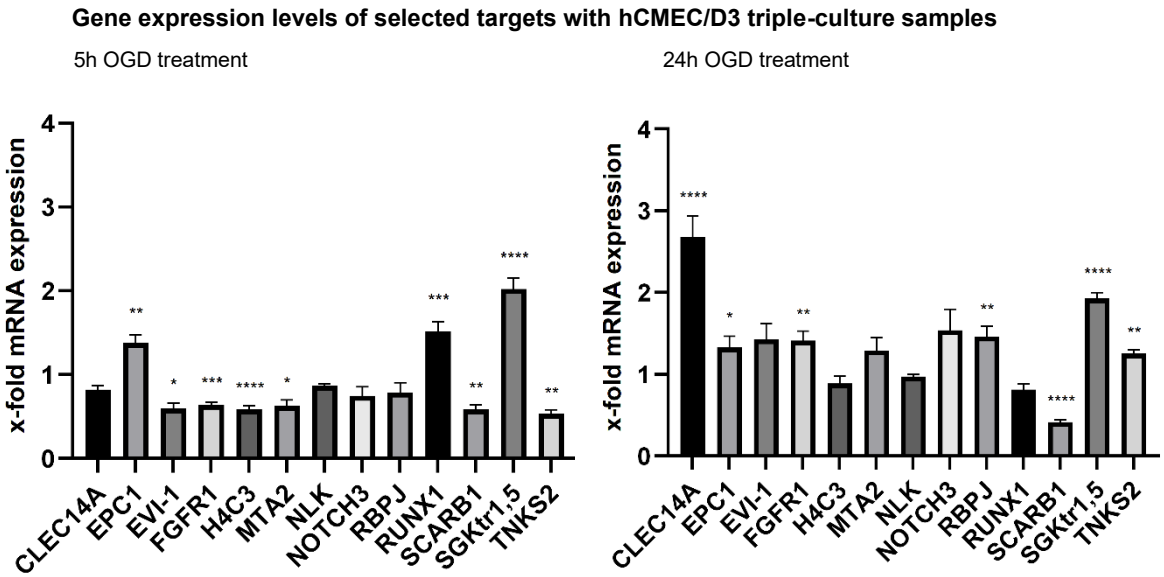

Figure 47: Summary of analysis of selected targets at the mRNA level with triple-culture samples; OGD x-fold values related to normoxia in hCMEC/D3 triple-culture after 5 hours OGD and 19 hours reoxygenation and 5 hours OGD only; OGD: Dulbecco´s Modified Eagle´s Medium without glucose (DMEM - G), 0.1% O_2 , n=5-6; hCMEC/D3 triple-culture with human astrocytes and human pericytes; data are presented as mean ± SEM; housekeeping gene: *18SrRNA*; ns: p>0.05, *: p≤0.05, **:p≤0.01, ***: p≤0.001, ****:p≤0.0001

4.3 Determination of mRNA expression of selected targets in hiPS-EC triple-culture with astrocytes and pericytes after OGD treatment

To assess the reproducibility of the found data, the same targets were measured in another human BBB model based on hiPSCs. For this, hiPS-EC cells were cultivated and treated under OGD conditions on transwell model system as triple-culture with astrocytes and pericytes.

4.3.1 *CLEC14A* mRNA expression in hiPS-EC after OGD treatment

To observe how the OGD treatment affects individual groups, all values (shown as bar plots – difference between means ± SEM, p-value) were related to the normoxia group of the respective culture condition. As shown in **Figure 48**, expression of *CLEC14A* after two different OGD timepoints did not significantly change in the triple-culture of hiPS-EC cells with astrocytes and pericytes from two independent differentiations. First OGD timepoint comprised stimulation of OGD conditions for the duration of 6 hours. Second OGD timepoint was after 6 h OGD treatment followed by a 18 h recovery period under normoxic conditions and addition of glucose.

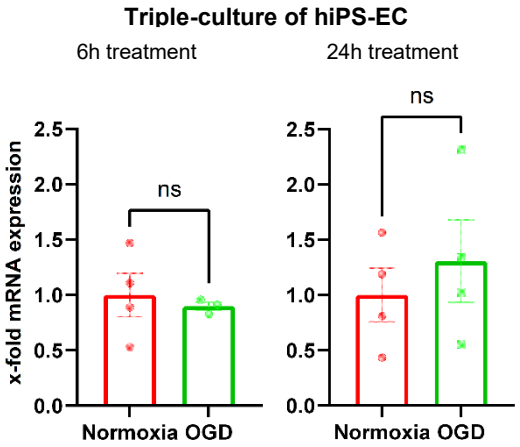

Figure 48: *CLEC14A* x-fold mRNA expression (shown as bar plots) related to normoxia culture condition in hiPS-EC triple-culture after 5 hours OGD and 19 hours reoxygenation and 5 hours OGD only; Normoxia: Dulbecco´s Modified Eagle´s Medium with glucose (DMEM + G), normoxic conditions 21% O_2, n=4; OGD: Dulbecco´s Modified Eagle´s Medium without glucose (DMEM - G), 0.1% O_2 , n=3-4; hiPS-EC triple-culture with human astrocytes and human pericytes; in OGD group of 6h treatment an outlier was removed (Grubbs´s test); housekeeping gene: *18SrRNA*; ns: p>0.05

4.3.2 *EPC1* mRNA expression in hiPS-EC after OGD treatment

After OGD treatment, no significant differences were determined in *EPC1* x-fold mRNA expression in neither of the OGD groups in relation to the respective normoxia DMEM+G groups.

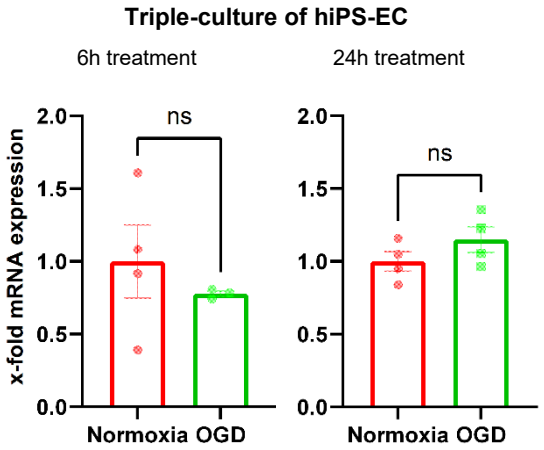

Figure 49: *EPC1* x-fold mRNA expression (shown as bar plots) related to normoxia culture condition in hiPS-EC triple-culture after 5 hours OGD and 19 hours reoxygenation and 5 hours OGD only; Control: Dulbecco´s Modified Eagle´s Medium with glucose (DMEM + G), normoxic conditions 21% O_2, n=4; OGD: Dulbecco´s Modified Eagle´s Medium without glucose (DMEM - G), 0.1% O_2 , n=3-4; hiPS-EC triple-culture with human astrocytes and human pericytes; in OGD group of 6h treatment an outlier was removed (Grubbs´s test); housekeeping gene: *18SrRNA*; ns: p>0.05

4.3.3 *MECOM* mRNA expression in hiPS-EC after OGD treatment

In **Figure 50**, the effect of the OGD treatment on independent differentiations of hiPS-EC triple-culture can be observed. After 6 h treatment, a significant decrease in *MECOM* mRNA expression levels was determined (0.66 ± 0.09, p=0.0441).

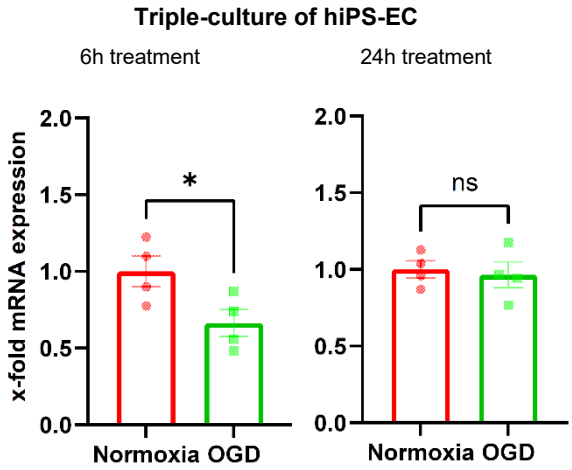

Figure 50: *MECOM* x-fold mRNA expression (shown as bar plots) related to normoxia culture condition in hiPS-EC triple-culture after 5 hours OGD and 19 hours reoxygenation and 5 hours OGD only; Normoxia: Dulbecco´s Modified Eagle´s Medium with glucose (DMEM + G), normoxic conditions 21% O_2, n=4; OGD: Dulbecco´s Modified Eagle´s Medium without glucose (DMEM - G), 0.1% O_2 , n=4; hiPS-EC triple-culture with human astrocytes and human pericytes; housekeeping gene: *18SrRNA*; ns: p>0.05, *: p≤0.05

4.3.4 *FGFR1* mRNA expression in hiPS-EC after OGD treatment

In this experimental set-up, 6 h OGD treatment as well as treatment of 6 hours of OGD treatment followed by 18 hours of reoxygenation did not significantly impact the mRNA expression of *FGFR1*.

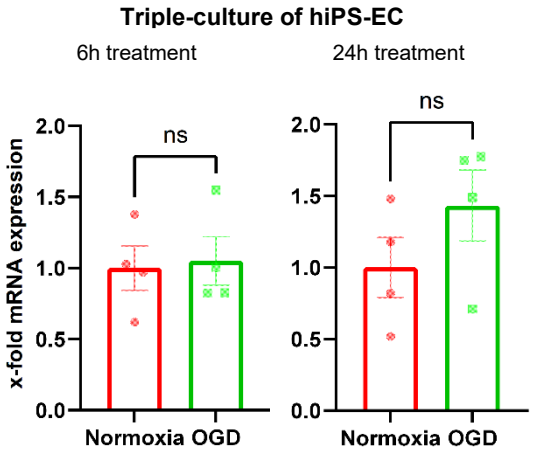

Figure 51: *FGFR1* x-fold mRNA expression (shown as bar plots) related to normoxia culture condition in hiPS-EC triple-culture after 5 hours OGD and 19 hours reoxygenation and 5 hours OGD only; Normoxia: Dulbecco´s Modified Eagle´s Medium with glucose (DMEM + G), normoxic conditions 21% O_2, n=4; OGD: Dulbecco´s Modified Eagle´s Medium without glucose (DMEM - G), 0.1% O_2 , n=4; hiPS-EC triple-culture with human astrocytes and human pericytes; housekeeping gene: *18SrRNA*; ns: p>0.05

4.3.5 *H4C3* mRNA expression in hiPS-EC after OGD treatment

H4C3 x-fold change values decreased significantly after 6 h OGD treatment (0.75 ± 0.05, p=0.0294).

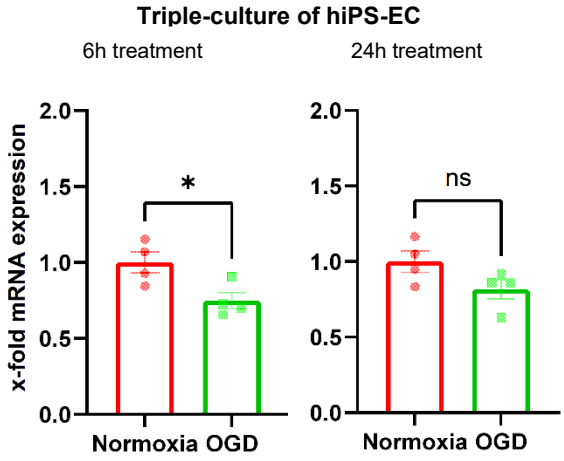

Figure 52: *H4C3* x-fold mRNA expression (shown as bar plots) related to normoxia culture condition in hiPS-EC triple-culture after 5 hours OGD and 19 hours reoxygenation and 5 hours OGD only; Normoxia: Dulbecco´s Modified Eagle´s Medium with glucose (DMEM + G), normoxic conditions 21% O_2, n=4; OGD: Dulbecco´s Modified Eagle´s Medium without glucose (DMEM - G), 0.1% O_2 , n=4; hiPS-EC triple-culture with human astrocytes and human pericytes; housekeeping gene: *18SrRNA*; ns: p>0.05, *: p≤0.05

4.3.6 *MTA2* mRNA expression in hiPS-EC after OGD treatment

A significant decrease in *MTA2* x-fold mRNA expression was observed after 6 h OGD treatment (0.56 ± 0.06, p=0.0016).

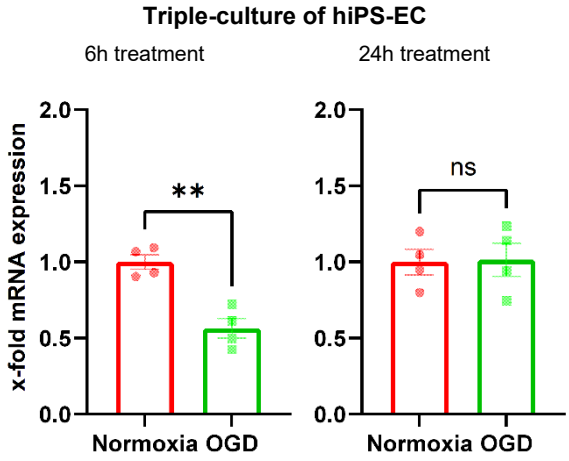

Figure 53: *MTA2* x-fold mRNA expression (shown as bar plots) related to normoxia culture condition in hiPS-EC triple-culture after 5 hours OGD and 19 hours reoxygenation and 5 hours OGD only; Normoxia: Dulbecco´s Modified Eagle´s Medium with glucose (DMEM + G), normoxic conditions 21% O_2, n=4; OGD: Dulbecco´s Modified Eagle´s Medium without glucose (DMEM - G), 0.1% O_2 , n=4; hiPS-EC triple-culture with human astrocytes and human pericytes; housekeeping gene: *18SrRNA*; ns: p>0.05, *: p≤0.05, **:p≤0.01

4.3.7 *NLK* mRNA expression in hiPS-EC after OGD treatment

NLK gene expression levels remained unaffected by significant changes after the two distinct OGD timepoints.

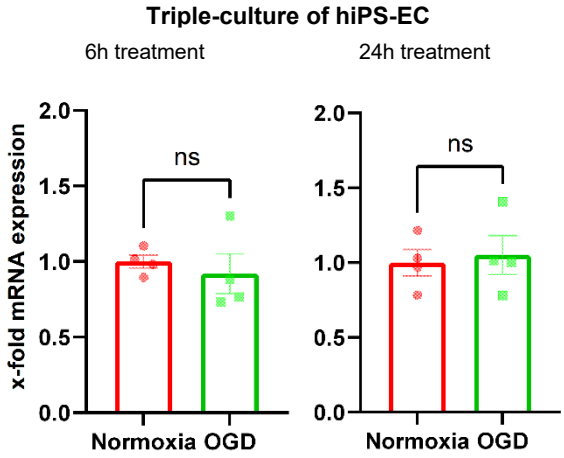

Figure 54: *NLK* x-fold mRNA expression (shown as bar plots) related to normoxia culture condition in hiPS-EC triple-culture after 5 hours OGD and 19 hours reoxygenation and 5 hours OGD only; Normoxia: Dulbecco´s Modified Eagle´s Medium with glucose (DMEM + G), normoxic conditions 21% O_2, n=4; OGD: Dulbecco´s Modified Eagle´s Medium without glucose (DMEM - G), 0.1% O_2 , n=4; hiPS-EC triple-culture with human astrocytes and human pericytes; housekeeping gene: *18SrRNA*; ns: p>0.05

4.3.8 *NOTCH3* mRNA expression in hiPS-EC after OGD treatment

Investigation of *NOTCH3* mRNA expression after the OGD treatment revealed a significant downregulation after 6 hours of treatment in hiPS-EC triple-culture with astrocytes and pericytes (0.56 ± 0.03, p=0.0007).

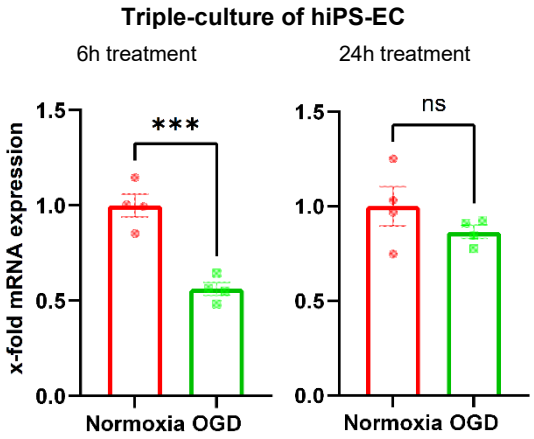

Figure 55: *NOTCH3* x-fold mRNA expression (shown as bar plots) related to normoxia culture condition in hiPS-EC triple-culture after 5 hours OGD and 19 hours reoxygenation and 5 hours OGD only; Normoxia: Dulbecco´s Modified Eagle´s Medium with glucose (DMEM + G), normoxic conditions 21% O_2, n=4; OGD: Dulbecco´s Modified Eagle´s Medium without glucose (DMEM - G), 0.1% O_2 , n=4; hiPS-EC triple-culture with human astrocytes and human pericytes; housekeeping gene: *18SrRNA*; ns: p>0.05, *: p≤0.05, **:p≤0.01, ***: p≤0.001

4.3.9 *RBPJ* mRNA expression in hiPS-EC after OGD treatment

Simulation of OGD conditions for the duration of 6 hours (6 h treatment) and for 6 hours followed by 18 hour reoxygenation (24 h treatment) did not result in significant changes of *RBPJ* mRNA expression.

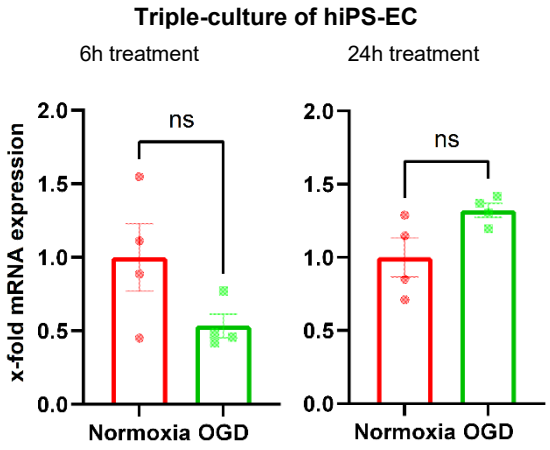

Figure 56: *RBPJ* x-fold mRNA expression (shown as bar plots) related to normoxia culture condition in hiPS-EC triple-culture after 5 hours OGD and 19 hours reoxygenation and 5 hours OGD only; Normoxia: Dulbecco´s Modified Eagle´s Medium with glucose (DMEM + G), normoxic conditions 21% O_2, n=4; OGD: Dulbecco´s Modified Eagle´s Medium without glucose (DMEM - G), 0.1% O_2 , n=4; hiPS-EC triple-culture with human astrocytes and human pericytes; housekeeping gene: *18SrRNA*; ns: p>0.05

4.3.10 *RUNX1* mRNA expression in hiPS-EC after OGD treatment

In **Figure 57**, the effect of OGD treatment on mRNA expression of target *RUNX1* is summarised. In comparison to normoxia DMEM+G group, a significant *RUNX1* mRNA expression upregulation was determined after 6 hours of the OGD treatment (2.13 ± 0.01, p=0.0040).

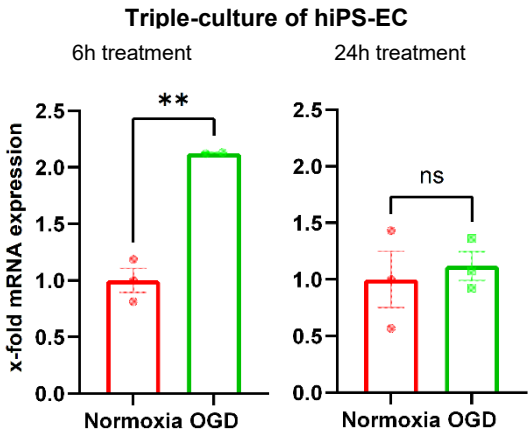

Figure 57: *RUNX1* x-fold mRNA expression (shown as bar plots) related to normoxia culture condition in hiPS-EC triple-culture after 5 hours OGD and 19 hours reoxygenation and 5 hours OGD only; Normoxia: Dulbecco´s Modified Eagle´s Medium with glucose (DMEM + G), normoxic conditions 21% O_2, n=3; OGD: Dulbecco´s Modified Eagle´s Medium without glucose (DMEM - G), 0.1% O_2 , n=2-3; hiPS-EC triple-culture with human astrocytes and human pericytes; in OGD group of 6h treatment an outlier was removed (Grubbs´s test); housekeeping gene: *18SrRNA*; ns: p>0.05, *: p≤0.05, **:p≤0.01

4.3.11 *SCARB1* mRNA expression in hiPS-EC after OGD treatment

Furthermore, OGD treatment of hiPS-EC triple-culture in two independent differentiations did not lead to any significant changes in *SCARB1* mRNA expression levels.

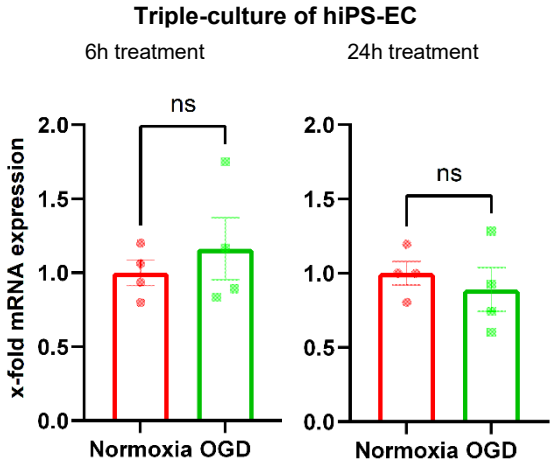

Figure 58: *SCARB1* x-fold mRNA expression (shown as bar plots) related to normoxia culture condition in hiPS-EC triple-culture after 5 hours OGD and 19 hours reoxygenation and 5 hours OGD only; Normoxia: Dulbecco´s Modified Eagle´s Medium with glucose (DMEM + G), normoxic conditions 21% O_2, n=4; OGD: Dulbecco´s Modified Eagle´s Medium without glucose (DMEM - G), 0.1% O_2 , n=4; hiPS-EC triple-culture with human astrocytes and human pericytes; housekeeping gene: *18SrRNA*; ns: p>0.05

4.3.12 *SGK1* mRNA expression in hiPS-EC after OGD treatment

SGK1 expression in hiPS-EC triple-culture was evaluated using two different *SGK1* transcript variants, namely *SGK1* transcript variant 1-4/5 and *SGK1* transcript variant 1-5/5. *SGK1* (transcript variant 1-4/5) mRNA expression significantly increased after six hours of OGD treatment (5.44 ± 0.78, p=0.0013). When investigating gene expression levels of *SGK1* (transcript variant 1-5/5), also a significant upregulation of *SGK1* after 6h treatment was recorded (8.13 ± 1.33, p=0.0060).

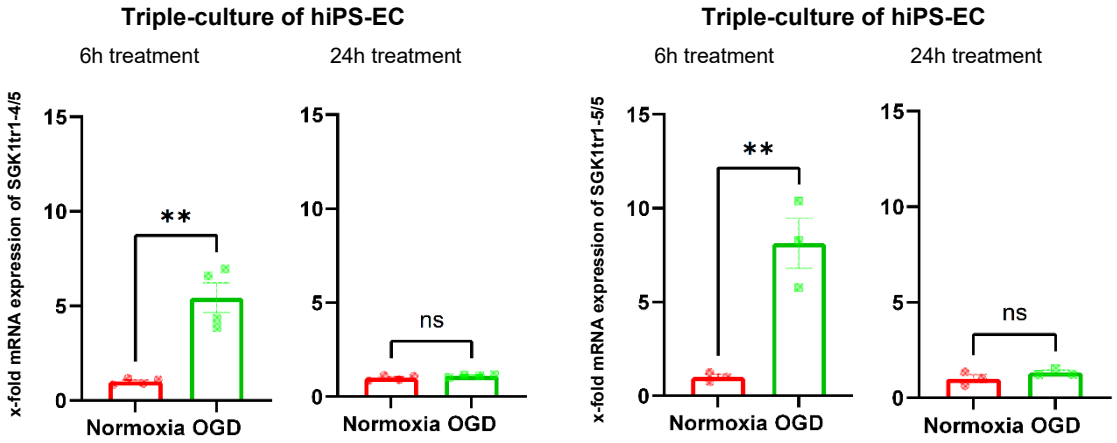

Figure 59: *SGK1* x-fold mRNA expression (shown as bar plots) related to normoxia culture condition in hiPS-EC triple-culture after 5 hours OGD and 19 hours reoxygenation and 5 hours OGD only; Normoxia: Dulbecco´s Modified Eagle´s Medium with glucose (DMEM + G), normoxic conditions 21% O_2, n=3-4; OGD: Dulbecco´s Modified Eagle´s Medium without glucose (DMEM - G), 0.1% O_2 , n=3-4; hiPS-EC triple-culture with human astrocytes and human pericytes; housekeeping gene: *18SrRNA*; ns: p>0.05, *: p≤0.05, **:p≤0.01

4.3.13 *TNKS2* mRNA expression in hiPS-EC after OGD treatment

OGD simulation induced for the duration of 6 hours followed by 18 hours of recovery phase (24 h treatment) resulted in a significant *TNKS2* overexpression at mRNA level (1.55 ± 0.16, p=0.0182).

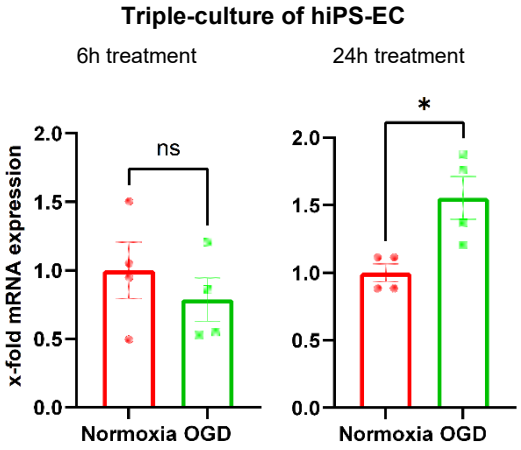

Figure 60: *TNKS2* x-fold mRNA expression (shown as bar plots) related to normoxia culture condition in hiPS-EC triple-culture after 5 hours OGD and 19 hours reoxygenation and 5 hours OGD only; Normoxia: Dulbecco´s Modified Eagle´s Medium with glucose (DMEM + G), normoxic conditions 21% O_2, n=4; OGD: Dulbecco´s Modified Eagle´s Medium without glucose (DMEM - G), 0.1% O_2 , n=4; hiPS-EC triple-culture with human astrocytes and human pericytes; housekeeping gene: *18SrRNA*; ns: p>0.05, *: p≤0.05

4.3.14 Summary of mRNA expression studies with selected targets in hiPS-EC triple-culture with astrocytes and pericytes after OGD treatment

To make a summary of the effect OGD treatment exerted on the mRNA expression of selected regulated targets in hiPS-EC triple-culture with astrocytes and pericytes, expression of all targets was summarised. **Figure 61** shows all OGD values of mRNA expression levels of the respective targets from the two distinct OGD timepoints. Thus, OGD groups seen in the figure below were calibrated to the corresponding normoxic control DMEM+G groups, equal to one.

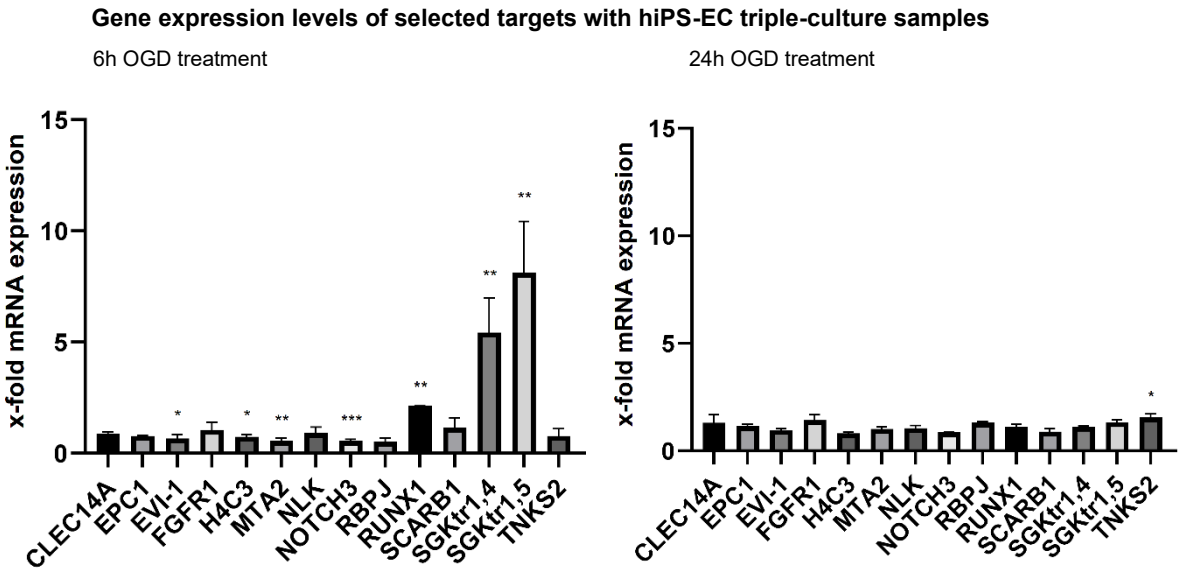

Figure 61: Summary of analysis of selected targets at the mRNA level with triple-culture samples from the two independent differentiations; OGD x-fold values related to normoxia in hiPS-EC triple-culture after 5 hours OGD and 19 hours reoxygenation and 5 hours OGD only; OGD: Dulbecco´s Modified Eagle´s Medium without glucose (DMEM - G), 0.1% O_2, n=2-4; hCMEC/D3 triple-culture with human astrocytes and human pericytes; data are presented as mean ± SEM; housekeeping gene: *18SrRNA*; ns: p>0.05, *: p≤0.05, **:p≤0.01, ***: p≤0.001

4.4 Determination of mRNA expression of selected targets in human TBI biopsy patient samples

Human TBI biopsy samples from four different patients were examined at mRNA level with selected regulated targets. The influence of respective TBIs on gene expression levels of the targets was evaluated. For every patient, four individual samples were taken. Contralateral samples were taken from the contralateral side of the brain, while contusional samples were taken from the injured side of the brain. For each brain side, total brain lysates as well as lysates of isolated capillaries were investigated. Always, the samples from a particular patient were normalized to the contralateral sample of the brain. For sample analysis two endogenous gene controls, namely *B2M* and *PPIA*, were chosen.

4.4.1 *CLEC14A* mRNA expression in human TBI biopsy samples

In respect to housekeeping gene *B2M*, *CLEC14A* was enriched in contralateral capillaries in every patient. Equally, target *CLEC14A* was enriched in contusional capillaries of every patient with exception of the patient 2 with survival time of 4 hours after the TBI. When comparing two total brain samples, *CLEC14A* seemed to be downregulated in patient 1 and patient 4, while upregulated in patient 2 and patient 3. When comparing two capillary samples, *CLEC14A* seemed to be downregulated in patient 1 and 3, while upregulated in patient 2 and 4. To better estimate whether *CLEC14A* was upregulated or downregulated in the capillaries after the respective TBIs, ratios between corresponding x-fold values of the contralateral and contusional capillaries were determined. Calculation of ratios was performed by dividing x-fold value of contusional capillary by the x-fold value of contralateral capillary which was followed by division of the obtained value by the x-fold value of divided contusional brain by the x-fold value of the contralateral brain. Inclusion of the factor derived from the ratio of the two total brain samples allows to include possible different capillary enrichment performance. However, this is only meaningful with the assumption that the target was regulated in all cell types in the total brain in a similar manner. Based on calculated values of ratios, *CLEC14A* mRNA levels were upregulated in patient 4 (ratio = 2.33). *CLEC14A* gene expression levels were on the other hand downregulated in patient 2 (ratio = 0.21) and patient 3 (ratio = 0.66). Determined ratio in patient 1 (ratio = 1.13) suggested no *CLEC14A* gene regulation (**Figure 62**).

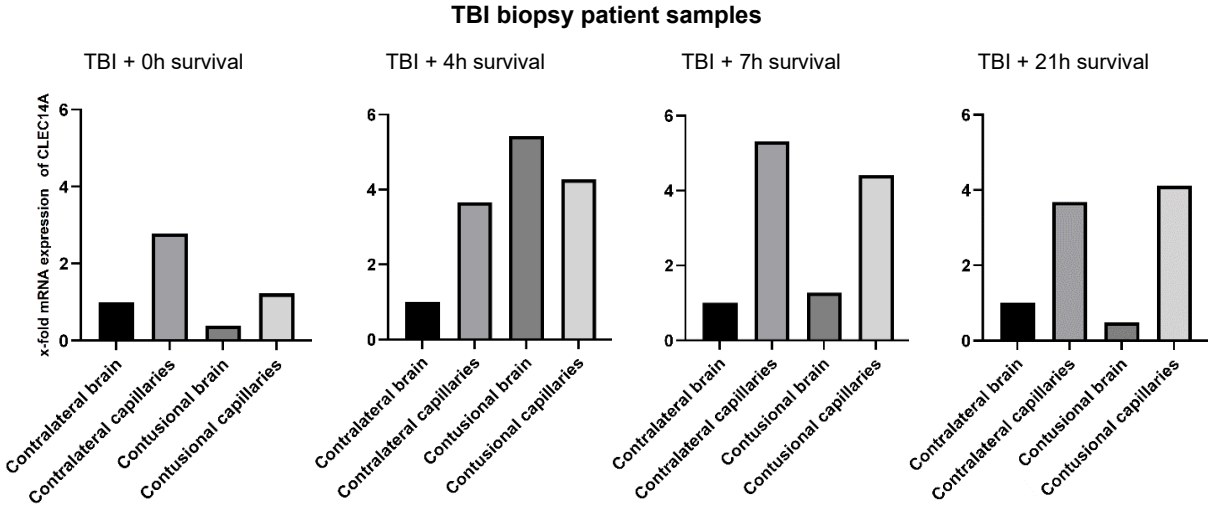

Figure 62: *CLEC14A* mRNA expression (shown as bar plots) in human TBI biopsy patient samples related to contralateral brain – Contralateral brain: contralateral side of the brain, n=1; Contralateral capillaries: contralateral side of the capillaries, n=1; Contusional brain: damaged/injured side of the brain after TBI, n=1; Contusional capillaries: damaged/injured side of the capillaries after TBI, n=1; Patient 1: 0h survival post TBI; Patient 2: 4h survival post TBI; Patient 3: 7h survival post TBI; Patient 4: 21h survival post TBI; housekeeping gene: *B2M*

In respect to housekeeping gene *PPIA*, *CLEC14A* was enriched in contralateral capillaries as well as in contusional capillaries of every patient when compared to specific brain samples. When comparing two total brain samples, *CLEC14A* seemed to be downregulated in patient 1, patient 3, and patient 4, and upregulated in patient 2. When comparing two capillary samples, *CLEC14A* seemed to be downregulated in every patient. Determined ratios of *CLEC14A* at the BBB suggested downregulation of gene expression levels in patient 1 (ratio = 0.59), patient 2 (ratio = 0.04), patient 3 (ratio = 0.58), and also in patient 4 (ratio = 0.50) after TBI (**Figure 63**).

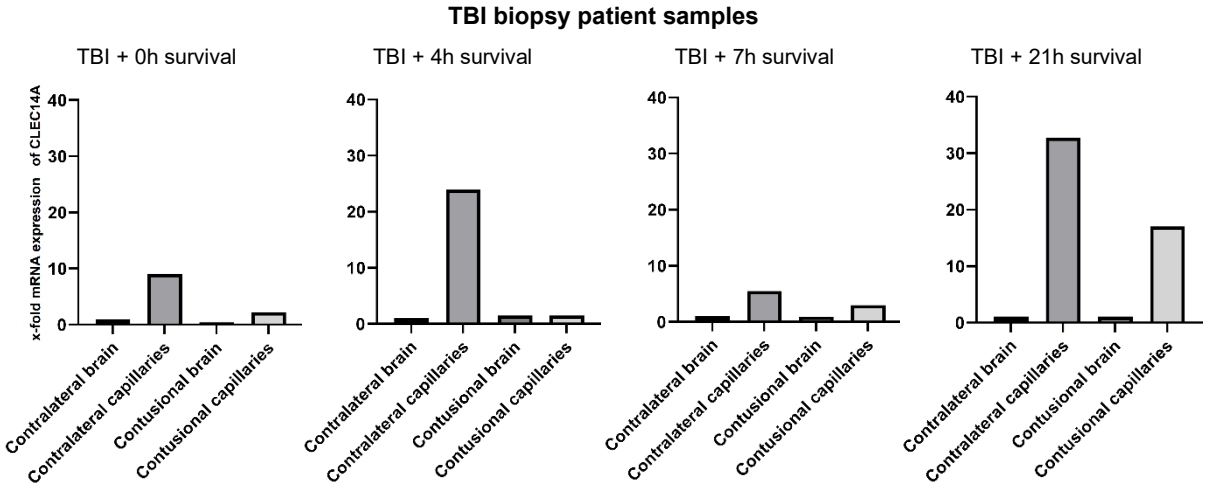

Figure 63: *CLEC14A* mRNA expression (shown as bar plots) in human TBI biopsy patient samples related to contralateral brain – Contralateral brain: contralateral side of the brain, n=1; Contralateral capillaries: contralateral side of the capillaries, n=1; Contusional brain: damaged/injured side of the brain after TBI, n=1; Contusional capillaries: damaged/injured side of the capillaries after TBI, n=1; Patient 1: 0h survival post TBI; Patient 2: 4h survival post TBI; Patient 3: 7h survival post TBI; Patient 4: 21h survival post TBI; housekeeping gene: *PPIA*

4.4.2 *EPC1* mRNA expression in human TBI biopsy samples

With *B2M* as endogenous control, *EPC1* was enriched in contralateral capillaries in patient 1 and patient 3. *EPC1* decreased in contralateral capillaries in patient 2 and patient 4. Moreover, *EPC1* was enriched in contusional capillaries at the BBB in every patient except of the patient 2 where it decreased. When comparing two total brain samples, *EPC1* seemed to be downregulated in patient 1, patient 4, and upregulated in patient 2, and patient 3. When comparing two capillary samples, *EPC1* seemed to be upregulated in every patient. Calculated ratios showed upregulation of *EPC1* in capillaries in patient 1 (ratio = 2.36), patient 3 (ratio = 1.37), and also in patient 4 (ratio = 4.61) after TBI. In patient 2 (ratio = 1.19), *EPC1* did not seem to be regulated (**Figure 64**).

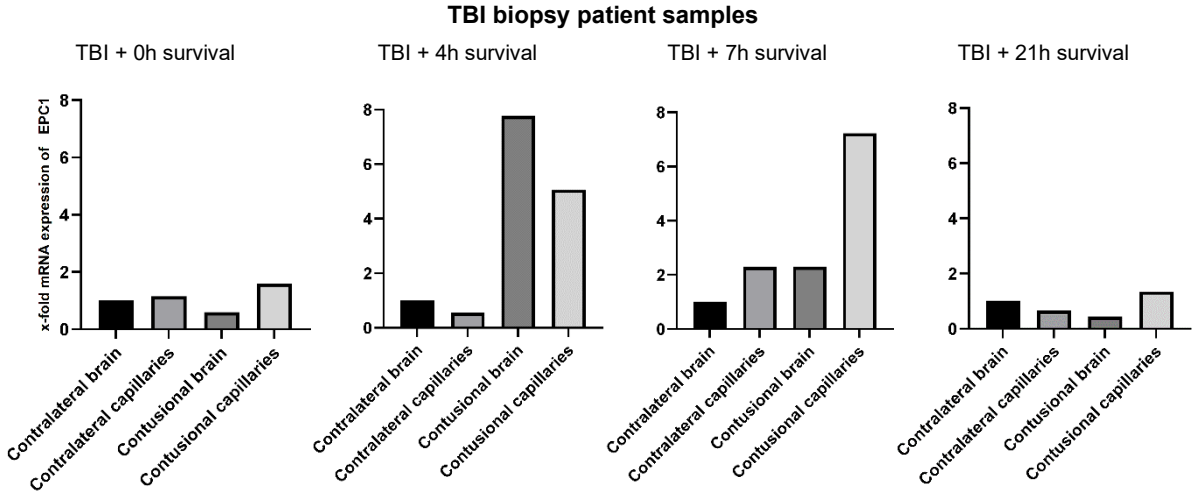

Figure 64: *EPC1* mRNA expression (shown as bar plots) in human TBI biopsy patient samples related to contralateral brain – Contralateral brain: contralateral side of the brain, n=1; Contralateral capillaries: contralateral side of the capillaries, n=1; Contusional brain: damaged/injured side of the brain after TBI, n=1; Contusional capillaries: damaged/injured side of the capillaries after TBI, n=1; Patient 1: 0h survival post TBI; Patient 2: 4h survival post TBI; Patient 3: 7h survival post TBI; Patient 4: 21h survival post TBI; housekeeping gene: *B2M*

With *PPIA* as endogenous control, *EPC1* was enriched in contralateral capillaries of every patient. Equally, *EPC1* was enriched in contusional capillaries of every patient except of the patient 2. When comparing two total brain samples, *EPC1* seemed to be downregulated in patient 1, patient 4, and upregulated in patient 2, and patient 3. When comparing two capillary samples, *EPC1* seemed to be downregulated in patient 1, patient 2, patient 4, and upregulated in patient 3. Based on the determined ratios, *EPC1* mRNA expression was overexpressed in patient 1 (ratio = 1.22) and patient 3 (ratio = 1.20) while remained downregulated in patient 2 (ratio = 0.23) at the BBB post-TBI. Furthermore, *EPC1* did not seem to be regulated in patient 4 (ratio = 0.99) (**Figure 65**).

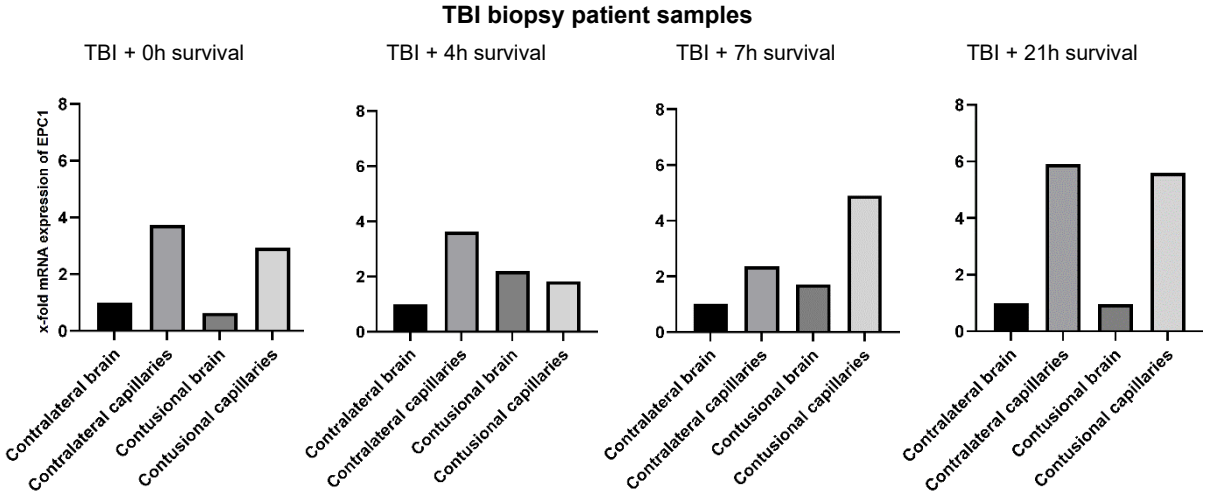

Figure 65: *EPC1* mRNA expression (shown as bar plots) in human TBI biopsy patient samples related to contralateral brain – Contralateral brain: contralateral side of the brain, n=1; Contralateral capillaries: contralateral side of the capillaries, n=1; Contusional brain: damaged/injured side of the brain after TBI, n=1; Contusional capillaries: damaged/injured side of the capillaries after TBI, n=1; Patient 1: 0h survival post TBI; Patient 2: 4h survival post TBI; Patient 3: 7h survival post TBI; Patient 4: 21h survival post TBI; housekeeping gene: *PPIA*

4.4.3 *MECOM* mRNA expression in human TBI biopsy samples

When *B2M* was applied as a housekeeping gene for *MECOM*, target *MECOM* was enriched in contralateral capillaries as well as in contusional capillaries of every patient in comparison to the respective total brain samples. When comparing two total brain samples, *MECOM* was upregulated in patient 1, patient 2, and downregulated in patient 3, and patient 4. When comparing two capillary samples, *MECOM* was downregulated in every patient with the exception of patient 4. Determined ratios demonstrated decrease of *MECOM* x-fold change values in patient 1 (ratio = 0.40), patient 2 (ratio = 0.74), and patient 3 (ratio = 0.33). Increase of *MECOM* mRNA levels was recorded in patient 4 (ratio = 1.64) (**Figure 66**).

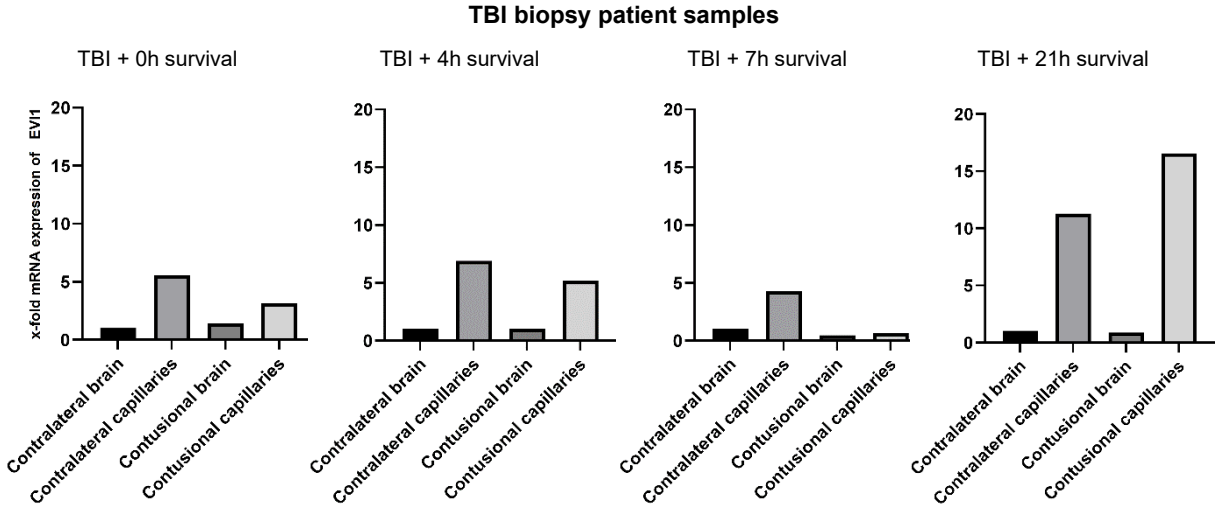

Figure 66: *MECOM* mRNA expression (shown as bar plots) in human TBI biopsy patient samples related to contralateral brain – Contralateral brain: contralateral side of the brain, n=1; Contralateral capillaries: contralateral side of the capillaries, n=1; Contusional brain: damaged/injured side of the brain after TBI, n=1; Contusional capillaries: damaged/injured side of the capillaries after TBI, n=1; Patient 1: 0h survival post TBI; Patient 2: 4h survival post TBI; Patient 3: 7h survival post TBI; Patient 4: 21h survival post TBI; housekeeping gene: *B2M*

When *PPIA* was selected as a housekeeping gene for *MECOM*, target *MECOM* was enriched in contralateral capillaries as well as in contusional capillaries of every patient in comparison to the corresponding total brain samples. When comparing two total brain samples, *MECOM* was upregulated in patient 1, patient 4, and downregulated in patient 2, and patient 3. When comparing two capillary samples, *MECOM* seemed to be downregulated in every patient. Calculated ratios displayed downregulation of *MECOM* gene expression values in patient 1 (ratio = 0.17), patient 2 (ratio = 0.58), patient 3 (ratio = 0.18), and patient 4 (ratio = 0.28) at the BBB after the respective TBIs (**Figure 67**).

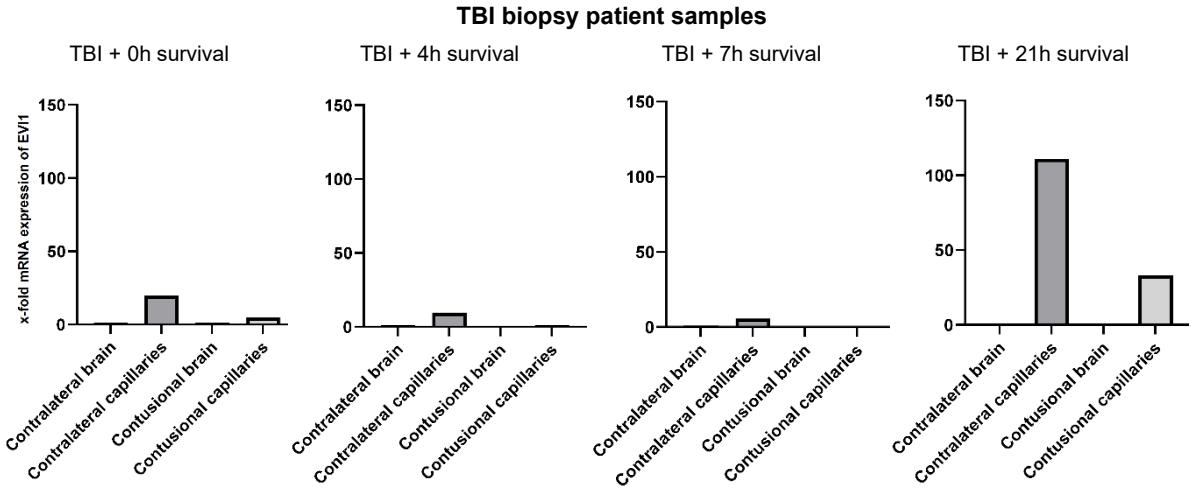

Figure 67: *MECOM* mRNA expression (shown as bar plots) in human TBI biopsy patient samples related to contralateral brain – Contralateral brain: contralateral side of the brain, n=1; Contralateral capillaries: contralateral side of the capillaries, n=1; Contusional brain: damaged/injured side of the brain after TBI, n=1; Contusional capillaries: damaged/injured side of the capillaries after TBI, n=1; Patient 1: 0h survival post TBI; Patient 2: 4h survival post TBI; Patient 3: 7h survival post TBI; Patient 4: 21h survival post TBI; housekeeping gene: *PPIA*

4.4.4 *FGFR1* mRNA expression in human TBI biopsy samples

Using *B2M*, target *FGFR1* decreased in contralateral capillaries and contusional capillaries of every patient. When comparing two total brain samples, *FGFR1* was upregulated in patient 1, patient 2, and downregulated in patient 3, and patient 4. When comparing two capillary samples, *FGFR1* was downregulated in patient 1, patient 3, and upregulated in patient 2, and patient 4. Based on determined ratios, *FGFR1* was downregulated at the BBB after TBI in patient 1 (ratio = 0.62) and upregulated in patient 2 (ratio = 2.63), and patient 4 (ratio = 2.00). *FGFR1* seemed to be not regulated in patient 3 (ratio = 1.19) (**Figure 68**).

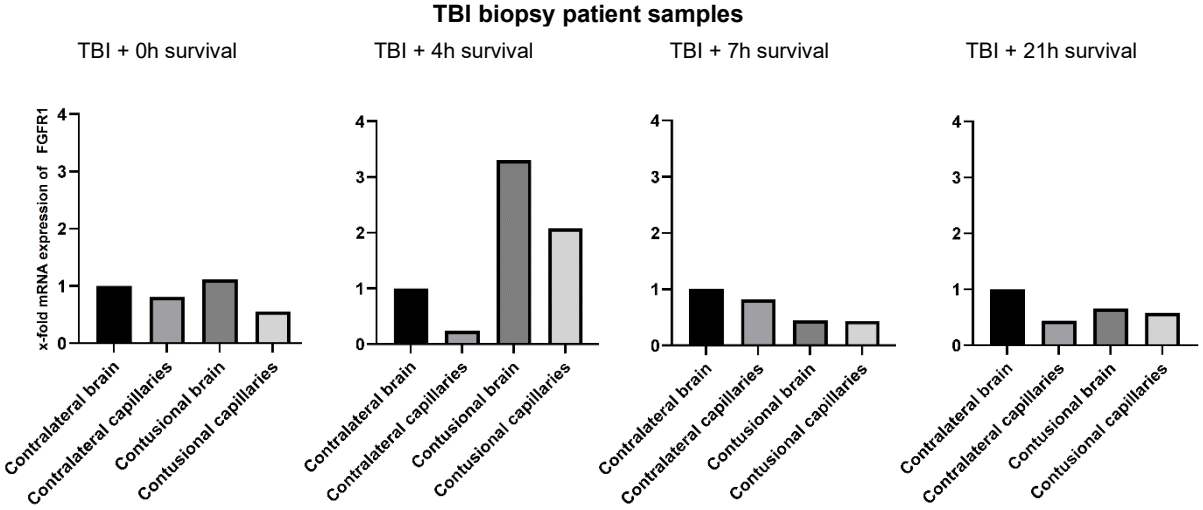

Figure 68: *FGFR1* mRNA expression (shown as bar plots) in human TBI biopsy patient samples related to contralateral brain – Contralateral brain: contralateral side of the brain, n=1; Contralateral capillaries: contralateral side of the capillaries, n=1; Contusional brain: damaged/injured side of the brain after TBI, n=1; Contusional capillaries: damaged/injured side of the capillaries after TBI, n=1; Patient 1: 0h survival post TBI; Patient 2: 4h survival post TBI; Patient 3: 7h survival post TBI; Patient 4: 21h survival post TBI; housekeeping gene: *B2M*

Using *PPIA, FGFR1* was enriched in contralateral capillaries in every patient except of the patient 3 where it decreased. Also, target *FGFR1* decreased in contusional capillaries in every patient except of the patient 4 where it was enriched. When comparing two total brain samples, *FGFR1* was upregulated in patient 1, patient 4, and downregulated in patient 2, and patient 3. When comparing two capillary samples, *FGFR1* was downregulated in every patient. Ratios depicted downregulation of *FGFR1* in patient 1 (ratio = 0.33), patient 2 (ratio = 0.52), and patient 4 (ratio = 0.43). *FGFR1* was observed not to be regulated in patient 3 (ratio = 1.05) (**Figure 69**).

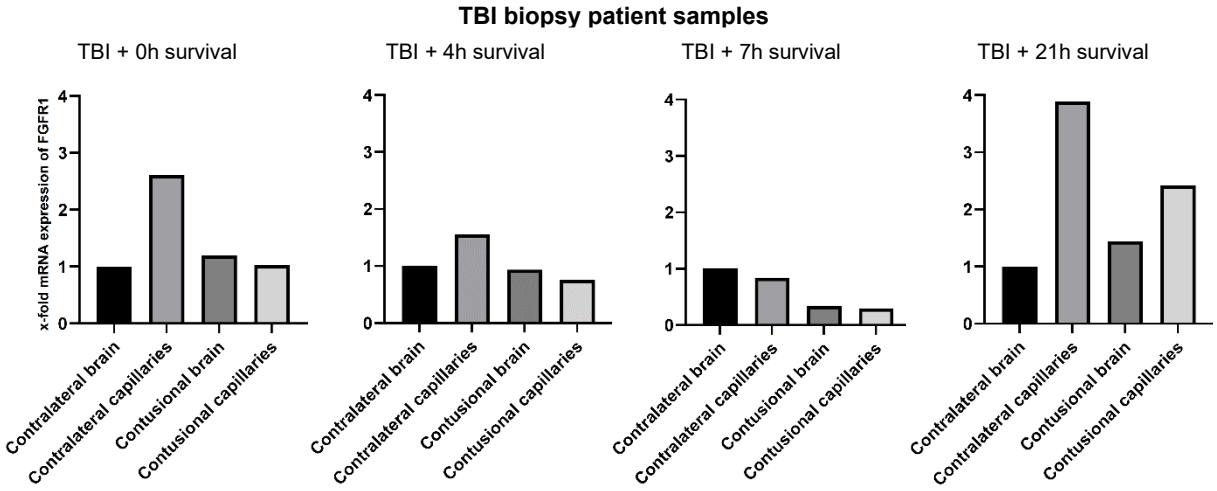

Figure 69: *FGFR1* mRNA expression (shown as bar plots) in human TBI biopsy patient samples related to contralateral brain – Contralateral brain: contralateral side of the brain, n=1; Contralateral capillaries: contralateral side of the capillaries, n=1; Contusional brain: damaged/injured side of the brain after TBI, n=1; Contusional capillaries: damaged/injured side of the capillaries after TBI, n=1; Patient 1: 0h survival post TBI; Patient 2: 4h survival post TBI; Patient 3: 7h survival post TBI; Patient 4: 21h survival post TBI; housekeeping gene: *PPIA*

4.4.5 *H4C3* mRNA expression in human TBI biopsy samples

With *B2M*, both contralateral and contusional capillaries decreased in *H4C3* expression in every patient when compared with corresponding total brain samples. When comparing two total brain samples, *H4C3* was upregulated in every patient with the exception of patient 4. When comparing two capillary samples, *H4C3* was upregulated in every patient. After additional normalization that included calculation of ratios when comprising also ratio of the two total brain samples, *H4C3* was observed to be downregulated in patient 1 (ratio = 0.72) at the level of capillaries. Also, *H4C3* mRNA expression was upregulated in patient 2 (ratio = 2.43), patient 3 (ratio = 1.63), and patient 4 (ratio = 2.36) (**Figure 70**).

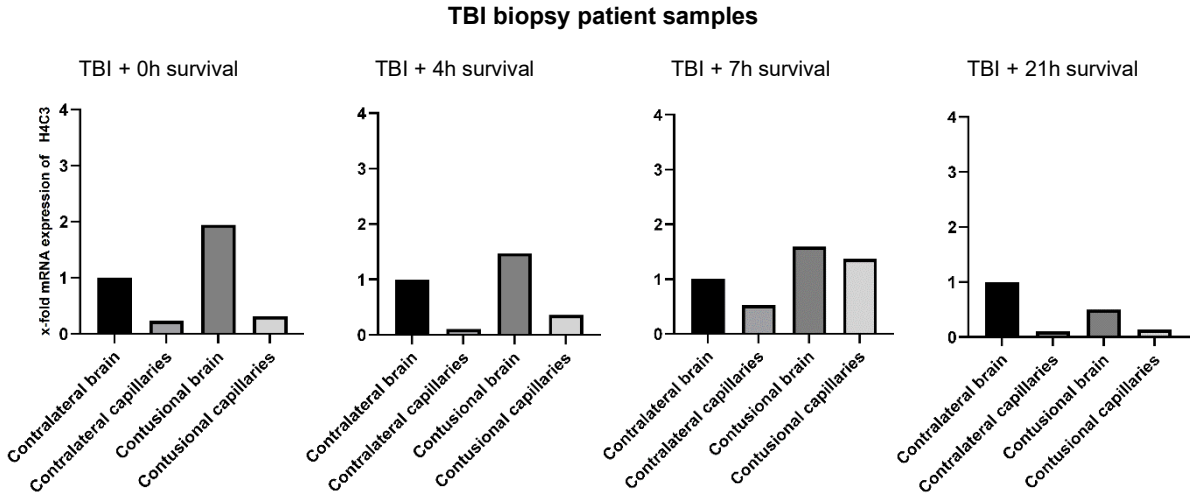

Figure 70: *H4C3* mRNA expression (shown as bar plots) in human TBI biopsy patient samples related to contralateral brain – Contralateral brain: contralateral side of the brain, n=1; Contralateral capillaries: contralateral side of the capillaries, n=1; Contusional brain: damaged/injured side of the brain after TBI, n=1; Contusional capillaries: damaged/injured side of the capillaries after TBI, n=1; Patient 1: 0h survival post TBI; Patient 2: 4h survival post TBI; Patient 3: 7h survival post TBI; Patient 4: 21h survival post TBI; housekeeping gene: *B2M*

With *PPIA*, both contralateral and contusional capillaries decreased in *H4C3* expression in every patient. When comparing two total brain samples independently, *H4C3* was upregulated in every patient with the exception of patient 2. When comparing two capillary samples, *H4C3* was downregulated in every patient with the exception of patient 3. With regard to determined ratios, *H4C3* gene expression was overexpressed in patient 3 (ratio = 1.45). Equally, *H4C3* mRNA expression decreased in patient 1 (ratio = 0.37), patient 2 (ratio = 0.45), and patient 4 (ratio = 0.53) (**Figure 71**).

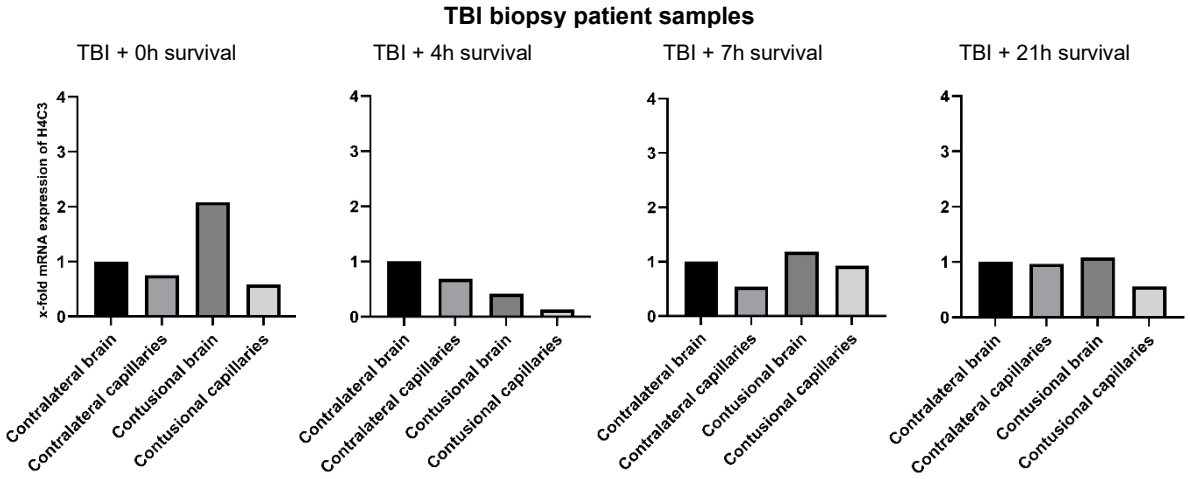

Figure 71: *H4C3* mRNA expression (shown as bar plots) in human TBI biopsy patient samples related to contralateral brain – Contralateral brain: contralateral side of the brain, n=1; Contralateral capillaries: contralateral side of the capillaries, n=1; Contusional brain: damaged/injured side of the brain after TBI, n=1; Contusional capillaries: damaged/injured side of the capillaries after TBI, n=1; Patient 1: 0h survival post TBI; Patient 2: 4h survival post TBI; Patient 3: 7h survival post TBI; Patient 4: 21h survival post TBI; housekeeping gene: *PPIA*

4.4.6 *MTA2* mRNA expression in human TBI biopsy samples

In respect to *B2M* as selected endogenous control, *MTA2* decreased in contralateral capillaries of patient 1, patient 2, and patient 4. MTA2 was enriched in contralateral capillaries of patient 2 as well as in contusional capillaries of patient 4. Furthermore, target *MTA2* decreased in the contusional capillaries of patient 1, patient 2, and patient 3. When comparing two total brain samples independently, *MTA2* was upregulated in patient 1, patient 2, and downregulated in patient 3, and patient 4. When comparing two capillary samples, *MTA2* was upregulated in patient 1, patient 4, and downregulated in patient 2, and patient 3. Determined ratios suggest decreased *MTA2* mRNA expression in patient 2 (ratio = 0.26). Increased *MTA2* gene expression was observed in patient 3 (ratio = 1.20) and in patient 4 (ratio = 1.63). *MTA2* seemed not to be regulated in patient 1 (ratio = 0.92) (**Figure 72**).

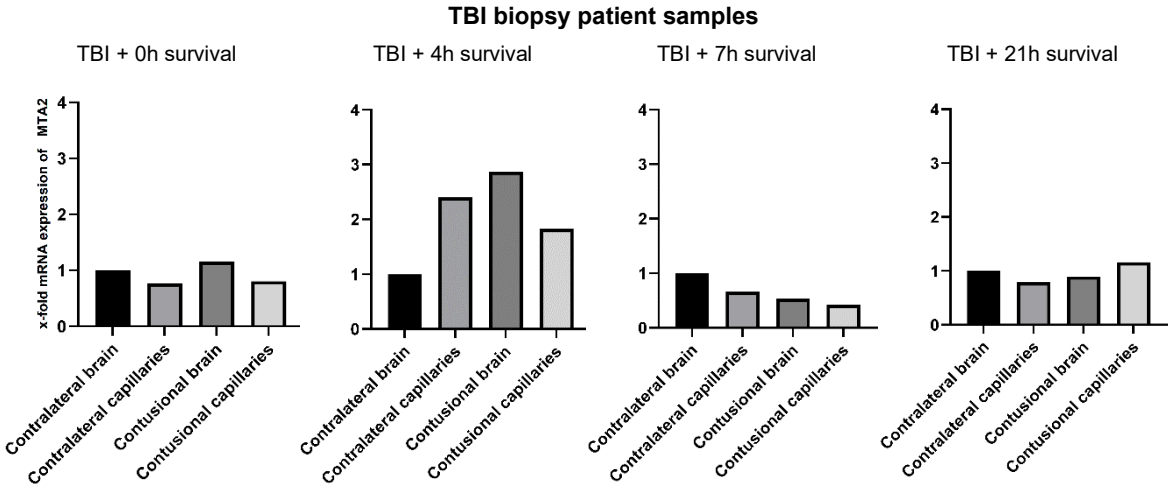

Figure 72: *MTA2* mRNA expression (shown as bar plots) in human TBI biopsy patient samples related to contralateral brain – Contralateral brain: contralateral side of the brain, n=1; Contralateral capillaries: contralateral side of the capillaries, n=1; Contusional brain: damaged/injured side of the brain after TBI, n=1; Contusional capillaries: damaged/injured side of the capillaries after TBI, n=1; Patient 1: 0h survival post TBI; Patient 2: 4h survival post TBI; Patient 3: 7h survival post TBI; Patient 4: 21h survival post TBI; housekeeping gene: *B2M*

In respect to *PPIA* as selected endogenous control, *MTA2* decreased in contralateral capillaries in patient 3 and enriched in patient 1, patient 2, and patient 4. *MTA2* decreased in contusional capillaries in patient 2 and patient 3. Moreover, *MTA2* was enriched in contusional capillaries in patient 1 and patient 4. When comparing two total brain samples, *MTA2* was upregulated in patient 1, patient 4, and downregulated in patient 2, and patient 3. When comparing two capillary samples, *MTA2* was downregulated in every patient. Calculated ratios showed a decrease in *MTA2* mRNA expression in patient 1 (ratio = 0.38), patient 2 (ratio = 0.21), patient 3 (ratio = 0.65), and also in patient 4 (ratio = 0.28) (**Figure 73**).

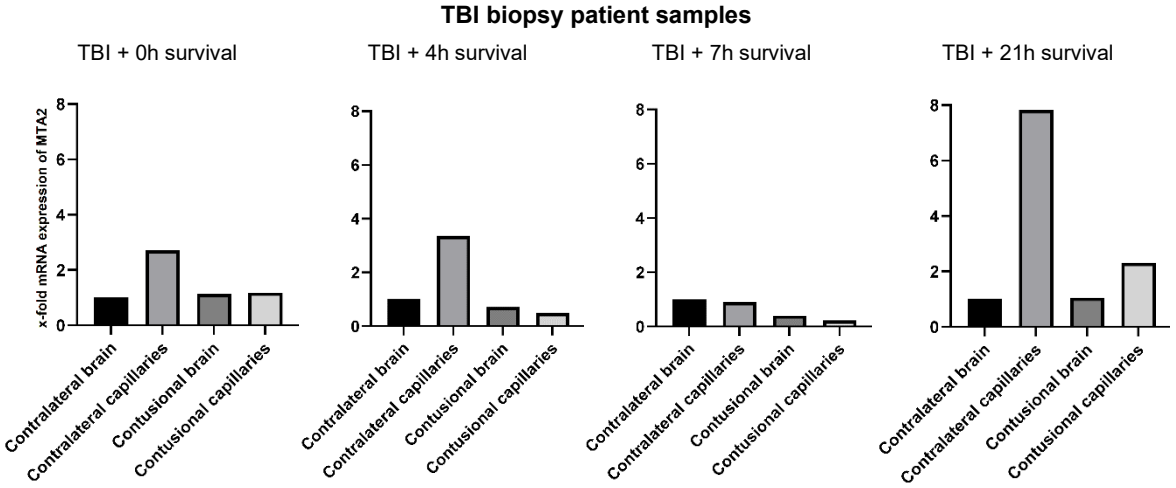

Figure 73: *MTA2* mRNA expression (shown as bar plots) in human TBI biopsy patient samples related to contralateral brain – Contralateral brain: contralateral side of the brain, n=1; Contralateral capillaries: contralateral side of the capillaries, n=1; Contusional brain: damaged/injured side of the brain after TBI, n=1; Contusional capillaries: damaged/injured side of the capillaries after TBI, n=1; Patient 1: 0h survival post TBI; Patient 2: 4h survival post TBI; Patient 3: 7h survival post TBI; Patient 4: 21h survival post TBI; housekeeping gene: *PPIA*

4.4.7 *NLK* mRNA expression in human TBI biopsy samples

With *B2M*, *NLK* decreased in contralateral as well as contusional capillaries in every patient when compared with respective total brain samples. When comparing two total brain samples, *NLK* was upregulated in every patient with the exception of patient 3. When comparing two capillary samples, *NLK* was downregulated in every patient with the exception of patient 4. Calculated ratios demonstrated downregulation of *NLK* mRNA expression in patient 1 (ratio = 0.28), patient 2 (ratio = 0.23), and patient 3 (ratio = 0.91) at the BBB after TBI. *NLK* upregulation was observed in patient 4 (ratio = 1.50) (**Figure 74**).

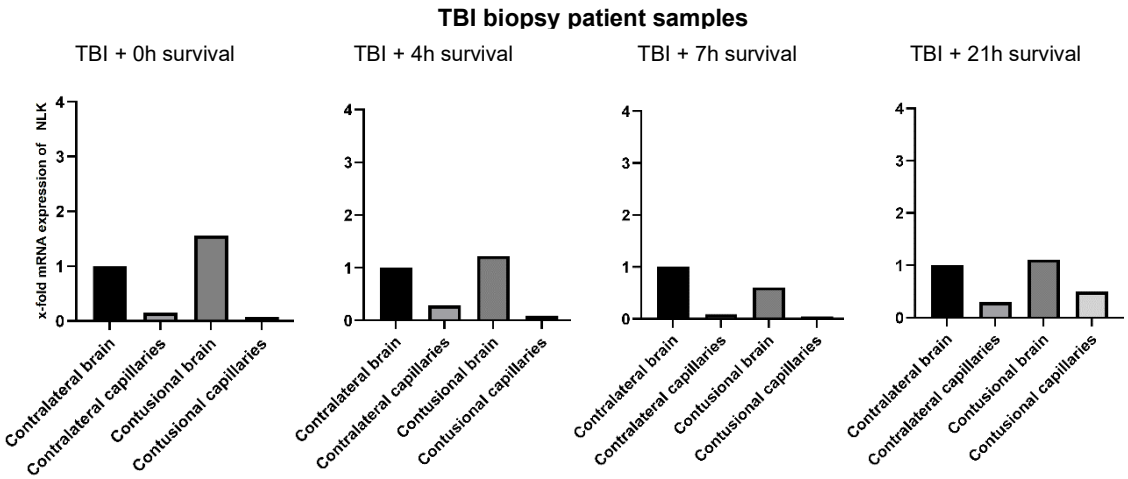

Figure 74: *NLK* mRNA expression (shown as bar plots) in human TBI biopsy patient samples related to contralateral brain – Contralateral brain: contralateral side of the brain, n=1; Contralateral capillaries: contralateral side of the capillaries, n=1; Contusional brain: damaged/injured side of the brain after TBI, n=1; Contusional capillaries: damaged/injured side of the capillaries after TBI, n=1; Patient 1: 0h survival post TBI; Patient 2: 4h survival post TBI; Patient 3: 7h survival post TBI; Patient 4: 21h survival post TBI; housekeeping gene: *B2M*

With *PPIA*, *NLK* decreased in contralateral as well as contusional capillaries in every patient except of the contralateral capillaries in patient 4 where *NLK* was enriched. When comparing two total brain samples independently, *NLK* was upregulated in patient 1, patient 4, and downregulated in patient 2, and patient 3. When comparing two capillary samples, *NLK* was downregulated in every patient. Based on the determined ratios, *NLK* mRNA expression decreased in patient 1 (ratio = 0.13), patient 2 (ratio = 0.17), patient 3 (ratio = 0.54), and also in patient 4 (ratio = 0.26) (**Figure 75**).

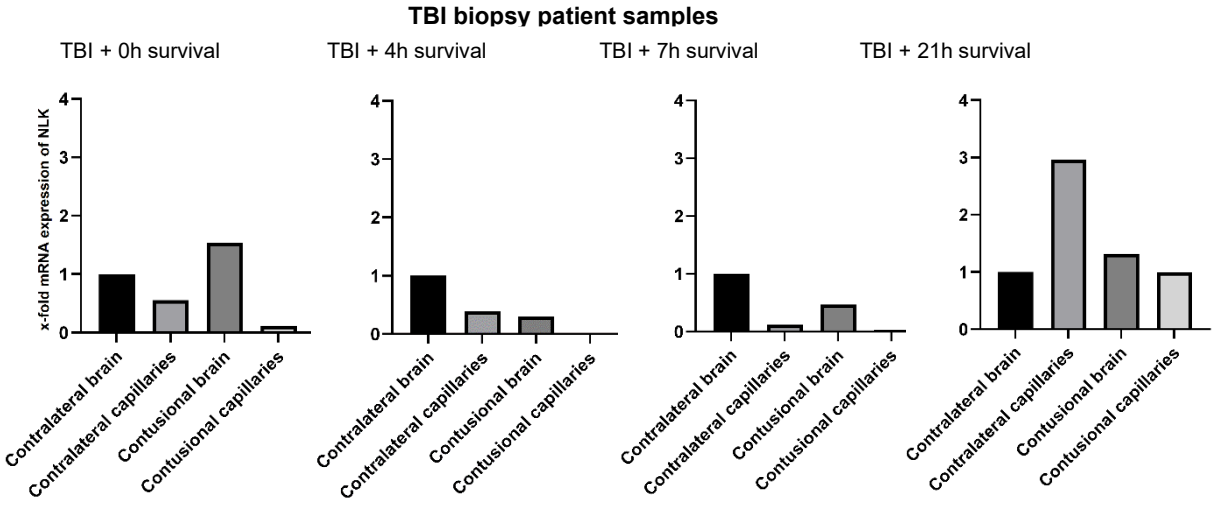

Figure 75: *NLK* mRNA expression (shown as bar plots) in human TBI biopsy patient samples related to contralateral brain – Contralateral brain: contralateral side of the brain, n=1; Contralateral capillaries: contralateral side of the capillaries, n=1; Contusional brain: damaged/injured side of the brain after TBI, n=1; Contusional capillaries: damaged/injured side of the capillaries after TBI, n=1; Patient 1: 0h survival post TBI; Patient 2: 4h survival post TBI; Patient 3: 7h survival post TBI; Patient 4: 21h survival post TBI; housekeeping gene: *PPIA*

4.4.8 *NOTCH3* mRNA expression in human TBI biopsy samples

Using *B2M* as housekeeping gene, target *NOTCH3* was enriched in both contralateral and contusional capillaries in every patient in comparison to the corresponding brain samples. When comparing two total brain samples, *NOTCH3* seemed to be upregulated in patient 1, patient 4, and downregulated in patient 2, and patient 3. When comparing two capillary samples, *NOTCH3* seemed to be downregulated in every patient with the exception of patient 4. Moreover, *NOTCH3* mRNA expression was observed to be downregulated in the capillaries after the TBI in patient 1 (ratio = 0.20) and patient 2 (ratio = 0.59). *NOTCH3* gene expression increased in the capillaries after the TBI in patient 3 (ratio = 2.90) and patient 4 (ratio = 1.53) (**Figure 76**).

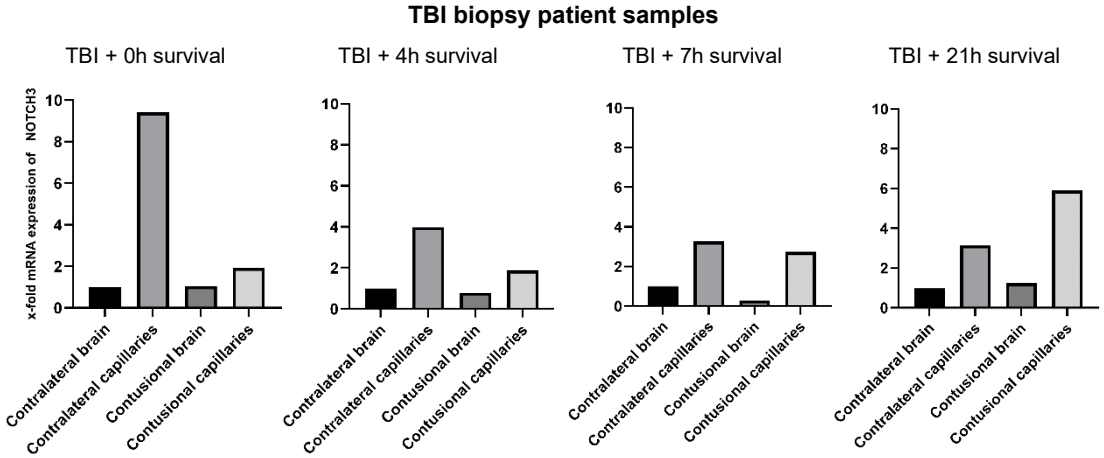

Figure 76: *NOTCH3* mRNA expression (shown as bar plots) in human TBI biopsy patient samples related to contralateral brain – Contralateral brain: contralateral side of the brain, n=1; Contralateral capillaries: contralateral side of the capillaries, n=1; Contusional brain: damaged/injured side of the brain after TBI, n=1; Contusional capillaries: damaged/injured side of the capillaries after TBI, n=1; Patient 1: 0h survival post TBI; Patient 2: 4h survival post TBI; Patient 3: 7h survival post TBI; Patient 4: 21h survival post TBI; housekeeping gene: *B2M*

Using *PPIA* as housekeeping gene, *NOTCH3* was enriched in both contralateral and contusional capillaries in every patient. When comparing two total brain samples, *NOTCH3* seemed to be upregulated in patient 1, patient 4, and downregulated in patient 2, and patient 3. When comparing two capillary samples, *NOTCH3* seemed to be downregulated in every patient. Based on determined ratios, *NOTCH3* x-fold values decreased in patient 1 (ratio = 0.08), patient 2 (ratio = 0.45), and patient 4 (ratio = 0.26) in the capillaries at the BBB post-TBI. *NOTCH3* gene expression increase was recorded in patient 3 (ratio = 1.58) (**Figure 77**).

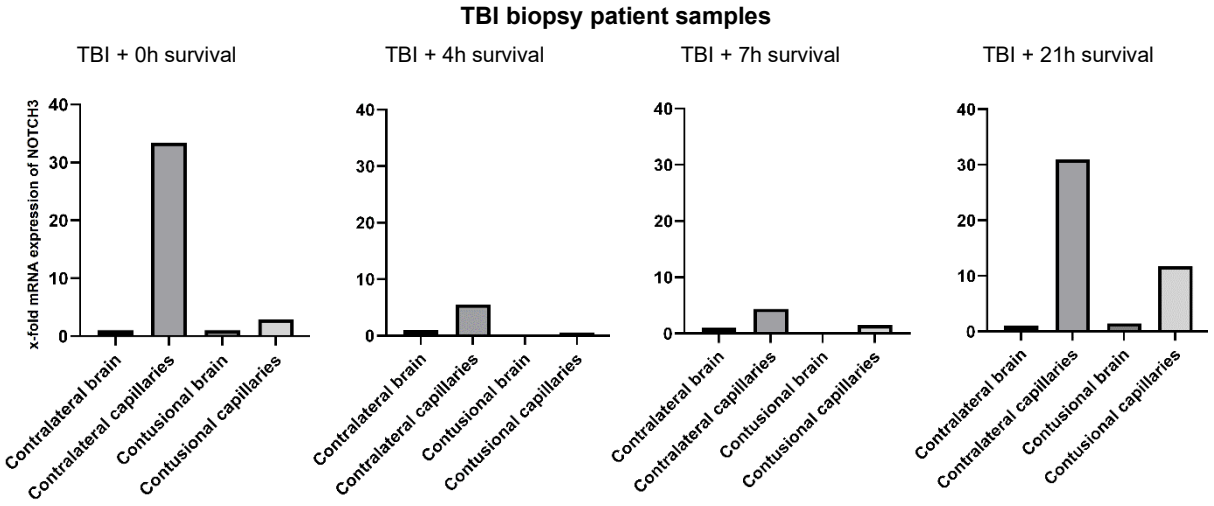

Figure 77: *NOTCH3* mRNA expression (shown as bar plots) in human TBI biopsy patient samples related to contralateral brain – Contralateral brain: contralateral side of the brain, n=1; Contralateral capillaries: contralateral side of the capillaries, n=1; Contusional brain: damaged/injured side of the brain after TBI, n=1; Contusional capillaries: damaged/injured side of the capillaries after TBI, n=1; Patient 1: 0h survival post TBI; Patient 2: 4h survival post TBI; Patient 3: 7h survival post TBI; Patient 4: 21h survival post TBI; housekeeping gene: *PPIA*

4.4.9 *RBPJ* mRNA expression in human TBI biopsy samples

When *B2M* was applied, interestingly *RBPJ* decreased in contralateral capillaries of every patient in respect to the contralateral brain samples. Target *RBPJ* was enriched in contusional capillaries of every patient except of the patient 3 where it decreased. When comparing two total brain samples, *RBPJ* seemed to be downregulated in patient 1, patient 4, and upregulated in patient 2, and patient 3. When comparing two capillary samples, *RBPJ* seemed to be upregulated in every patient. After additional normalization step, obtained ratios between contralateral and contusional capillaries suggested upregulation of *RBPJ* mRNA expression at the BBB after the TBI in patient 1 (ratio = 4.27), patient 2 (ratio = 1.49), and patient 4 (ratio = 6.43). Slight *RBPJ* mRNA expression decrease was recorded in patient 3 (ratio = 0.80) (**Figure 78**).

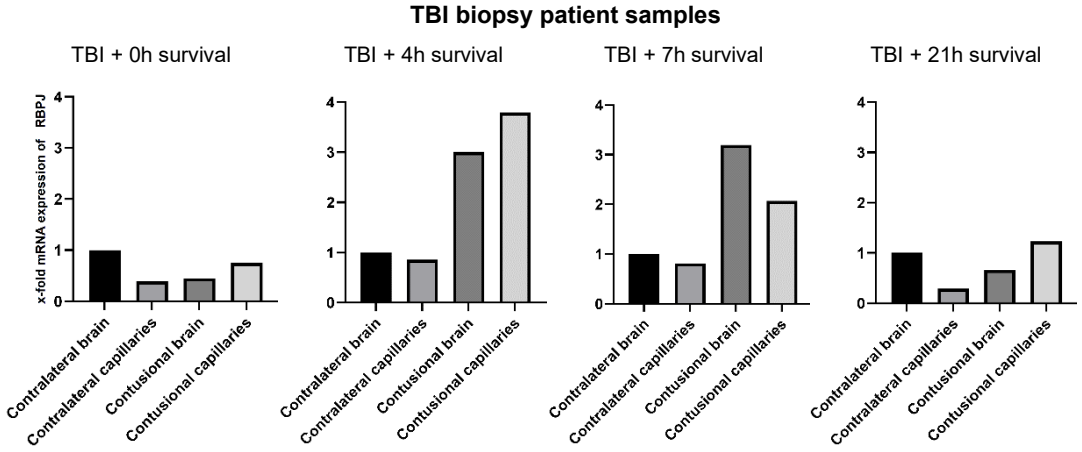

Figure 78: *RBPJ* mRNA expression (shown as bar plots) in human TBI biopsy patient samples related to contralateral brain – Contralateral brain: contralateral side of the brain, n=1; Contralateral capillaries: contralateral side of the capillaries, n=1; Contusional brain: damaged/injured side of the brain after TBI, n=1; Contusional capillaries: damaged/injured side of the capillaries after TBI, n=1; Patient 1: 0h survival post TBI; Patient 2: 4h survival post TBI; Patient 3: 7h survival post TBI; Patient 4: 21h survival post TBI; housekeeping gene: *B2M*

When *PPIA* was applied, *RBPJ* was enriched in contralateral and contusional capillaries of every patient except of the contusional capillaries of patient 3 where target *RBPJ* decreased. When comparing two total brain samples, *RBPJ* seemed to be downregulated in every patient with the exception of patient 3. When comparing two capillary samples, *RBPJ* seemed to be downregulated in every patient with the exception of patient 3 where rather no *RBPJ* gene regulation was observed. Capillary ratios demonstrated *RBPJ* mRNA overexpression at the BBB after the TBI in patient 1 (ratio = 1.80). No *RBPJ* gene regulation was observed in patient 2 (ratio = 1.13) and patient 4 (ratio = 1.11). Furthermore, *RBPJ* mRNA expression downregulation was observed in patient 3 (ratio = 0.43) (**Figure 79**).

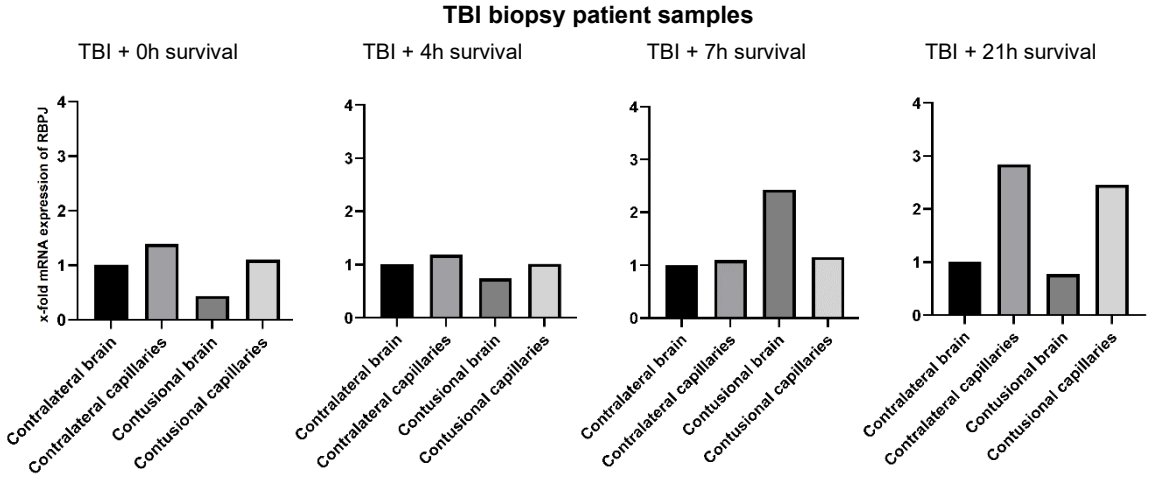

Figure 79: *RBPJ* mRNA expression (shown as bar plots) in human TBI biopsy patient samples related to contralateral brain – Contralateral brain: contralateral side of the brain, n=1; Contralateral capillaries: contralateral side of the capillaries, n=1; Contusional brain: damaged/injured side of the brain after TBI, n=1; Contusional capillaries: damaged/injured side of the capillaries after TBI, n=1; Patient 1: 0h survival post TBI; Patient 2: 4h survival post TBI; Patient 3: 7h survival post TBI; Patient 4: 21h survival post TBI; housekeeping gene: *PPIA*

4.4.10 *RUNX1* mRNA expression in human TBI biopsy samples

When using *B2M* as endogenous control for *RUNX1*, target *RUNX1* was not detected in every experimental condition. However, derichment of *RUNX1* was recorded in contralateral capillaries of patient 2, patient 3, and patient 4 as well as in contusional capillaries of patient 4. When comparing two total brain samples, *RUNX1* seemed to be upregulated in patient 1, patient 4, and downregulated in patient 3. When comparing two capillary samples, *RUNX1* seemed to be downregulated in patient 2 and upregulated in patient 4. After additional normalization step, determined ratio between contralateral and contusional capillaries in patient 4 showed *RUNX1* mRNA expression upregulation (ratio = 3.01) (**Figure 80**).

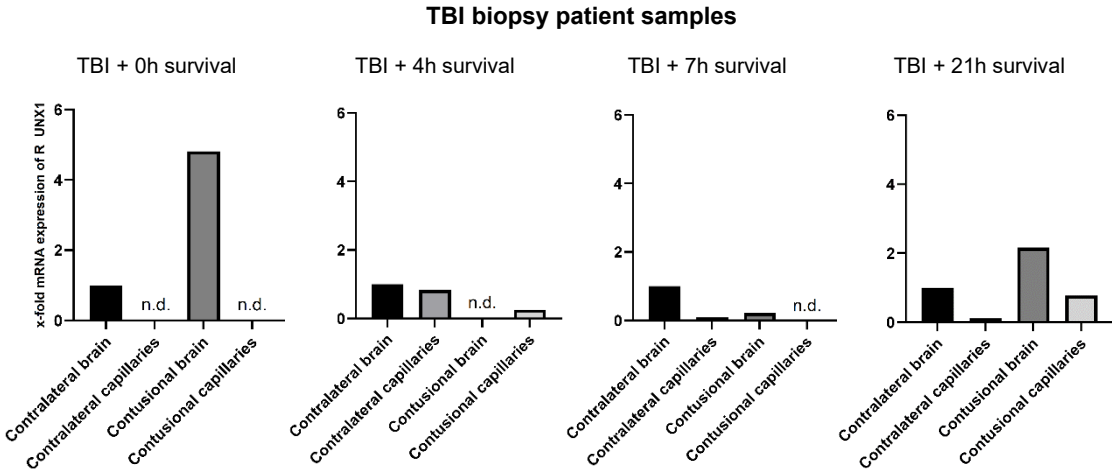

Figure 80: *RUNX1* mRNA expression (shown as bar plots) in human TBI biopsy patient samples related to contralateral brain – Contralateral brain: contralateral side of the brain, n=1; Contralateral capillaries: contralateral side of the capillaries, n=1; Contusional brain: damaged/injured side of the brain after TBI, n=1; Contusional capillaries: damaged/injured side of the capillaries after TBI, n=1; Patient 1: 0h survival post TBI; Patient 2: 4h survival post TBI; Patient 3: 7h survival post TBI; Patient 4: 21h survival post TBI; n.d. = not detectable; housekeeping gene: *B2M*

When using *PPIA* as endogenous control, detected *RUNX1* was enriched in contralateral capillaries of patient 2 and patient 4. Also, *RUNX1* decreased in contralateral capillaries of patient 3 and contusional capillaries of patient 4. When comparing two total brain samples, *RUNX1* seemed to be upregulated in patient 1, patient 4, and downregulated in patient 3. When comparing two capillary samples, *RUNX1* seemed to be downregulated in patient 2 and upregulated in patient 4. Based on calculated ratios, *RUNX1* mRNA expression was downregulated in patient 4 (ratio = 0.50) at the BBB after TBI (**Figure 81**).

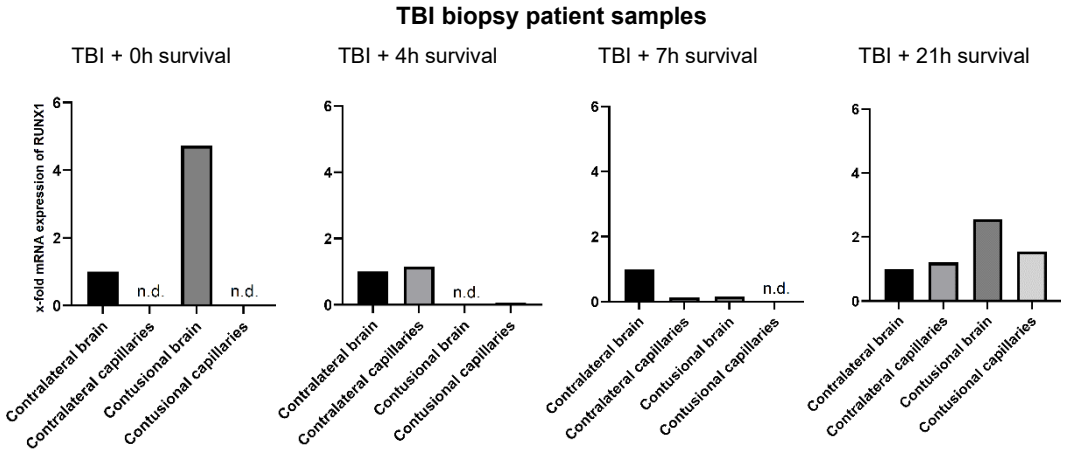

Figure 81: *RUNX1* mRNA expression (shown as bar plots) in human TBI biopsy patient samples related to contralateral brain – Contralateral brain: contralateral side of the brain, n=1; Contralateral capillaries: contralateral side of the capillaries, n=1; Contusional brain: damaged/injured side of the brain after TBI, n=1; Contusional capillaries: damaged/injured side of the capillaries after TBI, n=1; Patient 1: 0h survival post TBI; Patient 2: 4h survival post TBI; Patient 3: 7h survival post TBI; Patient 4: 21h survival post TBI; n.d. = not detected; housekeeping gene: *PPIA*

4.4.11 *SCARB1* mRNA expression in human TBI biopsy samples

With *B2M* as housekeeping gene, *SCARB1* was enriched in contralateral capillaries of every patient when compared with respective total brain samples. Equally, *SCARB1* was enriched in contusional capillaries of patient 2 and patient 4 as well as decreased in contusional capillaries of patient 1 and patient 3. When comparing two total brain samples, *SCARB1* seemed to be downregulated in every patient with the exception of patient 1. When comparing two capillary samples, *SCARB1* seemed to be downregulated in every patient with the exception of patient 4. Determined ratios between contralateral and contusional capillaries revealed decrease in *SCARB1* mRNA expression at the BBB after the TBI in patient 1 (ratio = 0.23), patient 2 (ratio

= 0.60), and patient 3 (ratio = 0.15). In patient 4, *SCARB1* was overexpressed (ratio = 1.52) (**Figure 82**).

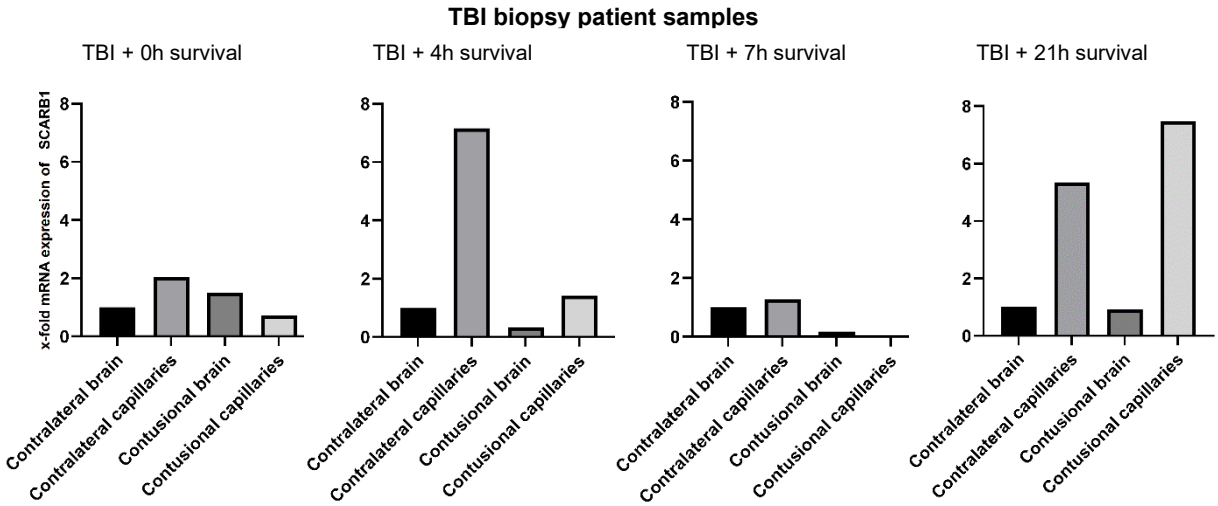

Figure 82: *SCARB1* mRNA expression (shown as bar plots) in human TBI biopsy patient samples related to contralateral brain – Contralateral brain: contralateral side of the brain, n=1; Contralateral capillaries: contralateral side of the capillaries, n=1; Contusional brain: damaged/injured side of the brain after TBI, n=1; Contusional capillaries: damaged/injured side of the capillaries after TBI, n=1; Patient 1: 0h survival post TBI; Patient 2: 4h survival post TBI; Patient 3: 7h survival post TBI; Patient 4: 21h survival post TBI; housekeeping gene: *B2M*

With *PPIA* as housekeeping gene, *SCARB1* was enriched in contralateral capillaries of every patient. In respect to contusional capillaries, *SCARB1* decreased in patient 1 and patient 3 as well as enriched in patient 2 and patient 4. When comparing two total brain samples, *SCARB1* seemed to be upregulated in patient 1, downregulated in patient 2, patient 3, as well as not regulated in patient 4. When comparing two capillary samples, *SCARB1* seemed to be downregulated in every patient. Based on acquired ratios between contralateral and contusional capillaries, target *SCARB1* was downregulated at mRNA level at the BBB after the TBI in patient 1 (ratio = 0.10), patient 2 (ratio = 0.48), patient 3 (ratio = 0.09), and patient 4 (ratio = 0.26) (**Figure 83**).

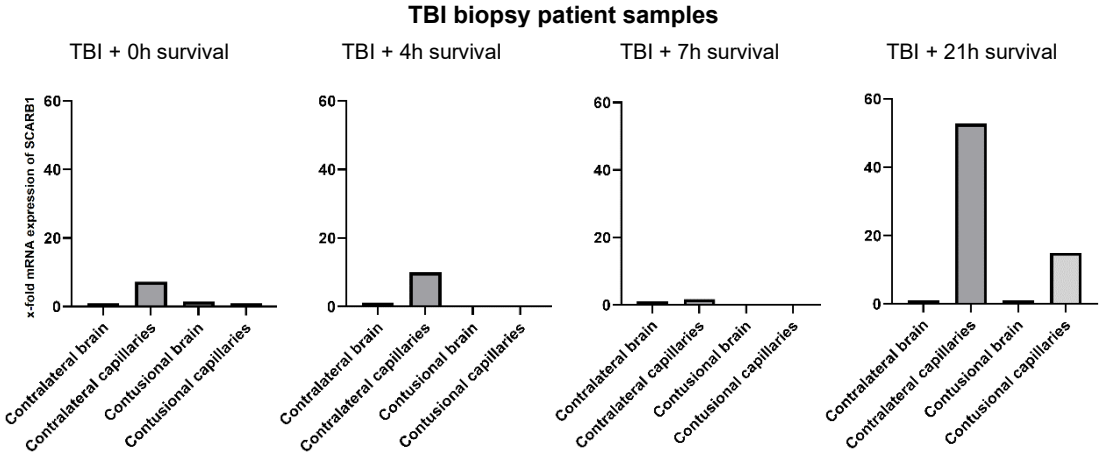

Figure 83: *SCARB1* mRNA expression (shown as bar plots) in human TBI biopsy patient samples related to contralateral brain – Contralateral brain: contralateral side of the brain, n=1; Contralateral capillaries: contralateral side of the capillaries, n=1; Contusional brain: damaged/injured side of the brain after TBI, n=1; Contusional capillaries: damaged/injured side of the capillaries after TBI, n=1; Patient 1: 0h survival post TBI; Patient 2: 4h survival post TBI; Patient 3: 7h survival post TBI; Patient 4: 21h survival post TBI; housekeeping gene: *PPIA*

4.4.12 *SGK1* mRNA expression in human TBI biopsy samples

When using *B2M* as endogenous control, *SGK1* transcript variant SGK1tr1-4/5 decreased in both contralateral and contusional capillaries when compared to corresponding contralateral and contusional brain samples. When comparing two total brain samples independently, *SGK1* seemed to be not regulated in patient 1, upregulated in patient 2, patient 3, and downregulated in patient 4. When comparing two capillary samples, *SGK1* seemed to be upregulated in every patient. In capillaries after the TBI, *SGK1* was upregulated in patient 1 (ratio = 1.27) and patient 4 (ratio = 1.62), not regulated in patient 2 (ratio = 0.98) and downregulated in patient 3 (ratio = 0.37). *SGK1* transcript variant SGK1tr1-5/5 decreased in contralateral capillaries of patient 1, patient 3, and patient 4. Moreover, *SGK1* decreased in contusional capillaries of patient 2, patient 3, and patient 4. Thus, this *SGK1* transcript variant was enriched in contralateral capillaries of patient 2 and contusional capillaries of patient 1. When comparing two total brain samples independently, *SGK1* seemed to be not regulated in patient 1, and upregulated in every other patient. When comparing two capillary samples, *SGK1* seemed to be upregulated in every patient except of the patient 2 where *SGK1* seemed to be not regulated. In capillaries after the TBI, *SGK1* was estimated to be decreased at the mRNA level in patient 2 (ratio = 0.55), and not regulated in patient 3 (ratio = 0.97), and patient 4 (ratio = 0.92). Equally, *SGK1* was estimated to be increased at the mRNA level in patient 1 (ratio = 1.35) (**Figure 84**).

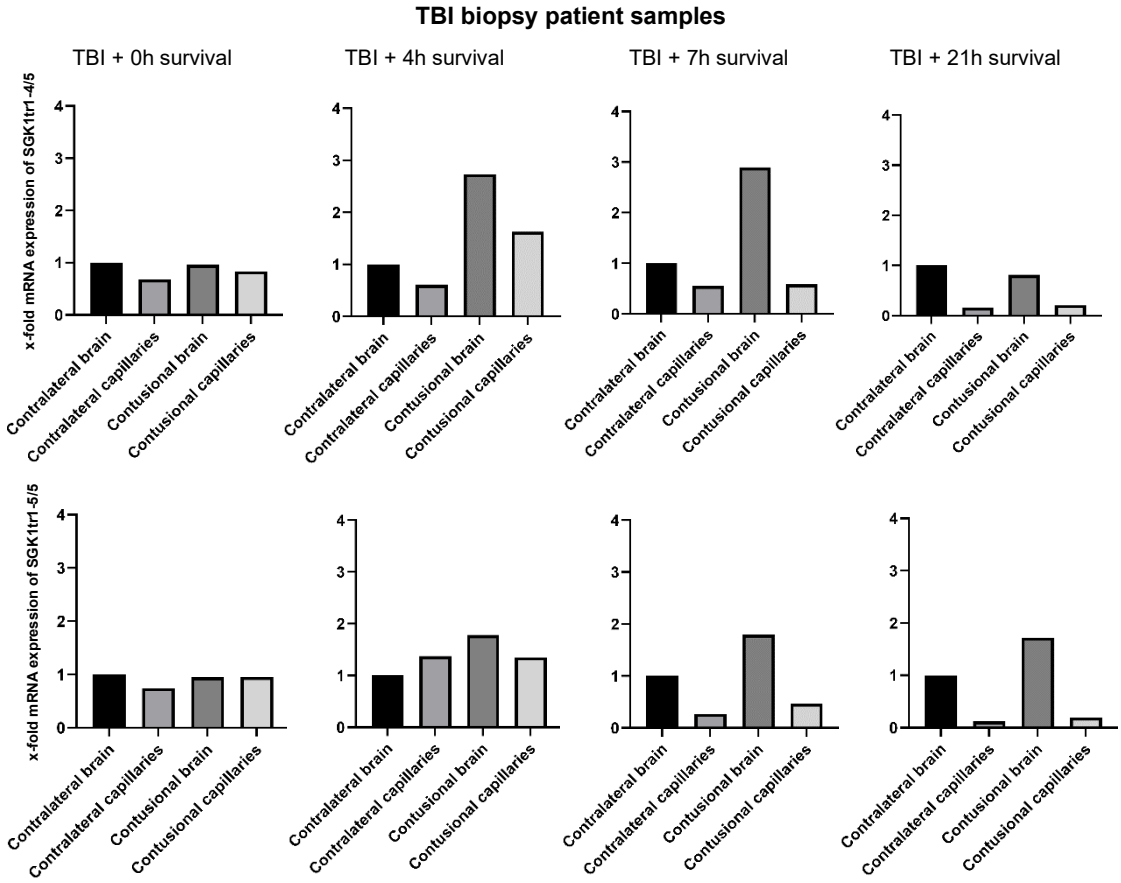

Figure 84: *SGK1* (transcript variants SGK1tr1-4/5 and SGK1tr1-5/5) mRNA expression (shown as bar plots) in human TBI biopsy patient samples related to contralateral brain – Contralateral brain: contralateral side of the brain, n=1; Contralateral capillaries: contralateral side of the capillaries, n=1; Contusional brain: damaged/injured side of the brain after TBI, n=1; Contusional capillaries: damaged/injured side of the capillaries after TBI, n=1; Patient 1: 0h survival post TBI; Patient 2: 4h survival post TBI; Patient 3: 7h survival post TBI; Patient 4: 21h survival post TBI; housekeeping gene: *B2M*

When using *PPIA* as endogenous control, *SGK1* transcript variant SGK1tr1-4/5 was enriched in contralateral capillaries of every patient except of the patient 3 where *SGK1* decreased. Moreover, this transcript variant of *SGK1* decreased in contusional capillaries of every patient except of the patient 1 where *SGK1* was enriched. When comparing two total brain samples independently, *SGK1* seemed to be not regulated in patient 1, downregulated in patient 2, and upregulated in patient 3, and patient 4. When comparing two capillary samples, *SGK1* seemed to be downregulated in every patient. Determined ratios suggested *SGK1* downregulation at the BBB after respective TBIs in patient 1 (ratio = 0.67), patient 2 (ratio = 0.19), patient 3 (ratio = 0.32), and patient 4 (ratio = 0.35). *SGK1* transcript variant SGKtr1-5/5 was enriched in

contralateral capillaries of every patient except of the patient 3 where *SGK1* decreased. Furthermore, *SGK1* decreased in contusional capillaries of every patient except of the patient 1 where *SGK1* was enriched. When comparing two total brain samples, *SGK1* seemed to be not regulated in patient 1, downregulated in patient 2, and upregulated in patient 3, and patient 4. When comparing two capillary samples, *SGK1* seemed to be downregulated in every patient. Calculated ratios depicted downregulation of *SGK1* at the BBB after respective TBIs in patient 1 (ratio = 0.57), patient 2 (ratio = 0.43), patient 3 (ratio = 0.53), and patient 4 (ratio = 0.16) (**Figure 85**).

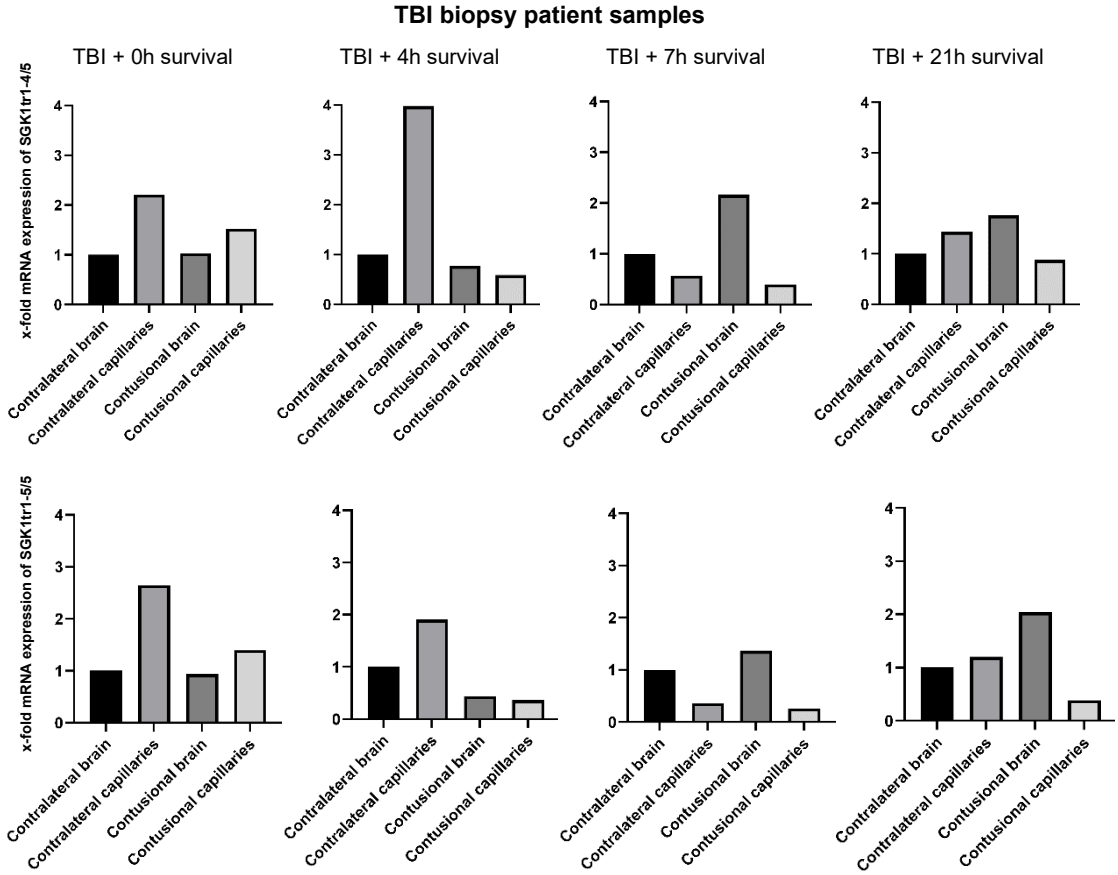

Figure 85: *SGK1* (transcript variants SGK1tr1-4/5 and SGK1tr1-5/5) mRNA expression (shown as bar plots) in human TBI biopsy patient samples related to contralateral brain – Contralateral brain: contralateral side of the brain, n=1; Contralateral capillaries: contralateral side of the capillaries, n=1; Contusional brain: damaged/injured side of the brain after TBI, n=1; Contusional capillaries: damaged/injured side of the capillaries after TBI, n=1; Patient 1: 0h survival post TBI; Patient 2: 4h survival post TBI; Patient 3: 7h survival post TBI; Patient 4: 21h survival post TBI; housekeeping gene: *PPIA*

4.4.13 *TNKS2* mRNA expression in human TBI biopsy samples

Using *B2M* as housekeeping gene for *TNKS2*, target *TNKS2* decreased in contralateral capillaries of every patient except of the patient 2 where it was enriched. Also, *TNKS2* decreased in contusional capillaries of patient 2, patient 3, and patient 4. When comparing two total brain samples independently, *TNKS2* seemed to be upregulated in every patient with the exception of patient 4. When comparing two capillary samples, *TNKS2* seemed to be downregulated in patient 2, patient 4, and upregulated in patient 3. In relation to determined ratios between contralateral and contusional capillaries, *TNKS2* was downregulated at mRNA level in patient 2 (ratio = 0.18) and patient 3 (ratio = 0.54) after TBI. Upregulation of *TNKS2* was recorded in patient 4 (ratio = 1.67) (**Figure 86**).

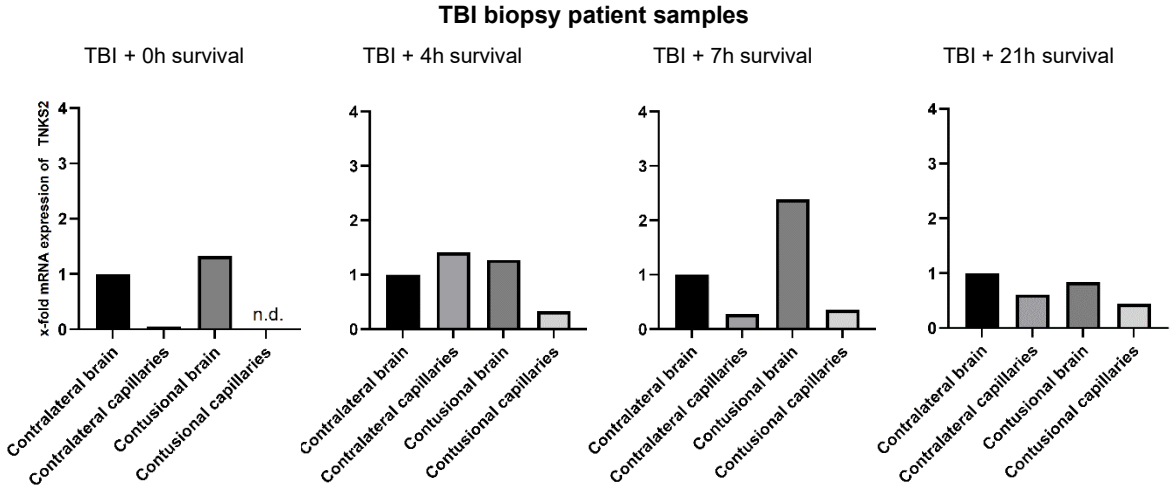

Figure 86: *TNKS2* mRNA expression (shown as bar plots) in human TBI biopsy patient samples related to contralateral brain – Contralateral brain: contralateral side of the brain, n=1; Contralateral capillaries: contralateral side of the capillaries, n=1; Contusional brain: damaged/injured side of the brain after TBI, n=1; Contusional capillaries: damaged/injured side of the capillaries after TBI, n=1; Patient 1: 0h survival post TBI; Patient 2: 4h survival post TBI; Patient 3: 7h survival post TBI; Patient 4: 21h survival post TBI; n.d. = not detected; housekeeping gene: *B2M*

Using *PPIA* as housekeeping gene for *TNKS2,* target *TNKS2* decreased in contralateral capillaries of patient 1 and patient 3 as well as enriched in contralateral capillaries of patient 2 and patient 4. When comparing two total brain samples, *TNKS2* seemed to be upregulated in patient 1, patient 3, downregulated in patient 2, and not regulated in patient 4. When comparing two capillary samples, *TNKS2* seemed to be downregulated in patient 2, patient 3, and patient 4. Calculated ratios estimated *TNKS2* downregulation in patient 2 (ratio = 0.14), patient 3 (ratio

= 0.30), and patient 4 (ratio = 0.15) in the capillaries at the BBB after respective TBIs (**Figure 87**).

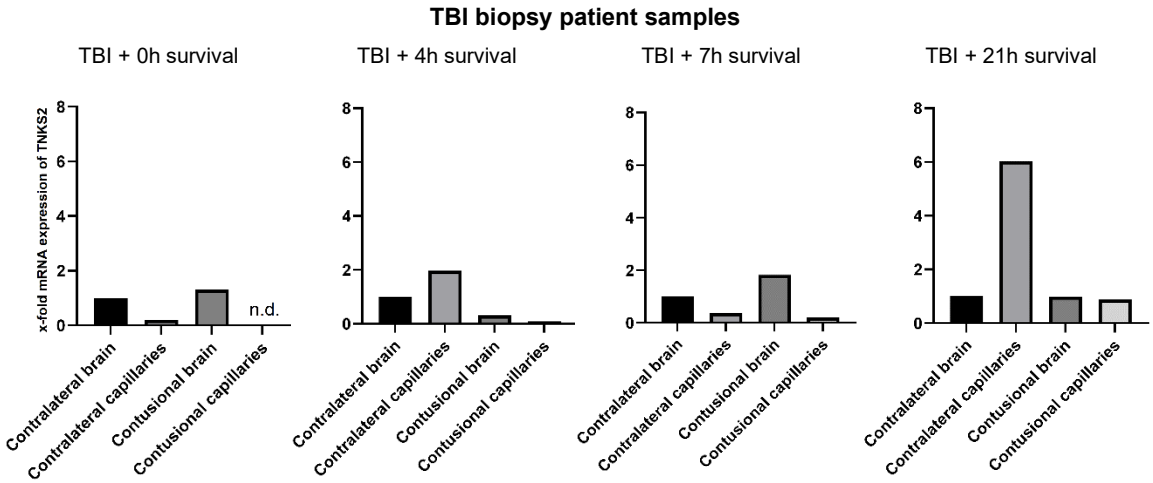

Figure 87: *TNKS2* mRNA expression (shown as bar plots) in human TBI biopsy patient samples related to contralateral brain – Contralateral brain: contralateral side of the brain, n=1; Contralateral capillaries: contralateral side of the capillaries, n=1; Contusional brain: damaged/injured side of the brain after TBI, n=1; Contusional capillaries: damaged/injured side of the capillaries after TBI, n=1; Patient 1: 0h survival post TBI; Patient 2: 4h survival post TBI; Patient 3: 7h survival post TBI; Patient 4: 21h survival post TBI; n.d. = not detected; housekeeping gene: *PPIA*

4.5 Influence of OGD treatment on the protein expression of *MECOM*, *MTA2*, *RBPJ*, *RUNX1*, and *TNKS1/2*

MECOM, *MTA2*, *RBPJ*, *RUNX1*, and *TNKS2* were amongst those targets that showed significant changes at the mRNA level after the OGD treatment in different cell culture conditions. That is the reason why they were chosen to be analysed also at the protein level. OGD experiments were performed with hCMEC/D3 mono-culture using two distinct OGD timepoints: 5 h OGD treatment only and 5 h OGD treatment followed by 19 h of reoxygenation (24 h treatment). This experiment was repeated for three times in a row in consecutive experimental weeks. Normoxia conditions were used for each OGD timepoint as corresponding control groups.

4.5.1 Western blots

For the quantification of the EVI-1 (MECOM) antibody a double-band was used. To note, antibodies from the **Figures 88-90** were not incubated on the same membrane, rather on multiple membranes. Furthermore, membranes were stripped in maximum of three times in a row due to a limited amount of samples.

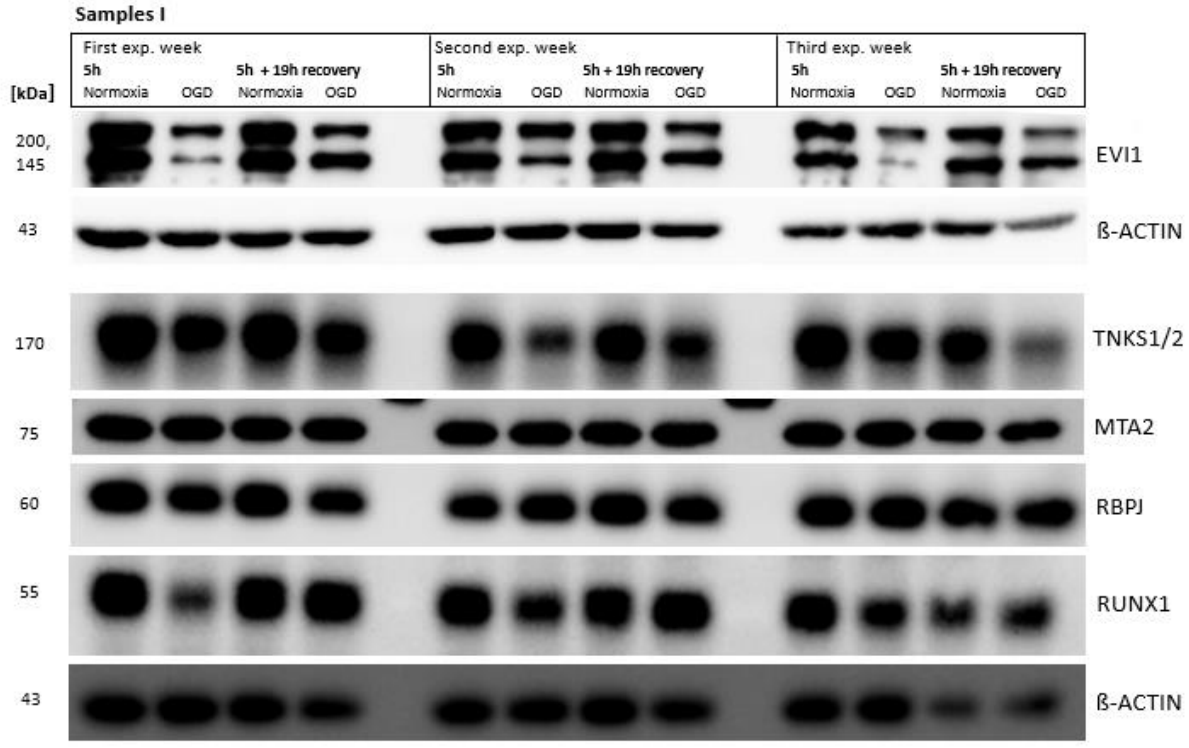

Figure 88: Western blot membrane of the isolated proteins of experiment I, first set of samples from the three consecutive experimental weeks consisting of 5 h OGD treatment and 5 h OGD treatment followed by 19 h of reoxygenation in hCMEC/D3 mono-culture: expression of *EVI-1 (MECOM)*, *MTA2*, *RBPJ*, *RUNX1*, and *TNKS1/2*

according to the size and the respective endogenous control *ß-actin* – Normoxia: Dulbecco´s Modified Eagle´s Medium with glucose (DMEM+G), normoxic conditions 21% O_2; OGD: Dulbecco´s Modified Eagle´s Medium without glucose (DMEM-G), 0.1% $O_{2;}$, kDa: kilodalton, Protein Ladder: Thermo Scientific PageRuler Plus Prestained Protein Ladder, 10 to 250 kDa

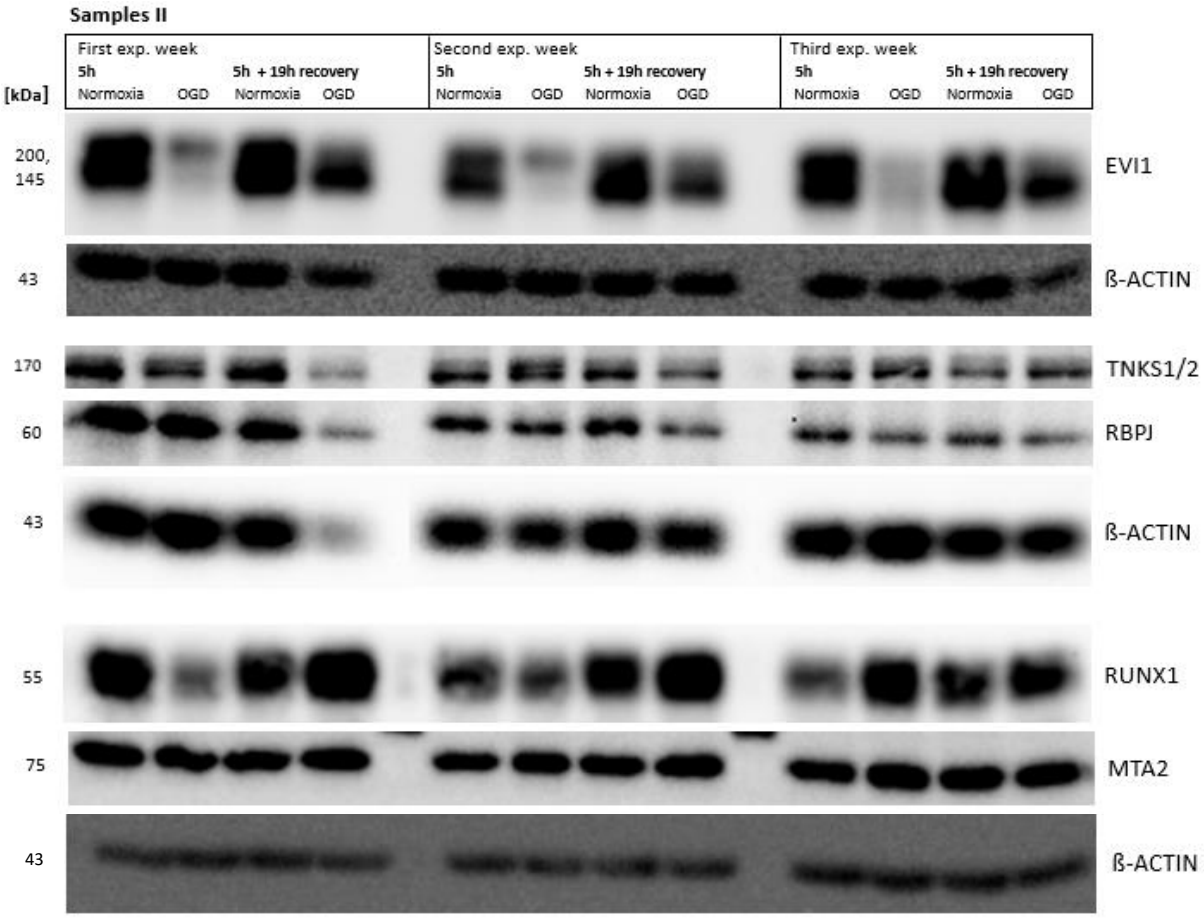

Figure 89: Western blot membrane of the isolated proteins of experiment II, second set of samples from the three consecutive experimental weeks consisting of 5 h OGD treatment and 5 h OGD treatment followed by 19 h of reoxygenation in hCMEC/D3 mono-culture: expression of *EVI-1 (MECOM)*, *MTA2*, *RBPJ*, *RUNX1*, and *TNKS1/2* according to the size and the respective endogenous control *ß-actin* – Normoxia: Dulbecco´s Modified Eagle´s Medium with glucose (DMEM+G), normoxic conditions 21% O_2; OGD: Dulbecco´s Modified Eagle´s Medium without glucose (DMEM-G), 0.1% $O_{2;}$, kDa: kilodalton, Protein Ladder: Thermo Scientific PageRuler Plus Prestained Protein Ladder, 10 to 250 kDa

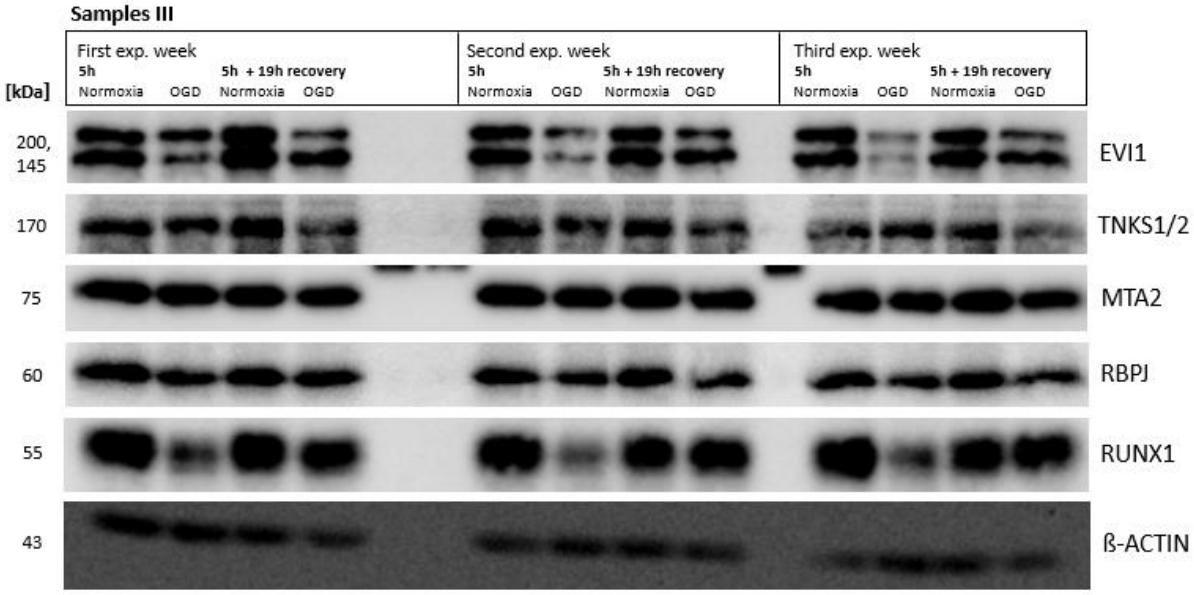

Figure 90: Western blot membrane of the isolated proteins of experiment III, third set of samples from the three consecutive experimental weeks consisting of 5 h OGD treatment and 5 h OGD treatment followed by 19 h of reoxygenation in hCMEC/D3 mono-culture: expression of *EVI-1 (MECOM)*, *MTA2*, *RBPJ*, *RUNX1*, and *TNKS1/2* according to the size and the respective endogenous control *ß-actin* – Normoxia: Dulbecco´s Modified Eagle´s Medium with glucose (DMEM+G), normoxic conditions 21% O_2; OGD: Dulbecco´s Modified Eagle´s Medium without glucose (DMEM-G), 0.1% $O_{2;}$, kDa: kilodalton, Protein Ladder: Thermo Scientific PageRuler Plus Prestained Protein Ladder, 10 to 250 kDa

4.5.2 Densitometric analysis

Densitometric analysis served for comparison of protein abundance between individual set of samples. Obtained values from the analysis were then normalized to the respective endogenous *ß-actin* control of every single sample.

4.5.2.1 *MECOM* protein expression in hCMEC/D3 after OGD treatment

The expression of *MECOM* on the protein level was significantly downregulated after 5 h OGD treatment (0.24 ± 0.05, $p<0.0001$) (**Figure 91**). Even though 24 h treatment did not result in any significant changes at the protein level, change of the OGD treatment over time resulted in significant *MECOM* overexpression (4.57 ± 1.07, $p=0.0029$). This was also confirmed by the fact that normoxia control conditions were not altered over time (**Figure 92**).

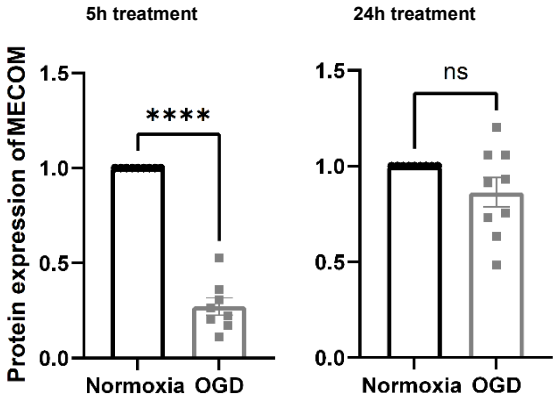

Figure 91: *MECOM* protein expression (shown as bar plots) related to respective normoxia control in hCMEC/D3 mono-culture after 5 h OGD treatment and 5 h OGD treatment followed by 19 h of reoxygenation – Normoxia: Dulbecco´s Modified Eagle´s Medium with glucose (DMEM+G), normoxic conditions 21% O_2, n=8-9; OGD: Dulbecco´s Modified Eagle´s Medium without glucose (DMEM-G), 0.1% O_2, n=9; endogenous control: *ß-actin*; ns: p>0.05, *: p≤0.05, **:p≤0.01, ***: p≤0.001, ****:p≤0.0001

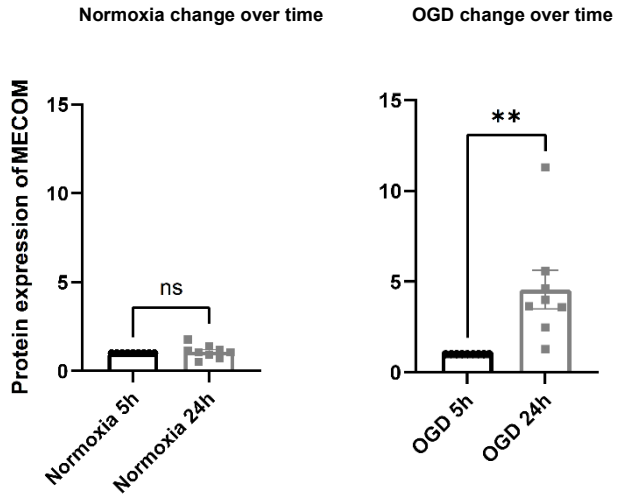

Figure 92: *MECOM* protein expression (shown as bar plots) related to 5 h normoxia control in hCMEC/D3 mono-culture depicting the change of the target´s expression in the control conditions over time (left) – Normoxia: Dulbecco´s Modified Eagle´s Medium with glucose (DMEM+G), normoxic conditions 21% O_2, n=9; *MECOM* protein expression related to 5 h OGD culture condition in hCMEC/D3 mono-culture displaying the change of the target´s expression in the hypoxia conditions over time (right) – OGD: Dulbecco´s Modified Eagle´s Medium without glucose (DMEM-G), 0.1% O_2, n=8-9 ; in OGD group of 24 h treatment an outlier was removed (Grubbs´s test); endogenous control: *ß-actin*; ns: p>0.05, *: p≤0.05, **:p≤0.01

4.5.2.2 *MTA2* protein expression in hCMEC/D3 after OGD treatment

The expression of *MTA2* on the protein level did not change significantly after neither of the two different OGD timepoints (**Figure 93**). However, over time, *MTA2* expression increased significantly in respect to the OGD treatment (1.29 ± 0.08, p=0.0021). This change was also proved by the *MTA2* expression changing not significantly in respect to the normoxia control conditions over the time (**Figure 94**).

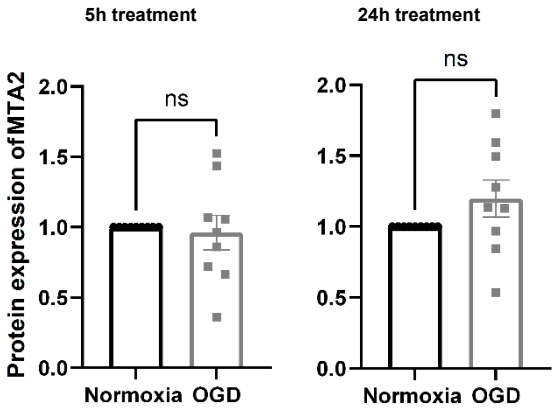

Figure 93: *MTA2* protein expression (shown as bar plots) related to respective normoxia control in hCMEC/D3 mono-culture after 5 h OGD treatment and 5 h OGD treatment followed by 19 h of reoxygenation – Normoxia: Dulbecco´s Modified Eagle´s Medium with glucose (DMEM+G), normoxic conditions 21% O_2, n=9; OGD: Dulbecco´s Modified Eagle´s Medium without glucose (DMEM-G), 0.1% O_2, n=9; endogenous control: *ß-actin*; ns: p>0.05

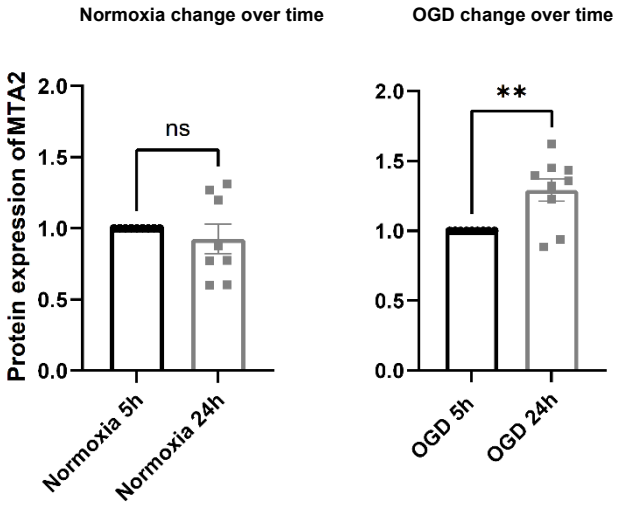

Figure 94: *MTA2* protein expression (shown as bar plots) related to 5 h normoxia control in hCMEC/D3 mono-culture depicting the change of the target´s expression in the control conditions over time (left) – Normoxia: Dulbecco´s Modified Eagle´s Medium with glucose (DMEM+G), normoxic conditions 21% O_2, n=8-9; *MTA2* protein expression related to 5 h OGD culture condition in hCMEC/D3 mono-culture displaying the change of the target´s expression in the hypoxia conditions over time (right) – OGD: Dulbecco´s Modified Eagle´s Medium without glucose (DMEM-G), 0.1% O_2, n=9 ; endogenous control: *ß-actin*; ns: p>0.05, *: p≤0.05, **:p≤0.01

4.5.2.3 *RBPJ* protein expression in hCMEC/D3 after OGD treatment

Impact of the OGD treatment on the protein expression of the target *RBPJ* is summarised in **Figure 95**. After 5 h OGD treatment in the hCMEC/D3 mono-culture, expression of *RBPJ* decreased significantly (0.71 ± 0.09, p=0.0072). After 24 h treatment, decrease in *RBPJ* expression was not significant. In **Figure 96**, the change of *RBPJ* expression over the time is presented. *RBPJ* expression in normoxia control conditions did not change over the two different timepoints. However, in relation to 5 h OGD condition, there was a significant upregulation of *RBPJ* expression recorded after 24 h treatment (1.49 ± 0.15, p=0.0057).

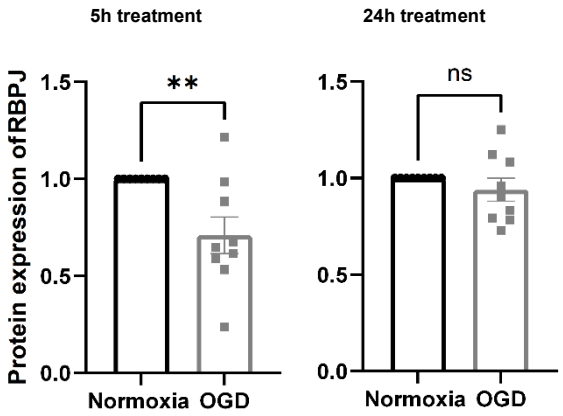

Figure 95: *RBPJ* protein expression (shown as bar plots) related to respective normoxia control in hCMEC/D3 mono-culture after 5 h OGD treatment and 5 h OGD treatment followed by 19 h of reoxygenation – Normoxia: Dulbecco´s Modified Eagle´s Medium with glucose (DMEM+G), normoxic conditions 21% O_2, n=9; OGD: Dulbecco´s Modified Eagle´s Medium without glucose (DMEM-G), 0.1% O_2, n=9; endogenous control: *ß-actin*; ns: p>0.05, *: p≤0.05, **:p≤0.01

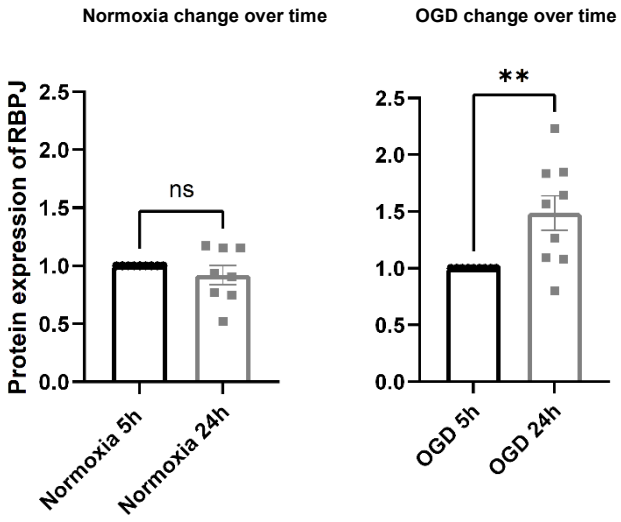

Figure 96: *RBPJ* protein expression (shown as bar plots) related to 5 h normoxia control in hCMEC/D3 mono-culture depicting the change of the target´s expression in the control conditions over time (left) – Normoxia: Dulbecco´s Modified Eagle´s Medium with glucose (DMEM+G), normoxic conditions 21% O_2, n=8-9; *RBPJ* protein expression related to 5 h OGD culture condition in hCMEC/D3 mono-culture displaying the change of the target´s expression in the hypoxia conditions over time (right) – OGD: Dulbecco´s Modified Eagle´s Medium without glucose (DMEM-G), 0.1% O_2, n=9 ; in normoxia group of 24 h treatment an outlier was removed (Grubbs´s test); endogenous control: *ß-actin*; ns: p>0.05, *: p≤0.05, **:p≤0.01

4.4.2.4 *RUNX1* protein expression in hCMEC/D3 after OGD treatment

In relation to respective normoxia controls, *RUNX1* expression decreased significantly after 5 h OGD treatment (0.44 ± 0.09, p<0.0001) while increased significantly after 5 h OGD treatment followed by 19 h of recovery phase (1.59 ± 0.19, p=0.0064) (**Figure 97**). When related to 5 h OGD timepoint, *RUNX1* expression was significantly overexpressed after 24 h OGD timepoint (3.15 ± 0.44, p=0.0002). Moreover, *RUNX1* protein expression in normoxia control conditions did not change significantly over the two distinct timepoints which further confirmed the relevance of the significance of the OGD treatment over the time (**Figure 98**).

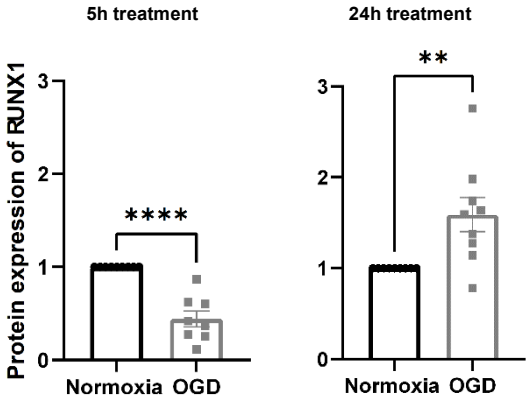

Figure 97: *RUNX1* protein expression (shown as bar plots) related to respective normoxia control in hCMEC/D3 mono-culture after 5 h OGD treatment and 5 h OGD treatment followed by 19 h of reoxygenation – Normoxia: Dulbecco´s Modified Eagle´s Medium with glucose (DMEM+G), normoxic conditions 21% O_2, n=9; OGD: Dulbecco´s Modified Eagle´s Medium without glucose (DMEM-G), 0.1% O_2, n=8-9; in OGD group of 5 h treatment an outlier was removed (Grubbs´s test); endogenous control: *ß-actin*; ns: p>0.05, *: p≤0.05, **:p≤0.01, ***: p≤0.001, ****:p≤0.0001

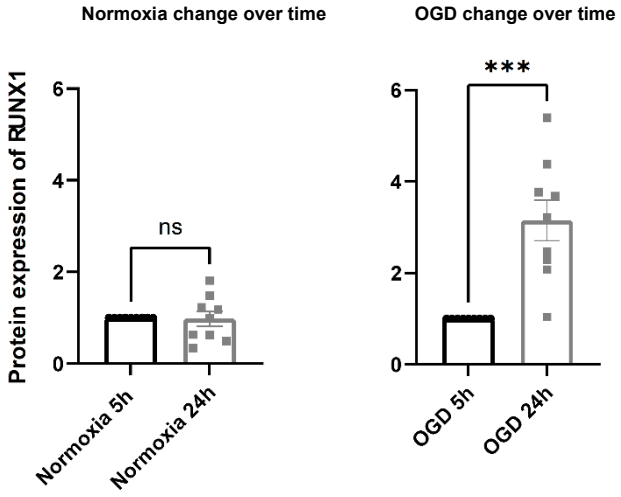

Figure 98: *RUNX1* protein expression (shown as bar plots) related to 5 h normoxia control in hCMEC/D3 mono-culture depicting the change of the target´s expression in the control conditions over time (left) – Normoxia: Dulbecco´s Modified Eagle´s Medium with glucose (DMEM+G), normoxic conditions 21% O_2, n=9; *RUNX1* protein expression related to 5 h OGD culture condition in hCMEC/D3 mono-culture displaying the change of the target´s expression in the hypoxia conditions over time (right) – OGD: Dulbecco´s Modified Eagle´s Medium without glucose (DMEM-G), 0.1% O_2, n=9 ; endogenous control: *ß-actin*; ns: p>0.05, *: p≤0.05, **:p≤0.01, ***: p≤0.001

4.5.2.5 *TNKS1/2* protein expression in hCMEC/D3 after OGD treatment

When investigating the effect of the OGD treatment on the target *TNKS2* on the protein level, antibody directed against *TNKS1* and *TNKS2* at the same time was chosen. OGD treatment of 5 h of OGD conditions induced a significant downregulation in *TNKS1/2* protein expression (0.65 ± 0.06, p=0.0117). However, 24 h treatment composed out of 5 h OGD conditions and 19 h reoxygenation did not promote alteration in the expression of *TNKS1/2* (**Figure 99**). In addition, change of the OGD treatment over time resulted in significant TNKS1/2 overexpression (1.36 ± 0.14, p=0.0232) while normoxia control conditions did not change over the two distinct timepoints (**Figure 100**).

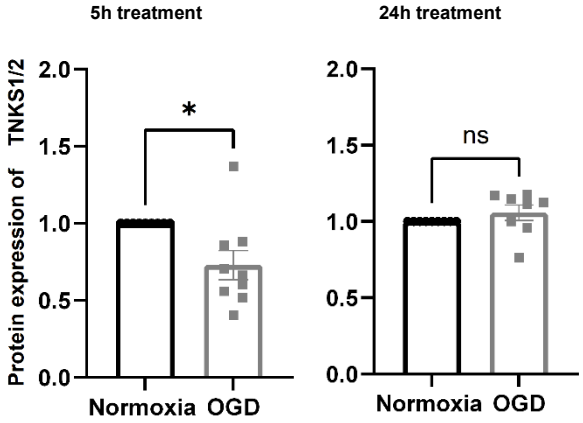

Figure 99: *TNKS1/2* protein expression (shown as bar plots) related to respective normoxia control in hCMEC/D3 mono-culture after 5 h OGD treatment and 5 h OGD treatment followed by 19 h of reoxygenation – Normoxia: Dulbecco´s Modified Eagle´s Medium with glucose (DMEM+G), normoxic conditions 21% O_2, n=9; OGD: Dulbecco´s Modified Eagle´s Medium without glucose (DMEM-G), 0.1% O_2, n=8-9; in OGD group of 5 h treatment and 24 h an outlier was removed (Grubbs´s test); endogenous control: *ß-actin*; ns: p>0.05, *: p≤0.05

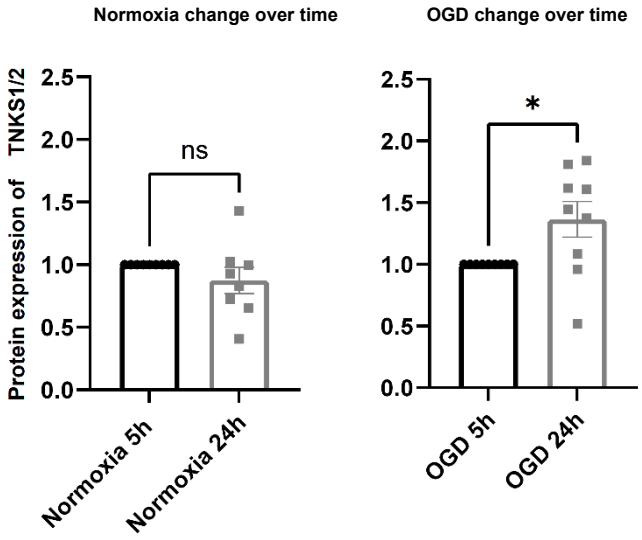

Figure 100: *TNKS1/2* protein expression (shown as bar plots) related to 5 h normoxia control in hCMEC/D3 mono-culture depicting the change of the target´s expression in the control conditions over time (left) – Normoxia: Dulbecco´s Modified Eagle´s Medium with glucose (DMEM+G), normoxic conditions 21% O_2, n=8-9; *TNKS1/2* protein expression related to 5 h OGD culture condition in hCMEC/D3 mono-culture displaying the change of the target´s expression in the hypoxia conditions over time (right) – OGD: Dulbecco´s Modified Eagle´s Medium without glucose (DMEM-G), 0.1% O_2, n=9 ; endogenous control: *ß-actin*; in normoxia group of 24 h treatment an outlier was removed (Grubbs´s test); ns: p>0.05, *: p≤0.05

4.6 Impact of *SGK1* inhibitor on OGD induced barrier disruption in the hCMEC/D3-C6 co-culture model

To evaluate the effect of OGD treatment on the integrity of the BBB when applying *SGK1* inhibitor GSK-650394, hCMEC/D3 transwell model in co-culture with glioma C6 cells was selected. Integrity of the BBB model was assessed by the measurement of TEER before and after OGD. Permeability of the BBB model after the treatment was determined by the transport of the FITC-dextran 4000.

4.6.1 Effects of 10 µM and 30 µM *SGK1* inhibitor on the BBB after OGD

High concentrations of *SGK1* inhibitor GSK-650394 such as 10 µM or 30 µM applied to the cells before OGD conditions for five hours resulted in lower TEER values and higher permeability coefficient values in comparison to the respective OGD control groups. Thus, use of GSK-650394 inhibitor in these concentrations caused higher leakage of the BBB than OGD treatment alone. Specifically, TEER values of 30 µM *SGK1* inhibitor group decreased significantly in comparison to OGD control group (37.66% ± 0.55, p=0.0232).

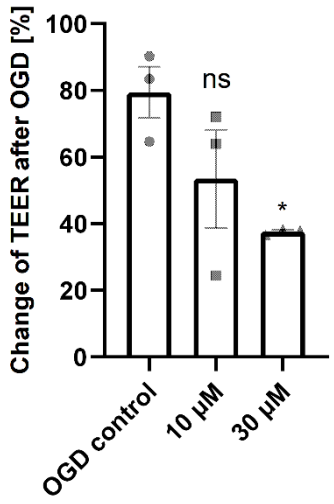

Figure 101: Assessment of the impact of 10 µM and 30 µM *SGK1* inhibitor GSK-650394 on the BBB after 5 h OGD treatment by TEER measurement; TEER change normalized to the TEER progression of the respective OGD control in the hCMEC/D3 transwell model – OGD: Dulbecco´s Modified Eagle´s Medium without glucose (DMEM-G), 1.0% O_2, hCMEC/D3 in co-culture with C6 cells (n=3) and in co-culture with C6 cells with 10 µM (n=3) or 30 µM (n=3) *SGK1* inhibitor GSK-650394 concentration; data are presented as mean ± SEM; One-way ANOVA with all pairwise multiple comparison Dunnett in case of normal distribution and equal variances, ns: p>0.05, *: p≤0.05

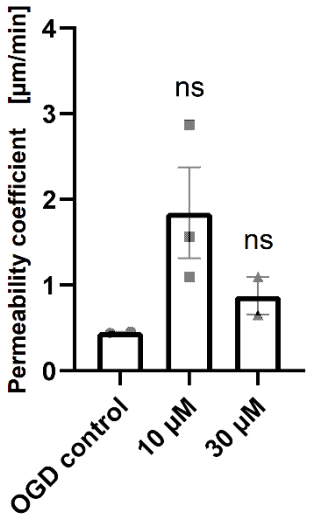

Figure 102: Assessment of the impact of 10 µM and 30 µM *SGK1* inhibitor GSK-650394 on the BBB after 5 h OGD treatment by permeability coefficient determination; Permeability coefficient [µm/min] of FD4 across hCMEC/D3 transwell model in OGD for 5 hours – OGD: Dulbecco´s Modified Eagle´s Medium without glucose (DMEM-G), 1.0% O_2, hCMEC/D3 in co-culture with C6 cells (n=2) and in co-culture with C6 cells with 10 µM (n=3) or 30 µM (n=2) *SGK1* inhibitor GSK-650394 concentration; in OGD control group and 30 µM group an outlier was removed (Grubbs´s test); data are presented as mean ± SEM; One-way ANOVA with all pairwise multiple comparison Dunnett in case of normal distribution and equal variances, ns: p>0.05

4.6.2 Effects of 0.1 µM, 1 µM, and 10 µM *SGK1* inhibitor on the BBB after OGD

As higher amounts of *SGK1* inhibitor GSK-650394 seemed to further induce BBB breakdown along with OGD treatment, in the next experimental set-up lower concentrations of the *SGK1* inhibitor were applied. As shown in **Figure 103** and **Figure 104**, the detrimental action of 10 µM *SGK1* inhibitor group on the cells could be confirmed also in this experimental set-up. Interestingly, use of lower concentrations of *SGK1* inhibitor seemed to induce rather a protective effect on the cells and thus on the BBB as well. From TEER change values it can be observed that OGD control group (62.28% ± 5.55, p=0.0198) decreased significantly in comparison to the normoxia group (137.02% ± 22.32, p=0.0198). This suggested that OGD treatment efficiently led to BBB disruption. Furthermore, in relation to the normoxia group (137.02% ± 22.32, p=0.0198), OGD control group (62.28% ± 5.55, p=0.0198), 10 µM *SGK1* inhibitor group (32.69% ± 17.31, p=0.0063) as well as 1 µM *SGK1* inhibitor group (62.31% ± 3.61, p=0.0336) showed significantly lower TEER values. On the other hand, values obtained from the calculations of permeability coefficients demonstrate no significant changes between the individual experimental groups. Nevertheless, the values still depict a damaging effect of the experimental set-up comprising of 10 µM *SGK1* inhibitor. In addition, calculated values of

permeability coefficients propose that 1 µM and 0.1 µM concentrations of *SGK1* inhibitor provoked not only stronger BBB tightness properties in comparison to the control OGD group but also in comparison to the control normoxia group where no injury to the cells was promoted.

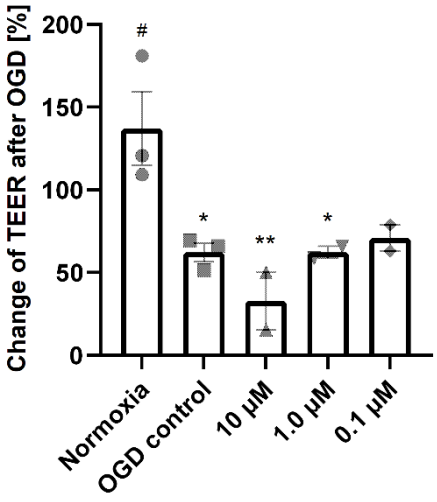

Figure 103: Assessment of the impact of 0.1 µM, 1 µM, and 10 µM *SGK1* inhibitor GSK-650394 on the BBB after 5 h OGD treatment by TEER measurement; TEER change normalized to the TEER progression of the respective OGD and normoxia control in the hCMEC/D3 transwell model – Normoxia: Dulbecco´s Modified Eagle´s Medium with glucose (DMEM+G), normoxic conditions 21% O_2, hCMEC/D3 in co-culture with C6 cells (n=3); OGD: Dulbecco´s Modified Eagle´s Medium without glucose (DMEM-G), 0.1% O_2, hCMEC/D3 in co-culture with C6 cells (n=3) and in co-culture with C6 cells with 0.1 µM (n=2) or 1.0 µM (n=2) or 10 µM (n=2) *SGK1* inhibitor GSK-650394 concentration; data are presented as mean ± SEM; One-way ANOVA with all pairwise multiple comparison Dunnett in case of normal distribution and equal variances; #: statistical significant versus OGD hCMEC/D3 + C6, p≤0.05; *: Statistical significant versus normoxia hCMEC/D3, *: p≤0.05, **:p≤0.01

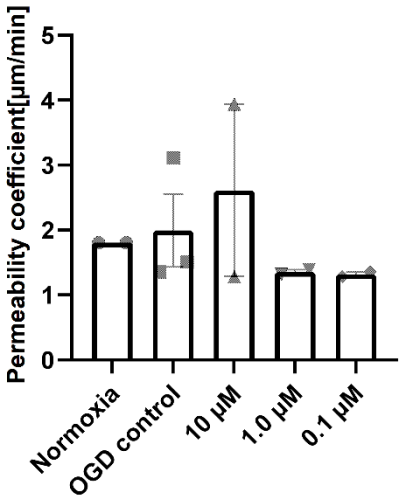

Figure 104: Assessment of the impact of 0.1 µM, 1 µM, and 10 µM *SGK1* inhibitor GSK-650394 on the BBB after 5h OGD treatment by permeability coefficient determination; Permeability coefficient [µm/min] of FD4 across hCMEC/D3 transwell model in OGD for 5 hours – Normoxia: Dulbecco´s Modified Eagle´s Medium with glucose (DMEM+G), normoxic conditions 21% O_2, hCMEC/D3 in co-culture with C6 cells (n=2); OGD: Dulbecco´s Modified Eagle´s Medium without glucose (DMEM-G), 0.1% O_2, hCMEC/D3 in co-culture with C6 cells (n=3) and in co-culture with C6 cells with 0.1 µM (n=2) or 1.0 µM (n=2) or 10 µM (n=2) *SGK1* GSK-650394 inhibitor concentration; data are presented as mean ± SEM; One-way ANOVA with all pairwise multiple comparison Dunnett in case of normal distribution and equal variances

4.6.3 Effects of 0.01 µM, 0.03 µM, 0.1 µM, 0.3 µM, and 1 µM *SGK1* inhibitor on the BBB after OGD

The third experimental set-up used lower *SGK1* inhibitor GSK-650394 concentrations on the hCMEC/D3 cells co-cultured with glioma C6 cells in the transwell model. Summarized TEER change values from three consecutive experiments displayed significant change in normoxia (116.13% ± 12.67, p=0.0004) group when related to OGD control group (78.31% ± 5.89). Equally, significant change between OGD control group and 0.1 µM (100.53% ± 5.18, p=0.0435) and 0.03 µM (105.23% ± 5.64, p=0.0091) *SGK1* inhibitor groups was recorded. These findings together suggested that OGD treatment during the experiment worked accordingly as well as demonstrated very strong protective effects on the BBB integrity resulting from the application of respective *SGK1* inhibitor concentrations on the hCMEC/D3 cells before the start of the OGD treatment. Significant changes were also determined between normoxia group and OGD control group (78.31% ± 5.89, p=0.0004) with 1 µM *SGK1* inhibitor group (79.63% ± 2.81, p=0.0015) (**Figure 105**).

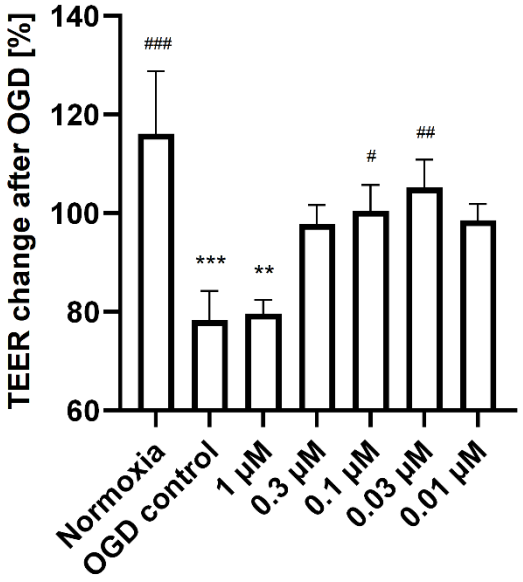

Figure 105: Assessment of the impact of 0.01 µM, 0.03 µM, 0.1 µM, 0.3 µM, and 1 µM *SGK1* inhibitor GSK-650394 on the BBB after 5 h OGD treatment by TEER measurement; TEER change normalized to the TEER progression of the respective normoxia or OGD control in the hCMEC/D3 transwell model – Normoxia: Dulbecco´s Modified Eagle´s Medium with glucose (DMEM+G), normoxic conditions 21% O_2, hCMEC/D3 in co-culture with C6 cells (n=9); OGD: Dulbecco´s Modified Eagle´s Medium without glucose (DMEM-G), 0.1% O_2, hCMEC/D3 in co-culture with C6 cells (n=12) and in co-culture with C6 cells with 0.01 µM (n=9), 0.03 µM (n=12), 0.1 µM (n=12), 0.3 µM (n=9), and 1.0 µM (n=9) *SGK1* inhibitor concentration; data are presented as mean ± SEM from three independent experiments; One-way ANOVA with all pairwise multiple comparison Dunnett in case of normal distribution and equal variances, #: statistical significant versus OGD hCMEC/D3 + C6, $p<0.05$, ##: $p\leq0.01$, ###: $p\leq0.001$; *: Statistical significant versus normoxia hCMEC/D3, *: $p\leq0.05$, **:$p\leq0.01$, ***: $p\leq0.001$

Data obtained from the transport studies suggested similar outcome of the experiment as determined TEER change values. For instance, in respect to normoxia group, permeability coefficient of the OGD group increased significantly (100.00 ± 13.83, p=0.0203). Significant changes were also determined between OGD control group and normoxia group (48.06 ± 13.23, p=0.0246), 0.1 µM *SGK1* inhibitor group (37.45 ± 10.79, p=0.0003), 0.3 µM *SGK1* inhibitor group (50.06 ± 20.15, p=0.0044), as well as 0.03 µM *SGK1* inhibitor group (43.82 ± 6.31, p=0.0008) (**Figure 106**).

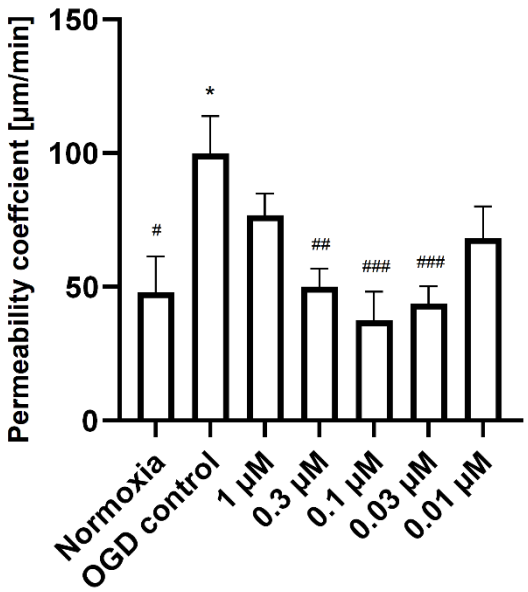

Figure 106: Assessment of the impact of 0.01 µM, 0.03 µM, 0.1 µM, 0.3 µM, and 1 µM *SGK1* inhibitor GSK-650394 on the BBB after 5 h OGD treatment by permeability coefficient determination; Permeability coefficient [µm/min] of FD4 across hCMEC/D3 transwell model in OGD for 5 hours – Normoxia: Dulbecco´s Modified Eagle´s Medium with glucose (DMEM+G), normoxic conditions 21% O_2, hCMEC/D3 in co-culture with C6 cells (n=4); OGD: Dulbecco´s Modified Eagle´s Medium without glucose (DMEM-G), 0.1% O_2, hCMEC/D3 in co-culture with C6 cells (n=8) and in co-culture with C6 cells with 0.01 µM (n=9), 0.03 µM (n=10), 0.1 µM (n=9), 0.3 µM (n=8), and 1.0 µM (n=8) *SGK1* inhibitor concentration; data are presented as mean ± SEM from three independent experiments; One-way ANOVA with all pairwise multiple comparison Dunnett in case of normal distribution and equal variances, #: statistical significant versus OGD hCMEC/D3 + C6, $p<0.05$, ##: $p\leq0.01$, ###: $p\leq0.001$; *: Statistical significant versus normoxia hCMEC/D3, *: $p\leq0.05$

5. Discussion

The BBB is responsible for maintaining tightly controlled chemical composition of the neuronal milieu necessary for accurate and effective neuronal signaling which merely preserves brain homeostasis [82]. CNS diseases are often linked to BBB dysfunction. For instance, BBB breakdown is associated with poor prognosis in stroke and TBI [83]. Both of these neurodegenerative disorders are accompanied by cerebral ischemia. Cerebral ischemia represents a condition in which e.g. a blockage in an artery causes insufficient blood supply to the brain. To better understand what happens at the BBB during and after cerebral ischemia, a human cerebral ischemia *in vitro* model of the BBB can be applied. In this case, OGD treatment can be used to simulate cerebral ischemia [43].

Furthermore, the emerging field of epigenetics shows a great promise to solve the problem with currently limited options for treatment and biomarkers destined for cerebral ischemia induced BBB damage as well as post stroke recovery. Recent studies demonstrate namely dual function of the DNA methylation that is correlated with BBB injury and BBB recovery in stroke at the same time [39]. The fact that DNA methylation serves solely for purpose of gene silencing was contradicted in the recent years. Increasing evidence depicts DNA methylation being implicated also in the gene activation, splicing regulation, recruitment of transcription factors, or nucleosomes positioning. Noticeably, gene activation occurs only within transcribed regions while gene body methylation was observed to increase the rate of transcription. Thus, role of the DNA methylation in the gene regulation arises as much more complex and multi-faceted epigenetic process as initially estimated [84].

5.1 Relevance of selected regulated targets

DNA methylation EPIC array analysis with over 850.000 datapoints per sample of OGD treated hCMEC/D3 cells identified targets with altered methylation patterns. Relevance of the targets chosen for further analysis was assured by investigation of function of individual targets, analysis of pathways and interactions in which the particular targets participate as well as running STRING database analysis with proteins that are important for the proper function of the BBB.

Based on the Kegg Pathway Database, targets *MECOM* and *RUNX1* are involved together in several cancer pathways including the pathway of chronic myeloid leukemia. *MECOM* is considered a proto-oncogene due to exhibition of anti-apoptotic effects in multiple cancer types along with chronic myeloid leukemia [85]. *RUNX1* regulates hematopoietic development and

thus mutations in this gene are often connected with development of hematological malignancies [86]. In skeletal muscle during ischemia, *RUNX1* expression was increased and promoted muscle regeneration after the injury [87]. Constant upregulation of *RUNX1* was confirmed in a rat model of chronic myocardial ischemia [88]. Function of *RUNX1* shows to be essential also in intracranial hemorrhage as *RUNX1* regulates the expression of tight junction proteins and thus the overall state of the BBB permeability [89]. After TBI, *RUNX1* seems to induce neuroprotective effects comprising of microglial and neural stem cell activation and proliferation [90].

Next, Kegg Pathway Database analysis revealed linkage of targets *RBPJ* and *NOTCH3* in a signaling cascade promoting Th1 cellular immunity. As the main interest of this particular project lies rather in acute CNS disorders, interestingly, DNA methylation targets *SGK1* and *NLK* were observed to inhibit *FOXO* in a *FOXO* signaling cascade. The family of *FOXOs* transcription factors possesses an essential role in neuronal function. More precisely, *FOXOs* are implicated in the control of neural stress responses, lineage commitment, neuronal signaling, apoptosis, or promotion of cell survival by autophagy in the brain. Activity of *FOXOs* is mainly regulated by PI3K/AKT signaling that is responsible for regulation of neuronal apoptosis. In response to PI3K/AKT signaling, neuroprotective action against reactive oxygen species was recorded [91]. Furthermore, *FOXOs* are involved in the neuroprotection followed after cerebral ischemia insult and TBI. It was reported that *FOXO* inactivation promotes neuroprotection in adult rats after exposure to hypoxic preconditioning 1-2 days prior to ischemia [92]. Moreover, treatment with artesunate improved post stroke recovery by inhibition of *FOXO3a* which further activated PI3K/AKT pathway and promoted $p27^{kip1}$ downregulation and neural stem cell proliferation [93]. Thus, it seems that neurons could be rescued from delayed neuronal death in cerebral ischemia by *FOXO* inhibition which further blocks death signals in neurons [94]. However, another study showed that upregulation of *FOXO3* transcription factor stimulated autophagy in a rat MCAO model, provoking protective effects on the I/R injury [95].

When investigating the role of *FOXO* in TBI it was shown, that after TBI, human brains were enriched in *FOXO*. In mice, ipsilateral cerebral cortex was collected at distinct timepoints following the brain injury. Here, the highest peak of *FOXO* protein levels was reached at 24h timepoint while the expression was neuron-specific [96]. In a rat model of TBI, *FOXO3a* knockdown induced neuroprotection in form of motor behavioral recovery, as well as suppressed memory impairment and partially reversed neuronal damage. Without *FOXO3a*

knockdown, nuclear accumulation of *FOXO3a* increased the expression of neuronal autophagy genes which then caused post-TBI neurological impairments [97]. Thus, blocking the activation of autophagy may provide a new direction for the treatment of acute CNS disorders [98].

Targets *SGK1* and *NLK* which are involved in the inhibition of *FOXO* in *FOXO* signaling pathway are also implicated in the stroke pathogenesis. For example, *SGK1* overexpression has been associated over the past years with the development and progression of multiple pathological conditions including stroke and thrombosis [79]. *NLK* is an enzyme and member of the MAPK family. MAPK regulates wide range of cellular processes including inflammation and stress responses. Moreover, it plays a pivotal role in the stroke pathology. It was reported that MAPK in particular may represent a promising therapeutic target for the treatment of stroke and post-stroke related disabilities [67], [99].

Selected regulated target of cerebral ischemia, *RBPJ*, was examined for its implication in the stroke and TBI as well. In one study, postnatal inactivation of *RBPJ* gene in mice increased local TGFβ signaling and triggered profound changes in endothelial cell phenotype. Noticeably, loss of *RBPJ* gene in adult mice promoted aggravated brain damage upon stroke incidence [72]. Another study demonstrated that *RBPJ* knockdown which subsequently blocked Notch signaling, combined with stroke insult, resulted in a higher recruitment of astrocytes to neurogenesis. Also, it was deduced that blockage of Notch signaling in stroke raised the neurogenic response to stroke by a factor of 3.5 fold [73].

5.2 Regulation of DNA methylation targets at the mRNA level

Chosen regulated targets of cerebral ischemia were examined at mRNA level with set a of samples from four different conditions. The aim here was to observe mRNA expression changes of the selected targets when using different experimental set-ups and to evaluate whether expression level changes from mono-culture experiments were conserved also in different experimental conditions. In **Table 25**, expression changes of DNA methylation targets from different experimental set-ups were summarized. In detail, table 25 shows b-value differences or p-values (EVI-1, NOTCH3) for initial DNA epic array data, mean x-fold change values for mRNA data from hCMEC/D3 mono-culture, hCMEC/D3 triple-culture, and hiPS-EC triple-culture experiments, human TBI biopsy samples of two patients in form of normalized ratios, as well as protein expression data from hCMEC/D3 mono-culture after the OGD treatment. To interpret DNA epic array data, negative b-value differences suggest less DNA

methylation and thus mRNA levels are supposed to be upregulated. On the other hand, positive b-value differences suggest higher degree of DNA methylation and thus according mRNA should be downregulated in theory. Some targets were also termed as positive for Bumphunt analysis. Bumphunt analysis involves analysis of several CpG islands localized on the same gene that are summarized to test whether sum of small similar regulations might lead to a total strong regulation of a gene. Based on determined results, targets positive for Bumhunt analysis were *CLEC14A* and *H4C3*. Also, *MECOM* was correlated with p-value lower than 0.0001 which demonstrated significance of this target. The same was shown for *NOTCH3*, while *NOTCH3* was additionally found to be linked to *RBPJ* via STRING analysis.

Table 33: Summary table of expression changes of DNA methylation targets at DNA methylation, mRNA, and protein level after OGD treatment under different conditions; data are presented as b-value differences (in case of DNA epic array data), p-values (in case of EVI-1 and NOTCH3 in DNA epic array data), mean x-fold change values, ratios after normalization (in case of TBI biopsy samples) and mean protein expression data (in case of WB); n.d. = not detected; B = Bumphunt; ns: p>0.05, *: p≤0.05, **:p≤0.01, ***: p≤0.001, ****:p≤0.0001

Experimental condition	*Mono-culture (DNA Epic Array)*		*Mono-culture*		*Triple-culture*		*Triple-culture*		*TBI biopsy samples*		*TBI biopsy samples*		*Mono-culture (WB)*	
Cell type	*hCMEC/D3*		*hCMEC/D3*		*hCMEC/D3*		*hiPS-EC*						*hCMEC/D3*	
Control gene	-		*18SrRNA*		*18SrRNA*		*18SrRNA*		*B2M*		*PPIA*		*ß-actin*	
Treatment	*5h*	*24h*	*5h*	*24h*	*5h*	*24h*	*6h*	*24h*	*4h*	*21h*	*4h*	*21h*	*5h*	*24h*
CLEC14A		B	0.88	0.75	0.82	2.68****	0.90	1.31	0.21	2.33	0.04	0.50	-	-
EPC1		0.19	0.87	2.88	1.38**	1.33*	0.78	1.15	1.19	4.61	0.23	0.99	-	-
MECOM	0.0001		0.43***	3.46	0.60*	1.43	0.66*	0.96	0.74	1.64	0.58	0.28	0.24****	0.86
FGFR1	-0.35		0.43***	1.77	0.64***	1.41**	1.05	1.43	2.63	2.00	0.52	0.43	-	-
H4C3		B	0.26****	0.85	0.58****	0.89	0.75*	0.82	2.43	2.36	0.45	0.53	-	-
MTA2		-0.21	0.36**	2.04	0.63*	1.29	0.56**	1.02	0.26	1.63	0.21	0.28	0.96	1.20
NLK		-0.18	0.68	3.10	0.87	0.97	0.92	1.05	0.23	1.50	0.17	0.26	-	-
NOTCH3	0.0001		0.90	1.42	0.75	1.54	0.56***	0.86	0.59	1.53	0.45	0.26	-	-
RBPJ		-0.14	0.76	1.88	0.79	1.46**	0.53	1.32	1.49	6.43	1.13	1.11	0.71**	0.94
RUNX1		B	0.53*	3.28	1.52***	0.81	2.13***	1.12	n.d.	3.01	n.d.	0.50	0.61****	1.59**
SCARB1	0.45		0.69	3.24***	0.59**	0.42****	1.16	0.89	0.60	1.52	0.48	0.26	-	-
SGK1tr1-4/5	-0.38		1.64	3.52**	-	-	5.44**	1.12	0.98	1.62	0.19	0.35	-	-
SGK1tr1-5/5	-0.38		1.79****	3.64**	2.02****	1.93****	8.13**	1.33	0.55	0.92	0.43	0.16	-	-
TNKS2		-0.20	0.36***	2.66	0.54**	1.25**	0.79	1.55*	0.18	1.67	0.14	0.15	0.73*	0.99

To examine expression changes in evaluated targets at mRNA level, for instance, mRNA expression levels of the target *CLEC14A* were significantly upregulated in hCMEC/D3 triple-culture after 24 h OGD timepoint (2.68 ± 0.26, p<0.0001). *CLEC14A* mRNA expression levels determined from TBI biopsy samples normalized with *B2M* endogenous control correspond well to *in vitro* data by suggesting an increase in patient with survival of 21 hours after the TBI when comparing two capillary samples as well as when applying normalized ratio.

When summarizing mRNA expression changes of the target *EPC1*, a significant upregulation in OGD treated hCMEC/D3 triple-culture after 5 h OGD treatment (1.38 ± 0.11, p=0.0096) and after 24 h OGD treatment (1.33 ± 0.15, p=0.0471) was determined. In human TBI biopsy samples, significant increase of *EPC1* mRNA expression levels was observed with endogenous control *B2M* in patient with survival of 21 hours after the TBI.

MECOM x-fold change decreased significantly in the OGD treated hCMEC/D3 mono-culture after 5 hours (0.43 ± 0.04, p=0.0002). *MECOM* gene expression downregulation was demonstrated also hCMEC/D3 triple-culture after 5 h OGD timepoint (0.60 ± 0.06, p=0.0454) and in the hiPS-EC triple-culture after 6 h OGD timepoint (0.66 ± 0.09, p=0.0441). In respect to human TBI biopsy samples, varying degrees of *MECOM* gene expression downregulation were shown with both endogenous controls at the BBB after respective TBIs in every patient with exception of the patient with survival time of 21 hours post-TBI when applying *B2M* as housekeeping gene.

In regard to mRNA expression changes of the target *FGFR1*, *FGFR1* downregulation was found in the OGD treated hCMEC/D3 mono-culture after 5 hours (0.43 ± 0.06, p=0.0007) as well as in OGD treated hCMEC/D3 triple-culture after 24 hours (0.64 ± 0.03, p=0.0006). Here, determined negative b-value difference after 5 h OGD treatment did not match demonstrated upregulation at mRNA level after 5 hours of treatment. Upregulation of *FGFR1* gene expression was shown in hCMEC/D3 triple-culture after 24 h OGD treatment (1.41 ± 0.11, p=0.0057). *FGFR1* mRNA expression change in TBI biopsy samples resulted in *FGFR1* upregulation in patients with survival times of 4 h and 21 h post-TBI based on determined ratios when using *B2M* as endogenous control. However, with *PPIA*, *FGFR1* mRNA expression decreased in patients with survival times of 4 h and 21 h post-TBI.

Studies with the hCMEC/D3 mono-culture led to a significant decrease in *H4C3* mRNA expression after 5 h OGD treatment (0.26 ± 0.05, p<0.0001). Significant change in *H4C3* x-fold values was observed also in the hCMEC/D3 triple-culture after 5 h OGD treatment (0.58

± 0.05 p<0.0001) as well as in the hiPS-EC triple-culture after 6h OGD treatment (0.75 ± 0.05, p=0.0294). Investigation of the *H4C3* x-fold change in human brain TBI biopsy samples revealed downregulation of *H4C3* in patient with 0h survival time when using *B2M*. Here, *H4C3* upregulation was shown for patients with survival times of 4h, 7h, and 21h. For patients with survival time of 0 h, 4 h, and 21 h, using *PPIA* estimated *H4C3* gene expression downregulation. Here, *H4C3* upregulation was observed solely in patient with survival time of 7 h post-TBI.

Next, target *MTA2* mRNA expression levels showed a significant downregulation in the OGD treated hCMEC/D3 mono-culture at 5h timepoint (0.36 ± 0.09, p=0.0024), in the hCMEC/D3 triple-culture at 5 h OGD timepoint (0.63 ± 0.07, p=0.0160), and in the hiPS-EC triple-culture after 6 h OGD timepoint (0.56 ± 0.06, p=0.0016). Also, negative b-value difference after 24 h treatment fits to the observed upregulation at mRNA level after treatment of 24 hours. Investigation of *MTA2* x-fold change in human TBI biopsy samples depicted downregulation of *MTA2* mRNA expression in every patient when applying *PPIA* as gene control. With *B2M*, *MTA2* decreased in patients with survival time of 4 h, while increased in patients with survival time of 7 h and 21 h post-TBI.

Determined *NLK* x-fold change values did not display any significant changes at mRNA level in OGD treated hCMEC/D3 mono-culture, hCMEC/D3 triple-culture, or hiPS-EC triple-culture. Human TBI biopsy samples showed decreased *NLK* mRNA expression levels in all four patients when applying *PPIA* as endogenous control. Equally, using *B2M*, *NLK* mRNA levels decreased in every patient except of the patient 4 with survival time of 21 h after the TBI.

X-fold change values for the next target, *NOTCH3*, were significant in hiPS-EC triple-culture after 6 h OGD timepoint (0.56 ± 0.03, p=0.0007). With regard to human TBI biopsy samples and endogenous control *B2M*, a *NOTCH3* mRNA expression decrease was observed in patients with survival time of 0 h and 4 h post-TBI, while an increase was recorded in patients with survival time of 7 h and 21 h. With *PPIA, NOTCH3* gene expression decreased in patients with survival time of 0 h, 4 h, and 21 h, but increased in patient with survival time of 7 h after TBI.

RBPJ mRNA expression increased significantly in hCMEC/D3 triple-culture after 24 h OGD timepoint (1.46 ± 0.12, p=0.0034) that included 5 h OGD treatment and 19 hours of reoxygenation. This also fits to the determined negative b-value difference based on DNA epic array data. In human TBI biopsy samples, upregulation of *RBPJ* x-fold change values in every

patient when applying *B2M* as housekeeping gene was found with the exception of patient 3 with survival time of 7 hours post-TBI where *RBPJ* was downregulated at mRNA level. With *PPIA*, *RBPJ* mRNA expression significantly increased only in patient with 0 h survival time and decreased in patient with 7 h survival time.

Gene expression of *RUNX1* was significantly downregulated in the OGD treated mono-culture after 5 h timepoint (0.53 ± 0.14, p=0.0265), while displayed upregulation in the hCMEC/D3 triple-culture after 5 h OGD timepoint (1.52 ± 0.11, p=0.0005) as well as in the hiPS-EC triple-culture after 6 h OGD treatment (2.13 ± 0.01, p=0.0040). Despite *RUNX1* not being detected in every sample of human TBI biopsy samples, *RUNX1* was upregulated at the capillaries after the TBI in patient with survival time of 21 h when applying *B2M*, while remained downregulated in the same patient when applying housekeeping gene *PPIA*.

Target *SCARB1* showed to be downregulated in the OGD treated hCMEC/D3 mono-culture after 24 h timepoint (0.29 ± 0.04, p=0.0002) as well as in hCMEC/D3 triple-culture after 5 h OGD treatment (0.59 ± 0.05, p=0.0016) and after 24 h OGD treatment (0.42 ± 0.03, p<0.0001). Thus, determined positive b-value difference from DNA epic array data accurately predicted *SCARB1* downregulation at mRNA level after 5 h OGD treatment. Results from human brain TBI biopsy samples suggested downregulation of *SCARB1* mRNA levels in every patient when using both endogenous controls with the exception of patient with survival time of 21 hours where *SCARB1* mRNA expression was upregulated when applying solely *B2M* as endogenous control.

SGK1 was significantly upregulated in the OGD treated hCMEC/D3 mono-culture using *SGK1* transcript variant 1-4/5 after 24 h treatment (3.52 ± 0.34, p=0.0017) and using *SGK1* transcript variant 1-5/5 after 5 h treatment (1.53 ± 0.01, p<0.0001) and 24 h treatment (3.64 ± 0.40, p=0.0027). *SGK1* increased also in hCMEC/D3 triple-culture after 5 h OGD treatment (2.02 ± 0.14, p<0.0001) and 24 h OGD treatment (1.93 ± 0.07, p<0.0001) when using *SGK1* transcript variant 1-5/5. *SGK1* upregulation was also detected after 6 h OGD in hiPS-EC triple-culture when using *SGK1* transcript variant 1-4/5 (5.44 ± 0.78, p=0.0013) as well as when using *SGK1* transcript variant 1-5/5 (8.13 ± 1.33, p=0.0060). Also in relation to obtained positive b-value differences for both *SGK1* transcript variants based on DNA epic array data, *SGK1* was downregulated at mRNA level after 5 h OGD treatment. Interestingly, in human brain biopsy samples, target *SGK1* was decreased at the mRNA level in every patient when using both *SGK1* transcript variants in relation to selected housekeeping gene *PPIA*. Using *B2M* and

SGK1 transcript variant 1-4/5, *SGK1* mRNA expression increased in patient 1 and patient 4, while was not regulated in patient 2, and decreased in patient 3. Moreover, using *B2M* and *SGK1* transcript variant 1-5/5, *SGK1* mRNA expression increased in patient 1, while decreased in patient 2, and was not regulated in patient 3 as well as in patient 4.

X-fold change values in the selected target, *TNKS2,* showed a significant downregulation in the OGD treated hCMEC/D3 mono-culture after 5h OGD timepoint (0.36 ± 0.06, p=0.0004). In triple-culture experimental set-ups with hCMEC/D3 cells, a significant downregulation of *TNKS2* mRNA expression levels was recorded after 5 h OGD treatment (0.54 ± 0.04, p=0.0025), while a significant *TNKS2* overexpression was determined after 24 h OGD treatment (1.25 ± 0.04, p=0.0014). In addition, *TNKS2* upregulation at mRNA level was detected also in the hiPS-EC triple-culture after 24 h OGD treatment (1.55 ± 0.16, p=0.0182). *TNKS2* upregulation at mRNA level after 24 h OGD treatment coincided well with the determined negative b-value difference from DNA methylation array data. Based on the investigation of *TNKS2* mRNA expression in human TBI biopsy samples, patient 1 with survival time of 0 h seemed to have no *TNKS2* mRNA expression detected at the capillaries after the TBI. Meanwhile, there was a decrease in *TNKS2* gene expression determined with *B2M* in patients with survival time of 4 h and 7 h, and an increase in patient with survival time of 21 h. When using *PPIA*, *TNKS2* downregulation at mRNA level at the BBB was recorded in every patient with the exception of patient with survival time of 0 h where *TNKS2* expression remained undetected.

5.3 Regulation of *MECOM*, *MTA2*, *RBPJ*, *RUNX1*, and *TNKS1/2* at the protein level

After investigation of the expression of the selected regulated targets at the mRNA level, some targets were further chosen to be examined also at the protein level using OGD treated hCMEC/D3 mono-culture samples.

For instance, *MECOM* was significantly downregulated at the protein level after 5 h OGD treatment (0.24 ± 0.05, p<0.0001). Moreover, at 24 h OGD timepoint *MECOM* was significantly overexpressed, depicting high increase in the *MECOM* protein expression during OGD change over the time (4.57 ± 1.07, p=0.0029). This suggested that some amount of *MECOM* protein that was lost during 5 h OGD treatment was rescued after 24 hours.

Target *MTA2* did not show any significant changes in the protein expression after 5 h and 24 h OGD treatment. However, there was observed a significant *MTA2* upregulation at the protein

level after 24 hours when comparing OGD change over the time (1.29 ± 0.08, p=0.0021). This showed that *MTA2* could accumulate at the BBB during the course of cerebral ischemia.

Concerning the change of the protein expression of *RBPJ*, a significant decrease was determined after 5 h OGD treatment (0.71 ± 0.09, p=0.0072). In addition, OGD change over the time revealed a significant *RBPJ* upregulation after 24 hours (1.49 ± 0.15, p=0.0057). This demonstrated that some amount of *RBPJ* protein that was lost during 5 h OGD timepoint was rescued after 24 h reoxygenation phase.

Protein expression of the target *RUNX1* decreased significantly after 5 h OGD treatment (0.44 ± 0.09, p<0.0001) while increased significantly after 24 h OGD treatment (1.59 ± 0.19, p=0.0064). OGD change over the time resulted in a significant *RUNX1* protein overexpression after 24 hours (3.15 ± 0.44, p=0.0002). This outcome suggested that some amount of *RUNX1* that was lost during 5 h OGD treatment at the protein level and was recovered after 24-hour recovery phase.

Target *TNKS1/2* was significantly downregulated at the protein level after 5 h OGD treatment (0.65 ± 0.06, p=0.0117). OGD change over the time revealed a significant *TNKS1/2* protein overexpression (1.36 ± 0.14, p=0.0232), proposing that the amount of *TNKS1/2* protein lost during 5 h OGD timepoint was recovered after reoxygenation that followed the OGD treatment.

5.4 Function of *SGK1* in stroke and TBI

SGK1 is a member of serine/threonine kinase family located downstream of PI3K signaling pathway [77]. A mediator of PI3K signaling is known to be *AKT* [100]. Activity of *SGK1* enzyme is induced for instance by stress or growth factors. *SGK1* expression is also stimulated by *TGFβ* while at the same time *SGK1* promotes inhibitory action towards *TGFβ* degradation in a feedback loop [78]. Action of *SGK1* contributes to the proper function and regulation of ion channel opening, metabolite transport, hormone release, inflammation, cell proliferation, and apoptosis in neurons. Overexpression of *SGK1* was over the past years associated with multiple pathological conditions and their progression such as hypertension, diabetes, stroke, ischemia, thrombosis, obesity, tumour growth, fibrosis, or neurodegenerative diseases [74], [76,77]. Furthermore, targeting of *SGK1* for the treatment in different conditions was proposed [101].

For example, ischemic preconditioning improved the outcome of the renal I/R injury by the activation of the autophagy via *SGK1* signaling pathway. More precisely, protective effect was stimulated by *SGK1* overexpression that in turn increased expression levels of *FOXO3* and

HIF-1α, and thus activated the autophagy [102]. Neuroprotection by *SGK1* through anti-apoptotic effects was suggested also in AD [103]. In I/R injury in rat hippocampal neurons *in vitro* and *in vivo* studies, it was demonstrated that *SGK1* overexpression suppresses apoptosis and induces neuroprotection during cerebral ischemia via PI3K/AKT/GSK3β pathway [104]. The role of the autophagy in state of disease may be not only beneficial for the outcome of the disease but also detrimental. Aggravation of myocardial I/R injury associated with excessive amount of autophagy was also regulated by the *SGK1* signaling cascade [105].

Moreover, there were multiple studies concerning the role of *SGK1*-specific inhibitor GSK-650394 in cerebral ischemia. This inhibitor inhibits not only *SGK1* but also other *SGK* members [106]. It was stated that use of the mentioned *SGK1* inhibitor may help to attenuate injury and damage caused by cerebral ischemia. Use of the inhibitor in asphyxia cardiac arrest rat model promoted protection against neuroinflammation, memory deficits, and neuronal cell death. On the contrary, overexpression of *SGK1* has been linked with the aggravation of the injury originating during the course of cerebral ischemia [107]. Further identification of the function of the inhibitor in mice suggested that *SGK1* inhibitor attenuated brain injury mediated by stroke and induced protective effects against N-methyl-D-aspartate (NMDA) neurotoxicity. In general, NMDA receptors represent a major cause of cell death promoted during stroke [106]. Due to contradictory outcomes from the studies concerning *SGK1* and its role in stroke and other neurodegenerative diseases, we decided to apply the inhibitor on hCMEC/D3 cells in co-culture with C6 glioma cells in a transwell model system in different concentrations to observe its effect on the BBB *in vitro* during cerebral ischemia. Obtained results suggested that applications of high concentrations of *SGK1* inhibitor including 10 μM and 30 μM concentrations promoted exacerbating effects on the BBB breakdown during OGD treatment. However, applications of lower concentrations ideally comprising of 0.03 μM and 0.1 μM of *SGK1* inhibitor seemed to induce neuroprotective effects on the BBB integrity, and thus on the damage induced during stroke. We can hypothesize that *SGK1* signaling is crucial for restorative processes following cerebral ischemia, although exceeding certain threshold of *SGK1* expression seemed to mediate also damage to the BBB. That could be the reason why some degree of *SGK1* inhibition was observed to induce neuroprotective effects upon the injury resulting from cerebral ischemia or stroke. Another possibility is that *SGK1* inhibitor GSK-650394 exerts adverse non-target side effects at higher concentrations.

5.5 General experimental considerations

First of all, in many samples from the hCMEC/D3 OGD treated mono-culture data to be examined at mRNA level, strong deviations in the single datapoints were observed. Unfortunately, low sample size of hCMEC/D3 24 h mono-culture data accompanied by identified deviations did not allow meaningful statistical analysis with every chosen target. In general, the reason why the triplicates of the same cultural condition could sometimes differ might be for instance attributed to technical errors such as pipetting errors or use of the wrong media, as well as insufficient cell confluency during the OGD experiment.

Regarding experiments performed at mRNA level with human samples, due to small sample size and diversity of the TBI biopsy samples from patients no statistical significance of the biopsy results could be determined. Even though all other experimental conditions to be investigated at the mRNA level were normalized to *18SrRNA*, we observed considerable changes in the gene expression levels with this housekeeping gene in human TBI biopsy samples. That is the reason why *B2M* and *PPIA* were selected for evaluation of mRNA expression of selected targets in TBI biopsy samples. The reason why the individual patients showed quite different expression profiles after analysis at mRNA level seemed to be mainly due to heterogeneity of the respective TBIs and unique genetic profile of every individual. Not only the extent of the injury and brain damage or location of the injury in the brain differed from patient to patient. Also, the environment and thus the type of accident that led to the TBI might be responsible for the different expression profile of individual patient (e.g. car accident, suicide, etc.).

Investigation of the protein expression changes with selected regulated targets of cerebral ischemia involved also use of anti-*SGK1* antibody and anti-*SGK1*-phospho antibody. Unfortunately, these antibodies acted nonspecifically and thus data obtained from them could not be included in this master´s thesis. Moreover, *SGK1* inhibitor studies did not reveal any significant changes in the permeability coefficients data from the first two initial experiments. The reason for that might be insufficient sample size to reach reproducibility as well as inconsistent blank values of the media used during individual cell culture experiments which represent a prerequisite for the accurate determination of the permeability coefficients.

5.6 Conclusion

In summary, observed epigenetic changes at the DNA methylation level during cerebral ischemia model with hCMEC/D3 cells provided us with promising targets that may be

implicated in the stroke induced BBB damage or in the regenerative processes that follow after the brain injury. Experimental set-ups using different cell culture conditions and human TBI biopsy samples demonstrated that significant DNA methylation changes detected at the DNA level were translated in many cases also to the mRNA level and subsequently to the protein level. For instance, target *MECOM* was significantly downregulated at the mRNA level after 5 h OGD treatment in many of the applied experimental conditions as well as at the protein level. Target *MTA2* was significantly downregulated at the mRNA level even though this decrease was not translated to the protein expression level. *RBPJ* was upregulated at mRNA level in hCMEC/D3 triple-culture after 24 h OGD treatment while *RBPJ* protein expression was downregulated after 5 h OGD treatment at the protein level. Upregulation of *RBPJ* at mRNA level after 24 h treatment correlates positively also with the negative b-value from DNA epic array data after 24 hours. Selected target *RUNX1* showed inconclusive changes at the mRNA level as it was downregulated in hCMEC/D3 OGD treated mono-culture after 5h treatment but upregulated in hCMEC/D3 triple-culture after 5 h OGD timepoint as well as in hiPS-EC triple-culture after 6 h OGD timepoint. At protein level, *RUNX1* was significantly downregulated after 5 h OGD treatment and became significantly upregulated after 24 h OGD treatment. Our last target that was examined both at the mRNA and at the protein level was *TNKS2*. *TNKS2* was downregulated at the mRNA level after 5 h OGD treatment while remained upregulated after 24 h OGD treatment in many of the applied experimental set-ups. Upregulation of *TNKS2* at the mRNA level after 24 hours also coincides well with its negative b-value after 24 hours based on DNA epic array data. At the protein level, *TNKS2* was significantly downregulated after 5 h OGD treatment. When examining OGD change over time in all targets that were examined both at the mRNA level and at the protein level, it was revealed, that a significant upregulation of every target after 24 hours of OGD conditions was recorded. This demonstrated that all of these targets may be crucially involved in the restorative processes that follow after cerebral ischemia. These studies also depicted that translation from the DNA methylation level to the mRNA level can occur differently as further translation to the protein level. The reason for that might be generally poor genome-wide correlation between expression levels of mRNA and protein. This inconsistency is typically associated with other levels of regulation between transcript and protein product [108]. We can hypothesize that lost protein during OGD treatment was in many cases compensated by high production on mRNA level.

Based on studies with *SGK1* at the mRNA level and *SGK1* inhibitor experiments, target *SGK1* seems to represent a promising biomarker due to its significant upregulation during OGD in different experimental conditions. Equally, it possesses a promising therapeutic potential as use of *SGK1* inhibitor in smaller concentrations seems to restore the BBB breakdown followed after the OGD treatment *in vitro*.

In future studies, more of the selected targets could be chosen to be examined at mRNA as well as at protein level. Also, the DNA methylation targets that were so far investigated only at the mRNA level could be additionally investigated at the protein level. Examination of human TBI biopsy samples could be performed in higher sample size that would further allow statistical analysis to be performed. Mono-culture experiments with hCMEC/D3 cells could be repeated to obtain a better data basis for statistical analysis. This could also demonstrate in a more reproducible way how exactly are the epigenetic changes of the selected regulated targets translated to the mRNA level *in vivo*.

Concerning target *SGK1*, its protein expression during cerebral ischemia could be analyzed with novel anti-*SGK1* specific antibodies to gain insight on how are the epigenetic changes of *SGK1* translated to the protein level. *SGK1* inhibitor studies could be repeated using the same experimental set-up to confirm reproducibility of permeability coefficients data and to study molecular effects of *SGK1* inhibition at the BBB. For studies of *SGK1*, additionally siRNA technique could be employed to further confirm our current hypothesis about the role of *SGK1* in stroke.

In conclusion, this project led to the characterization of multiple OGD relevant functional targets at the BBB which were originally identified from DNA methylation data and subsequently revealed to be translated to the RNA level, protein level as well as to the functional level in case of *SGK1*.

6. List of abbreviations

AD	Alzheimer´s disease
AML	Acute myeloid leukemia
APS	Ammonium persulfate
BBB	Blood-brain barrier
BHS	Blut-Hirn-Schranke
BM	Basement membrane
BSA	Bovine serum albumin
cDNA	Complementary DNA
CNS	Central nervous system
DMSO	Dimethyl sulfoxide
Dnmts	DNA methyltransferases
D-PBS	Dulbecco´s Phosphate Buffered Saline
EBM-2	Endothelial Cell Growth Basal Medium-2
ECM	Extracellular matrix
ECs	Endothelial cells
EPIC	HumanMethylationEPIC BeadChip
FBS	Fetal bovine serum
FITC-dextran	Fluorescein isothiocyanate-dextran
hCMEC/D3	Human cerebral microvascular endothelial cell line
hiPSCs	Human induced pluripotent stem cells
HRP	Horseradish peroxidase
I/R	Ischemia reperfusion
MCAO	Middle cerebral artery occlusion
MECP2	Methyl-CpG-binding protein 2
NVU	Neurovascular unit
OGD	Oxygen-glucose deprivation
PhosSTOP	Phosphatase Inhibitor
PIC	Protease Inhibitor
PI3K	Phosphatidylinositide-3 kinase
PVDF	Hydrophilic polyvinylidene fluoride
qPCR	Quantitative polymerase chain reaction
SDS	Sodium dodecyl sulfate

SGE	Sauerstoff- und Glukoseentzug
SHT	Schädel-Hirn Trauma
TBI	Traumatic brain injury
TEER	Transepithelial/transendothelial electrical resistance
TEMED	Tetramethylethylenediamine
Tet	Ten-eleven translocation
TRIS	Tris(Hydroxymethyl)aminomethane

7. List of figures

8. List of tables

9. References

[1] Roy, Rupa & Pattnaik, Sambhavi & Sivagurunathan, Suganya & Chidambaram, Subbulakshmi. (2020). Small ncRNA binding protein, PIWI: A potential molecular bridge between Blood Brain Barrier and Neuropathological conditions. Medical Hypotheses. 138. 109609. 10.1016/j.mehy.2020.109609.

[2] Rajagopal, N.; Irudayanathan, F.J.; Nangia, S. Computational Nanoscopy of Tight Junctions at the Blood–Brain Barrier Interface. *Int. J. Mol. Sci.* 2019, 20, 5583. https://doi.org/10.3390/ijms20225583.

[3] N. R. Saunders *et al.*, “The rights and wrongs of blood-brain barrier permeability studies: a walk through 100 years of history.,” *Front. Neurosci.*, vol. 8, p. 404, 2014, doi: 10.3389/fnins.2014.00404.

[4] Chow, B. W., & Gu, C. (2015). The molecular constituents of the blood-brain barrier. *Trends in neurosciences, 38*(10), 598–608. https://doi.org/10.1016/j.tins.2015.08.003.

[5] Wilhelm, I., Nyúl-Tóth, Á., Suciu, M., Hermenean, A., & Krizbai, I. A. (2016). Heterogeneity of the blood-brain barrier. *Tissue barriers, 4*(1), e1143544. https://doi.org/10.1080/21688370.2016.1143544.

[6] N. J. Abbott, L. Rönnbäck, and E. Hansson, “Astrocyte-endothelial interactions at the blood-brain barrier.,” *Nat. Rev. Neurosci.*, vol. 7, no. 1, pp. 41–53, 2006, doi: 10.1038/nrn1824.

[7] H. Kadry, B. Noorani, and L. Cucullo, “A blood-brain barrier overview on structure, function, impairment, and biomarkers of integrity.,” *Fluids Barriers CNS*, vol. 17, no. 1, p. 69, 2020, doi: 10.1186/s12987-020-00230-3.

[8] Greene, C., & Campbell, M. (2016). Tight junction modulation of the blood brain barrier: CNS delivery of small molecules. *Tissue barriers, 4*(1), e1138017. https://doi.org/10.1080/21688370.2015.1138017.

[9] M. D. Sweeney, A. P. Sagare, and B. V Zlokovic, “Blood-brain barrier breakdown in Alzheimer disease and other neurodegenerative disorders.,” *Nat. Rev. Neurol.*, vol. 14, no. 3, pp. 133–150, 2018, doi: 10.1038/nrneurol.2017.188.

[10] J. Keaney and M. Campbell, “The dynamic blood-brain barrier.,” *FEBS J.*, vol. 282, no. 21, pp. 4067–4079, 2015, doi: 10.1111/febs.13412.

[11] L. Xu, A. Nirwane, and Y. Yao, “Basement membrane and blood-brain barrier,” *Stroke Vasc. Neurol.*, vol. 4, no. 2, pp. 78–82, 2018, doi: 10.1136/svn-2018-000198.

[12] A. H. Bell, S. L. Miller, M. Castillo-Melendez, and A. Malhotra, “The Neurovascular Unit: Effects of Brain Insults During the Perinatal Period ,” *Frontiers in Neuroscience* , vol. 13. p. 1452, 2020, [Online]. Available: https://www.frontiersin.org/article/10.3389/fnins.2019.01452.

[13] B. Obermeier, R. Daneman, and R. M. Ransohoff, “Development, maintenance and disruption of the blood-brain barrier.,” *Nat. Med.*, vol. 19, no. 12, pp. 1584–1596, 2013, doi: 10.1038/nm.3407.

[14] E. Zenaro, G. Piacentino, and G. Constantin, “The blood-brain barrier in Alzheimer’s disease.,” *Neurobiol. Dis.*, vol. 107, pp. 41–56, 2017, doi: 10.1016/j.nbd.2016.07.007.

[15] Daneman, R., & Prat, A. (2015). The blood-brain barrier. *Cold Spring Harbor perspectives in biology, 7*(1), a020412. https://doi.org/10.1101/cshperspect.a020412

[16] E. M. Rhea and W. A. Banks, “Role of the Blood-Brain Barrier in Central Nervous System Insulin Resistance,” *Frontiers in Neuroscience*, vol. 13. p. 521, 2019, [Online]. Available: https://www.frontiersin.org/article/10.3389/fnins.2019.00521.

[17] S. Liebner, R. M. Dijkhuizen, Y. Reiss, K. H. Plate, D. Agalliu, and G. Constantin, “Functional morphology of the blood-brain barrier in health and disease.,” *Acta Neuropathol.*, vol. 135, no. 3, pp. 311–336, 2018, doi: 10.1007/s00401-018-1815-1.

[18] I. Cockerill, J.-A. Oliver, H. Xu, B. M. Fu, and D. Zhu, “Blood-Brain Barrier Integrity and Clearance of Amyloid-β from the BBB.,” *Adv. Exp. Med. Biol.*, vol. 1097, pp. 261–278, 2018, doi: 10.1007/978-3-319-96445-4_14.

[19] C. P. Profaci, R. N. Munji, R. S. Pulido, and R. Daneman, “The blood-brain barrier in health and disease: Important unanswered questions.,” *J. Exp. Med.*, vol. 217, no. 4, 2020, doi: 10.1084/jem.20190062.

[20] Y. Kim, J. O. Davidson, C. R. Green, L. F. B. Nicholson, S. J. O’Carroll, and J. Zhang, “Connexins and Pannexins in cerebral ischemia.,” *Biochim. Biophys. acta. Biomembr.*, vol. 1860, no. 1, pp. 224–236, 2018, doi: 10.1016/j.bbamem.2017.03.018.

[21] H.-C. Diener and G. J. Hankey, “Primary and Secondary Prevention of Ischemic Stroke and Cerebral Hemorrhage: JACC Focus Seminar.,” *J. Am. Coll. Cardiol.*, vol. 75, no. 15, pp. 1804–1818, 2020, doi: 10.1016/j.jacc.2019.12.072.

[22] O. A. Sveinsson, O. Kjartansson, and E. M. Valdimarsson, “[Cerebral ischemia/infarction - epidemiology, causes and symptoms].,” *Laeknabladid*, vol. 100, no. 5, pp. 271–279, 2014, doi: 10.17992/lbl.2014.05.543.

[23] B. Ovbiagele and M. N. Nguyen-Huynh, “Stroke epidemiology: advancing our understanding of disease mechanism and therapy,” *Neurotherapeutics*, vol. 8, no. 3, pp. 319–329, 2011, doi: 10.1007/s13311-011-0053-1.

[24] R. H. C. Lee *et al.*, “Cerebral ischemia and neuroregeneration.,” *Neural Regen. Res.*, vol. 13, no. 3, pp. 373–385, 2018, doi: 10.4103/1673-5374.228711.

[25] H. Kassis, A. Shehadah, M. Chopp, and Z. G. Zhang, “Epigenetics in Stroke Recovery.,” *Genes (Basel).*, vol. 8, no. 3, 2017, doi: 10.3390/genes8030089.

[26] T. W. McAllister, “Neurobehavioral sequelae of traumatic brain injury: evaluation and management,” *World Psychiatry*, vol. 7, no. 1, pp. 3–10, 2008, doi: 10.1002/j.2051-5545.2008.tb00139.x.

[27] A. Salehi, J. H. Zhang, and A. Obenaus, “Response of the cerebral vasculature following traumatic brain injury.,” *J. Cereb. blood flow Metab. Off. J. Int. Soc. Cereb. Blood Flow Metab.*, vol. 37, no. 7, pp. 2320–2339, 2017, doi: 10.1177/0271678X17701460.

[28] K. Hackenberg and A. Unterberg, “[Traumatic brain injury].,” *Nervenarzt*, vol. 87, no. 2, pp. 203–206, 2016, doi: 10.1007/s00115-015-0051-3.

[29] H. Atif and S. D. Hicks, “A Review of MicroRNA Biomarkers in Traumatic Brain Injury.,” *J. Exp. Neurosci.*, vol. 13, p. 1179069519832286, 2019, doi: 10.1177/1179069519832286.

[30] A. Dadas, J. Washington, R. Diaz-Arrastia, and D. Janigro, “Biomarkers in traumatic brain injury (TBI): a review,” *Neuropsychiatr. Dis. Treat.*, vol. 14, pp. 2989–3000, 2018, doi: 10.2147/NDT.S125620.

[31] L. D. Moore, T. Le, and G. Fan, “DNA methylation and its basic function.,” *Neuropsychopharmacol. Off. Publ. Am. Coll. Neuropsychopharmacol.*, vol. 38, no. 1,

pp. 23–38, 2013, doi: 10.1038/npp.2012.112.

[32] P. A. Jones, “Functions of DNA methylation: islands, start sites, gene bodies and beyond.,” *Nat. Rev. Genet.*, vol. 13, no. 7, pp. 484–492, 2012, doi: 10.1038/nrg3230.

[33] J. Krupinski *et al.*, “DNA Methylation in Stroke. Update of Latest Advances.,” *Comput. Struct. Biotechnol. J.*, vol. 16, pp. 1–5, 2018, doi: 10.1016/j.csbj.2017.12.001.

[34] B. G. Jorgensen *et al.*, “DNA methylation, through DNMT1, has an essential role in the development of gastrointestinal smooth muscle cells and disease,” *Cell Death Dis.*, vol. 9, no. 5, p. 474, 2018, doi: 10.1038/s41419-018-0495-z.

[35] R. Lister *et al.*, “Human DNA methylomes at base resolution show widespread epigenomic differences,” *Nature*, vol. 462, no. 7271, pp. 315–322, 2009, doi: 10.1038/nature08514.

[36] Nevin C, Carroll M (2015) Sperm DNA Methylation, Infertility and Transgenerational Epigenetics. J Genet Genomic Sci 1: 004.

[37] Z. Hu, B. Zhong, J. Tan, C. Chen, Q. Lei, and L. Zeng, “The Emerging Role of Epigenetics in Cerebral Ischemia,” *Mol. Neurobiol.*, vol. 54, no. 3, pp. 1887–1905, 2017, doi: 10.1007/s12035-016-9788-3.

[38] R. Stanzione *et al.*, “Pathogenesis of Ischemic Stroke: Role of Epigenetic Mechanisms.,” *Genes (Basel).*, vol. 11, no. 1, 2020, doi: 10.3390/genes11010089.

[39] S. M. Stamatovic, C. M. Phillips, G. Martinez-Revollar, R. F. Keep, and A. V Andjelkovic, “Involvement of Epigenetic Mechanisms and Non-coding RNAs in Blood-Brain Barrier and Neurovascular Unit Injury and Recovery After Stroke.,” *Front. Neurosci.*, vol. 13, p. 864, 2019, doi: 10.3389/fnins.2019.00864.

[40] W. Neuhaus, “In Vitro Models of the Blood-Brain Barrier.,” *Handb. Exp. Pharmacol.*, 2020, doi: 10.1007/164_2020_370.

[41] F. Sivandzade and L. Cucullo, “In-vitro blood-brain barrier modeling: A review of modern and fast-advancing technologies.,” *J. Cereb. blood flow Metab. Off. J. Int. Soc. Cereb. Blood Flow Metab.*, vol. 38, no. 10, pp. 1667–1681, 2018, doi: 10.1177/0271678X18788769.

[42] W. Neuhaus, “Human induced pluripotent stem cell based in vitro models of the blood-

brain barrier: the future standard?," *Neural Regen. Res.*, vol. 12, no. 10, pp. 1607–1609, 2017, doi: 10.4103/1673-5374.217326.

[43] A. Gerhartl, N. Pracser, A. Vladetic, S. Hendrikx, H.-P. Friedl, and W. Neuhaus, "The pivotal role of micro-environmental cells in a human blood-brain barrier in vitro model of cerebral ischemia: functional and transcriptomic analysis.," *Fluids Barriers CNS*, vol. 17, no. 1, p. 19, 2020, doi: 10.1186/s12987-020-00179-3.

[44] W. Neuhaus, T. Krämer, A. Neuhoff, C. Gölz, S. C. Thal, and C. Y. Förster, "Multifaceted Mechanisms of WY-14643 to Stabilize the Blood-Brain Barrier in a Model of Traumatic Brain Injury," *Front. Mol. Neurosci.*, vol. 10, p. 149, 2017, doi: 10.3389/fnmol.2017.00149.

[45] M. Saunders, "Transplacental transport of nanomaterials.," *Wiley Interdiscip. Rev. Nanomed. Nanobiotechnol.*, vol. 1, no. 6, pp. 671–684, 2009, doi: 10.1002/wnan.53.

[46] Tornabene, E., Helms, H., Pedersen, S. F., & Brodin, B. (2019). Effects of oxygen-glucose deprivation (OGD) on barrier properties and mRNA transcript levels of selected marker proteins in brain endothelial cells/astrocyte co-cultures. *PloS one, 14*(8), e0221103. https://doi.org/10.1371/journal.pone.0221103

[47] A. R. Santa-Maria *et al.*, "Transport Studies Using Blood-Brain Barrier In Vitro Models: A Critical Review and Guidelines.," *Handb. Exp. Pharmacol.*, 2020, doi: 10.1007/164_2020_394.

[48] N. Fernandez-Jimenez *et al.*, "Comparison of Illumina 450K and EPIC arrays in placental DNA methylation.," *Epigenetics*, vol. 14, no. 12, pp. 1177–1182, 2019, doi: 10.1080/15592294.2019.1634975.

[49] P. Du *et al.*, "Comparison of Beta-value and M-value methods for quantifying methylation levels by microarray analysis," *BMC Bioinformatics*, vol. 11, p. 587, 2010, doi: 10.1186/1471-2105-11-587.

[50] A. Subramanian *et al.*, "Gene set enrichment analysis: a knowledge-based approach for interpreting genome-wide expression profiles.," *Proc. Natl. Acad. Sci. U. S. A.*, vol. 102, no. 43, pp. 15545–15550, 2005, doi: 10.1073/pnas.0506580102.

[51] A. Appelt-Menzel *et al.*, "Establishment of a Human Blood-Brain Barrier Co-culture Model Mimicking the Neurovascular Unit Using Induced Pluri- and Multipotent Stem

Cells.," *Stem cell reports*, vol. 8, no. 4, pp. 894–906, 2017, doi: 10.1016/j.stemcr.2017.02.021.

[52] S. Oerter, C. Förster, and M. Bohnert, "Validation of sodium/glucose cotransporter proteins in human brain as a potential marker for temporal narrowing of the trauma formation.," *Int. J. Legal Med.*, vol. 133, no. 4, pp. 1107–1114, 2019, doi: 10.1007/s00414-018-1893-6.

[53] S. A. Bustin *et al.*, "The MIQE Guidelines: Minimum Information for Publication of Quantitative Real-Time PCR Experiments," *Clin. Chem.*, vol. 55, no. 4, pp. 611–622, 2009, doi: 10.1373/clinchem.2008.112797.

[54] B. Gericke *et al.*, "A face-to-face comparison of claudin-5 transduced human brain endothelial (hCMEC/D3) cells with porcine brain endothelial cells as blood-brain barrier models for drug transport studies.," *Fluids Barriers CNS*, vol. 17, no. 1, p. 53, 2020, doi: 10.1186/s12987-020-00212-5.

[55] D. Giakoumettis, A. Kritis, and N. Foroglou, "C6 cell line: the gold standard in glioma research.," *Hippokratia*, vol. 22, no. 3, pp. 105–112, 2018.

[56] B. Srinivasan, A. R. Kolli, M. B. Esch, H. E. Abaci, M. L. Shuler, and J. J. Hickman, "TEER measurement techniques for in vitro barrier model systems.," *J. Lab. Autom.*, vol. 20, no. 2, pp. 107–126, 2015, doi: 10.1177/2211068214561025.

[57] C. Chaves, F. Remiao, S. Cisternino, and X. Decleves, "Opioids and the Blood-Brain Barrier: A Dynamic Interaction with Consequences on Drug Disposition in Brain," *Curr. Neuropharmacol.*, vol. 15, no. 8, pp. 1156–1173, 2017, doi: 10.2174/1570159X15666170504095823.

[58] S. A. Ihezie, I. E. Mathew, D. W. McBride, A. Dienel, S. L. Blackburn, and P. K. Thankamani Pandit, "Epigenetics in blood-brain barrier disruption," *Fluids Barriers CNS*, vol. 18, no. 1, p. 17, 2021, doi: 10.1186/s12987-021-00250-7.

[59] H. Steinkellner *et al.*, "An electrochemiluminescence based assay for quantitative detection of endogenous and exogenously applied MeCP2 protein variants," *Sci. Rep.*, vol. 9, no. 1, p. 7929, 2019, doi: 10.1038/s41598-019-44372-3.

[60] Y. Kim *et al.*, "CLEC14A deficiency exacerbates neuronal loss by increasing blood-brain barrier permeability and inflammation," *J. Neuroinflammation*, vol. 17, no. 1, p.

48, 2020, doi: 10.1186/s12974-020-1727-6.

[61] Y. Wang *et al.*, “Epigenetic factor EPC1 is a master regulator of DNA damage response by interacting with E2F1 to silence death and actifile:///C:/Users/HP/Downloads/PMC4716764.risvafile:///C:/Users/HP/Downloads/PMC4716764.riste metastasis-related gene signatures,” *Nucleic Acids Res.*, vol. 44, no. 1, pp. 117–133, 2016, doi: 10.1093/nar/gkv885.

[62] A. Hou *et al.*, “Expression of MECOM is associated with unfavorable prognosis in glioblastoma multiforme,” *Onco. Targets. Ther.*, vol. 9, pp. 315–320, 2016, doi: 10.2147/OTT.S95831.

[63] J. Z. Drago *et al.*, “FGFR1 Amplification Mediates Endocrine Resistance but Retains TORC Sensitivity in Metastatic Hormone Receptor-Positive (HR(+)) Breast Cancer,” *Clin. Cancer Res.*, vol. 25, no. 21, pp. 6443–6451, 2019, doi: 10.1158/1078-0432.CCR-19-0138.

[64] Y. Lu, Y. Liu, S. Oeck, G. J. Zhang, A. Schramm, and P. M. Glazer, “Hypoxia Induces Resistance to EGFR Inhibitors in Lung Cancer Cells via Upregulation of FGFR1 and the MAPK Pathway.,” *Cancer Res.*, vol. 80, no. 21, pp. 4655–4667, 2020, doi: 10.1158/0008-5472.CAN-20-1192.

[65] P. B. Talbert and S. Henikoff, “Histone variants--ancient wrap artists of the epigenome.,” *Nat. Rev. Mol. Cell Biol.*, vol. 11, no. 4, pp. 264–275, 2010, doi: 10.1038/nrm2861.

[66] S. Zhu *et al.*, “Reciprocal loop of hypoxia-inducible factor-1α (HIF-1α) and metastasis-associated protein 2 (MTA2) contributes to the progression of pancreatic carcinoma by suppressing E-cadherin transcription.,” *J. Pathol.*, vol. 245, no. 3, pp. 349–360, 2018, doi: 10.1002/path.5089.

[67] J. Sun and G. Nan, “The Mitogen-Activated Protein Kinase (MAPK) Signaling Pathway as a Discovery Target in Stroke.,” *J. Mol. Neurosci.*, vol. 59, no. 1, pp. 90–98, 2016, doi: 10.1007/s12031-016-0717-8.

[68] Y. Huang, Y. Yang, Y. He, and J. Li, “The emerging role of Nemo-like kinase (NLK) in the regulation of cancers.,” *Tumour Biol. J. Int. Soc. Oncodevelopmental Biol. Med.*, vol. 36, no. 12, pp. 9147–9152, 2015, doi: 10.1007/s13277-015-4159-7.

[69] S. Hosseini-Alghaderi and M. Baron, “Notch3 in Development, Health and Disease.,” *Biomolecules*, vol. 10, no. 3, 2020, doi: 10.3390/biom10030485.

[70] L. Keat Wei, L. R. Griffiths, L. Irene, and C. W. Kooi, “Association of NOTCH3 Gene Polymorphisms with Ischemic Stroke and its Subtypes: A Meta-Analysis.,” *Medicina (Kaunas).*, vol. 55, no. 7, 2019, doi: 10.3390/medicina55070351.

[71] P. Zhang *et al.*, “Endothelial Notch activation promotes neutrophil transmigration via downregulating endomucin to aggravate hepatic ischemia/reperfusion injury.,” *Sci. China. Life Sci.*, vol. 63, no. 3, pp. 375–387, 2020, doi: 10.1007/s11427-019-1596-4.

[72] R. Diéguez-Hurtado *et al.*, “Loss of the transcription factor RBPJ induces disease-promoting properties in brain pericytes.,” *Nat. Commun.*, vol. 10, no. 1, p. 2817, 2019, doi: 10.1038/s41467-019-10643-w.

[73] G. Santopolo, J. P. Magnusson, O. Lindvall, Z. Kokaia, and J. Frisén, “Blocking Notch-Signaling Increases Neurogenesis in the Striatum after Stroke.,” *Cells*, vol. 9, no. 7, 2020, doi: 10.3390/cells9071732.

[74] M. Lie-A-Ling *et al.*, “RUNX1 Dosage in Development and Cancer.,” *Mol. Cells*, vol. 43, no. 2, pp. 126–138, 2020, doi: 10.14348/molcells.2019.0301.

[75] I. L. Tourkova *et al.*, “The high-density lipoprotein receptor Scarb1 is required for normal bone differentiation in vivo and in vitro.,” *Lab. Invest.*, vol. 99, no. 12, pp. 1850–1860, 2019, doi: 10.1038/s41374-019-0311-0.

[76] T.-T. Zeng, D.-J. Tang, Y.-X. Ye, J. Su, and H. Jiang, “Influence of SCARB1 gene SNPs on serum lipid levels and susceptibility to coronary heart disease and cerebral infarction in a Chinese population.,” *Gene*, vol. 626, pp. 319–325, 2017, doi: 10.1016/j.gene.2017.05.020.

[77] C. Yang, J. Li, F. Sun, H. Zhou, J. Yang, and C. Yang, “The functional duality of SGK1 in the regulation of hyperglycemia,” *Endocr. Connect.*, vol. 9, no. 7, pp. R187–R194, 2020, doi: 10.1530/EC-20-0225.

[78] F. Artunc and F. Lang, “Mineralocorticoid and SGK1-sensitive inflammation and tissue fibrosis.,” *Nephron. Physiol.*, vol. 128, no. 1–2, pp. 35–39, 2014, doi: 10.1159/000368267.

[79] F. Lang, C. Stournaras, and I. Alesutan, “Regulation of transport across cell

membranes by the serum- and glucocorticoid-inducible kinase SGK1.," *Mol. Membr. Biol.*, vol. 31, no. 1, pp. 29–36, 2014, doi: 10.3109/09687688.2013.874598.

[80] B. Schoenebeck, V. Bader, X. R. Zhu, B. Schmitz, H. Lübbert, and C. C. Stichel, "Sgk1, a cell survival response in neurodegenerative diseases.," *Mol. Cell. Neurosci.*, vol. 30, no. 2, pp. 249–264, 2005, doi: 10.1016/j.mcn.2005.07.017.

[81] P. Kirubakaran, G. Kothandan, S. J. Cho, and K. Muthusamy, "Molecular insights on TNKS1/TNKS2 and inhibitor-IWR1 interactions.," *Mol. Biosyst.*, vol. 10, no. 2, pp. 281–293, 2014, doi: 10.1039/c3mb70305c.

[82] M. D. Sweeney, Z. Zhao, A. Montagne, A. R. Nelson, and B. V Zlokovic, "Blood-Brain Barrier: From Physiology to Disease and Back," *Physiol. Rev.*, vol. 99, no. 1, pp. 21–78, 2019, doi: 10.1152/physrev.00050.2017.

[83] R. Prakash and S. T. Carmichael, "Blood-brain barrier breakdown and neovascularization processes after stroke and traumatic brain injury," *Curr. Opin. Neurol.*, vol. 28, no. 6, pp. 556–564, 2015, doi: 10.1097/WCO.0000000000000248.

[84] R. Tirado-Magallanes, K. Rebbani, R. Lim, S. Pradhan, and T. Benoukraf, "Whole genome DNA methylation: beyond genes silencing," *Oncotarget; Vol 8, No 3*, 2016, [Online]. Available: https://www.oncotarget.com/article/13562/text/.

[85] T. Sato *et al.*, "Evi1 defines leukemia-initiating capacity and tyrosine kinase inhibitor resistance in chronic myeloid leukemia.," *Oncogene*, vol. 33, no. 42, pp. 5028–5038, 2014, doi: 10.1038/onc.2014.108.

[86] R. Sood, Y. Kamikubo, and P. Liu, "Role of RUNX1 in hematological malignancies.," *Blood*, vol. 129, no. 15, pp. 2070–2082, 2017, doi: 10.1182/blood-2016-10-687830.

[87] M. Bao *et al.*, "Runx1 promotes satellite cell proliferation during ischemia - Induced muscle regeneration.," *Biochem. Biophys. Res. Commun.*, vol. 503, no. 4, pp. 2993–2997, 2018, doi: 10.1016/j.bbrc.2018.08.083.

[88] S. Gattenlöhner, C. Waller, G. Ertl, B.-D. Bültmann, H.-K. Müller-Hermelink, and A. Marx, "NCAM(CD56) and RUNX1(AML1) are up-regulated in human ischemic cardiomyopathy and a rat model of chronic cardiac ischemia.," *Am. J. Pathol.*, vol. 163, no. 3, pp. 1081–1090, 2003, doi: 10.1016/S0002-9440(10)63467-0.

[89] Ren, S., Wu, G., Huang, Y., Wang, L., Li, Y., & Zhang, Y. (2021). MiR-18a Aggravates

Intracranial Hemorrhage by Regulating RUNX1-Occludin/ZO-1 Axis to Increase BBB Permeability. *Journal of stroke and cerebrovascular diseases : the official journal of National Stroke Association, 30*(8), 105878. https://doi.org/10.1016/j.jstrokecerebrovasdis.2021.105878.

[90] Logan, T. T., Villapol, S., & Symes, A. J. (2013). TGF-β superfamily gene expression and induction of the Runx1 transcription factor in adult neurogenic regions after brain injury. *PloS one, 8*(3), e59250. https://doi.org/10.1371/journal.pone.0059250.

[91] E. E. Santo and J. Paik, “FOXO in Neural Cells and Diseases of the Nervous System,” *Curr. Top. Dev. Biol.*, vol. 127, pp. 105–118, 2018, doi: 10.1016/bs.ctdb.2017.10.002.

[92] L. Zhan, T. Wang, W. Li, Z. C. Xu, W. Sun, and E. Xu, “Activation of Akt/FoxO signaling pathway contributes to induction of neuroprotection against transient global cerebral ischemia by hypoxic pre-conditioning in adult rats.,” *J. Neurochem.*, vol. 114, no. 3, pp. 897–908, 2010, doi: 10.1111/j.1471-4159.2010.06816.x.

[93] K. Zhang *et al.*, “Artesunate promotes the proliferation of neural stem/progenitor cells and alleviates Ischemia-reperfusion Injury through PI3K/Akt/FOXO-3a/p27(kip1) signaling pathway.,” *Aging (Albany. NY).*, vol. 12, no. 9, pp. 8029–8048, 2020, doi: 10.18632/aging.103121.

[94] K. Fukunaga and N. Shioda, “Pathophysiological relevance of forkhead transcription factors in brain ischemia.,” *Adv. Exp. Med. Biol.*, vol. 665, pp. 130–142, 2009, doi: 10.1007/978-1-4419-1599-3_10.

[95] H. Zhou, X. Wang, L. Ma, A. Deng, S. Wang, and X. Chen, “FoxO3 transcription factor promotes autophagy after transient cerebral ischemia/reperfusion.,” *Int. J. Neurosci.*, vol. 129, no. 8, pp. 738–745, 2019, doi: 10.1080/00207454.2018.1564290.

[96] Liu, X. L., Gao, C. C., Qi, M., Han, Y. L., Zhou, M. L., & Zheng, L. R. (2021). Expression of FOXO transcription factors in the brain following traumatic brain injury. *Neuroscience letters, 753*, 135882. https://doi.org/10.1016/j.neulet.2021.135882.

[97] L. Sun *et al.*, “Suppression of FoxO3a attenuates neurobehavioral deficits after traumatic brain injury through inhibiting neuronal autophagy.,” *Behav. Brain Res.*, vol. 337, pp. 271–279, 2018, doi: 10.1016/j.bbr.2017.08.042.

[98] Y. Mo, Y.-Y. Sun, and K.-Y. Liu, “Autophagy and inflammation in ischemic stroke.,” *Neural Regen. Res.*, vol. 15, no. 8, pp. 1388–1396, 2020, doi: 10.4103/1673-5374.274331.

[99] Y. Zheng, Z. Han, H. Zhao, and Y. Luo, “MAPK: A Key Player in the Development and Progression of Stroke.,” *CNS Neurol. Disord. Drug Targets*, vol. 19, no. 4, pp. 248–256, 2020, doi: 10.2174/1871527319666200613223018.

[100] A. Di Cristofano, “SGK1: The Dark Side of PI3K Signaling.,” *Curr. Top. Dev. Biol.*, vol. 123, pp. 49–71, 2017, doi: 10.1016/bs.ctdb.2016.11.006.

[101] F. Lang and J. Voelkl, “Therapeutic potential of serum and glucocorticoid inducible kinase inhibition.,” *Expert Opin. Investig. Drugs*, vol. 22, no. 6, pp. 701–714, 2013, doi: 10.1517/13543784.2013.778971.

[102] Y. Xie *et al.*, “Ischemic preconditioning attenuates ischemia/reperfusion-induced kidney injury by activating autophagy via the SGK1 signaling pathway.,” *Cell Death Dis.*, vol. 9, no. 3, p. 338, 2018, doi: 10.1038/s41419-018-0358-7.

[103] P. Sahin, C. McCaig, J. Jeevahan, J. T. Murray, and A. H. Hainsworth, “The cell survival kinase SGK1 and its targets FOXO3a and NDRG1 in aged human brain.,” *Neuropathol. Appl. Neurobiol.*, vol. 39, no. 6, pp. 623–633, 2013, doi: 10.1111/nan.12023.

[104] W. Zhang, C. yun Qian, and S. Q. Li, “Protective effect of SGK1 in rat hippocampal neurons subjected to ischemia reperfusion.,” *Cell. Physiol. Biochem. Int. J. Exp. Cell. Physiol. Biochem. Pharmacol.*, vol. 34, no. 2, pp. 299–312, 2014, doi: 10.1159/000363000.

[105] H. Jiang, J. Xiao, B. Kang, X. Zhu, N. Xin, and Z. Wang, “PI3K/SGK1/GSK3β signaling pathway is involved in inhibition of autophagy in neonatal rat cardiomyocytes exposed to hypoxia/reoxygenation by hydrogen sulfide.,” *Exp. Cell Res.*, vol. 345, no. 2, pp. 134–140, 2016, doi: 10.1016/j.yexcr.2015.07.005.

[106] K. Inoue, T. Leng, T. Yang, Z. Zeng, T. Ueki, and Z.-G. Xiong, “Role of serum- and glucocorticoid-inducible kinases in stroke.,” *J. Neurochem.*, vol. 138, no. 2, pp. 354–361, 2016, doi: 10.1111/jnc.13650.

[107] Lee, R. H., Grames, M. S., Wu, C. Y., Lien, C. F., Couto E Silva, A., Possoit, H. E.,

Clemons, G. A., Citadin, C. T., Neumann, J. T., Pastore, D., Lauro, D., Della-Morte, D., & Lin, H. W. (2020). Upregulation of serum and glucocorticoid-regulated kinase 1 exacerbates brain injury and neurological deficits after cardiac arrest. *American journal of physiology. Heart and circulatory physiology, 319*(5), H1044–H1050. https://doi.org/10.1152/ajpheart.00399.2020.

[108] Koussounadis, A., Langdon, S. P., Um, I. H., Harrison, D. J., & Smith, V. A. (2015). Relationship between differentially expressed mRNA and mRNA-protein correlations in a xenograft model system. *Scientific reports, 5*, 10775. https://doi.org/10.1038/srep10775.